The Dorsal Subiculum And Long-term Spatial Memory: A Behavioural And Electrophysiological Study

Chiara Franceschi

A thesis submitted for the degree of

Doctor of Philosophy

Cardiff University

March 2025

ABSTRACT

The subiculum is a major output region of the hippocampus. While its involvement in spatial working memory is known, its contributions to reference memory have not been established. This work aimed at filling this gap. Silencing the dorsal subiculum through muscimol infusions was performed at different stages of a spatial radial-arm maze (RAM) task: acquisition, and memory processing during rest. In both instances, muscimol impaired the animals' performance, confirming a role of the area in spatial working memory and indicating a subicular contribution to spatial reference memory. The manipulation of subicular activity was additionally tested when pre-exposure to the task was carried out. Here, no impact on performance was detected, which suggests that prior task knowledge might reduce the contribution of the subiculum in reference memory.

The second part of this thesis focused on developing and implementing an electrophysiological methodology that allows characterisation of neuronal activity across consecutive days. Neuropixels probes were implanted and recorded while rats explored an open field apparatus and performed the RAM task, intermingled with sleep sessions. Stability of the recordings was assessed through waveform features using a PCA approach, which showed that it is feasible to reliably track the same cells across days. A circular clustering approach allowed to identify four subgroups of excitatory neurons, based on their theta preference. These groups differed in position along the radial axis, burstiness, mean firing, and spatial information content. Characterisation of their firing during sharp-wave ripple events was also assessed. During learning, group 1 consisted of more spatial, plastic cells. Reactivation of firing assemblies during sleep confirmed that subicular cells reactivate more on the first two days of the task, consistent with learning.

Collectively, this data provides a first indication of the involvement of the dorsal subiculum in reference memory, from both a behavioural and an electrophysiological standpoint.

LIST OF CONTENTS

AKNOWLEDGEMENTS

I would like to express my sincerest gratitude to Joe whose guidance and support was invaluable over these four and a half years. His patience and academic insight helped greatly in shaping who I am today as a scientist. I could not have undertaken this journey without Cardiff University and the School of Psychology in particular, for all the support provided by them to PhD students.

I am also grateful to my fellow colleagues for their moral support and avid discussions. Honourable mentions go to Sungmin Kang for helping in developing the probe recordings, and Hanna Wyszynska for always bringing a smile to work and sharing all of the stress of being a PhD student without blinking an eye.

I would not be here if not for the support of my family who were there for me since the beginning of this adventure. Despite the physical distance, they always encouraged me and pushed me to bring the best version of myself into every day. My oldest friends Auri, Ire, and Simo, for providing me with little moments of respite in between the days which made me smile and forget all my worries. Isa and Nori, who have been pillars of strength when times were difficult. Their belief in me has helped me stay motivated and positive throughout this process. Soorya, Jack, Kim, Miriam and Bri, who have provided me with the comfort of a group of friends I could always rely on, and who have given me so many board games throughout the years that I am sure I will never be bored again. I look forward to being able to play them with them more often now that this journey has ended.

Lastly, a huge thank you goes to Marcus, for believing I could do this even when I couldn’t see it. He helped me through some of the darkest times of my life and never gave up on me, despite my foul moods and, sometimes, horrible words. I would not have been able to finish this thesis without him, and I hope he knows I will be there to support him just as much whatever might come our way.

ABBREVIATIONS

AP	Action potential (when talking about the electrophysiological recordings) or anterior-posterior (when talking about coordinates in the brain)
AV	Antero-ventral nucleus of the thalamus
BVC	Boundary-vector cell
CA1-4	Cornu Ammonis or Ammon's Horn, subergions 1-4
CI	Confidence intervals
DG	Dentate gyrus
DLC	DeepLabCut
DMSO	Dimethyl Sulfoxide
DV	Dorso-ventral (axis of the brain)
EC	Entorhinal cortex
EEG	Electroencephalography
fMRI	Functional Magnetic Resonance Imaging
GABA	Gamma-aminobutyric acid (primary inhibitory neurotransmitter in the central nervous system)
IFR	Instantaneous firing rate
ISO	Isoflurane
LEC	Lateral Entorhinal cortex
LED	Light-emitting diode (glows when a voltage is applied)
LFP	Local field potential
LTD	Long-term depression
LTP	Long-term potentiation
MEC	Medial Entorhinal cortex
ML	Medio-lateral (axis of the brain)
MMB	Medial mammillary body
MWM	Morris Water Maze
NAC	Nucleus accumbens
NMDA	N-methyl-D-aspartate (subtype of glutamate ionotropic receptors)
NPX 1.0/2.0	Neuropixels probe, version 1.0 or 2.0
PBS	Phosphate buffered saline
PC	Pyramidal cell

PCA	Principal component analysis
PFA	Paraformaldehyde
RAM	Radial-arm maze
RME	Reference memory error
RSC	Retrosplenial cortex
SD	Standard deviation
SEM	Standard error of the mean
SI	Spatial information
SOP	Sometimes-opponent processes (theory)
SWR	Sharp-wave ripple
TTL	Transistor-transistor logic (signal)
VTC	Vector-trace cell
WME	Working memory error

Chapter 1 - General Introduction

Spatial memory is “the ability of an animal to keep track of its location in space by remembering where it has been” (Olton, 1977). It has been studied as a concept for decades in close relation to episodic memory, with the latter being defined as the ability to remember specific events, experiences, and situations that happen in everyday life. Episodic and spatial mnemonic systems are believed to require the hippocampus, before information is then communicated to the rest of the brain for higher level processing (see Squire, 2004). Decades of work have been spent elucidating the role of the hippocampal formation in memory; however, not all components of these regions have received thorough attention. One such component is the subiculum, which represents the main output region from the hippocampus to the rest of the brain (Rosene & Van Hoesen, 1977). While up and down stream regions of the hippocampal formation have equally been implicated in both short and long-term spatial memory (e.g. O’Mara & Aggleton, 2019), the step in between (the subiculum) has been under-explored in the literature so far, and there has been no consensus regarding its possible involvement in long-term memory processing. This introduction will first describe the concepts of episodic and spatial memory and how they are processed in the brain, then explore the subiculum’s involvement in these processes, and finally identify those questions that remain unanswered regarding the function of this brain region.

The role of the hippocampus in episodic memory

What is episodic memory? Episodic memory is a cognitive process that stores information on events that happen in one’s life, particularly the “what”, the “where”, and the “when”, as cleverly put by Nyberg and colleagues (1996). The concept was first introduced by Tulving (1972) to make a distinction with semantic memory: while the latter concerns memories of general, objective facts, the former stores information of personally experienced events. Episodic memory operates on two main dimensions, a temporal and a spatial one, which

together allow navigation of one's experience by creating maps of spatiotemporal relations.

Episodic memories can be divided based on the time frame of information processing, from the short-term (within seconds) to long-term (spanning across days or years; see Kesner & Hunsaker, 2010). The way information inside these time periods is processed has been described to involve three stages: acquisition, storage, and retrieval (Diekelmann & Born, 2010; Squire, 2004; Tulving, 2002). While the initial encoding of information allows for a first, short-term acquisition (which involves the active process of working memory; Atkinson & Shiffrin, 1968), the subsequent long-term storage of memory traces occurs through a slower process of consolidation, enabling the recall of events over a lifetime (reviewed by McGaugh, 2000). This storing and updating of information in the brain occurs through changes in structure, function, and organization of neurons and synapses (i.e. neuroplasticity) as a result of learning (see Turrigiano & Nelson, 2004). These changes span from large-scale modifications such as creating new neurons and synapses (structural plasticity), to microscale changes in the connections between neurons (synaptic plasticity). This last type of plasticity is a key mechanism in enabling mnemonic processing, through both strengthening (long-term potentiation, or LTP), and weakening of synapses (long-term depression, or LTD; see Luscher & Malenka, 2012). Many forms of LTP and LTD have been recognized, which rely on different molecular mechanisms (such as different neurotransmitters, or postsynaptic receptors such as NMDA and AMPA). Overall, these mechanisms occur at nearly every synapse and brain circuit, providing a way for salient information to be emphasized (e.g., by strengthening the synapses of cofiring neurons).

Along with providing information on "what" and "when" an event happens, episodic memories store information on the "where". From here comes the notion of spatial memory, the ability of an animal to store representations of where it has been in an environment. This particular aspect of the mnemonic function is what this thesis will focus on.

Both the temporal and the spatial components of episodic memory likely involve complex interactions between multiple brain regions over time. However, the hippocampus has been shown to play a central role in each stage of memory formation (Riedel et al., 1999),

by providing an internal representation of space (O'Keefe et al., 1978) and time (Kesner & Hunsaker, 2010). As part of a wide set of regions defined as the hippocampal formation (see below), the subiculum has also been implicated in the processing of spatial information and spatial memories (O'Mara et al., 2009), although its role in each of the three stages (acquisition, storage, and retrieval) has not been clearly delineated. As the subiculum is the main output of the hippocampus (Amaral et al., 1991), one has to first understand the role of the hippocampus in episodic memory in order to better understand the specific contributions of the subiculum to this function.

First discoveries of the hippocampal function. Two main lines of research initially fuelled the interest in the connection between the hippocampus and episodic memory. First, Scoville and Milner (1957) observed a patient (H.M.) after surgical removal of his hippocampus and other parahippocampal structures as a treatment for epilepsy. After surgery, this patient exhibited an impairment in generating new memories for places and events, while memories formed in the distant past appeared spared. This observation first linked the human hippocampus to the generation of new episodic memories. After, numerous studies have come to the same conclusion, with replications both in humans and non-human primates (reviewed by Zola-Morgan & Squire, 1990).

In parallel with this analysis, research conducted in rodents began to point towards the hippocampus and its involvement in spatial learning and navigation. First, Tolman (1948) conducted a series of maze learning experiments on rats (***Figure 1A***). He observed that, after learning a roundabout route to a goal location, the animals were able to switch to a more direct route if the familiar one was unavailable. He concluded that these animals could create cognitive maps of the environments in order to navigate inside them. Then, O'Keefe and Dostrovsky (1971) uncovered how different excitatory cells of the CA1 subfield ("place cells", see below) become active when the animal explores defined regions of an environment. Groups of such cells collectively form a patchwork of spatial fields across any given environment to form a "cognitive map of space" (O'Keefe et al., 1978), supporting the conclusions drawn by Tolman three decades earlier. From these first studies, it appeared clear that the hippocampus has a role in processing both mnemonic and, more specifically, spatial information.

Lesion studies in the hippocampal formation. Stemming from these discoveries, an entire line of rodent studies focused on analysing the results of hippocampal lesions. Along with trying to compare results with those found by observing the damaged hippocampus in human patients such as H.M., these studies benefitted from being able to induce lesions on specific and restricted targeted areas, without the need for them to happen "naturally" due to accidents, disease or surgical intervention. With this advantage, the hippocampus in rodents has been tested in a variety of navigation and spatial memory tasks (see ***Figure 1***). One key example of such tasks was performed on the Radial Arm Maze (RAM), an environment made up of (usually) 8 arms radiating from a central chamber (***Figure 1B***). This maze was first implemented to study the role of the hippocampus in spatial memory by Olton (1977), who would place pieces of food at the end of each arm to test the ability of the rats to collect the rewards without re-entering any of the previously visited arms (in a task that is now referred to, in literature, as "all-arms baited" or "working memory" RAM task). Olton demonstrated that lesioning the connections from the hippocampus to the rest of the brain (via either the entorhinal cortex or the fornix) causes irreversible damage to the animal's ability to perform the task, thus highlighting the importance of the hippocampus in spatial memory. Later, Jarrard (1993) implemented a similar version of this task, with only 4 out of the 8 arms baited (***Figure 1B, right***), and used focused lesions of the hippocampus itself while sparing its connections with other brain regions. He concluded that hippocampal lesions greatly affect learning a complex spatial task, compared to an equally complex non-spatial one. Similar conclusions were reached in the more navigational demanding Morris Water Maze (MWM, ***Figure 1C***) task, in which animals have to find a submerged platform without the "aid" of fixed routes to search within (Morris et al., 1982).

Importantly, one of the two pathways impacted by the lesion studies conducted by Olton (1977), the fornix, contains approximately 60% of projections arising from the subicular complex in the macaque (of which more than half arise from the subiculum proper; Saunders & Aggleton, 2007). In the rodent, these percentages are even higher (Swanson & Cowan, 1977), highlighting the importance of the subiculum as the main output region from the hippocampus. This suggests that the subiculum is at least involved in communicating hippocampal spatial information to other regions of the brain. Consistent

with this idea, lesioning the subiculum during the MWM and RAM tasks reveals similar deficits compared to lesioning the hippocampus only (Morris et al., 1990; Potvin et al., 2007). At the same time, lesioning both regions results in greater deficits than lesioning either region individually. These additive effects indicate that the deficits of subicular lesions are not only due to a loss of hippocampal inputs to other brain areas, but rather suggest that the subiculum itself has a role in processing spatial information (Potvin et al., 2006).

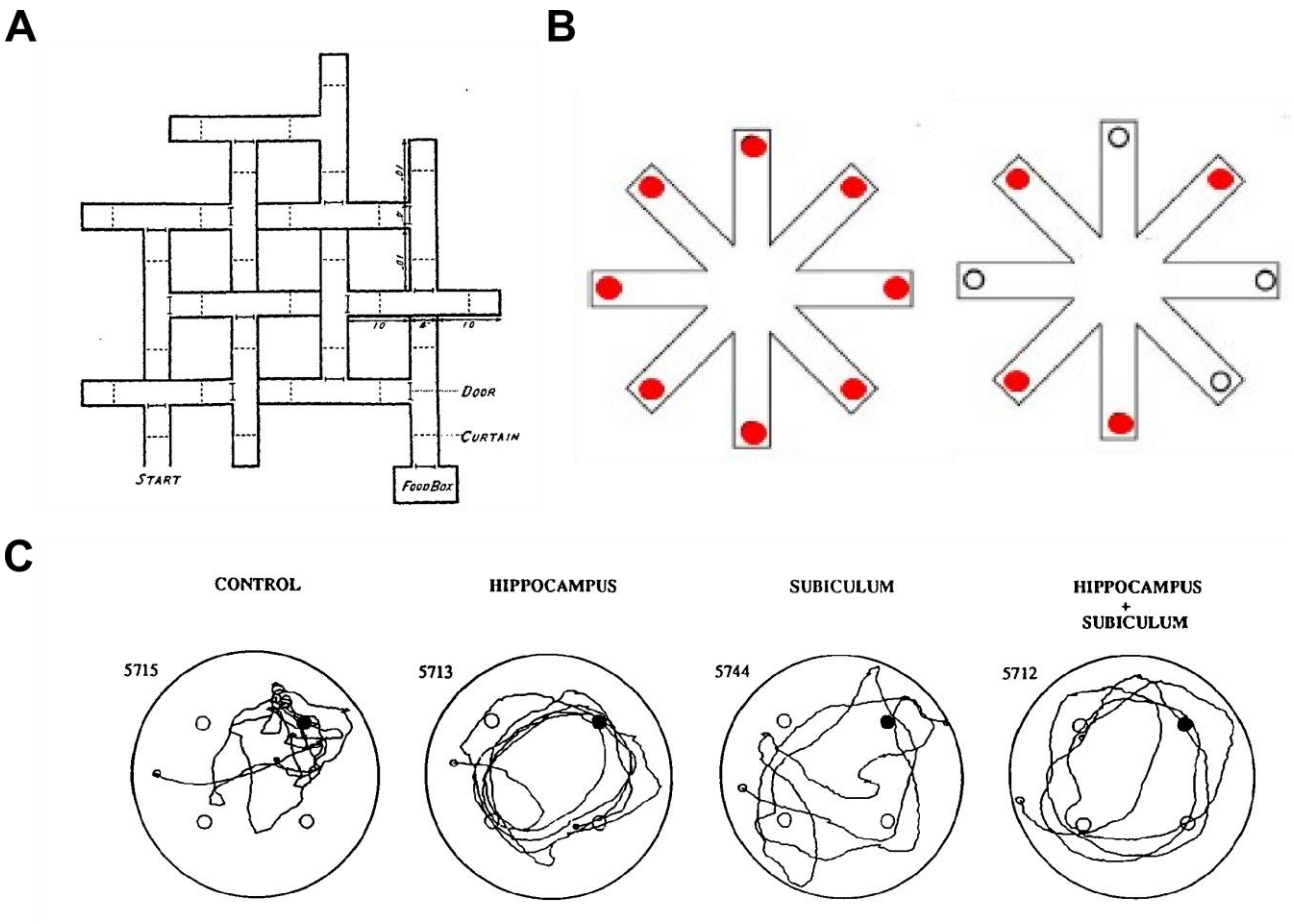

Figure 1. A variety of spatial memory tasks can be implemented to study spatial memory in rodents. *(A) Example layout of one of the mazes used by Tolman (1948) to test the ability of rats to learn routes to goal locations. (B) Example of radial-arm maze (RAM) tasks. Left: all-arms baited version, where the animals, starting from the central chamber, must enter each of the 8 arms to collect all rewards and conclude the trial. This type of task is usually used to assess spatial working memory. Right: more complex version of the task, where animals only have to find 4 goal locations. Entering a non-baited arm is considered a "reference memory error". Figure taken from Palombi and colleagues (2022). (C) Example of results of a Morris Water Maze (MWM) task, taken from Morris and colleagues (1990). In this task, animals are positioned inside a circular environment filled with opaque water and have to find their way to an elevated platform (solid black circle). In the series of experiments carried out by Morris and colleagues, lesions were performed in either the hippocampus only, subiculum only, or both hippocampus and subiculum. Compared to the control group, all three lesion groups exhibited an impaired ability to find the submerged platform, which can be seen by the more widespread locations that were explored inside the maze (the lines represent the path the animal took during a trial). This suggested an involvement of both hippocampus and subiculum in the mnemonic processing of spatial information.*

The timeline of hippocampal information processing. The lesion studies mentioned above indicate a general role of the hippocampus in spatial memory processing. However, as previously mentioned, memory processing involves three main stages (acquisition, storage, retrieval) and the studies explored so far only focus on acquisition of information. A study conducted by Riedel and colleagues (1999) fills this gap by implementing reversible inactivation of the dorsal hippocampus at different times during a modified long-term memory MWM task. In this experiment, the activity of the dorsal hippocampus was disrupted either during training (the encoding phase) or before retention (tested 16 days after training to determine any effects on the retrieval phase). The inhibition of the dorsal hippocampus in both cases resulted in impaired performances in the spatial task, suggesting the importance of this region not only for memory encoding, but also for consolidation of information, and its subsequent retrieval. It is relevant to take notice, for the aims of thesis, of the specific method implemented in this experiment. The studies described above that explored hippocampal function had done so by inducing permanent damage to the area in order to tests its function. The ability to generate a reversible inhibition is a key aspect when testing the mnemonic function. By inducing “lesions” that could only last for several hours, one can test the involvement of an area in both acquisition of information (by inducing the inhibition before the start of the task), and in long-term consolidation and retrieval of that information. This is done by inducing the inhibition during a resting period after the task, and testing the behaviour after the drug has been metabolised and the function of the area has returned to baseline. This could also benefit the use of specific techniques to record the activity of a specific area, such as electrophysiological recordings.

The hippocampus is not the only region involved in these three stages. Both cortical and subcortical structures to which the hippocampus projects to have been shown to play a role in spatial memory processing (Aggleton & Brown, 1999; Ranganath & Ritchey, 2012; Vann et al., 2009; Vann, 2010). These regions include, among others, the anterior thalamic nucleus, the retrosplenial and entorhinal cortices, as well as the mammillary bodies. They have all been implicated in both short-term acquisition and consolidation of spatial information (Sweeney-Reed et al., 2021; Vann et al., 2009; Vann & Aggleton, 2004), and they all receive hippocampal projections from the subiculum (Aggleton & Christiansen, 2015). Noticeably, two of these regions, the anterior thalamic nucleus and the mammillary bodies, exclusively receive their inputs from the subicular region in the rodent brain (see

Figure 2C). Since both the upstream and downstream areas projecting to and from the subiculum are implicated in acquisition and long-term retrieval of spatial memories, one could hypothesise that the subiculum should also be involved in both processes. Past studies, however, do not seem to fully support this notion.

The role of the subiculum in acquisition and short-term retention of spatial information has been unanimously identified through the years. For example, Morris and colleagues (1990) observed that performance following subiculum lesioning is impaired in a matching-to-place working memory task performed in the MWM (where the location of the hidden platform is re-learned every day), albeit the impact on performance is lower than when lesioning the hippocampus proper (see ***Figure 1C***). These results have been replicated in other working memory spatial tasks, such as the T-maze alternation task (Potvin et al., 2007).The results of these studies support, in part, the hypothesis formulated above, with regions of the hippocampus, regions to which the hippocampus projects to, *and* the subiculum all being involved in processing spatial information for short-term memory.

Less clear is the role of the subiculum in long-term retention, or consolidation, of spatial information. Rodent studies often utilise “reference memory” (Honig, 1978) tests to evaluate the formation of long-term memories by training animals to learn the location of goals within an environment, with recall tests at a later point (typically over the course of days or weeks). Previous work shows that the hippocampus proper is required for reference memory (e.g. Morris et al., 1982), and that the same can be said for downstream structures such as the anterior thalamic nucleus and the retrosplenial cortex (e.g. (Milczarek & Vann, 2020; Warburton & Aggleton, 1998);. When it comes to the subiculum, conclusions are harder to reach. Some studies have claimed that lesioning the subiculum during a reference memory task does not impair the animals’ performance (Galani et al., 1998; Cembrowski et al., 2018). Others have been less inclined to draw the same conclusions, showing instead an impairment in performance in the MWM task (Morris et al., 1990; Bolhius et al., 1994). One piece of evidence in support of this view comes from disconnecting the entorhinal cortex inputs to CA1 and subiculum, performed by Remondes and Schuman (2004). In this experiment, lesioning the direct entorhinal projections to the two hippocampal areas 24 hours after learning of the task resulted in an impaired ability to find the submerged platform, suggesting that this projection is required for long-term consolidation of spatial information. The suggestion that the entorhinal cortex input to the

CA1 and subiculum is required for the consolidation stage implicates a role for both regions in processing information in a long-term timescale.

A potential confound for any study of long-term spatial memory is that it is hard to separate working and reference memory deficits within an experimental paradigm. That is, any disruption in working memory reduces the ability to consistently locate goals, which could in turn prevent acquisition of a long-term memory of their location. While initially generated in the context of associative learning, the Sometimes-Opponent Processes theory of Wagner (SOP; Wagner, 1976, 1981) is a helpful theoretical framework in this situation. The SOP states that there are two independent processes that govern the memory function, a short- and a long-term one, which both contribute to the process of “habituation”. As defined by Wagner, “habituation” is the process through which there is a decline in the tendency to respond to a stimulus following a previous exposure to it, which leads animals to choose less familiar/more novel options when exploring an environment. This process is believed to drive the performance of animals when a choice is required between alternative paths (e.g. in the RAM, or the T-maze). Short-term habituation is believed to reflect priming of the memory of a stimulus (which, in maze learning, could be a specific arm path leading to a goal), with accumulation of that stimulus’ information into an “active state” with each exposure (Sanderson et al., 2010). This process depends on recency of the presented stimulus. Long-term habituation, on the other hand, happens when the stimulus is associated with its context, such as the cues present in the environment. It relies on the strength of the association between the stimulus and the context. According to the SOP theory, working and reference memory processes are competing mechanisms, as the short-term memory of a stimulus can delay its subsequent association with the context by rendering the presence of the stimulus “unsurprising”, and thus reducing the amount of attention that is paid to that stimulus (Wagner, 1981). While the “stimulus” in maze learning is less defined than in associative learning, with this theory in mind, it is conceivable that deficits in working memory may indirectly give rise to problems in encoding reference memory, given that goal locations cannot be maintained in mind while searching an environment (Sanderson et al., 2010; Schmitt et al., 2003). An animal that is unable to remember where it has just been (thus failing to recognise that location as “more familiar” than others) could then repeatedly revisit the same location, which in turn would influence the ability of the animal to find specific goal locations.

One possible solution to this problem would be to assess performance after disruption of post-task consolidation, instead of during memory acquisition itself (similar to what has been done in the CA1 by Riedel, et al., 1999). In this way, the task could be performed without any influence of working memory impairment, while still testing the role of the subiculum in reference memory. Initial evidence of a possible subicular involvement in consolidation has been provided in a study by Torromino and colleagues (2019). The authors have shown that silencing projections from the ventral subiculum to the ventral striatum after learning impairs subsequent performance in a MWM task. Nonetheless, a more thorough confirmation of whether the subiculum participates in consolidation of spatial information has still not been clearly made.

Connecting rodent and human studies. The lesion studies described above have highlighted a contribution of the hippocampus in spatial memory formation, from its early acquisition stages to the recall of stored information. How do these discoveries made in the rat's brain connect to the deficits found in H.M. and other human patients?

In the rodent brain, the hippocampal system plays a crucial role developing cognitive maps. Here, place cells in the CA1 work in conjunction with spatially selective neurons in nearby hippocampal regions, such as grid cells (which exhibit firing fields arranged in an hexagonal regular pattern to map the location of the animal; Hafting et al., 2005), head-direction cells (which fire based on the orientation of the animal's gaze relative to environmental landmarks; Taube et al., 1990), and border and boundary cells (which, respectively, encode for the animal's proximity to geometric borders or environmental boundaries; Lever et al., 2009; Solstad et al., 2008). As it will be explored later in this chapter, examples of these cells can be found in the subiculum. In the human brain, this spatial hippocampal system is believed to have developed into episodic memory due to the addition of verbal and temporal inputs (Epstein et al., 2017). Using fMRI (functional Magnetic Resonance Imaging), authors have uncovered that humans engage an extended network of brain regions when performing navigational tasks, including the hippocampus along with other cortical and subcortical structures (Aguirre et al., 1996; Ghaem et al., 1997; Maguire et al., 1998). Additionally, intracranial electrophysiological recordings performed in the hippocampal system of epileptic patients undergoing surgery have

revealed the presence of cells with similar coding schemes to those seen in the rat. These include place and grid-like cells, along with view cells (which encode the direction of a person's gaze) and cells with mixed selectivity. This supports the notion that the human hippocampus processes both spatial (similarly to rodents) and non-spatial inputs to formulate episodic memories (Ekstrom et al., 2003; Jacobs et al., 2013).

Lesion studies, electrophysiology, and scans of the healthy brain have all suggested a primary role of the hippocampal system in navigation and episodic (and spatial) memory. The first chapter of this thesis will focus on testing the role of the subiculum in long-term spatial memory (reference memory) in rats performing a behavioural task. The aim will be to silence the activity of the dorsal subiculum, which has been associated with spatial information processing (as it will be explored in depth below), using a specific drug that will temporarily inactivate the area at defined times of the behavioural paradigm. The action of this drug, muscimol, is often referred to as a "temporary lesion", and the drug itself has been used in many studies to temporarily inactivate the hippocampus (e.g. Jarrard, 1993). Muscimol is a psychotropic drug originally identified in extracts of the mushroom *Amanita muscaria*, and it is a potent $GABA_A$ agonist (Johnston, 2014). That is, application of muscimol increases inhibition and suppresses excitatory cells firing. In *Chapter 2* of this thesis, this will allow testing the involvement of the dorsal subiculum at different timepoints, while also granting retention of the normal functions of the area after the drug has been metabolised.

While lesion studies and behavioural tasks can help shine a light on the function of the hippocampal formation in spatial information processing, investigating the properties of neuronal populations can provide further insight into the behavioural functions of this area, as happened with the discovery of place cells in the CA1 (O'Keefe et al., 1971). In the following sections, the current knowledge of the spatial coding within the hippocampal system will be outlined, along with how information is transmitted to the rest of the brain, as well as what information reaches the neurons in the subiculum through efferent input.

The organization of the hippocampal system

The terminology to define the hippocampus and nearby areas can vary from author to author. For simplicity, this thesis will refer to the "hippocampal formation" as the group of cortical areas of the medial temporal lobe which includes the entorhinal cortex (EC), dentate gyrus (DG), hippocampus proper (comprising of the cornu ammonis subfields, CA1-4), presubiculum, parasubiculum, and subiculum proper, along with the postsubiculum in the rodent brain (Witter et al., 1989). While other authors have regarded the subiculum as part of the hippocampus proper (e.g. Aggleton, 2012), we will refer to them as two distinct parts of the hippocampal formation. Thus, when referring to the hippocampus, we are referring to only a part of the hippocampal system, the "hippocampus proper", which is only one of the regions in the temporal lobe area that have shown involvement in episodic memory processing.

Historically, information has been believed to flow in the hippocampal formation through the so called "hippocampal trisynaptic circuit" (see ***Figure2A, bottom row***). Sensory information coming from neocortical areas can be fed into the EC, which then projects to the DG through the "perforant pathway". From there, processed information can be transmitted to the hippocampus proper, specifically first to the CA3, then to the CA1 through the "Shaffer collateral pathway" (Amaral, et al., 1989). Regions in this area also communicate with each other through a variety of alternative connections that diverge from this canonical circuit (***Figure 2B***). The CA2, for example, receives inputs from both the CA3 and the EC (Chevaleyre & Siegelbaum, 2010; Hitti & Siegelbaum, 2014), which then projects to the CA1 (Hitti & Siegelbaum, 2014). The CA1, on the other hand, has been shown to send the majority of its projections to the subiculum (Amaral, 1993; Amaral & Witter, 1989; Naber et al., 2001). Moreover, both the CA1 and subiculum receive direct projections from the EC (the "temporoammonic pathway"; Lorente de Nó, 1934; Witter et al., 1988). Both of these regions can then also send projections back to the EC (Naber et al., 2001; Witter, 1986). Other backwards projections have been found from the CA3 to the DG (Li et al., 1994; Scharfman, 2007), and from the subiculum to the CA1 (Berger et al., 1980; X. Xu et al., 2016).

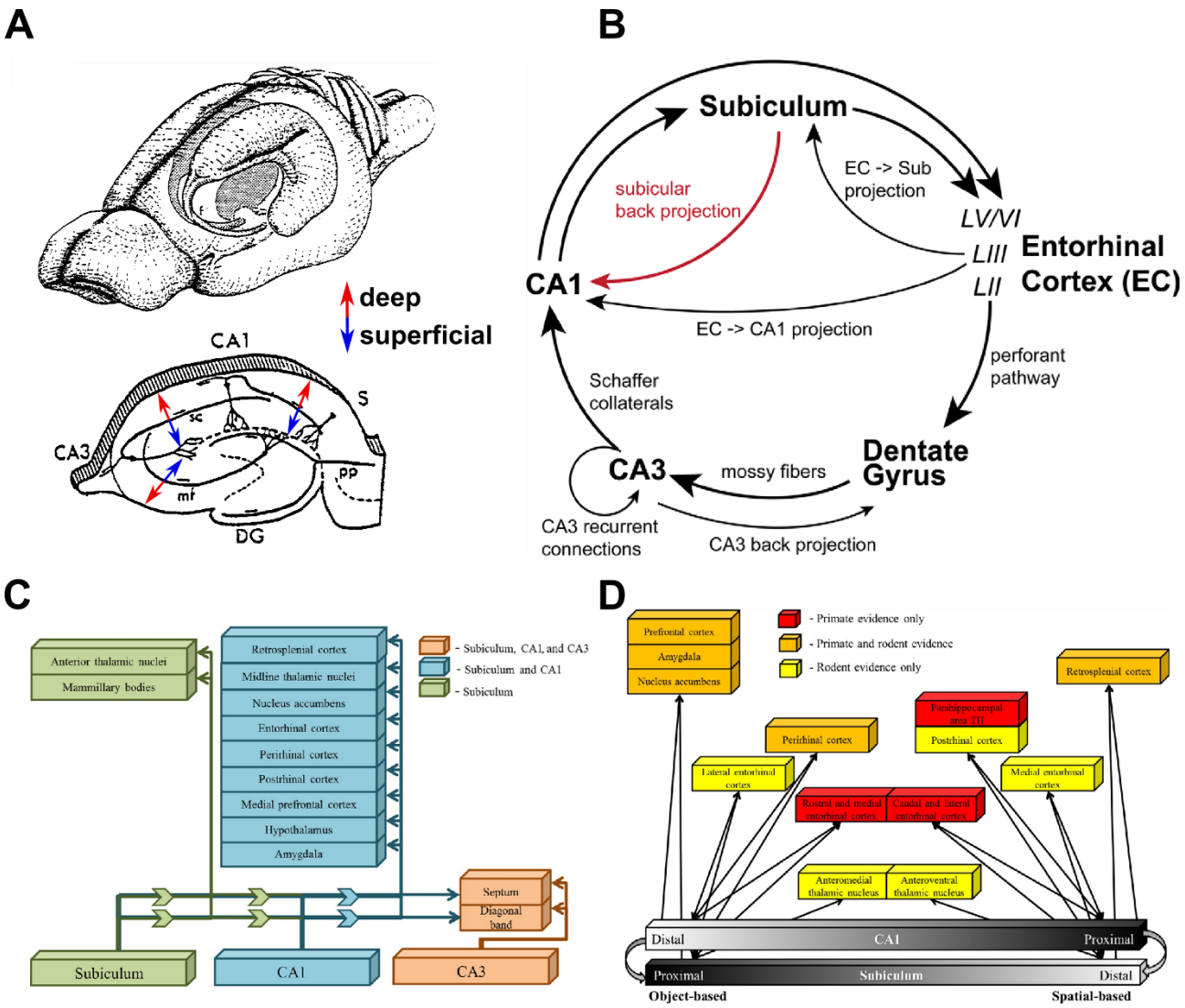

Figure 2. Distribution of connections within the hippocampal formation. *(A) Drawing depicting the location and size of the hippocampus in the rodent (top) and the subdivision in dentate gyrus, CA subfields and subiculum (DG, CA1 and 3, S; bottom). Bottom image also shows example projections of the so called "hippocampal trisynaptic circuit", from DG to CA3 to CA1. Coloured arrows represent the conventional nomenclature of different layers along the hippocampal cortex. (B) Circuit diagram of the canonical and noncanonical connections within the hippocampal formation. The canonical feedforward and unidirectional projections are depicted as black lines with large directional arrows. (C) Diagram depicting the projections in the rat from subiculum only (green), subiculum + CA1 (blue) and subiculum + CA1 + CA3. (D) Diagram of the specific connections of CA1 and subiculum with other brain areas, specifying whether the connections is with the proximal or distal portions. All projects are reciprocal, except those to the restrosplenial and prefrontal cortices. Red represents projections only present in the primate brain, orange in primates and rodents, and yellow in rodents only. (A) is adapted from O'Mara (2005); (B) taken from Xu and colleagues (2016); and (C-D) taken from Aggleton and Christiansen (2015).*

Of particular interest to this thesis is the communication from the CA1 to the subiculum, and then to the rest of the brain. As outlined above, the majority of projections coming from the CA1 reach the rest of the brain via the subiculum, marking this area the “last station” in this hippocampal circuit. With this notion in mind, looking at what is processed in upstream areas can help in better understanding what information reaches the subiculum before being sent to extrahippocampal areas.

The flow of information from the EC to the CA regions. The EC, first main step of the hippocampal circuit, is organised from a cytoarchitectonic point of view into two subregions, the lateral (LEC) and the medial (MEC) entorhinal cortices (Steward, 1976). These two subregions receive and process inputs from sensory cortices (Kerr et al., 2007). The LEC is believed to relay to the hippocampus information on the “what”, by encoding for objects and environmental context. Neurons in this area have been found to respond to specific odours (Young et al., 1997), objects (Deshmukh & Knierim, 2011), or the location of previously encountered objects (Tsao et al., 2013). Additionally, a recent study has found that individual cells in the LEC code for temporal information (Tsao et al., 2018), linking this area to one of the two core dimensions of episodic memory. The LEC relays its processed information to both the DG and the distal CA1 area. The MEC, on the other hand, relays information on the “where” to the DG and the proximal hippocampus (Steward, 1976). It contains neurons that fire in a regular, grid-like pattern of locations, and have thus been referred to as “grid cells” (***Figure 3, top***). These cells are believed to support the coding for metric distances (Hafting et al., 2005), and the MEC has for this reason been implicated in path integration and navigation (McNaughton et al., 2006). Other spatial-related cells that are found in this area are head direction cells and boundary/border cells (Sargolini et al., 2006; Savelli et al., 2008; Solstad et al., 2008). However, emerging evidence suggests that at least grid cells play a role beyond navigation. Indeed, grid cells partially remap to represent goal locations and become less “grid-like” when animals learn to locate them (Boccara et al., 2019). At the same time, these cells may participate in working memory processes by encoding future choice and trial information during a forced choice task on the T-maze (O’Neill et al., 2017). Finally, grid cells are believed to work in conjunction with place cells in the CA regions to form the

basis for a quantitative spatiotemporal representation of experiences (reviewed by Moser et al., 2008).

These two information streams from the EC (MEC and LEC) are believed to convey contextual information to the hippocampus to support the encoding of objects and events in a spatial context. Interestingly, while projecting to the DG and CA subfields, both LEC and MEC have also been found to have direct connections with the subiculum. The topographical organization of these projections correlates with the EC inputs to the CA1, where the LEC projects to the proximal part of the subiculum, while the MEC projects to its distal area (Tamamaki & Nojyo, 1995). The subiculum thus receives EC inputs (both spatial and non-spatial) from both a direct and an indirect (going through the DG and CA before reaching the subiculum) pathways (see ***Figure 2D***).

Through the indirect pathway, spatial information leaving the EC is canonically processed by the DG. This region has been hypothesised to be implicated in spatial pattern separation, for example by facilitating spatial discrimination of objects based on their distance from each other (Gilbert et al., 2001). It has also been implicated in separation of emotionally salient contexts (McHugh et al., 2007). This and similar evidence suggests a role of the DG in separating memories (reviewed by Aimone et al., 2011) before they reach more downstream regions. Indeed, like the CA1, granule cells in the DG are also thought to show spatial selectivity, although their rate maps are often multipeaked with multiple place fields (Jung & McNaughton, 1993). These neurons are exquisitely sensitive to small changes in the environment, consistent with a role in disambiguating similar spatial information (Leutgeb et al., 2007).

From the DG, information reaches the most highly studied part of the hippocampus proper, composed of subfields CA1-4. This region is organised in a laminar fashion, with a deep layer comprising of efferent fibres coming from the DG (*stratum alveolus*), a following layer made up of inhibitory basket cells (*stratum oriens)*, an intermediate layer made up of the soma of pyramidal cells (*stratum pyramidale*), and more superficial layers containing apical dendrites of pyramidal cells and inhibitory neurons (*stratum radiatum*, and *stratum lacunosum-moleculare* in the CA3; Mercer & Thomson, 2017). Of note, because of the distinct “C” shape of the hippocampal cortex (which wraps around the DG), the definition of “deep” and “superficial” layers of the various areas of the hippocampal formation is

sometimes counterintuitive. Superficial layers of the hippocampus are considered those closer the DG, while deep layers are furthest away from it. This means that in the CA1, which is positioned above the DG on the dorso-ventral axis, deeper layers are considered closer to the brain surface, while superficial layers are more ventrally located (see ***Figure 2A, bottom***). The same conventional names are kept for the subiculum layers as well (e.g. Amaral et al., 1991; Cembrowski et al., 2018; Kitanishi et al., 2021). This thesis will preserve the nomenclature used by previous authors when discussing laminar positions along the radial axis.

Mossy fibres of the DG preferentially target the area closest to the border, the CA3. Here, neurons are densely interconnected to propagate coherent populations synchronies such as theta and sharp-waves (Buzsáki et al., 1983), which have specific roles in memory processing (*discussed below*). Like in the CA1, CA3 neurons have shown to possess place fields, that is, they prevalently fire in high-frequency bursts inside restricted regions of the environment, while remaining relatively inactive in other areas (O'Keefe, et al., 1971). Like the DG, CA3 place cells exhibit the ability to change the position of their place fields in space, as well as changing their firing rate, when changes in the environment are introduced (a phenomenon called "remapping"; Leutgeb et al., 2005; Muller et al., 1991). This remapping phenomenon is a feature of neurons throughout the hippocampal formation, meaning that groups of neurons in these structures can collectively provide a unique map for each environment, as well as features within it (as discussed below). The CA3 sends few projections to the subiculum, but instead projects within the hippocampal circuit, principally to itself (Amaral et al., 1990; Amaral & Witter, 1989) and to another main subregion of the cornu ammonis, the CA1 (Ishizuka et al., 1990; Swanson et al., 1978). This recurrent architecture has inspired models of CA3 function that suggest it may act as an auto-associative network that plays a role in "pattern completion" (McNaughton & Morris, 1987). This process is the inverse operation of pattern separation, where CA3 neurons can recover a complete memory trace from partial or noisy cues. Pattern separation in the DG, which disambiguates spatial information with overlapping features, can, according to some, drive the CA3 to provide a recall of previously stored information (Rolls, 2013). The output of these computations then drives CA1 representations, the next step in the tri-synaptic pathway.

The CA1: central hub for spatial information processing. As the first area in which place fields were discovered, the CA1 has received significant attention. This region receives inputs from the CA3 Schaffer collateral pathway and preferentially sends its projections to the subiculum (Witter et al., 1989). It is widely recognised as the main subicular input region, with the EC being a close second (Amaral, 1993; Witter, 1993). CA1 functions can be subdivided along three main axes. First, a longitudinal axis, which spans along the dorsal-to-ventral regions in the rodent (posterior-to-anterior axis in the primate; Strange et al., 2014). Then, a transverse axis (proximal-to-distal, with the proximal region being the one closest to the CA3, and the distal CA1 being the region closest to the subiculum; reviewed by Igarashi et al., 2014). Lastly, a radial axis, or superficial-to-deep (reviewed by Soltesz & Losonczy, 2018). These subdivisions have shown differences in processing of spatial information and, thus, reflect different pathways of information flow into the subiculum.

The dorsal part of the CA1 is believed to mediate cognitive functions (in particular, spatial memory), while the ventral area is involved in processes such as emotional responses (Fanselow & Dong, 2010). This reflects a similar organization in the subiculum (with dorsal subiculum involved in spatial processing, and ventral in the stress-response system; see O'Mara et al., 2009). Additionally, there seems to be some level of anatomical arrangement that links subsets of CA1 neurons to different portions of the subiculum (Gigg, 2006).

Within the dorsal portion of the CA1 area, spatial selectivity varies as a function of transverse, or proximo-distal, location. CA1 neurons proximal to the CA3 have high spatial selectivity, enabling the region to distinguish between environments. On the other hand, neurons in the distal portion (closest to the subiculum), show more diffuse and multipeaked fields that presumably carry less spatial information (Henriksen et al., 2010). Moreover, distal CA1 neuronal firing are more likely to be influenced by nonspatial environmental features, such as odours, colours and shapes (e.g. Burke et al., 2011). Noticeably, this functional distinction along the transverse axis reflects the type of inputs received from the MEC (to proximal CA1) and the LEC (to distal CA1), described above (***Figure 2D***). Projections from the CA1 to the subiculum maintain this topographical organization, with the proximal CA1 prevalently projecting to the distal subiculum, and the distal CA1 to the proximal subiculum (Amaral et al., 1991).

One last subdivision of function has been recently highlighted along the radial axis, where deep and superficial pyramidal cells contribute to parallel and distinct processing of spatial information. For example, superficial CA1 cells seem to form more stable spatial maps than cells deeper in the layer, while neurons in the latter area seem to represent more dynamic features, for example by firing more at goal locations (Danielson et al., 2016).

Compared to the CA3, the CA1 contains smaller cell bodies, which are organised in an almost exclusively feed-forward network with little-to-no intrinsic excitatory connections (Amaral & Witter, 1989). These cells bodies predominantly belong to pyramidal excitatory cells, with only a small portion of interneurons (~10-15%, see Bezaire & Soltesz, 2013). Neurons in the CA1 have been classified as inhibitory or excitatory by a fixed set of parameters (see Csicsvari et al., 1999), which will be explored fully in *Chapter* 3 of this thesis. Excitatory neurons in the CA1 tend to carry spatial information by preferentially firing in specific locations of an environment (their place fields) while inhibitory neurons tend to present more widespread firing patterns. Different interneurons have been identified in this region based in their firing characteristics (Csicsvari et al., 1999; Somogyi & Klausberger, 2005), but their distinction goes beyond the focus of this thesis, since they are believed to mainly contribute to the regulation of excitation of pyramidal cells, as well as contributing to the modulation of population synchronies (e.g. Buzsáki & Chrobak, 1995).

Excitatory neurons in the CA1 generally show a tendency to be spatially selective (***Figure 3, top***). The number of spikes generated by a cell encodes information about the rat's position, to the point where just observing the rate output of 50 (or fewer) simultaneously recorded place cells allows the estimation of the position of the animal in an environment (Brown et al., 1998; Wilson & McNaughton, 1993). These CA1 neurons exhibit specific features that have been attributed to the hippocampal spatial memory function.

One of these important features lies in their ability to "remap", similar to neurons of the CA3 and DG regions. Remapping neurons change their location-specific firing (which makes up the place field of the cell, as seen above and in O'Keefe, et al., 1971) based on changes in the environment. CA1 cells have been found to expand their place fields over repeated exposures to the same environment (Mehta et al., 1997), suggesting a role in the process of updating acquired information. Additionally, they tend to remap between

different environments or different cues placed in the same environment (Muller & Kubie, 1987; Bostock et al., 1991), demonstrating an ability to discriminate between spatial representations. They have also shown to redirect their place fields to align with goal locations (e.g. Hok et al., 2007; Hollup et al., 2001; Dupret et al., 2010), which suggests a contribution to goal-directed learning. This remapping of CA1 neurons is present both in terms of spatial information, and in terms of firing rate, specifically when looking at their firing in conjunction with other pyramidal cells (their “cofiring”). Both firing and spatial properties changes in CA1 neurons suggest a defined role of this area in spatial memory processing, be it short-term (e.g. remapping between different environments) or long-term (e.g. remapping over time based on learning of goal locations).

The role of synchronised neuronal activity to memory processing. Neuronal activity in the hippocampus tends to exhibit high periods of synchronization, specifically during two phenomena: theta oscillations, and sharp-waves (Buzsáki, 2002, 2015). These local-field potential (LFP) events are generated by extracellular currents flowing inside the hippocampal formation.

The relevance of these oscillations inside the hippocampal formation has been extensively explored. Theta oscillations are one of the prominent patterns recorded in the hippocampus, with frequencies of 6-8 Hz. The generation of these synchrony patterns in the hippocampus has been attributed to two main areas, the pyramidal cell layer of the CA1 (Green et al., 1960; Petsche & Stumpf, 1960) and the outermost layer of the dentate gyrus (Winson, 1974). These two generators contribute to the propagation of theta oscillations in the hippocampal formation, and are believed to be influenced by theta activity generated in the medial septum, a region that forms connections with various cortical areas, hippocampus included (Vertes, 1982). Two types of theta oscillations have been identified, one which is prevalent in moving animals (type 1), and one that can be recorded in immobility, during periods in which the animal is preparing to move (type 2). Both of these types present a gradual shift in theta phase between the two main generators (the CA1 and the DG) but type 1 theta additionally presents a “null zone” of no visible theta along the gradual reversal, while type 2 does not exhibit the same phenomenon (Winson, 1974). The type of theta oscillations that has been most studied is

type 1, which is visible during locomotor activities, such as active exploration of an environment, while being generally absent outside of these epochs (Vanderwolf, 1969). These oscillations have been assumed to contribute to short-term memory processing by modulating the timing of spiking sequences (Dragoi & Buzsáki, 2006; Lisman & Idiart, 1995; Raghavachari et al., 2001). In the CA1 in particular, neurons are phase-locked, meaning they predominantly discharge on the negative phase of a theta cycle (Buzsáki et al., 1983; Fox & Ranck, 1981; Ranck, 1973). This is different from other regions, such as the EC, in which more superficial layers show an almost complete phase reversal compared to CA1 (e.g. Mitchell & Ranck, 1980). At the same time, in the CA1, a single place cell's distribution of spikes correlates with the position of the animal inside its place field: the spiking activity of the neuron will shift to earlier phases of the theta cycle while the animal passes through the location of the cell's place field, a phenomenon called "phase precession" (O'Keefe & Recce, 1993; see ***Figure 3, bottom***). This phenomenon is hypothesised to induce long-term potentiation for learning of spatial sequences (Skaggs et al., 1996). Theta oscillations are visible over the whole hippocampal formation (Winson, 1974), including the subiculum, making it a network event that synchronises neuronal activity across the whole area. As such, theta modulation and the possible presence of phase precession are useful tools to assess the spatial mnemonic functions of a region.

Another LFP event that has shown to correlate with mnemonic processing happens during sleep (or, more generally, resting periods; Buzsáki, 2015; Buzsáki et al., 1983), as well as in brief pauses during exploration (O'Neill et al., 2006). During these behavioural epochs, sharp waves (40-120 msec duration) can be intermittently observed in the CA1, coupled with high-frequency field oscillations called Sharp Wave/Ripples (SWRs, Buzsáki et al., 1983; O'Keefe et al., 1978; O'Neill et al., 2006). SWRs have an average frequency of ~150-200 Hz and are generated locally, initiated by bursts of activity in the CA3 (Csicsvari et al., 2000; Nakashiba et al., 2009) and CA2 (Oliva et al., 2016). The CA1 region has not only been found to generate ripple oscillations, but to propagate them to its neighbouring regions (Chrobak & Buzsáki, 1996). These oscillatory events have been recorded in rats, macaques and humans (Bragin et al., 1999; Skaggs et al., 2007; Staba et al., 2002). During SWRs, population synchrony in the CA3 and CA1 is shown to increase, which has been proposed as a mechanism for the strengthening of intra-hippocampal cell assemblies representing memory traces established during behaviour (i.e. during theta oscillations; Buzsáki, 1989; see ***Figure 3, bottom***). However, SWRs are also believed to be implicated

in the process of memory consolidation, which likely includes the transfer of memory traces from the hippocampus to the neocortex (Buzsáki, 1989; Marr et al., 1991; McClelland et al., 1995).

Evidence for this idea has been mounting since it was first proposed. Previous work indicated that the firing patterns withing SWRs are not random but rather reflect previous experience. Pavlides and Winson (1989) were the first to provide data showing that activity during SWRs reflected the previous waking behaviour. They found that neurons active during extended periods of exploration would increase their firing rate during SWRs occurring in the post-exploration sleep, suggesting that the hippocampus processes spatial information during “off-line” periods. Additionally, CA1 cells with overlapping place fields have also been shown to increase their correlation, or “cofiring”, during sleep that follows a period of exploration of an environment (Wilson & McNaughton, 1994). This “reactivation” of memory traces occurs predominantly during SWR events (Kudrimoti et al., 1999; O’Neill et al., 2008), but not exclusively (McHugh et al., 2024). Such reactivation does not only reflect the “cognitive map” in the previous exploration, but also what was learnt there. Using a “cheeseboard” maze, Dupret and colleagues (2010) demonstrated that newly learnt goal locations were preferentially activated during subsequent sleep, and that the frequency of goal location reactivation predicted subsequent recall in a probe test.

Finally, activity during SWRs can not only represent context or places, but also the movement trajectories made by the animal as they explore an environment. During SWRs, cells that display a strong temporal ordering (i.e. they fire consecutively) during exploration preserve that order of firing during sleep, indicating a “replay” of firing sequences (Lee & Wilson, 2002; Skaggs & McNaughton, 1996). Experiments analysing replay typically involve an animal shuttling up and down a narrow linear track. During exploration, place cells fire in specific order, driven by spatial selectivity. During SWR events, the same sequences are replayed, but on a much faster timescale (reviewed by Buzsáki, 2015; but also see Nádasdy et al., 1999). That is, sequential place cell activation during a 1-2 second traversal of linear track can be replayed in around 100ms SWRs. This is suggestive of a mechanism that would allow the high repetition of previously acquired information over a short period of time. In turn, this can facilitate the repeated replay of multiple memory traces during sleep, in a process akin to rehearsal, that may facilitate

consolidation. However, the precise underlying network mechanisms by which this off-line rehearsal facilitate memory processing have yet to be fully elucidated.

Direct evidence that reactivation/replay is involved in off-line memory processing has been provided through interventional experiments. First, disruption of SWRs occurring during post-training sleep has been shown to impair hippocampus-dependent memory consolidation (e.g. Girardeau et al., 2009). In this experiment, animals were trained to explore a RAM, in which they had to learn the hidden locations of food rewards (located in three out of the 8 available arms). With few trials each day, the animals' tendency to proceed directly to the baited arms improved over time, a process that was slowed by SWRs disruption. More recently, Gridchyn and colleagues (2020) demonstrated that *information* encoded during reactivation is critical for consolidation, and not just SWRs per se. They first trained animals on two different reference memory tasks (performed in two different environments) in parallel and then disrupted reactivation in post-learning sleep. They used a closed loop system, that enabled disruption to be triggered by brain activity. With this system, they decoded neuronal firing patterns during sleep to identify which of the two paradigms was being reactivated, and then selectively allowed one to avoid disruption. As a result, performance during subsequent recall was greater for the reactivated environment.

Considering the above, reactivation/replay during SWRs in sleep represents a strong candidate mechanism for the offline consolidation of spatial information. Nevertheless, a critical component of systems consolidation is communication between hippocampal and cortical structures. Indeed, SWRs trigger waves of increased activity across the neocortex (Logothetis et al., 2012), and drive increased firing and ripple oscillations in multiple areas. These include the EC, retrosplenial cortex, and neocortical limbic/associational areas, as well as the subiculum (Chrobak & Buzsaki, 1994, 1996; Khodagholy et al., 2017; Nitzan et al., 2020). Moreover, reactivation or replay is likely coordinated between the hippocampus and other areas of the brain to support a system-wide consolidation (Jadhav et al., 2016; Ji & Wilson, 2007; Ólafsdóttir et al., 2016; Rothschild et al., 2017; Wilson & McNaughton, 1994). As the subiculum is the primary link between the hippocampus and the rest of the brain, one hypothesis is that this area could act as a conduit for this hippocampal-neocortex dialogue for memory consolidation. Indeed, the subiculum has been shown to play a critical role in propagating SWR network activity from the CA1 region to the

restrosplenial cortex (Nitzan et al., 2020). In turn, this implicates the subiculum as playing a necessary role in long-term memory processing, as hypothesised by this thesis.

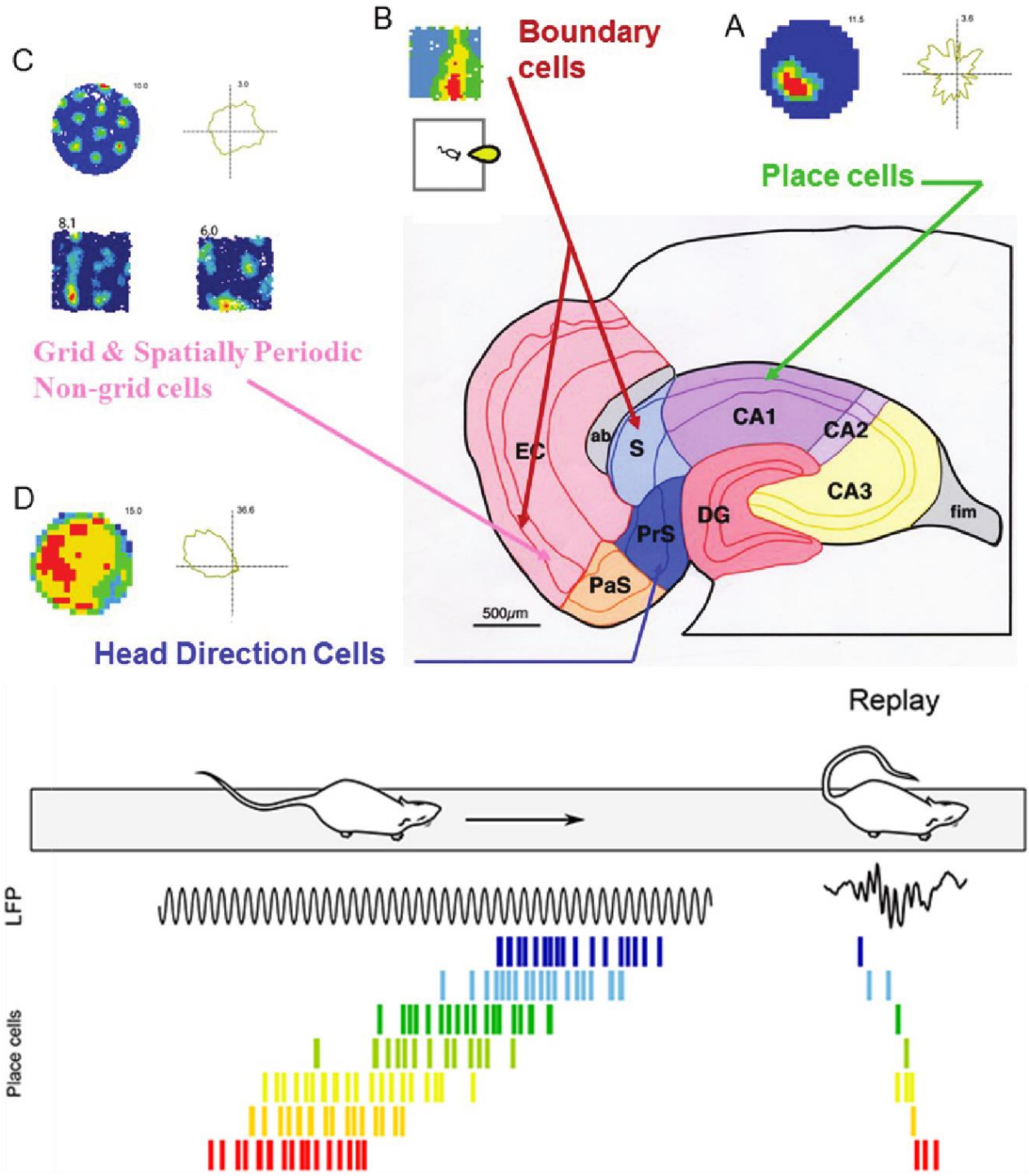

Figure 3. Cell firing profiles in the hippocampal formation. *Top: examples of different cell coding in the hippocampal formation. This includes place cells in the CA1 (A), grid cells in the EC (B), boundary cells in the subiculum (C) and head direction cells in the presubiculum (D). Bottom: Schematic of temporal coding in the hippocampus. While animals are running along a linear track (top), the LFP profile shows theta oscillations (middle). During these oscillations, place cells (bottom) fire at different locations along the track, shifting their firing relative to theta while moving forward. During rest, replay of firing sequences is carried out during periods of SWRs. Top figure*

taken from O'Keefe (2014); bottom figure taken from Drieu and Zugaro (2019). EC: entorhinal cortex; S: subiculum; PaS: parasubiculum; PrS: presubiculum; DG: dentate gyrus.

The subiculum: the overlooked part of the hippocampal formation

We have seen that spatial information is processed prevalently through the EC, then conveyed to the DG and the hippocampus proper, before reaching cortical and subcortical regions outside of the hippocampal system. The projections coming from the hippocampus proper prevalently come from the CA1, which projects out of the hippocampus either directly or, in the vast majority of cases, indirectly through the subiculum (Aggleton & Christiansen, 2015; Cenquizca & Swanson, 2007). These projections aimed at the subiculum make up the majority of CA1 projections in both rodents and primates (see above), marking this as the main route of information flow from the hippocampus to the neocortex. How is spatial information processed in this area? Moreover, spatial memory encoded in this hippocampal circuit is then broadcasted to the neocortex, at least for long-term storage and when recall is used to trigger a behavioural response. Does the subiculum contribute to this long-term memory circuit, and how? The next paragraphs will explore what is known about the subiculum in terms of spatial and mnemonic processing, and will highlight what are some key features, still unexplored, that would allow to provide answers to our questions.

Subicular projections and subdivisions. Once spatial information coming from the hippocampus reaches the subiculum, projections from this area extend towards a plethora of regions. Some projections share parallel routes with the CA1, such as the nucleus accumbens, perirhinal cortex, parahippocampal cortex, amygdala, and even back to the EC (Aggleton, 2012; Rosene & Van Hoesen, 1977). Even when an area receives projections from the CA1, it is usually accompanied by a parallel projection from the subiculum. Along with these parallel routes, other projections are almost exclusively arising from the subiculum. The targets of such projections include, in humans, the retrosplenial cortex, various thalamic nuclei, and the mammillary bodies (but only the anterior thalamic nucleus and the mammillary bodies in rodents; see Aggleton & Christiansen, 2015). As we have seen above, these downstream regions have been implicated in both short and long-term processing of spatial memories, marking the subiculum as a likely critical link in contributing to these types of mnemonic processing.

Similarly to the CA1, the subiculum can be divided using multiple criteria, and these subdivisions seem to have some specificity in terms of afferent inputs and efferent projections. On the transverse axis (as it happens in the CA1), the subiculum has been divided into proximal (the region closest to the CA1), and distal (furthest away from the CA1) subiculum. The proximal subiculum has been shown to project to the LEC, perirhinal cortex, prefrontal cortex, amygdala, and nucleus accumbens (Aggleton & Christiansen, 2015; ***Figure 2D***). This suggests a role of this subdivision in processing object-based information, similar to, for example, the LEC (see above). On the other hand, the distal subiculum projects to the MEC and the parahippocampal cortices, suggesting a role in processing spatial information. These two subdivisions have shown to present a gradient of changes in a variety of electrophysiological characteristics of their neurons (Kim & Spruston, 2012), including their firing rate and their spatial information (i.e. the locational information carried by their firing in an open field; Markus et al., 1994; Skaggs et al., 1992). In general, it seems that proximal subicular neurons show characteristics that include lower mean firing rates, fewer place fields per neuron, and less spatial information carried by each neuron. The more distal the cell is, the more these characteristics change, with neurons of the distal subiculum presenting with higher firing rates, multiple irregularly spaced place fields resembling the firing rate maps of grid cells in the EC, more extended place fields and single neurons carrying more spatial information (Cembrowski et al., 2018; Kim et al., 2012). The variability in the electrophysiological features of subicular neurons along the proximo-distal axis can make it difficult to properly characterise the cells of this area. For this reason, this thesis will focus on densely sampling cells from the middle portion of the subiculum, in order to try to restrict all possible differences found along the whole axis.

In addition to subdivisions on the transverse axis, separate areas of the subiculum have also been defined as “dorsal” and “ventral” subiculum. The ventral subiculum has been shown to project prevalently to the prefrontal cortex, amygdala, and nucleus accumbens, while the dorsal has shown to have connections with the retrosplenial cortex and the mammillary bodies (Aggleton & Christiansen, 2015). This suggests a similar division of functions along the longitudinal axis to that reported in the CA1, with the dorsal subiculum being prevalently linked with spatial information and the ventral to emotional inputs. As the main focus of this work is exploring the mnemonic functions of the subiculum in a spatial context, the electrophysiological recordings will be aimed at the dorsal part of the

subiculum. Another, less explored subdivision, identifies deeper layers of the subiculum as projecting prevalently to the anterior thalamic nucleus, while mid-layer neurons project to the mammillary bodies (Ishizuka, 2001). This laminar organization of subicular outputs may be attributed to differences in electrophysiological properties of the neurons along the radial axis, as we will explore below.

Variety of cells in the subiculum. Similarly to other regions of the hippocampus proper, the subiculum architecture can be subdivided into three main layers: a molecular layer, a pyramidal cell layer, and a polymorphic layer (O'Mara, 2005; O'Mara et al., 2001). The pyramidal layer contains the soma of subicular neurons, which are mostly large excitatory pyramidal cells (PCs). These cells are predominantly uniform in size and shape, with apical dendrites extending into the molecular layer, and basal dendrites reaching deeper areas of the pyramidal layer (Šmejda Haug, 1974). While similar in appearance, PCs have been shown to present distinct electrophysiological characteristics, resulting in two groups, based on spiking dynamics: bursting and regular-firing neurons (Stewart & Wong, 1993; Taube, 1993), although some studies have struggled with finding representatives of both groups in the area (see Kim et al., 2012). However, recent work by Cembrowski and colleagues (2018) indicates that the change from non-bursting to bursting occurs in a gradient across the proximo-distal axis. Here, regions in the central transitional portion have intermixed populations, consistent with previous report by Böhm and colleagues (2015). Using a transcriptomics approach, Cembrowski and colleagues (2018) identified separate classes of neurons, with two in the proximal area and a third in the distal. Neurons in these groups showed distinct afferent inputs and efferent targets, which broadly reflected the previous work describing the anatomy of the transverse axis (described above). To investigate the electrophysiological properties and coding schemes of these neuronal classes, one must sample along the transverse axis. Doing so requires densely sampling the region with expensive multi-shanked probes (e.g. the work done by Kitanishi et al., 2021), or by targeting different transverse regions in separate animals. Alternatively, one may target the transition region with the goal of recording from an area with heterogeneous cell populations (the approach taken in this thesis in *Chapters 3* and *4*).

Cembrowski and colleagues (2018) also identified a fourth, relatively small, group of neurons, which spanned the proximo-distal extent of the subiculum. These neurons were concentrated in the deep portion of the layer. Thus, subicular neurons can differ according to their position in the radial axis as well. Indeed, bursty and non-bursty excitatory subicular neurons have been shown to have different distributions across the radial axis in *in vitro* experiments, with busting cells mainly concentrated in the deep layer of the subiculum, and regular-firing ones found prevalently in superficial layers (Greene & Totterdell, 1997; Menendez De La Prida et al., 2003). There are *in vivo* reports of bursting and non-bursting cell types not presenting any noticeable differences in their firing properties (Sharp & Green, 1994), to the point where *in vitro* manipulations can even force them to turn from one type to the other by simply altering their membrane potential (Staff et al., 2000). However, more recent work has suggested that there *are* differences in firing properties of these cells, with bursting cells having higher global mean firing rates compared to regular-firing ones, along with presenting a deeper theta modulation (Lever et al., 2009).

Others have tried to further subdivide these two categories based on specific firing characteristics, for example whether their firing is modulated or not by theta oscillations (Sharp & Green, 1994). While it is true that there is a gradient of theta modulation across the transverse axis (with distal neurons more strongly modulated by theta than proximal cells; Kim et al., 2012), the vast majority of subicular (and hippocampal) neurons present firing rates modulated by theta oscillations, with very few showing no theta modulation at all (see Anderson & O'Mara, 2003). However, Kitanishi and colleagues (2021) identified three subgroups of excitatory neurons, based on their theta preference, located in the proximal, superficial-distal and deep-distal subiculum.

Along with excitatory PCs, the subiculum contains a number of inhibitory neurons which somas are positioned inside either of the three layers. These interneurons have similar discharge characteristics to the ones found in other regions of the hippocampus proper, and have been classified by O'Mara (2005) as "fast-spiking units" (to distinguish them from the other classes of excitatory neurons). Interneurons in the CA1 region (and indeed cortex) have been shown to be hugely diverse in terms of morphology, expression of receptors, and firing properties (reviewed by Somogyi & Klausberger, 2005). Together, these give rise to the diverse network functions underlying cognition. The subiculum also

shows a similar complex mix of these cell types. Indeed, Cembrowski and colleagues (2018) showed that, like the excitatory population, a subset of interneurons (expressing Neuropeptide Y) also varied as a function of proximo-distal location. However, other histological markers for interneurons commonly found in the CA1 were evenly distributed across the transverse axis. Thus, both excitatory cells and interneurons in the subiculum form diverse populations, expressing different proteins and exhibiting a range of firing properties. These include theta phase preference or modulation depth, bursting probability, and mean firing rates. This may increase the difficulties in separating interneurons and excitatory PCs from extracellular features alone. Indeed, it is worth noting that, while in the CA1 region a clear distinction between inhibitory and excitatory cells can be made solely based on their firing rate (see Csicsvari et al., 1999), that is not always the case for other brain areas, where firing rate alone does not result in two distinct clusters of neurons (e.g. Barthó et al., 2004; but also see Kitanishi et al., 2021 for subicular neurons). A classification based on extracellular features of recorded neurons will be carried out in *Chapter 3* of this thesis.

Overall, excitatory neurons seem to fall into two classes, bursty and non-bursty neurons, which occur in distal and proximal areas, respectively. However, recent transcriptomic/anatomical studies, along with electrophysiological characterisation, imply that the picture is more complicated. A critical question is how these cell-types contribute to mnemonic functions. Indeed, Cembrowski and colleagues (2018) showed that selectively inhibiting distal neurons in the subiculum disrupted spatial working memory, while inhibiting proximal cells had no effect on performance. In addition to intervention studies, previous work decoding the firing patterns of these neurons can provide an indication of their role in spatial processing.

Spatial properties of subicular neurons. According to the neuroanatomy of the hippocampal formation, spatial information is conveyed from the EC (specifically, its medial subdivision), into the DG, and then into the hippocampus proper, where it then reaches the subiculum. In addition, direct projections (from layer II of the MEC) convey grid, head direction, and border information directly to the CA1 and subiculum. As we have

seen above, most of the spatial information that reaches this area is integrated in the dorsal subiculum. How is this information expressed as spatial firing patterns?

Similar to the place cells that have been found in other areas of the hippocampus proper, subicular neurons have shown to exhibit a tendency in increasing their firing when the animal enters specific locations of an environment. These subicular place cells, different from those found in CA3 and CA1, tend to show multiple peaks of activity (Sharp & Green, 1994), and were first thought to have a rather low spatial specificity compared to their CA1 counterparts (Barnes et al., 1990). Initial reports also showed how these neurons tend not to remap across environments (Sharp, 1997; Sharp, 2006) and had a noisier representation of space compared to CA1 cells, while still being less noisy than EC cells (Muller et al., 1991). While it is true that subicular neurons tend to fire over larger portions of the environment, their higher mean and peak firing rates compared to CA1 cells allows them to convey a comparable (Kitanishi et al., 2021) or even greater amount of spatial information (Kim et al., 2012). This phenomenon seems to be possible due to a positive correlation between firing rate and spatial information, where subicular neurons have a comparatively lower per-spike information content, but due to the high firing rate have a higher *per-second* information content compared to CA1 cells (Kim et al., 2012; Kitanishi et al., 2021). When looking at the area's remapping ability, once again a more updated view is that, while there is a high degree of variability, subicular neurons demonstrate both firing rate and place field remapping (Kim et al., 2012). Additionally, like in the CA1, place fields of subicular neurons expand when the animal is placed in a similar, but bigger environment, to fit the size of the arena (Sharp, 1999), and most exhibit changes to their firing field(s) when a barrier is placed inside the environment, as highlighted by Poulter and colleagues in 2021 (a characteristic that was initially reported to not be present in subicular cells; see Sharp, 1999). Subicular neurons also seem to encode for speed, similarly to CA1 cells (McNaughton et al., 1983), and have shown to be more resistant to noise in both place and speed coding (Kitanishi et al., 2021).

The differences in encoding properties between the subiculum and the CA1 suggest that the subicular representation of space is not simply a result of multiple hippocampal inputs. To support this theory, while both CA1 and the subiculum have been reported to have spatially selective cells (Kitanishi et al., 2021), other classes of cells have been identified in the subiculum. Head-direction cells, for example, were first identified in the presubiculum

(which borders with the distal portion of the subiculum; see ***Figure 3, top***; Taube et al., 1990). In the subiculum proper, Muller and colleagues (1991) recorded head-direction cells that behave in a similar fashion to those in the presubiculum, firing in specific angular positions based on a cue card located on the wall of a cylindrical environment. According to a report by Kitanishi and colleagues (2021), there is a higher proportion of head direction cells in the subiculum than in the CA1. Other cells identified by Muller and colleagues (1991) present mixed characteristics between head direction cells and place cells, with their firing reflecting the position of the animal while also being modulated by two preferred head orientations (similar, but not identical to head direction-only cells, which have one preferred orientation; Taube et al., 1990). These cells have been later defined as axis-tuning cells by Olson and colleagues (2017). Axis-tuning cells can be detected in the context of route-running along a track but tend to not fire when an animal is foraging in an open arena (which is another characteristic that distinguishes them from head-direction cells). They are believed to fire in complete independence from environmental locations or visual cues (to the point where they are firing even when the animal is carrying out the task in darkness), and to use the environmental boundaries as their spatial frame of reference. In addition to these three classes (head-direction, axis-tuning, and place cell), other types of cells have been recognised among subicular neurons, such as grid-like and barrier-related cells (Brotons-Mas et al., 2017), boundary vector cells (BVCs; Lever et al., 2009) and vector-trace cells (VTCs; Poulter et al., 2021)

BVCs were first hypothesised to fire when an environmental boundary intersects the receptive field of the cell at a specific distance from the animal (Hartley et al., 2000). This firing would depend only on the location of the animal in relation to the environmental boundary, independent of the heading direction, resulting in broader firing fields when the peak of the receptive field was farther away from the animal (Barry & Burgess, 2007). Initially only theorised, BVCs have now been found in the dorsal subiculum of rats foraging in an open field (Lever et al., 2009). These cells fire along environmental boundaries, whether they are solid walls, sheer drops, or low ridges followed by a drop. Their firing fields tend to reflect the curvature of the boundary, and are independent of colour, shape, material of the walls or distal cues, to the point where they are clearly present even when the animal is running in darkness. Moreover, if a second barrier is inserted in the environment, the firing fields of BVCs tend to split and double to encode for both boundaries. These cells can be found in both proximal and distal subiculum, and they

appear to be both bursting and regular-firing pyramidal cells. Lever and colleagues (2009) estimated that ~24% of neurons in the dorsal subiculum can be classified as BVCs.

Another vector-based class of cells has been discovered recently, called vector-trace cells (VTCs). These cells also fire when the animal is at specific distances from environmental boundaries, but they additionally fire when a small or extended cue (acting as a “barrier”) is present. Moreover, their firing is bound by allocentric direction, differently from BVCs (Poulter et al., 2021). These cells also split their firing fields when a new barrier is introduced, but the second field (“vector field”) persists even after the cue is subsequently removed, creating a “vector trace field”. The implications of this characteristic in mnemonic processing will be explored in more details in the next paragraph.

How do these different types of subicular cells contribute to the general function of the area? One theory is that they all contribute to path integration, by constantly updating the position of the animal in relation to both egocentric (head-direction) and allocentric (place cells, grid cells, and BVCs) cues. According to this theory, the EC and the subiculum would then represent space as a universal map that can be implemented across different environments in helping the CA3 and CA1 generate a finer representation of a singular environment (Sharp, 1999). Some of these cell types have been identified in other regions, both in the hippocampal formation (grid cells, border cells, and putative boundary cells in the EC; Hafting et al., 2005; Savelli et al., 2008; Solstad et al., 2008), and in regions to which the subiculum projects to (e.g. head-direction cells in the anterior thalamic nucleus, Taube, 1995), which suggests a complementary role of subicular neurons and neurons in connected regions in processing spatial information.

Memory processing in subicular neurons. While some notion of a role of subicular neurons in spatial information processing has been uncovered over the years, less is known about their features during memory tasks. We have seen that place cells in the CA1 can re-orient their place fields (place remapping) to overlap with goal locations, suggesting a role of this region in acquiring and retaining spatial information across time. While place remapping has been explored in recordings of the subiculum (e.g. Kim et al., 2012), these studies have focused on remapping across different environments and cues, normally in the span

of a single day of recording, and no experiment to this date has analysed the remapping properties of subicular neurons during learning of goal locations.

There are two main pieces of evidence, at the time when this thesis is written, that suggest how at least some subicular neurons can process mnemonic information about the environment. The first evidence comes from the presence of phase procession, a phenomenon in which neurons shift their spiking activity to earlier phases of the theta cycle when passing through the place field of the cell (see above). This phenomenon was first identified in the CA1 region but has now also been recently demonstrated to happen in the subiculum (Kim et al., 2012). Neurons that exhibit phase precession are present along the whole proximo-distal axis of the subiculum and tend to have place fields centred around the trough of theta. While theta precession is equally present along the transverse axis, subicular neurons are differently distributed along based on their phase preference (i.e. tendency to fire at specific phases of the theta oscillation, see above). Distal neurons that are deep in the layer seem to fire at earlier phases of the theta cycle (around 285 degrees, with zero centred around the trough), while distal but more superficial cells fire later (~ 321 degrees), and proximal cells even later in the theta cycle (~9 degrees; Kitanishi et al., 2021). No study to our knowledge has explored possible differences in theta precession along the radial axis. In any case, the presence of theta precession, as for the CA1, suggests a role of subicular cells in storage and on-line retrieval of spatial information, at least in the short-term. This confirms a role of the subiculum in short-term retention of information, similar to what has been suggested by behavioural studies carried out in this area (e.g. Morris et al., 1990; Potvin et al., 2007).

The second evidence of mnemonic processing in the subiculum comes from the discovery of the aforementioned VTCs (Poulter et al., 2021). These cells respond to the introduction of a new cue in the environment by generating a new firing field (the cue field), which is maintained even when the cue is subsequently removed from the environment. Firing in the cue fields of these neurons can last for several hours (Poulter and colleagues tested it to up to 3 hours) and could be considered a first indication that there are “memory traces” in subicular neurons for (relatively) long-term retrieval of spatial information. Interestingly, VTCs seem to be more present in the distal subiculum than in the proximal (63% of the recoded distal cells, versus only 5% in the proximal). Distal VTCs also seem to fire at earlier phases of theta, similarly to what has been reported for other distal non-VT cells.

While both VTCs and other subicular neurons fire at similar phases during placement of the new cue (encoding phase), a difference between these two populations appears during the retrieval of information (happening once the cue has been removed from the environment). During this retrieval period, theta preference shifts to later phases for both neuronal types, but these changes appear to be bigger for VTCs (~50-60 degrees), suggesting a role of theta modulation in encoding for memory traces in the subiculum.

Theta precession and the presence of VTCs suggest how subicular cells can carry mnemonic information, at least for relatively short periods of time. This goes in accordance with what has been demonstrated in behavioural studies, where the subiculum has been implicated in the correct function of short-term spatial memory (see earlier in the chapter). Less is known about the characteristics of subicular cells that would implicate them in long-term memory and consolidation of spatial information. In the CA1, we have seen the phenomenon of reactivation of specific firing sequences during SWRs, which is believed to contribute to the consolidation of spatial information during periods of resting following a task (see above). In the subiculum, network activity has been implicated in the generation and propagation of SWRs (Imbrosci et al., 2021). SWRs have been found across the whole subiculum, but there seems to be possible differences on cells firing based on location. In a recent study by Kitanishi and colleagues (2021), for example, some neurons in the deep layer of the distal subiculum showed suppression of their firing rate during ripple activity, as opposed to the usual increase in firing found for CA1 and other subicular neurons. What the presence of these neurons means in the context of subicular network activity during rest has yet to be determined.

While electrophysiological studies have further explored the characteristics of subicular cells pre- and post-learning, the presence of these synchronous events in the area (which have been implicated in system-wide consolidation) and the discovery made by Kitanishi and colleagues (2021), suggest two critical points for this thesis: (1) that there might be more to the subicular function than just acquisition of information to be stored in a short period of time; and (2) that the contribution of subicular neurons during these events goes beyond a simple relaying of information from CA1 neurons.

Aims of this thesis

In the introduction to this thesis, we have explored the link between the hippocampus and episodic memory. In doing so, we have highlighted one area of the hippocampal formation, the subiculum, which constitutes the main output region of the hippocampus.

Behavioural studies focusing on this area have highlighted its the contribution to short-term spatial memory, but no consensus has been reached so far on its involvement in long-term spatial memory. Despite this, both regions projecting to the subiculum, and regions to which the subiculum projects to, have been implicated in both forms of spatial memory, marking the subiculum as a prime candidate in taking part in both processes. While behavioural studies can be a useful tool to pinpoint the contributions of a specific area to a behavioural output, looking at the electrophysiological characteristics of the neurons in the area can aid greatly in creating a better understanding of its function. With this in mind, the aims of the subsequent three experimental chapters are as follows:

(1) To test the role of the subiculum in long-term spatial memory, otherwise referred to as “reference memory”, in rats performing a behavioural task. The hypothesis is that silencing the subiculum will not only impact the acquisition stage of the task, impairing the animal’s performance in the short-term, but will also impact the consolidation of acquired spatial information, by impairing the ability of the animals to remember goal locations across days.
(2) To develop a method that will allow to track the neural activity of subicular cells across multiple days with electrophysiology, while also exploring the spatial characteristics of the recorded subicular neurons. While tracking of subicular cells across consecutive days has been previously performed with calcium imaging (see Sun et al., 2019), a report that allows the high resolution of results that comes with electrophysiological recordings has not yet been attempted.
(3) To explore the role of subicular neurons in spatial memory and learning, specifically the potential contributions of its neurons into spatial processing, both during learning and during post-task consolidation of information. To do so, different cell types will be characterised based on their theta preference, as well as firing and spatial features, in both a learning and a non-learning context. The hypothesis that memory-related phenomena such as rate remapping and reactivation will be

present in the subicular network will be tested, which may support the involvement of this area in long-term consolidation of spatial information.

Chapter 2 – Subicular inhibition during a long-term spatial memory task

Introduction

Given the central importance of the hippocampus in spatial memory that we have seen in the *General Introduction*, and that the subiculum represents its principal output region, one would expect that the latter region would play a similar role as its hippocampal input regions in spatial memory. Nonetheless, previous studies have struggled to make a connection between the subiculum and long-term spatial memory ("reference memory") in rodent studies. Some have suggested a link between this area and reference memory (see for example Bolhius et al., 1994; Morris et al., 1990), while others have not drawn the same conclusions (Cembrowski et al., 2018; Galani et al., 1998).

This chapter aims at shedding light into the involvement of the subiculum in spatial memory, with a focus on reference memory. An additional goal of this chapter is to establish a task that requires the subiculum to be correctly performed, in order to characterise the activity of neurons in this region during all stages of learning (see *Chapters 3* and *4*). In order to do so, a set of 3 experiments was employed (see ***Figure 1***). The first experiment aimed at developing a task that is subiculum-dependent while being able to assess both working memory and reference memory in the performance of the animals. Rats performed a spatial task in a radial 8-arm maze (RAM; a modified version of the task implemented by Olton & Samuelson, 1976), where they had to remember the location of three food rewards across multiple days, for 20 trials a day. To test the subicular involvement in spatial memory during the RAM task, the subiculum was inactivated with the $GABA_A$ agonist muscimol prior to the beginning of the task. Previous work has shown an involvement of the dorsal subiculum in spatial working memory (e.g. Morris et al., 1990; Potvin et al., 2007; see *General Introduction*). *Experiment 1* of this chapter aims at replicating these results, as well as evaluating how subicular inactivation impacts reference memory performance across days. Working memory performance was assessed by looking at working memory errors (WME), defined as the animals re-visiting a previously encountered arm. Reference memory was evaluated by the number of

reference memory errors (RME), defined as the animal visiting an arm that does not contain the food reward (Olton et al., 1979).

According to the SOP theory (Wagner, 1976, 1981; see *General Introduction*), the short-term memory of a stimulus (i.e. the arm visited) renders that stimulus "less surprising" than others, thus reducing the amount of attention that the animal pays to said stimulus. This, in theory, allows the animals to explore the RAM and find the hidden rewards in a relatively short period of time (i.e. without continuously re-visiting the same arm). On the other hand, an animal that is unable remember the arm it has just visited (thus failing to recognise it as "more familiar" than others) could repeat that visit whether the arm was baited or not, which in turn would potentially generate both working and reference memory errors as defined by Olton and colleagues (1979). It is then conceivable that deficits in working memory may indirectly give rise to problems encoding reference memory, given that goal locations cannot be maintained in mind while searching the maze (Sanderson et al., 2010; Schmitt et al., 2003; see *General Introduction*). Thus, while deficits in both working memory and reference memory measures would indicate a subicular dependence in spatial information processing, *Experiment 1* alone might not confirm a role for the subiculum in long-term reference memory formation.

Experiment 2 was aimed at testing the contribution of the subiculum to reference memory, independently of working memory. To do so, a second experiment was employed in which the animals performed the same task, but this time with muscimol infusions performed during subsequent rest, immediately after behavioural testing on the first 2 days. Here, *Experiment 2* leverages the role of rest and sleep in promoting consolidation of long-term memories (reviewed in McGaugh, 2000), in which the hippocampal formation plays a central role (Riedel et al., 1999; see *General Introduction*). In this way, inhibiting the subiculum during rest would allow testing of its involvement in spatial reference memory processing, while leaving working memory during the task unaffected.

A possible caveat of the second experiment lies in the possibility that inactivation of the subiculum could affect the ability of the animals to learn the rules of the task, which in turn could influence their performance. When learning a MWM task, providing a non-spatial training session prior to the task (which consists in masking any possible environmental cues) to the animals does not seem to aid in their ability to perform the task in the same

way that a spatial training (where environmental cues are visible and non-spatial components of the task can also be acquired) provides (Bannerman et al., 1995). This suggests that there are at least two different components in learning processes in the hippocampus, a spatial and a non-spatial one. These components can rely on different cellular processes, particularly involving NMDA receptors activity, which is believed to take up a role in specific types of learning and memory (Bliss & Collingridge, 1993; Collingridge et al., 1983) as well as in different cerebral circuits, as suggested by Bannerman and colleagues (1995). In *Experiments 1 and 2* of this chapter, the animal must not only learn the location of the food rewards based on extra-maze cues (spatial component), but also the structure of the task itself (non-spatial component, i.e. there are only three rewards, these are replaced after each trial, and the rewards remain in the same locations across trials/days, relative to external cues). The third experiment of this chapter sets to utilise an extended version of the behavioural task which allows testing of the performance of the animals once they have been trained on the RAM task and are then introduced to a new RAM environment, where the extra-maze cues and the position of the baited arms would differ from the previous environment. Inhibition of the dorsal subiculum was once again carried out during consolidation of information in this later “test” phase. In this way, the new timeline of inhibition would allow to test the contribution of the subiculum independently of the animals having to familiarise themselves with the task rules, thus controlling for the non-spatial component of learning.

Methods

Animals

A total of 36 rats (young male *Lister Hooded*, Envigo; age at surgery = 3.6 ± 2.69 m.o.; weight = 375.11 ± 29.34 gr) were used for this study: 8 for *Experiment 1*, 8 for *Experiment 2*, and 20 for *Experiment 3*. Rats were housed in plastic cages, with temperature maintained at approximately 20°C and humidity around 40%. Subjects were kept on a 12 h light-dark cycle with food and water available *ad libitum* prior to the start of the experiment. Before the beginning of the behavioural task, animals were kept under a restricted food diet to maintain 85-90% of their *ad libitum* weight. Access to water was given *ad libitum*.

The experiments were performed in accordance with the UK Animals (Scientific Procedures) Act, 1986.

Cannulation surgery and drug infusion

Rats were anaesthetised with isoflurane (ISO) at 4% concentration. They were then given meloxicam subcutaneously (0.06 ml of 5 mg/ml solution; Boehringer Ingelheim), before being moved to a stereotaxic frame (David Kopf Instruments) and kept at around 2% ISO. Lidocaine (0.1 ml of 20 mg/ml solution; B. Braun) was administered topically to the scalp during the procedure as an additional analgesic. A craniotomy was performed above the target region, and the dura cut to expose the cortex. Two mini guide cannulas (26-gauge, stainless steel, 4.5 mm length; Bilaney Consultants) were inserted bilaterally at coordinates AP - 5.9, ML ± 2.4, DV - 2.5, aiming at the central area of the dorsal subiculum. Coordinates were based on the results of a of pilot injections study previously performed in the lab. Cannulas were stabilised with dental cement attached to four screws implanted into the skull. At the end of the procedure, glucose saline solution was administered subcutaneously, and the rats were left in a heating chamber until awake, before being transferred to their home cage.

During the task, infusion of either 0.5 µl muscimol (1 mg/ml solution in 0.1 M Phosphate Buffer Saline, PBS; HelloBio) or saline (0.5 µl PBS) was performed using injectors (33-gauge, stainless steel internal cannulas, cut to fit the 4.5 mm cannulas; Bilaney Consultants) projecting 0.5 mm from the external cannulas. Solutions were delivered through a microinfusing pump at a speed of 0.5 µl/min, which was performed under general anaesthesia (<1.5% ISO concentration), or on lightly restrained awake animals (details on the restriction protocol below). One minute was given between the end of the infusion and removal of the injectors, after which the animals were taken off anaesthesia and put back in their home cage for recovery, which usually happened within 5 minutes.

A subset of rats (n = 7) was infused with 0.5 µl of conjugated muscimol (5.3 mg/ml solution in DMSO and PBS; HelloBio) at a speed of 0.25 µl/min to allow visualisation of the spread of the infusions into the targeted area. Two minutes were given between the end of the

infusion and removal of the injector, after which the animal was given 1 hour before termination through perfusion (see ***Figure 2***).

Behavioural paradigm

The behavioural task implemented for the evaluation of the effects of inhibition of the dorsal subiculum was a modified RAM task (Olton & Samuelson, 1976). The objective of the task was for the rat to collect food from three baited arms out of eight. The same three arms were baited across days. In this way, learning could be assessed across days, as well as the impact of silencing the subiculum during the encoding or consolidation phases of learning.

Materials. The animals were habituated to collect food reward during pellet chasing sessions in a circular (120 cm diameter) open field apparatus. The task was conducted on one (or 2 in *Experiment 3*) RAM, which consisted of a central circular chamber of 30 cm in diameter, with eight equidistant spaced arms, each 75 cm long. Wells were positioned at the end of each arm, so that the bait would be unseen from the central chamber. To minimise the possibility of the rat picking up odour cues, pellet dust was sprinkled on the apparatus. The room in which the RAM was positioned contained a series of extra-maze cues to aid the rat in navigating the environment. No intra-maze cues were given, to minimise the possibility that the animals would associate the food rewards with specific “objects” (the arm) as opposed to their location in space (dictated by their position in respect to the extra-maze cues).

Habituation to the RAM. Three days before the beginning of the task, animals were habituated to the maze(s). The animals were brought into the room(s) 10 minutes in advance. They were then placed inside the central chamber of the RAM, with closed doors. After around 30 seconds, the doors were lifted and the rats were left to explore the

apparatus, which contained several food pellets at the end of each arm. Every 2-5 minutes, the doors were dropped, and the rats were put back in the central chamber. This habituation phase for each RAM lasted around 10 minutes each day. The first day, rats housed tougher were habituated together, while the second and third day they were all individually habituated.

The task. The task began after the period of habituation and lasted a maximum of 7 days for *Experiments 1 and 2*, with an additional 4, 8, or 12 days for *Experiment 3* (see ***Figure 1***). Each rat was brought alone in the room 10 minutes before the start of the procedure. Of the eight arms, only three were baited, each with a single food pellet, in a semi-random configuration for each animal, chosen so that the three baited arms were never all adjacent to one another. Once the rat was put inside the central chamber, around 30 seconds were given before the doors were lifted. The trial would end once the animal had collected the three rewards - or after 5 minutes, after which the rat would be put back into the central chamber and the arms re-baited. Every 3-6 trials, the animal would be put back in the home cage, where drinking water would be available, and the maze would be rotated a random number of times, either clockwise or anticlockwise. One day of the task consisted of 20 trials. For *Experiment 3*, after 1 week of drug-free training, a “test” phase, during which the treatment was administered, was conducted in a second room. Rooms were switched to avoid the possibility that the animal would first search for the locations learnt in the training phase. The procedure was the same as during the training week, with a new configuration of three arms baited. In the experiments in which a second “test” was carried out, it was conducted in the first room, with a new set of arms baited (with a different configuration from the previous environment and with at least 2 out of the 3 baited arms differing from the training week configuration).

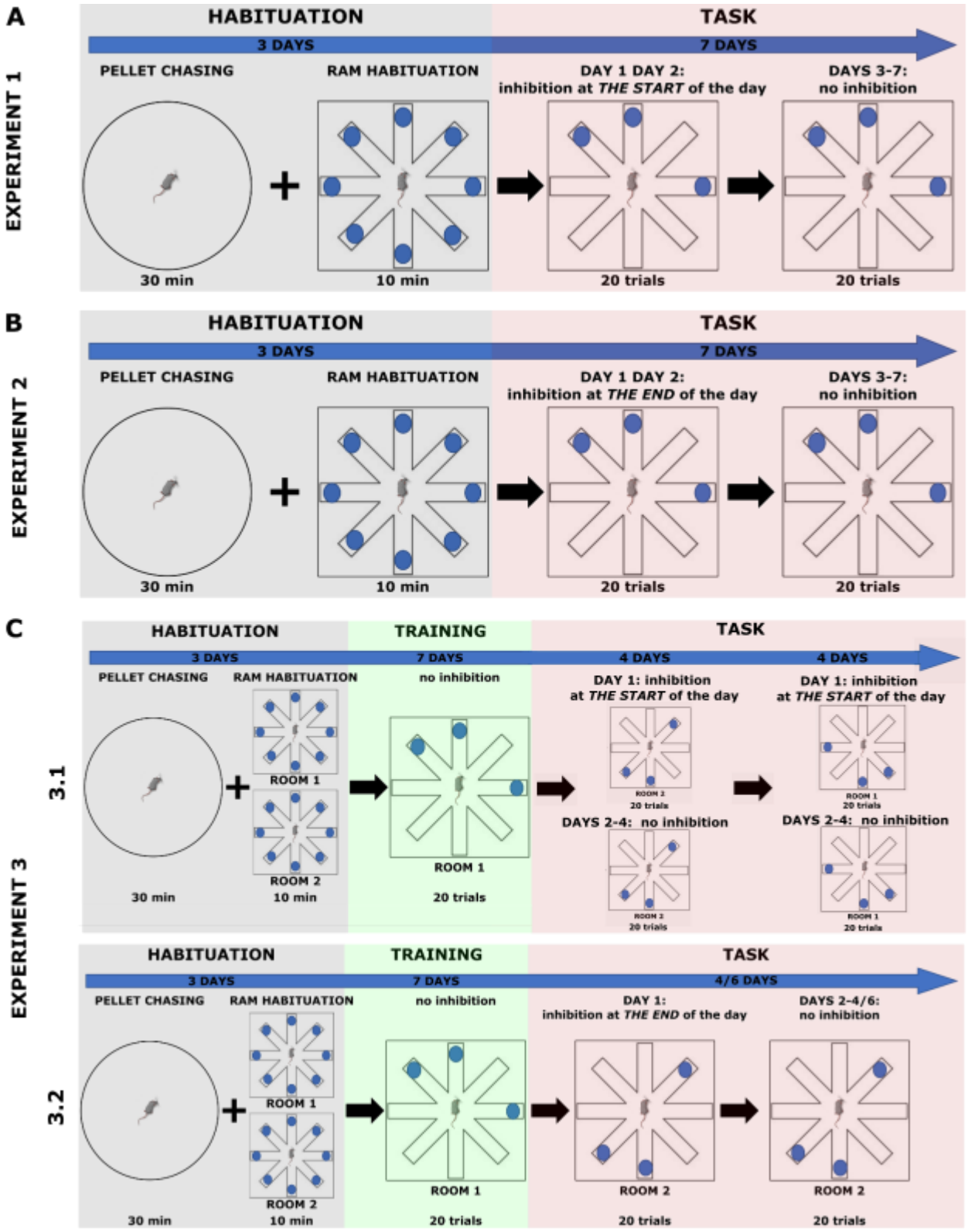

Figure 1. To test the involvement of the subiculum in reference memory, three sets of experiments were designed. *(A) Timeline of Experiment 1. Animals undergo three days of habituation to both in the open field (pellet chasing) and the RAM (with all arms baited). This was followed by 7 days performing the RAM, where muscimol (or saline) infusions were carried out*

immediately before the start of the task on days 1 and 2. (B) Timeline of Experiment 2. After the same habituation protocol as Experiment 1, animals performed the RAM for 7 days, when infusions were carried out immediately after the end of all trials on days 1 and 2. (C) Timeline of Experiment 3. Differently from the previous two experiments, animals were habituated to 2 separate RAM rooms. After, a period of 7 days of training was carried out in one of the rooms, followed by a "test" period. For experiment 3.1, two "tests" of 4 days each were carried out, where infusions were performed at the start of day 1. For Experiment 3.2, either 4 or 6 days of tests were carried out in a second room, with infusions performed or at the end of day 1.

To habituate the animals to the possibility of an intracranial infusion, animals were infused with saline (0.5 µl) either on days before the start of the task (*Experiments 1 and* 2) or on days 4 and 6 of training (*Experiment 3*). During the task, animals were infused with either muscimol or saline (0.5 µl). When inhibition was carried out before learning (*Experiment 1* and first part of *Experiment 3*), rats were infused under general anaesthesia, after which 20 minutes were given before the start of the task to avoid any aftereffects of the anaesthesia on the animals' performance. In the consolidation experiments (*Experiment 2* and the second part of *Experiment 3*), rats were infused while awake and lightly restrained by the experimenter within 5 minutes of the end of the task, and then again 2 hours after. Infusions were carried out on awake animals to avoid possible disruption of the consolidation process due to the use of anaesthetics (see Liu et al., 2010). Animals were habituated prior to the beginning of the experiment to a light restrain by hand to allow this procedure and were left undisturbed in their home cages after each infusion. As the half-life of muscimol in rats has been reported to be between 1.5 and 2 hours (Moroni et al., 1982), this set up allowed the drug to remain active in the brain for the whole duration of the task (when the drug was delivered prior to learning) and for a considerable amount of time after (when the drug was delivered after learning). Diagrams of the tasks and their timelines are shown in ***Figure 1***.

Histology

Rats were perfused under a biological hood at the end of the task. They were given a lethal dose of sodium pentobarbital (2 ml/kg, Dolethal; Vetoquinol UK Ltd) through intraperitoneal injection, and then transcardially perfused with 0.1 M PBS, followed by 4% paraformaldehyde (PFA) in 0.1 M PBS. Brains were collected in 4% PFA and left on a stirring plate for at least 4 hours, before being transferred in 25% sucrose solution overnight at room temperature on a stirring plate.

The tissues were cut using a freezing microtome (8000 sledge microtome; Bright Instruments). Brains were sectioned coronally in 80 µm thick slices. Most slices were cresyl stained, while those that belonged to animals in which the conjugated muscimol was infused were DAPI stained to visualise the somas of cells in the area.

Slices were then mounted on gelatine subbed glass slides and coverslipped using either DPX (for the cresyl-stained slices; Thermo Fisher Scientific) or FluoroMount (for the conjugated muscimol). Images were acquired using the Leica Microscope and the Leica Software using either a bright field (cresyl) or a green light filter (conjugated muscimol).

Data analysis

Behavioural results. Performance of the animals was measured in number of visits (a visit was scored when at least half of the rat's body was inside the arm), WME (animal re-entering a visited arm within a trial) and RME (animal entering a non-baited arm). The scoring was conducted by the experimenter, on pen and paper. The sequence of arms visited for each trial was manually entered on an Excel sheet to compute the mean number of visits, of WME and of RME for each animal on each day of the task.

Tracking. A camera was positioned above the maze to record the task, and the consequent videos were analysed to extract tracking for scoring confirmation and additional behavioural measures. Tracking data was analysed through DeepLabCut (DLC; Mathis et al., 2018) by marking the position of the head and the tail base. A DLC project was created for all the animals, using sample videos from the first recorded day. Forty frames were extracted from each video and labelled manually through the DLC graphical-user interface. The *resnet_50* network was then created with the *imgaug* augmentation method and trained for a maximum of 500000 iterations. The sample videos were analysed and percentage of tracked points with a likelihood below 0.7 were calculated to assess the model. If the model was considered unsatisfactory, outlier frames were extracted from the videos (with a combination of the jump, fitting, and uncertain methods from DLC, based on visual inspection of the tracked points) and then refined before the network was re-trained using the same parameters. The model was considered optimised once the percentage of tracked points' likelihood that was below 0.7 reached below 20%. Once optimised, the model was then run on all the recorded videos and further refinement of the tracking was computed using custom R code. Any points with a tracked likelihood below 0.7 and any point that was considered "jumpy" (distance from the point before and the point after > 20 cm) was removed and replaced by linear extrapolation using the

tracked points immediately before and after it. The position of the animal was then computed as the average between the position of the head and the tail base. To compute the distance travelled, the tracking data (collected at 15 frames-per-second) for each trial was first smoothed with a gaussian kernel (1SD = 2 samples) and the Euclidean distance between the rat position on each frame was computed. Instantaneous speed was calculated from the smoothed tracking for each frame. Due to issues with the camera equipment, two of the animals in *Experiment 1* were not recorded on day 3 (one for each group), so the consequent analysis of the tracked data considers a subset of all the animals that performed the behavioural tests.

Statistical analysis. A linear model was computed for each measure, using the formula *dv ~ group * day*, where *dv* was either the mean number of visits, RME or WME. Visual inspection of the residuals from the model was used to assess if the data met the assumptions to run an ANOVA analysis. Unpaired (or paired if the performance on the two "test" phases was combined) two-samples t-tests were computed for the analysis of differences between groups on individual days. ANOVA analyses were computed to compare the treatment groups across days, followed by pairwise t-tests, and the p values corrected using the Holm-Sidak correction method. To establish the level of chance performance, a Monte Carlo approach was used to simulate performance on the task. The simulation was set such that a limited range of WME were allowed. It was then run separately for 0 through to 5 maximum errors, and finally with unlimited WME (see Girardeau et al., 2009). Each simulation was run 1000 times, to produce a distribution of simulated performances that reflects a lack of reference memory, while incorporating a range of working memory capacities (see ***Figure 4C***). For the speed and distance analyses, a Kolmogorov-Smirnov test was computed to assess differences in the distributions between treatment groups. In *Experiment 3*, to assess the strength of the results, the Bayes factor was computed for each ANOVA analysis (Rouder et al., 2012).

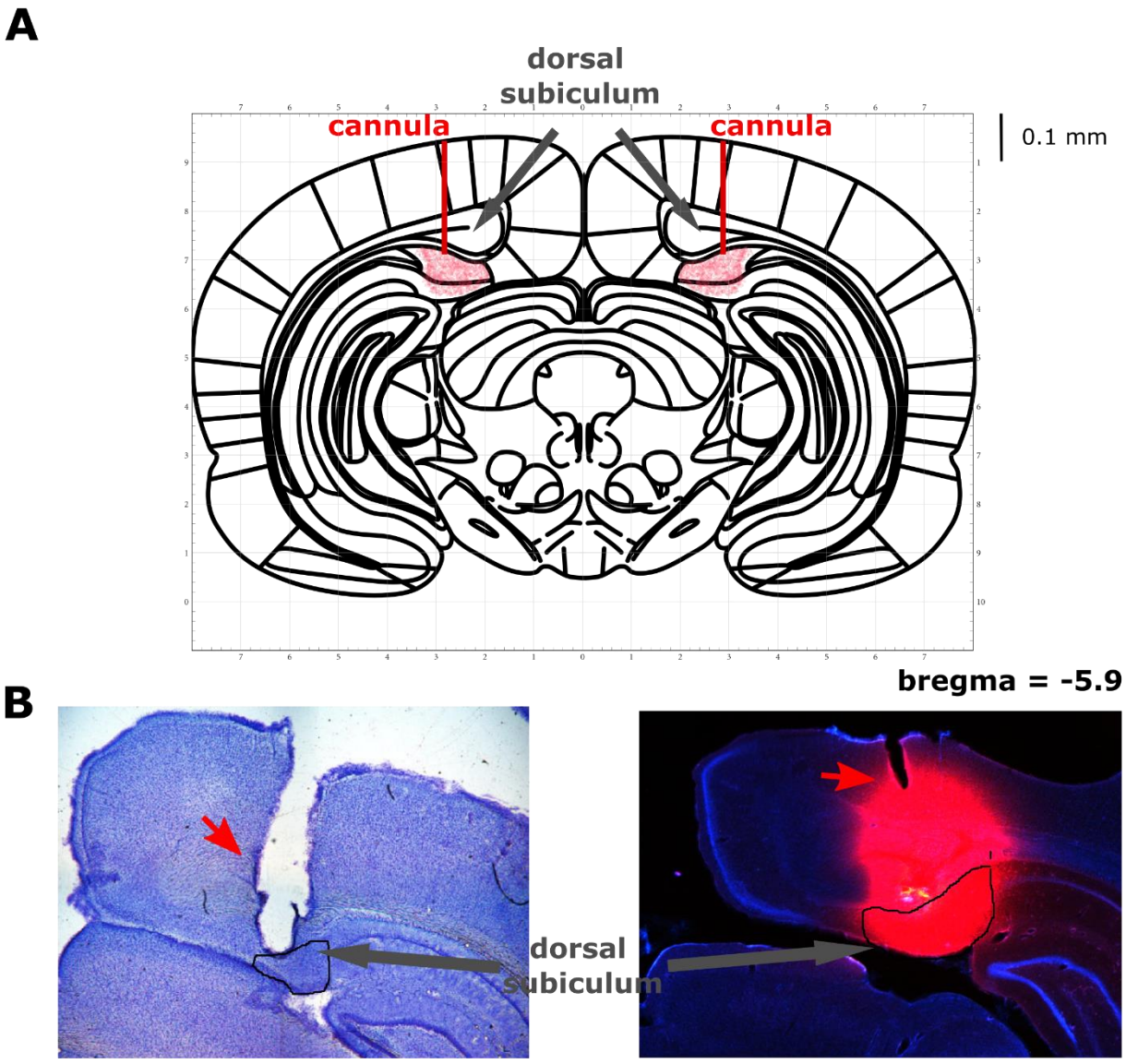

Figure 2. Animals were given bilateral infusions of muscimol to inhibit the activity of the subiculum. *(A) Schematic depicting the proposed position of cannulas (red lines) and spread of infused muscimol (red cloud). Cannulas were aimed at the mid portion of the subiculum on the proximo-distal axis, and the end of the cannulas was aimed at the very top of the layer, to ensure the drug would flow down into the structure. (B) Histological examples of position of the cannula (left, red arrow depicting the entrance point of the cannula in the cortex) and spread of the muscimol, which was considered comparable to the spread of conjugated muscimol (right, in red). Based on the histology, cannula placement was accurately aimed at the dorsal subiculum, and spread of the conjugated muscimol did not extend extensively into neighbouring regions.*

Histology. Position of the cannulas was confirmed through visualisation of brain slices. The spread of the muscimol infusions was estimated to be comparable to the spread of conjugated muscimol (see ***Figure 2B***), infused in a subset of animals at the same volume and comparable concentration of muscimol (considering that conjugated muscimol has 5.3 times the molecular weight of muscimol). This approach was similar to that used by Nelson and colleagues (2015).

Results

1. Experiment 1: inhibiting the dorsal subiculum prior to acquisition impacts performance on a spatial memory task

The first aim of this study was to confirm the involvement of the dorsal subiculum in spatial working memory (as previously suggested by Morris et al., 1990; Potvin et al., 2007, 2009), along with testing a possible involvement of the area in spatial long-term memory (previously suggested by Bolhius et al., 1994; Morris et al., 1990*;* see *General Introduction*). To do so, performance of a spatial memory-specific behavioural task was evaluated, after muscimol infusions aimed at the dorsal subiculum of rats (performed either before or after learning).

The task carried out in *Experiment 1* proceeded over 7 days (see *Methods*), in which inhibition was performed on days 1 and 2. The hypothesis was that the inhibition of the dorsal subiculum before learning would influence the ability of the rats to learn the position of the three baited arms, resulting in an impaired performance compared to controls (infused with saline on both days of treatment).

A total of 8 animals performed the task. Due to technical complications, of the animals completed only 5 out of the 7 days, hence all the following analyses will consider only days 1-5.

First, the overall performance was considered. To test whether infused animals tended to visit a greater number of arms to locate all food rewards, the sum of all visits for each day

and each rat was calculated (n = 4 for each treatment group; ***Figure 3A***). A one-tailed unpaired two-samples t-test, which showed as significant between these conditions ($t(6) = -4.167$, $p < 0.01$), consistent with a role for the dorsal subiculum in spatial memory.

Next, the difference in performance between the two groups was analysed across each day of learning. The mean number of visits for the two groups was computed for each day (n = 4, ***Figure 3B***). A mixed ANOVA analysis revealed a significant interaction between group and day in number of visits (between: experimental groups; within: days; main effect for group: $F(1,6) = 17.37$, $p < 0.01$; day: $F(4,24) = 27.974$, $p < 0.001$; group *x* day interaction: $F(4,24) = 5.174$, $p < 0.01$). To assess how performance differed between the two groups for each day, post-hoc pairwise t-tests were performed, which revealed differences on days 1-4 ($p < 0.01$ on day 1, and $p < 0.05$ on days 2-4). These results show how inhibiting the subiculum prior to the task influences the performance of the animals not only on the days of inhibition, but as far as 2 days after it.

Next, the influence of subicular inhibition on both working memory and reference memory was analysed. The expectation was that, if the subiculum is involved in both working and reference memory, both measures would show impairment in the treatment group on the days of muscimol delivery.

First, RME were considered separately, identified by the number of times the animal entered a non-baited arm. The average RME was computed for the two groups (***Figure 3C***) which were then analysed with a mixed ANOVA. These results paralleled the analysis of the number of visits, where the treatment group exhibited a significantly different number of RME compared to the control on days 1-3 (main effects of group: $F(1,6) = 28.39$, $p < 0.01$; and day $F(4,24) = 34.176$, $p < 0.001$; interaction effect: $F(4,24) = 6.837$, $p < 0.001$; pairwise t-test, day 1 $p < 0.01$, days 2 and 3 $p < 0.05$). This indicated an effect of long-term spatial memory errors in the muscimol group that was present not only on the two days of inhibition, but also on the following day.

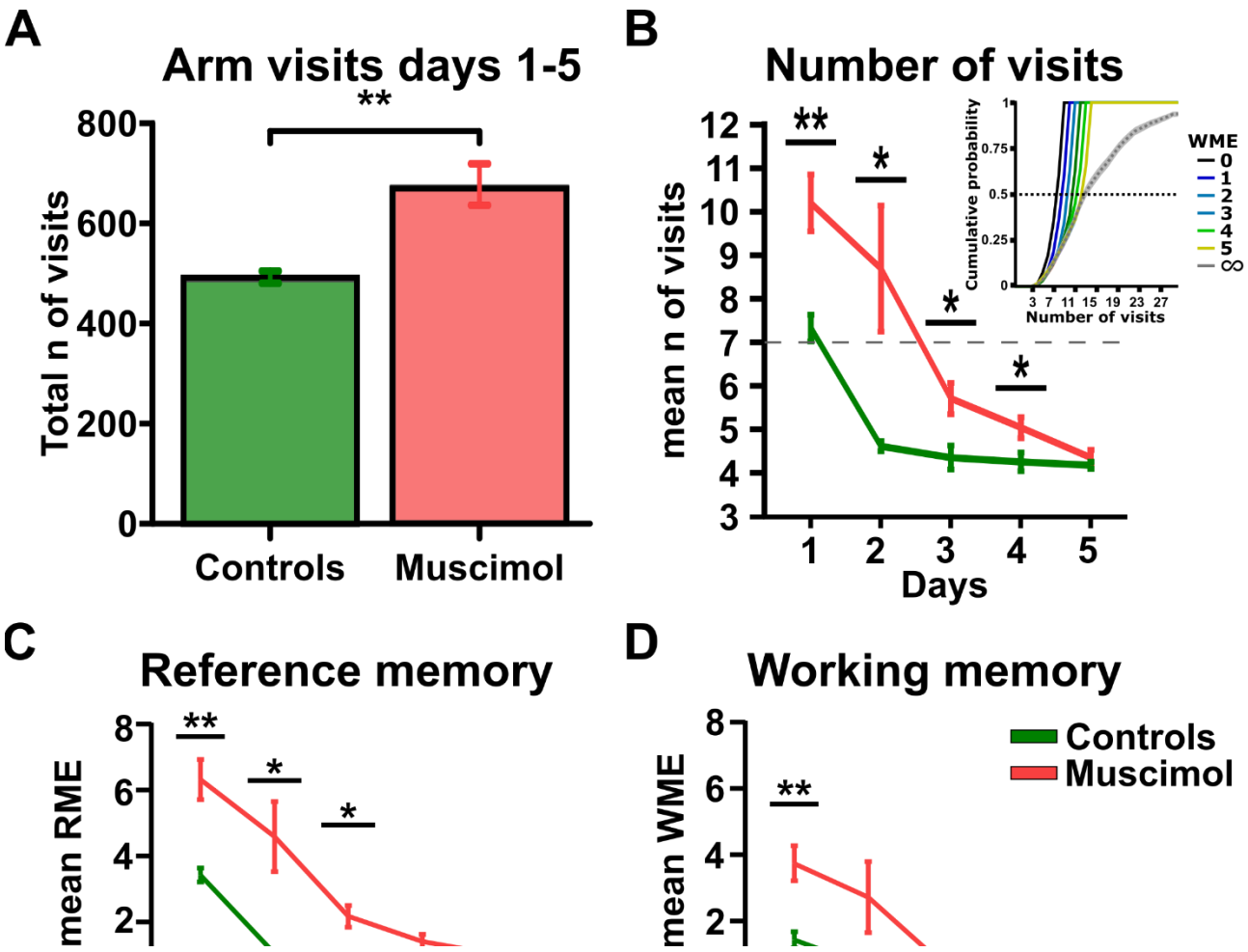

Figure 3. Inhibiting the subiculum prior to learning impacts performance on the RAM. *(A) The total number of visits across the 5 days of the task was computed for each animal and the average (n = 4) compared between the controls and muscimol groups using an unpaired two-samples t-test. (B) Mean number of visits per trial was computed for each animal and averaged for each group. Grey dotted line represents chance performance with perfect working memory, as assessed by our Monte Carlo approach (insert; see Methods). (C-D) Mean number of RME (C) and WME (D) per trial was assessed for each animal and averaged within the treatment groups. Differences between groups in (B), (C), and (D) were assessed with a mixed repeated Measures ANOVA and post-hoc pairwise comparisons t-tests. All error bars represent SEM. Significance levels: * $p < 0.05$, ** $p < 0.01$, *** $p < 0.001$, all Holm-Sidak corrected.*

Lastly, the mean number of WME was analysed for each group, identified as the animal re-entering a visited arm. This measure was expected to be impacted solely on the day of inhibition, as working memory is an active process that operates in a short time span (Atkinson & Shiffrin, 1968). A mixed ANOVA revealed a significant effect of muscimol infusions across the days (***Figure 3D***; main effect of group: $F(1,6) = 9.129$, $p < 0.05$); day: $F(4,24) = 14.182$, $p < 0.001$; group *x* day: $F(4,24) = 4.871$, $p < 0.01$). The post-hoc pairwise comparisons with t-tests confirmed a significant difference between the two groups on the first day of inhibition only ($p < 0.01$), confirming previous findings of the involvement of the subiculum in spatial working-memory (Morris et al., 1990; Potvin et al., 2007, 2009).

Of note, the number of failed trials was registered for each animal. A trial was considered as “failed” when exploration reached the 5 minutes limit before the animal had collected all the rewards. This phenomenon was only present in the first two days of the task and almost exclusively involved animals that received the muscimol infusions (treatment group day 1: 20/80 trials; day 2: 6/80 trials; control group day 1: 1/80 trials), suggesting how the muscimol group struggled with performing the task on the days of inhibition.

Taken together, these results show a general impairment in the muscimol-infused group on all three measurements of performance (visits, RME, and WME) on days of the task in which inhibition was carried out, indicating that the dorsal subiculum plays a role in both spatial working and reference memory. However, the difference in WME between the two groups on the first day of treatment highlights how this manipulation of subicular activity cannot let us draw any conclusions on its involvement in reference memory only, as an inability in remembering previously visited arms could impact the reference memory measurements (as discussed in the *Introduction* to this chapter).

2. Experiment 2: inhibiting the dorsal subiculum after acquisition impacts reference memory

In order to test reference memory without impacting working memory, a second experiment was performed where the dorsal subiculum was inactivated immediately after

learning on the first two days of the task, to disrupt consolidation processes. Here, the hypothesis was that the two muscimol-infused group would show an impaired performance on the days immediately subsequent to the treatment, similar to previous work that demonstrated a role for the CA1 in consolidation (Riedel et al., 1999; see *General Introduction*). Any deficit resulting from the inhibition of the dorsal subiculum during rest would affect the gross measurement of number of visits and the measurement of reference memory, while leaving working memory intact.

The number of visits, RME, and WME were all computed for both the muscimol-infused group (n = 4), and the control group (n = 4). As one of the animals completed only 6 out of the 7 days of the task, day 7 was excluded from the analysis. Additionally, as no treatment was carried out before the start of the task, but only at the end of day 1, it was assumed that the two groups would not differ in performance on this day. To check this, a two-tailed unpaired t-test was computed between the two groups for each of the performance measures mentioned above (see ***Figure 4B-D**).* All three tests revealed no significant difference between the two groups (all $p > 0.05$), so the performance on day 1 was no included in the following analyses.

For each measure, the difference in overall performance was first tested by comparing the total number of visits for each group (as performed in *Experiment 1*). A t-test to compare the two groups revealed no significant difference (two-tailed unpaired two-samples t-test: $t(6) = -1.4307$, $p = 0.202$; ***Figure 4A***) Next, the mean number of visits, RME and WME was computed and a mixed ANOVA performed (between: experimental groups; within: days) for days 2 to 6, followed by pairwise comparisons with t-tests to further explore any significant results.

The analysis of the number of visits revealed a significant effect of the treatment across days (main effect of day: $F(4,24) = 10.539$, $p < 0.001$, group *x* day: $F(4,24) = 5.327$, $p < 0.01$). This was further analysed by post-hoc pairwise comparisons t-tests, which confirmed a significant difference between the “consolidation block” and the control groups on days 5 and 6 ($p < 0.05$, ***Figure 4B***). These results revealed an effect of the subiculum inhibition that diverged from initial expectations, as the impairment in performance was seen not on the day immediately following the last drug treatment (day 3), but with a delay of two days.

This delay in the effect of “blocking” consolidation could reflect a lack of improvement in performance from day 3 onwards relative to control animals. In this way, differences between the two groups would be observed only when controls reached asymptotic performance at around day 4. To test this, pairwise t-tests were performed between days, for each group separately (***Figure 4B, insert on the right***). The results showed how the performance of the control group changed between day 2 and days 5 and 6 ($p < 0.05$), while it showed no change between any of the days for the treatment group, highlighting a lack of improvement in the muscimol group from the first day following treatment.

Similar results were evident when looking at RME. The muscimol group showed an impairment on days 5 and 6 (main effect of day: $F(4,24) = 19.586$, $p < 0.001$; group *x* day: $F(4,24) = 3.942$, $p < 0.05$; t-test p values on days 5 and 6: $p < 0.05$; ***Figure 4C***). This, combined with no difference found between the two groups on WME (all $p > 0.05$; ***Figure 4D***), indicated how inhibiting the subiculum during rest (and presumably consolidation) on the first two days of the task had an impact on reference memory, while leaving working memory intact.

As it was done in *Experiment 1*, the number of failed trials was also registered for each animal. This phenomenon was only sporadically present in the first day of the task and only in 2 animals (1 instance in the controls and 1 in the muscimol group), signifying that both groups had no particular issues in completing each trial every day.

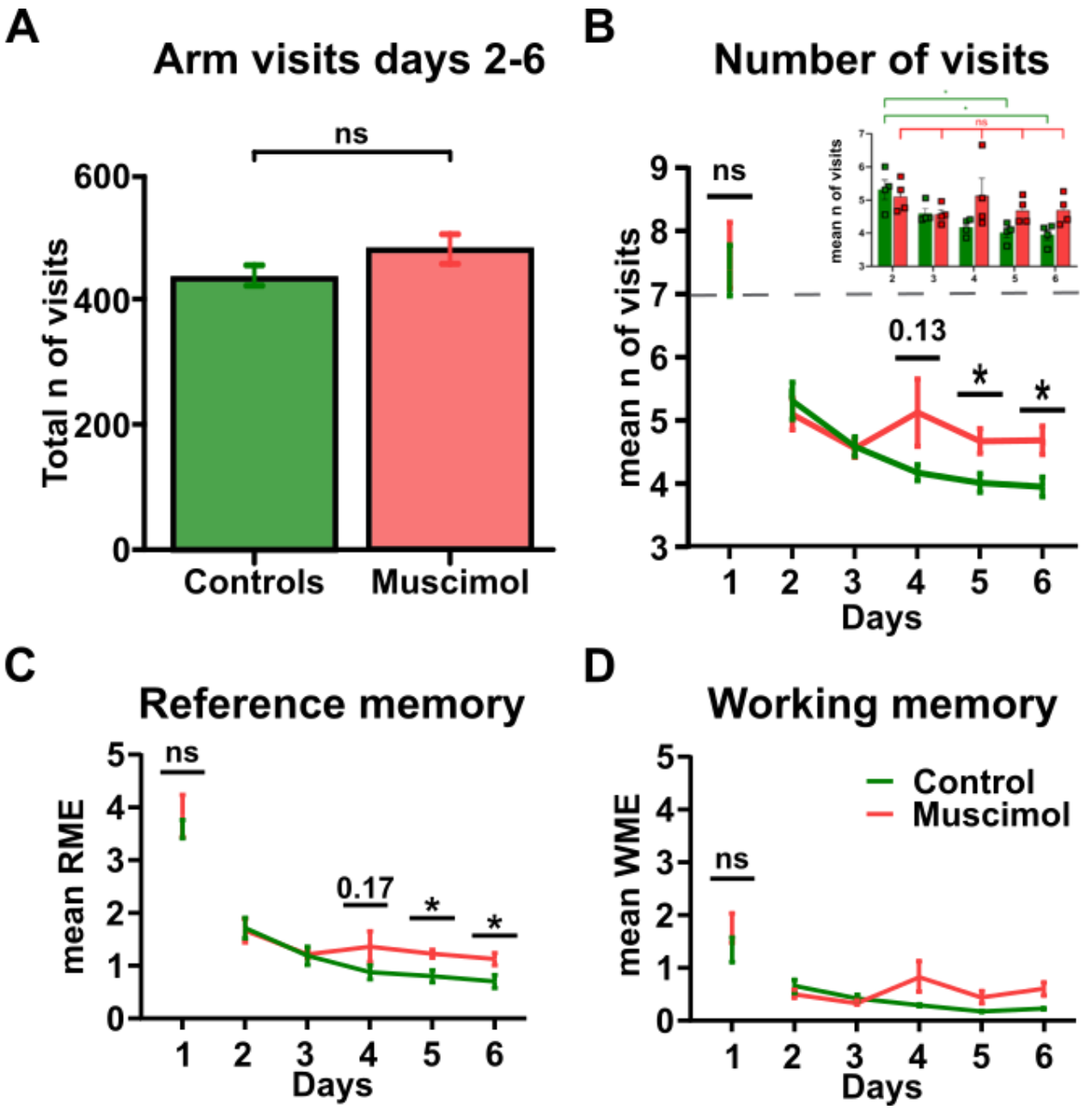

Figure 4. Inhibiting the subiculum immediately after acquisition impacts performance on the RAM. *(A) Total number of visits across days 2-6 of the task, computed for each treatment group ad compared with an unpaired two-samples t-test. (B) Mean number of visits for the two treatment groups. Day 1 performance was tested separately, as no treatment was carried out before the task on that day. Performance on days 2-6 was compared between groups and across days, as inhibition was carried out at the end of the task on days 1 and 2. Grey dotted line represents chance performance with perfect working memory (see Methods). Insert shows how performance for the control group (green) improves across days, while the performance of the treatment group (red) shows no difference across the 5 days after treatment. Single dots represent the mean number of visits for each animal. (C-D) Mean number of RME (C) and WME (D) for each treatment*

*group. For the performance of both groups on day 1, an unpaired t-test was performed. For the assessment of group differences across the other days, a mixed ANOVA was applied. All error bars represent SEM. Significance levels: * $p < 0.05$, ** $p < 0.01$, *** $p < 0.001$, all Holm-Sidak corrected.*

As a confirmatory analysis, the distance and speed travelled during the task were explored. This was performed on the tracking data extracted from video recordings (see *Methods*).

While the distance travelled on a trial could be considered as a reflection of the number of visits performed by the rats, an undecisive rat might exhibit an increase in time spent exploring the centre of the maze and the doors without making a clear arm choice, thus increasing the distance travelled (e.g. Schacter et al., 1989). The distance per trial (see *Methods*) was computed as the sum of all the distances on each trial. To compare the performance of the two groups on the day prior to treatment (day 1), a Kolmogorov-Smirnov test was applied to the two distributions of distances travelled. This revealed, as expected, no differences in the two groups ($D = 0.1125$; $p = 0.695$; ***Figure 5A, top row***). When looking at the distributions of distances on days 2-6 together, a significant difference was found between the control and the treatment group ($D = 0.143$, $p < 0.001$; ***Figure 5A, bottom row***). A mixed ANOVA revealed an effect on the interaction between the group and day of the task (mixed ANOVA on reciprocals; day effect: $F(4,22) = 10.394$, $p < 0.001$; group *x* day: $F(4, 22) = 7.016$, $p < 0.001$). The post-hoc analysis showed a difference between groups on days 5 and 6 (post-hoc pairwise t-test, days 5 and 6 $p < 0.05$, ***Figure 5B***).

A difference between groups in the distance travelled might reflect the notion of an "indecisive" animal (see Wiener et al., 2008 on path planning under uncertain conditions). However, one would expect the animals to run at similar speeds, as both groups are equally familiar with the environment they are exploring (see *Methods* for habituation procedure). The speed for each trial was taken as the mean of all instantaneous speeds (see *Methods*). As before, the distributions of speeds for the two groups were compared on the pre-treatment day (day 1), which revealed a significant difference (Kolmogorov-Smirnov test: $D = 0.2375$, $p < 0.05$; ***Figure 5C, top row***). This was also true for the distributions of speed on days 2-6 ($D = 0.2789$, $p < 0.001$; ***Figure 5C, bottom row***). Visualising the distributions of running speed for the two groups on day 1 only and days 2-6 together showed that the animals generally exhibited two clusters of speeds, one slower and one faster (represented by the grey dotted line on ***Figure 5C***). Given this, the proportion of time spent running fast or slow could be compared between the two groups ($p = t/total\ time$, where t is the time spent running at fast speed, and *total time* is the total

time of one trial). This analysis showed no differences in the amount of time the animals spent running at fast speed between the two groups (mixed ANOVA, day effect: $F(4,22) = 0.716$, $p = 0.590$; group effect: $F(1,4) = 0.149$, $p = 0.719$; group *x* day: $F(4, 22) = 0.124$, $p = 0.972$; ***Figure 5D***). This result suggests that general features of the animals' performance which are unrelated to learning, such as speed, are unaffected by the treatment.

Overall, these results show a difference in performance for most of the measures analysed, which suggests an involvement of the dorsal subiculum in reference memory. As mentioned above (see *Introduction*), these results open up a new line of enquiry on whether training the animals would influence our results. With the goal of testing the performance of the animals without it being influenced by the need to learn the rules of the task, animals were tested on a second room, after they had undergone a drug-free period of training.

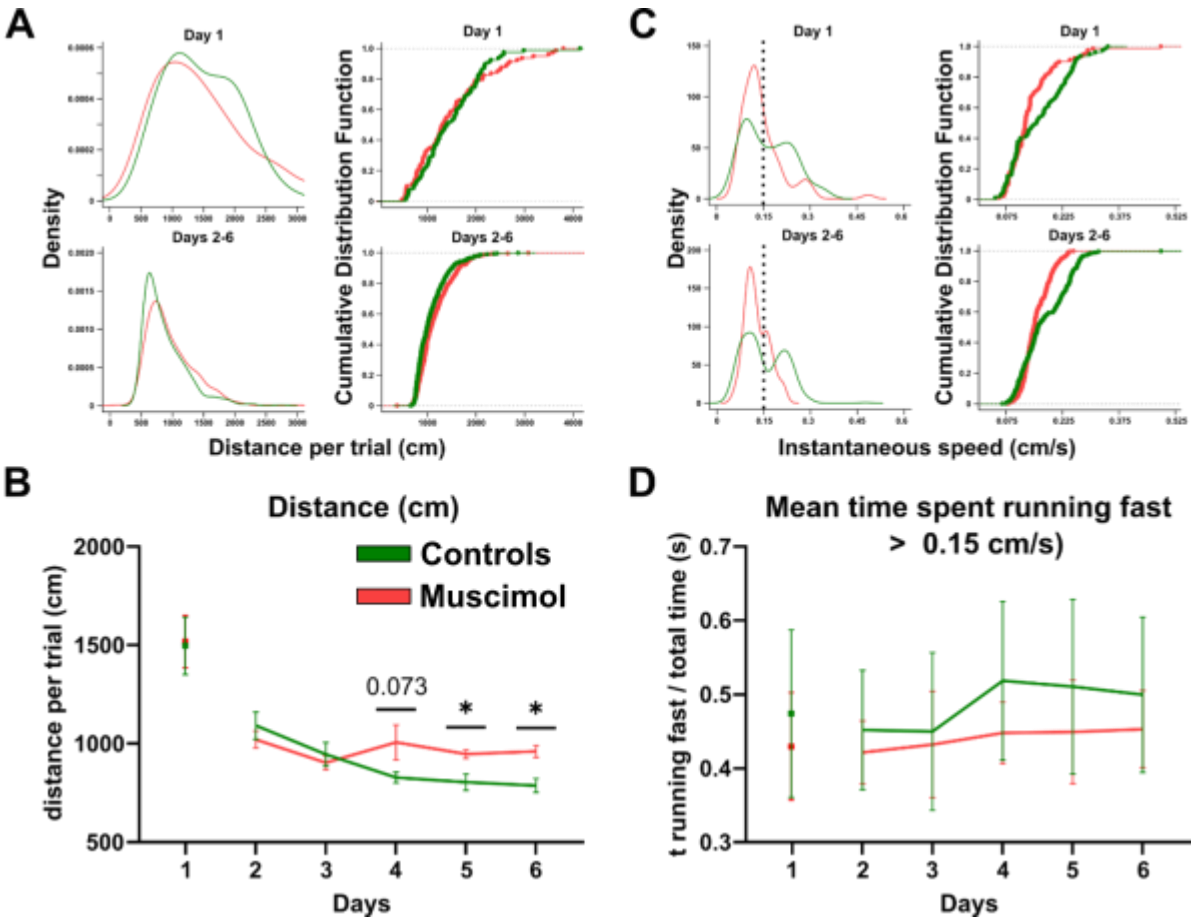

Figure 5. Animals treated with muscimol showed an increase in distance travelled per trial, but no difference in running speed. *(A) Density (left) and cumulative (right) distributions of the distance travelled by the two treatment groups, separately for day 1 (top) and days 2-6 (bottom). (B) Density (left) and cumulative (right) distributions of the speed of travel for each group, on day 1 (top) and days 2-6 (bottom). Dotted line represents possible separation of two clusters based on speed: fast speed, and slow speed. Differences between distributions were assessed using a Kolmogorov-Smirnov test. (C) Total distance travelled for each day by each treatment group. (D) Proportion of time spent running fast for each group on each day compared to total running time. Differences in the two groups across time were assessed with a mixed ANOVA approach. Error bars represent SEM. Significance values: * p < 0.05, with Holm-Sidak correction.*

3. Experiment 3: subicular dependence of working and reference memory in trained animals

3.1. Inhibiting the subiculum prior to learning on the "test" phase shows a deficit in performance

In order to test whether training the animals would influence their performance on the task (as suggested by Bannerman et al., 1995), the RAM task was modified as shown in ***Figure 1C***. In this version, animals underwent an initial period of 7 days of training in the RAM, after which they were brough to a second RAM room with a new set of baited arms (see *Methods*).

Before implementing the consolidation block, the subiculum-dependence of the task was tested in a cohort of 8 animals. To do so, infusions were performed at the beginning of day 1 to disrupt acquisition, in a similar fashion to *Experiment 1*. To reduce the number of rats that underwent this manipulation, the animals ran 2 "tests" of 4 days each, with the second being carried out in the same RAM as the training phase, so that each rat will carry out the experiment both in the control and treatment condition (counterbalancing the order of the treatments). A total of 8 rats underwent surgery for this experiment, but due to complications during the surgery, 2 rats were excluded prior to the beginning of the task.

The aim of this third experiment was to evaluate any effects of subicular inhibition on spatial memory by excluding the possibility that the drug treatment could influence acquisition of other non-spatial information, such as learning the rules of the task. This would assume that the animals have reached comparable levels of performance at the end of the training period. To verify that this was the case, performance was analysed in both groups on the last day of training. Analysis of the three performance measures (visits, RME, and WME), assessed through two sample t-tests, revealed no differences in the two groups on the day prior to the treatment (day 7 of the training period; visits: $t = -0.812$, $df = 4$, $p = 0.462$; RME: $t = -1.1$, $df = 4$, $p = 0.333$; WME: $t = -0.426$, $df = 4$, $p = 0.691$; see ***Figure 6A***). This was true not only when considering day 7 only, but also on an analysis of all 7 training days: the ANOVA test of each of the three measures revealed no effect of either treatment or an interaction between treatment and day on the task (group effect in number of visits: $F(1,4) = 0.056$, $p = 0.824$; RME; $F(1,4) = 0.055$, $p = 0.825$; WME: $F(1,4) =$

0.438; p = 0.544. Interaction effect in visits: F(6,24) = 1.615; p = 0.186; RME: F(6,24) = 2.082, p = 0.0934; WME: F(6,24) = 0.698, p = 0.654), with the only significant effect being on the day variable (main effect of day in visits: F(6,24) = 57.680, p < 0.001; RME: F(6,24) = 98.259, p < 0.001, WME: F(6,24) = 9.510, p < 0.001). This suggests that there were no differences between the performances of the two groups during training, with both groups showing learning throughout the days. Post-hoc one-way ANOVA on the effect of day independent of treatment confirmed a main effect for each group on the day variable (visits group1: F(6,12) = 20.4, p < 0.001; group2: F(6,12) = 44.3; p < 0.001; RME group1: F(6,12) = 46.5, p < 0.001; group2: F(6,12) = 53.1, p < 0.001; WME group1: F(6,12) = 2.98, p = 0.051; group2: F(6,12) = 8.55, p < 0.01). To assess changes in performance between day 1 and day 7, pairwise t-tests were run for each group. This revealed that the performance improved for both groups for number of visits and RME (t values for groups 1 and 2 in visits and RME respectively = 5.04, 7.85, 7.99, 9.53, all df = 2, all p < 0.05 with Holm-Sidak correction; see ***Figure 6A***). The WME results were not significant (group 1: t = 2.25, df = 2, p = 0.153; group 2: t = 3.47, df = 2, p = 0.074). These results suggest that the animals of each treatment group were learning over time.

Mean number of visits, mean RME and mean WME during the two “test” phases were then computed for the control and the treatment groups, averaging across the two “tests”, so that a total of n = 6 was reached for each group (i.e. each of the 6 rats performed both tests, once with saline and once with muscimol infusions). A two-way repeated measures ANOVA (within factors: experimental groups and days) was performed for each measure, followed by a post-hoc pairwise t-test for significant results.

All three measurements revealed an effect of the treatment across days (visits: group effect: F(1,5) = 12.91, p < 0.05; day: F(3,15) = 42.7, p < 0.001; group *x* day: F(3,15) = 5.674, p < 0.01; RME: group: (F(1,5) = 7.115, p < 0.05; day: F(3,15) = 63.73, p < 0.001; group *x* day: F(3,15) = 3.652, p < 0.05; WME: group: F(1,5) = 7.747, p < 0.05; day: F(3,15) = 18.54, p < 0.01; group *x* day: F(3,15) = 11.93, p < 0.01). Both visits and RME were impacted on both day 1 and day 2 (visits: p < 0.05; RME day 1 p < 0.01, day 2 p =0.08), while WME were impacted on day 1 only (p < 0.05; see ***Figure 6B, top right and bottom***). The impact on performance in the treatment group was also confirmed when analysing the overall number of visits performed during the task by the two groups (n = 6 for each group; pairwise t-test: t = -3.768, df = 2, p < 0.05; ***Figure 6B, top left***).

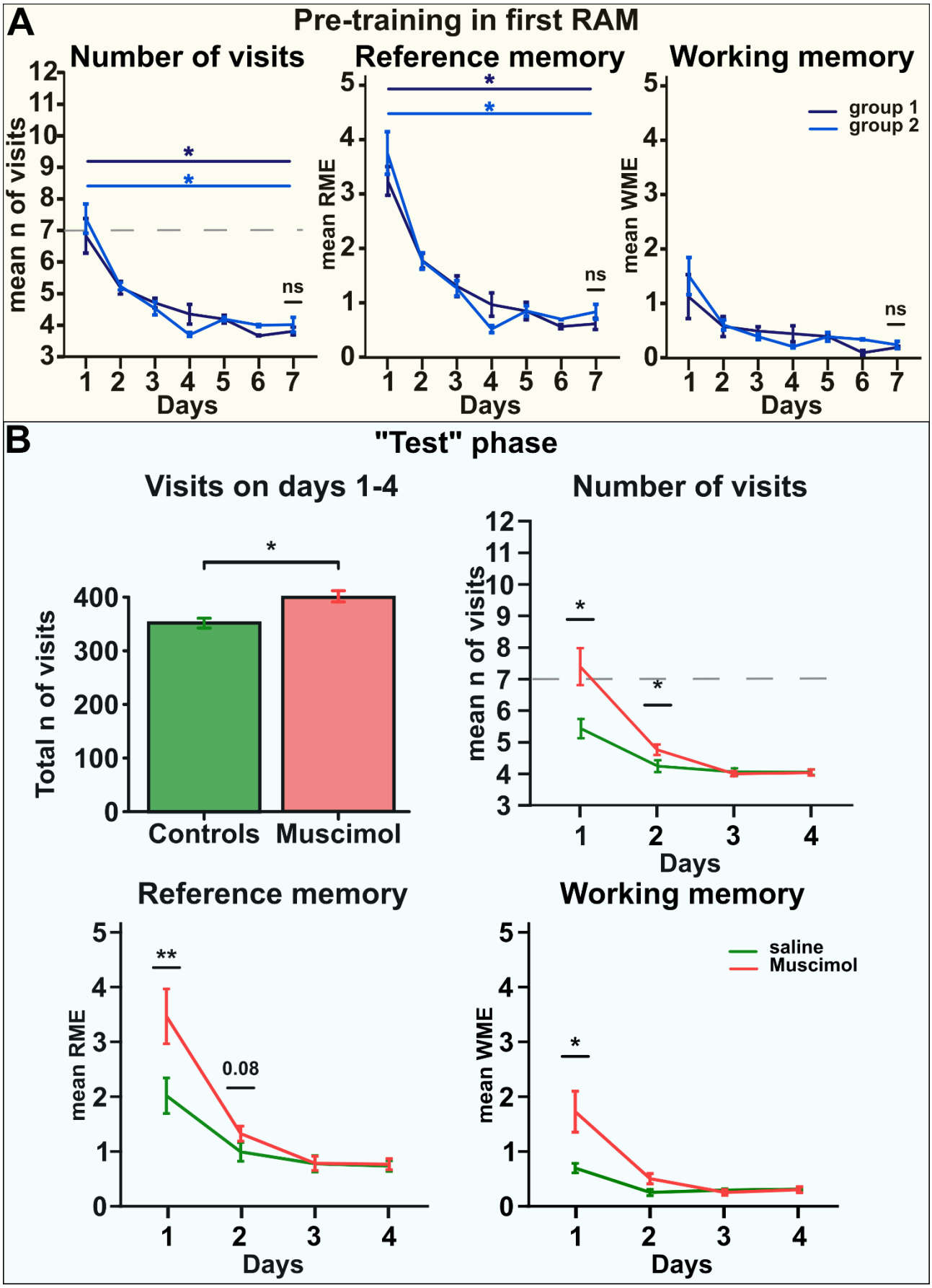
A
Pre-training in first RAM
Number of visits
Reference memory
Working memory
mean n of visits
mean RME
mean WME
Days
group 1
group 2
ns
*
B
"Test" phase
Visits on days 1-4
Total n of visits
Controls
Muscimol
Number of visits
Reference memory
Working memory
saline
Muscimol
**
0.08

Figure 6. Inhibiting the subiculum before learning impacts performance of animals that are previously trained on the RAM task. *(A) Number of visits (left), RME (centre) and WME (right) during training. For visualisation purposes, group 1 refers to the animals that were infused with saline on the first test (and consequently with muscimol on the second), while group 2 referes to those infused with muscimol on the first test (and saline on the second). Dotted grey line shows chance level with zero WME. (B) After the training period, animals underwent two "test" periods of 4 days each, so that both groups would receive both the muscimol and saline infusions (see Methods). Top left: total number of visits across the 4 days for the two "test" phases. The difference between groups was tested with a paired t-test. Top right: mean number of visits for each group across days. Grey dotted line represents chance performance with perfect working memory. Bottom left and right: mean RME and WME, respectively, for both groups across days. All comparisons of groups across days were made using an ANOVA design. Error bars represent SEM. Significance levels: * $p < 0.05$, ** $p < 0.01$.*

The results highlighted above indicate that there is a general impairment in the muscimol group in all three measures of performance on the first day of “tests”, with an additional impairment on the following treatment-free day for both number of visits and RME, which is not explained by differences in performance during the training phase. This aligns with the results found in *Experiment 1*, as it shows an involvement of the dorsal subiculum in both working and reference memory. It also adds to it by eliminating the confound given by the ability of the rat to learn the rules of the task. Thus, despite training, the task remains subiculum-dependent.

3.2. Inhibiting the dorsal subiculum after acquisition on a second RAM does not show any performance deficits

The second part of *Experiment 3* of this behavioural study aimed at testing the ability of the muscimol-infused cohort to perform the task after being familiarised with its rules, when the subiculum is inhibited during consolidation (i.e. working memory should remain intact). To do so, 12 new animals were trained drug-free for 7 days on the RAM, followed by 4 days of the task in a second maze, located in a different room, in which drug administration was carried out at the end of all trials on day 1. As the consolidation block carried out in *Experiment 2* highlighted a possible delay in the effect of treatment, the “test” phase was only performed once.

As both the control and treatment groups underwent a period of drug-free training, there were likely no differences in performance between the two groups. To verify that this was the case, the performance of both groups on the last day (day 7) of training was considered. The analysis of the three measures of performance was evaluated through two-sample t-tests, which each revealed no significant differences between the two groups (visits: $t = 1.327$; $df = 10$, $p = 0.214$; RME: $t = 1.42$, $df = 10$, $p = 0.186$; WME: $t = 0.826$, $df = 10$, $p = 0.427$; ***Figure 7A***). This analysis was then extended to the rest of the training period, to check any possible differences in the overall ability of the animals to learn the task. The mixed repeated measures ANOVA analysis of each of the three performance measures revealed no effect of treatment across days (group effect in number of visits: $F(1,10) = 1.499$, $p = 0.249$; RME; $F(1,10) = 1.523$, $p = 0.245$; WME: $F(1,10) = 0.605$; $p =$

0.455. Interaction effect in visits: F(6,60) = 0.198; p = 0.976; RME: F(6,60) = 0.142, p = 0.99; WME: F(6,60) = 0.204, p = 0.974). The only significant result was found as a main effect of day, consistent with the animals learning the task (effect of day in visits: F(6,60) = 69.615, p < 0.001; RME: F(6,60) = 108.935, p < 0.001; WME: F(6,60) = 30.567, p < 0.001). Post-hoc pairwise t-tests for each group showed an improvement in performance between day 1 and day 7 for each measure (t and p values for group 1 in visits, RME and WME, respectively t = 10.8, 12.1, 5.86, p <0.001, p < 0.0001, p < 0.01; for group 2 = 14.8, 14.8, 9.58, p < 0.0001, p < 0.0001, p < 0.001; all df = 5; p values computed with Holm-Sidak correction; see ***Figure 7A***). These results indicated an improvement in performance between the first and last day of training for both groups.

Similarly to *Experiment 2*, as no treatment was carried out on the first day in the second room, it was assumed that the two groups would not differ in performance on this day. This was verified by a t-test conducted on the three measures mentioned above on day 1 of the "test" phase, which revealed no significant differences (visits: t = 0.212, df = 10, p = 0.835; RME: t = 0.275, df = 10, p = 0.788; WME: t = 0.311, df = 10, p = 0.762; results shown as inserts to the left on ***Figure 7B, top right and bottom***). For this reason, the following analysis will only consider days 2-4 of the "test" phase.

As anticipated, WME did not differ across the two groups when the task was carried out in the second room (effect of group: F(1,10) = 0.334, p = 0.576; day: F(2,20) = 2.087, p = 0.150; group *x* day: F(2,20) = 1.379, p = 0.275; ***Figure 7A, bottom right****).* However, the analysis of both number of visits and RME also revealed no significant effect of treatment across the three post-treatment days (visits: effect of group: F(1,10) = 0.01, p = 0.923; day: F(2,20) = 4.698, p < 0.05; group *x* day: F(2,20) = 1.158, p = 0.334; RME: group effect: F(1,10) = 0.116, p = 0.741; day: F(2,20) = 4.542, p < 0.05; group *x* day: F(2,20) = 0.587, p = 0.565; ***Figure 7A, top right and bottom left***). This result was supported by the analysis of the total number of visits on the task (days 2-4 only), which did not reveal any significant difference between the two groups (unpaired t-test: W = -0.146, df = 10, p = 0.885; ***Figure 7A, top left***).

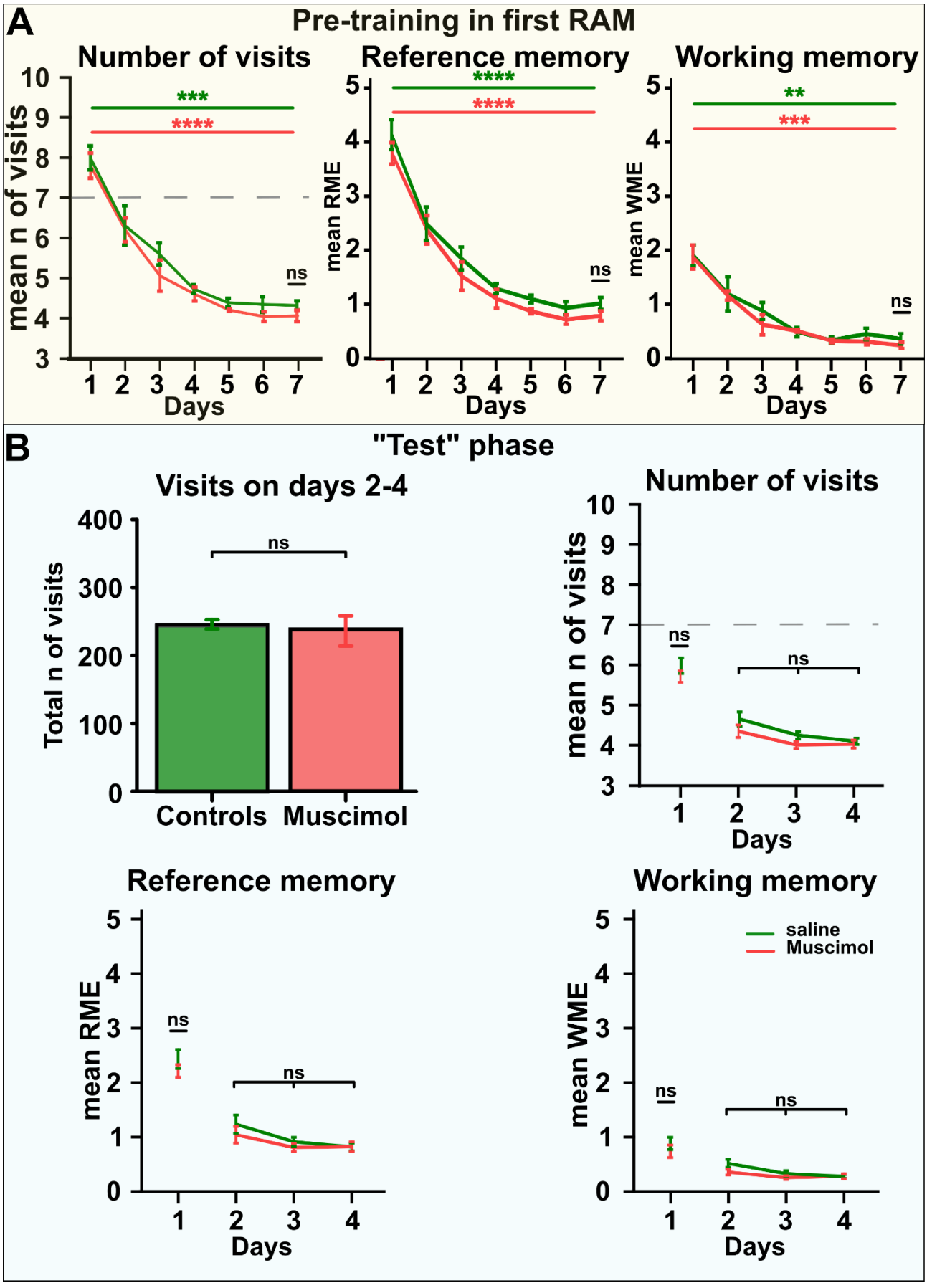
A
Pre-training in first RAM
Number of visits
Reference memory
Working memory
mean n of visits
mean RME
mean WME
***
****
**
ns
Days
B
"Test" phase
Visits on days 2-4
Total n of visits
Controls
Muscimol
Number of visits
Reference memory
Working memory
saline
Muscimol

Figure 7. Inhibiting the subiculum after learning does not impact performance when animals are trained on the RAM task. *(A) Number of visits (left), RME (centre) and WME (right) during training. Dotted grey line shows chance level with zero WME. (B) After the training period, animals underwent a "test" period of 4 days, in which infusions were carried out at the end of day 1 (see Methods). Top left: total number of visits across the 4 days for the "test" phase. Performance of the two groups was performed with a paired two-samples t-test. Top right: mean number of visits for each group across days. Grey dotted line represents chance performance with perfect working memory. Bottom left and right: mean RME and WME, respectively, for both groups across days. Differences among groups across days were computed with ANOVA designs. Error bars represent SEM. Significance levels: ** p < 0.01, *** p < 0.001, **** p < 0.0001.*

In order to clarify that the results truly confirmed the null hypothesis of there being no difference between the two groups, the Bayes factor was calculated for each ANOVA analysis. Bayes factors are usually implemented to provide positive evidence for a lack of an effect (see Jeffreys, 1998), and can be implemented on a linear model formula (see *Methods*). The results of the analysis indicate strong evidence for the null hypothesis (i.e. no difference between the two groups; visits: bf = 10.39; RME: bf = 67.95). The only result that was not confirmed was the WME ANOVA (bf = 0.59).

3.3 Prolonging the "test" phase to check for delayed effects

Experiment 2 of this chapter highlighted a delayed effect on performance compared to when the treatment was administered (see above). The results presented in the previous paragraph show a different phenomenon, in which training the animals before "testing" them on a second RAM shows no difference in performance up to 3 days after muscimol delivery. To exclude the possibility that a consolidation block could only show an effect after day 4 of the "test" phase, a subset of animals (n = 8) performed an extra 2 days in the new RAM, for a total of 6 days. Of these 8 animals, 1 did not complete all 6 days, so the following mixed ANOVA analyses (between: groups, within: days) was computed on a sample size of n = 4 for the control group, and n = 3 for the treatment group.

Considering the imbalance in sample sizes, it was decided to repeat the task a second time (similarly to what was done when inhibiting acquisition, see the start of this section). The task was then run a second time, counterbalancing the two groups so that each rat received both a muscimol and a saline infusion in the two "tests". Administration of either muscimol or saline was given at the end of trials on day 1. Mean number of visits, mean RME and mean WME were computed for the control and the treatment groups, so that a total of n = 14 was reached for both groups. Welch t-tests tests were computed for day 1 of "tests" between the two groups to assess any pre-drug differences in performance. All tests revealed no significant differences (visits: t = -1.337, df = 11.93, p = 0.206; RME: t = -0.973, df = 10.876, p = 0.351; WME: t = -1.209, df = 11.145, p = 0.251; see ***Figure 8***), so the following analysis considered only days 2-6 for both tests.

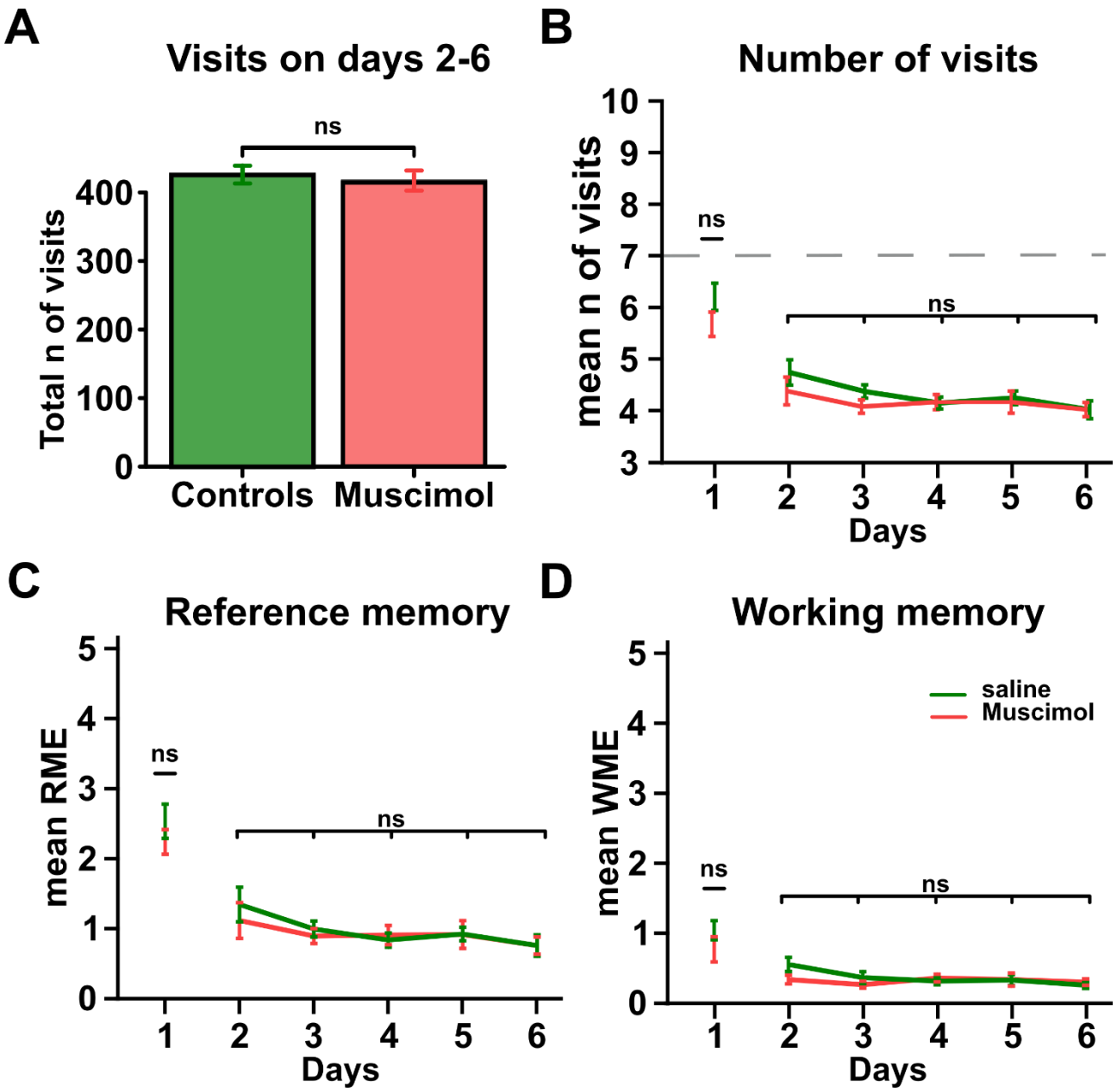

Figure 8. Extending the test phase after the consolidation block does not show differences between the treatment groups. *(A) Total number of visits for the two groups on days 2-6 of the two test phases together. The difference between the two groups was evaluated with a Welch t-test. (B-D) Number of visits (B), RME (C) and WME (D) during the two test phases. Dotted grey line shows chance level with zero WME. All comparisons of groups performance across days were computed with an ANOVA design. Error bars represent SEM.*

A two-way repeated measures ANOVA (within factors: group and days) was performed. As it was the case for the analysis that carried out only 4 days of test, the addition of two more days in the test phase did not show any significant effect of treatment across days (visits: effect of group: $F(1,30) = 1.532$, $p = 0.225$; day: $F(4,24) = 3.9$, $p < 0.05$; group *x* day: $F(4,30) = 1.006$, $p = 0.420$; RME: group effect: $F(4,30) = 0.585$, $p = 0.450$; day: $F(4,24) = 5.882$, $p < 0.01$; group *x* day: $F(4,30) = 0.559$, $p = 0.694$; WME: group effect: $F(1,30) = 1.609$, $p = 0.214$; day: $F(4,24) = 1.814$, $p = 0.159$; group *x* day: $F(4,30) = 2.044$, $p = 0.113$; see ***Figure 8B-D***). Again, this was supported by a Welch t-test on the total number of visits between the two group (considering only days 2-6), which did not show any significance ($t = -0.471$, $df = 11.629$, $p = 0.646$; ***Figure 8A***). The Bayes factor analysis indicated moderate evidence (visits: bf = 3.56; RME: bf = 5.73), with anecdotal evidence for the WME results (bf = 2.22).

Discussion

The three experiments detailed above set out to test the dependence of the subiculum on reference memory. These experiments first confirmed that the subiculum plays a role in spatial memory: inactivation of this structure prior to learning (*Experiment 1 and first part of Experiment 3*) gave rise to poorer performances across days in a RAM task, relative to controls. This impaired learning was quantified through increases in both WME and RME, the latter of which persisted into non-treatment days. However, as argued above, impairments in reference memory may solely occur as a result of disrupted working memory which, in turn, renders the task of memorising goal locations harder. To circumvent this issue, subicular inactivation was performed during post-learning rest, an epoch in which the hippocampal formation is believed to play a critical role in consolidation of long-term spatial memory (Riedel et al., 1999). Here, *Experiment 2* indicated a role for the subiculum in consolidation (and hence long-term spatial memory itself), at least when the task was novel to the animal. However, training the animal to the task removed this effect, so that learning proceeded at a similar rate between the “consolidation block” and the control groups (*second part of Experiment 3*). These data suggest that the subiculum plays a complex role in long-term memory, however further experiments will be required to delineate its function.

1. Inhibiting the dorsal subiculum prior to learning disrupts working memory performance on a spatial memory task

The aim of this study was to test the involvement of the subiculum in spatial long-term memory formation. As discussed in the *General Introduction*, previous work on the role of the subiculum has found deficits in working memory (Cembrowski et al., 2018; Morris et al., 1990; Potvin et al., 2007), pattern separation (Potvin et al., 2009), and reference memory (Bolhius et al., 1994; Morris et al., 1990). However, others have cast doubt on the role played by the subiculum in reference memory (Cembrowski et al., 2018; Galani et al., 1998). The results of this chapter suggest that the subiculum is at least critical for working memory, whether the animal is performing a novel task in a familiar environment (*Experiment 1*), or in a familiar task with novel reward locations (first part of *Experiment 3*). Indeed, the data from these experiments show that the inactivation of the subiculum with muscimol prior to learning causes the animal to revisit, within a trial, arms that had already been explored (i.e. WME), at a rate greater than controls. This effect was relatively acute, i.e. restricted to the day in which the subiculum was inhibited, which is consistent with an impact on working memory itself, rather than an indirect effect on spatial memory. In contrast, rats infused with muscimol continued to show signs of poor reference memory performance (assessed by the animals visiting non-baited arms) in the days after infusions had ceased, while working memory performance was indistinguishable from controls.

The precise role of the subiculum in spatial working memory is yet to be elucidated. Previous work indicates that regions of the hippocampus which are upstream of the subiculum are required for spatial working memory, whether using the T-maze (Bannerman et al., 2002; Potvin et al., 2006) or the RAM (e.g. Davis et al., 1986; Mahmmoud et al., 2015). Subsets of neurons in the CA1 (Wood et al., 2000) and in the subiculum (Kitanishi et al., 2021), as well as the MEC (Frank et al., 2000; O'Neill et al., 2017) and prefrontal cortices (Ito et al., 2015), all show prospective coding known as "splitter cells" during working memory tasks. Here, changes in rate predict the future choice of the animal when traversing a T-maze, and have been linked to assembly coding of working memory processes (Varga et al., 2024). The subiculum could represent a conduit, or relay, of this spatial coding, conveying information inherited from the CA1 region to cortical and subcortical areas. Conversely, the subiculum could generate independent mnemonic processing, with distal parts of the subiculum perhaps comparing MEC and proximal CA1

encoding of working memory. Future experiments aimed at disentangling these possibilities would involve silencing the CA1, or its inputs to the subiculum, combined with electrophysiological recordings. Optogenetic methods allow for silencing of synapses (e.g. Zhang et al., 2007), granting a possibility for the experimenter to (1) test the behavioural impacts of the CA1-subiculum pathway, and (2) characterise the change in subicular firing patterns during a working memory task (see *General Discussion*).

However, inhibition performed immediately before the task does not solely impact working memory. Indeed, muscimol treatment resulted in a deficit of reference memory, in both *Experiments 1* and *3*. Working and reference memory could be independent yet competing processes on the memory function. According to Sanderson and Bannerman (2012), working and reference memory are dissociable components of spatial information processing. Working memory relies on the timeframe of exposure to the stimulus, with more recent stimuli creating stronger memory traces (see *General Introduction)*. Reference memory, on the other hand, relies on the strength of the association between the stimulus and its context. These two processes, according to the authors, rely on different cellular mechanisms. Moreover, according to the SOP theory (Wagner, 1976, 1981), these two processes compete with each other: visiting an arm in the RAM would store that information in short-term memory, which would render the visited arm "unsurprising" and would then reduce the amount of attention paid to it. This would in turn prevent a long-term memory of the arm to be generated, as this memory depends on the strength of the association between a stimulus and its context (which relies on repeated exposures).

This theoretical framework would explain the results found in *Experiments 1* and *3* when inhibiting the subiculum prior to learning. Specifically, the deficit found in reference memory (as assessed by RME) could in fact indirectly reflect an inability of the animals to store in memory the position of the visited arms. Thus, while performing WME (i.e. re-entering a visited arm), animals would increase their number of RME as well, as their re-visits could either be to baited or unbaited arms.

2. Inhibiting the dorsal subiculum disrupts reference memory

The data presented in this chapter shows that RME increase when the subiculum was silenced. This effect continued into subsequent drug free behavioural sessions, indicating that ability of the animals to encode goal locations into long-term memory was impaired. The arguments presented here suggest an important role for the subiculum, as the output structure of the hippocampus, in system consolidation of long-term memory. Indeed, sharp-wave ripples (SWRs) are present in the subiculum which are a hallmark of hippocampal-dependent memory consolidation process (Buzsáki, 2015; see *General Introduction*). Moreover, the subiculum likely provides an important conduit between the hippocampus and the cortex, and can even generate SWRs independently of the CA1 (Imbrosci et al., 2021) In spite of this expectation, previous reports have provided a somewhat mixed picture in terms of its involvement in these memory processes. Morris and colleagues (1990) show that the subiculum is required to acquire new spatial reference memories over days, using the MWM task. However, it is unclear how the observed deficits in the experiment related to a disruption of subicular reference memory processing, or indirectly through working memory processes (see discussion above), for example. On the other hand, the disruption of consolidation processes would leave encoding during learning untouched. Thus, a disruption during rest periods would enable us to assess the subiculum's role in long-term memory, independent of incidental impacts on working memory, or on spatial memory encoding in general.

Experiment 2 shows that silencing the subiculum does give rise to increased RME during subsequent learning, albeit on the 5th and 6th day of learning (see ***Figure 4***). Consistent with this, treated animals also travelled further to collect rewards, on each trial. At first glance, this seems counter to expectations, given that day 2 is the first post-treatment learning session. An explanation can be provided by considering the processes driving performance across each day of learning. On the first day, when exposed for the first time to the task, rats must start to learn the associated rules, such as knowing that only three out of the eight arms contain food. Indeed, an animal performing the task with perfect working memory would complete the task in 7 trials, while an animal without a functioning working memory would require at least 12 trials to gather all the rewards (see ***Figure 3B, insert on the right***). Indeed, in all experiments, the average performance of control animals is above or around 7 visits. In *Experiment 1*, where the aim was to inhibit the

subiculum prior to learning (thus impacting working memory performance), the muscimol-infused animals visited around 10 arms on day 1, and around 9 on day two (the two days in which infusions were carried out). This goes in accordance with our Monte Carlo predictions, in which animals that performed at least 1 WME would visit more than 7 arms. Then, after day 1, the animals will increasingly rely on reference memory to complete the task, rather than working memory. This is clear both in the control groups of *Experiments 1 and 2*, where the number of visits on days 2 onward become lower and lower. Thus, degraded performance caused by disrupting the consolidation of learnt goal locations might be revealed in later behavioural sessions, as the animal becomes more reliant on reference memory. Consistent with this idea, treated animals in *Experiment 2* showed no improvement in performance between day 3 and day 6, while control animals showed a day-to-day improvement (***Figure 4D***). Disentangling when the animal becomes more reliant on subicular reference memory encoding in the task could be investigated further through modelling approaches.

A second possibility is that the subiculum is important in consolidation processes for remote recall. Previous work has shown that disrupting CA1 neuronal activity in sleep affects recall in the behavioural session that immediately follows it (e.g. Ego-Stengel & Wilson, 2010; Girardeau et al., 2009; Gridchyn et al., 2020; Jarrard, 1995). However, consolidation is a process that occurs over days and months. Memories for places and events are thought to switch from hippocampal dependence to becoming more reliant on cortical structures, particularly the prefrontal cortex (Dudai, 2004; Frankland & Bontempi, 2005; Marr, 1971; McClelland et al., 1995). The hippocampus would then play its main role in memory consolidation by encoding and storing information for limited periods of time, as opposed to the neocortex, which stores information for longer periods. In this scheme, subicular activity could facilitate coordination of hippocampal-cortical dialogue during sleep. Here, the effect of subicular disruption would only be revealed slowly, as the cortex is recruited for memory storage. Nevertheless, our behavioural paradigm cannot allow us to distinguish whether subicular activity in sleep supports more remote recall, or if the effect on performance is only revealed when the animal is reliant on reference memory (as discussed above). Clarification will first require expanding the sample size of *Experiment 2*. Indeed, while the sample size was sufficient to demonstrate a difference between treated and control groups, greater numbers will be required to draw more conclusions. First, to provide confidence in the main result, and second to reveal whether there are

small differences in performance on days 3 and 4, currently masked by the variance in the data and the small sample size.

Recent work shows that CA1 activity in sleep is required for later or remote recall of memories that are often regarded as hippocampal independent (Sawangjit et al., 2018). Here, the subiculum could be involved in consolidating non-spatial aspects of the task, without playing a direct role in encoding of goal locations. In this scheme, the subiculum might be critical for spatial working memory processing. Inactivating the subiculum during learning would then directly result in WME and, indirectly, in RME. However, a further possibility is whether the disrupted consolidation processes could relate to spatial components of the task, or perhaps non-spatial learning, for example the task rules. A corollary for this idea is the NMDA dependence of the Morris water maze (Bannerman et al., 1995).

3. The influence of training in subicular inhibition

To address the possible influence of training in the ability of subiculum-impaired animals in the RAM task, animals were first trained to “expert” levels of performance and the impact of silencing the subiculum was tested on spatial working and reference memory on a second RAM. This “raining” clearly improved performance, as can be seen in ***Figures 6 and 7***. Armed with this data, the hypothesis was that inhibiting the subiculum between days 1 and 2 would reveal a difference in performance on the day following the treatment, in contrast to the results of *Experiment 2*. However, no difference in performance was found between the treatment and the control groups, even when the test had been extended for a further 2 days, or when it was replicated a second time in the first RAM room.

Several explanations could reconcile the discrepancy between *Experiments 2* and *3*. First, the subiculum’s role in consolidation could be more pronounced when the task is relatively novel, as in *Experiment 2*. Data gathered in rodents show that CA1 reactivation during SWRs prioritises spatial coding of novel environments (O’Neill et al., 2008; Van De Ven et al., 2016). Here, CA1-driven reactivation or replay would prioritise newly formed

assemblies, which then would select maze-related coding in the subiculum for replay. In this scheme, reactivation in the subiculum might decay with experience. Electrophysiological recordings in the subiculum during learning and sleep (see *Chapters 4* and *5*), as well as joint recordings between the CA1 and the subiculum, could shed further light on the issue (see *General Discussion*). That said, CA1 assemblies representing novel goal locations are preferentially recruited during sleep, even in familiar environments and tasks (Dupret et al., 2010).

In addition, the dorsal subiculum does not provide the only hippocampal route to cortical structures. For example, the dorsal CA1 projects to the MEC via the nucleus reunions, a pathway implicated in memory consolidation (see Cassel et al., 2013; Frankland & Bontempi, 2005). At the same time, the CA1 also directly projects to layer V of the EC (Van Groen & Wyss, 1990), where cells fire during SWRs (Chrobak & Buzsáki, 1996), and where joint replay with CA1 cell assemblies is shown (Ólafsdóttir et al., 2016). Finally, the intervention carried out in this chapter affected the dorsal subiculum, while sparing the ventral compartment. Recent work implicated the ventral subiculum in consolidation of spatial information in a MWM task (Torromino et al., 2019). In this way, consolidation of spatial memory may occur through multiple routes. This raises the intriguing possibility that different components of hippocampal consolidation processes are broadcasted to the neocortex, across different timescales, which is addressed in the *General Discussion* of this thesis.

It also remains possible that aspects of the task cease to become solely hippocampal dependent with training, and instead rely more on egocentric responses (Packard & McGaugh, 1996). While a spatial strategy would presumably be required to locate the first baited arm, each animal could subsequently “respond” by turning in the direction of that arm. In this way, the task may become less sensitive to subicular disruption during rest. This idea is compatible with the deficits seen when inhibiting the subiculum prior to the beginning of the task (which shows subicular dependence). Here, disruption of reference memory during this manipulation may be mediated solely through working memory deficits, as described above.

Finally, this chapter’s data is consistent with the idea that the subiculum activity during rest promotes consolidation of task features, beyond goal location. In this way, long-term

memory formation of the task becomes less subicular dependent, once the animal becomes an “expert”.

4. Conclusions and future steps

The set of experiments carried out in this study shows clear evidence of the involvement of the dorsal subiculum, as previously seen, in spatial working memory, and provides some support of its role in reference memory as well. Increased confidence in these results will require further replications. Additionally, the use of muscimol as our inhibiting agent does not allow us to analyse fully the spread of the drug inside the brain, limiting our understanding of which areas are being affected. Infusing conjugated muscimol in a subset of the cannulated animals showed minimal spread outside the target area (see ***Figure 2***). However, conjugated muscimol has a different molecular weight (muscimol = 114.1 g/mol; conjugated muscimol = 607.46 g/mol). In order to match its concentration to that of muscimol used in this study, as done before by others (see e.g. Nelson et al., 2015), DMSO had to be implemented (a toxic substance for neurons; Galvao et al., 2014) to allow the compound to dissolve in saline. In turn this, to some degree, limits the interpretation of the data when using the labelled drug to characterise the spread of muscimol in the tissue during infusions.

Nonetheless, an important conclusion from these experiments is that the subiculum was confirmed to be involved in performing the task (both in *Experiment* 1 and *3*). This will be crucial for the next part of this thesis, in which the subicular cell activity will be explored through electrophysiology. Initially, the development of this type of task with a “test” phase was conceptualised with the aim of recording subicular activity using tetrodes (e.g. the original hippocampal tetrode study by O’Keefe & Recce, 1993). As tetrodes implants tend to become less stable when recorded from on multiple days (see Quirk & Wilson, 1999), the possibility to have a steep change in performance between day 1 and day 2 of the “test” phase provided the opportunity to record the subiculum during the task and during sleep. In this way, significant changes in performance could be correlated to subicular network activity, while maintaining stable recordings. However, the results presented above do show evidence of the subiculum playing a role in consolidation, while the

animals gradually learned goal locations when the task itself was novel (*Experiment 2).* Therefore, an alternative electrophysiology approach was implemented, with the aim of recording neuronal firing patterns from the same population of cells over several days, as described in the next chapter.

Chapter 3 - implementing a chronic probe recording technique to explore the electrophysiological characteristics of the dorsal subiculum

Introduction

In the introduction to this thesis, the subiculum has been described as one of the principal outputs of the hippocampal formation, conveying spatial information to other brain structures (Aggleton & Christiansen, 2015). On a broad scale, the subiculum can be characterised by two distinct regions: the ventral subiculum, shown to be involved in the stress-response system (Herman & Mueller, 2006); and the dorsal subiculum, which has been shown to prevalently encode spatial information (as highlighted by a series of lesion studies conducted by Potvin et al., 2006, 2007).

The experiments outlined in *Chapter 2* brought forward the notion that inhibiting the dorsal subiculum affects both working memory and reference memory. That is, silencing this structure during rest (when memory consolidation is thought to occur; see *General Introduction*) impairs learning across days. While these behavioural results provide some support for the idea that the subiculum is involved in long-term spatial memory processing, the type of role that this might be remains unclear. As previously discussed in the *General Introduction*, electrophysiological work in the CA1 region has demonstrated the critical network mechanisms that underline online and offline spatial memory processing, however little work has been undertaken to characterise subicular network activity.

Like the neighbouring CA1 region, the subiculum contains neurons with a great degree of spatial selectivity. However, these neurons exhibit a wider array of firing properties (Sharp & Green, 1994; but see *General Introduction*), providing a broader representation of the geometric relationships between locations in an environment. These include, among others, place cells and diffusely firing spatial cells (Sharp, 1997), boundary-vector cells (Lever et al., 2009), vector-trace cells (Poulter et al., 2021), and, most likely, grid cells (Brotons-Mas et al., 2017). This complex mix of spatial firing patterns has been suggested to be a coding scheme for efficient communication of spatial information to other brain regions (Kim et al., 2012). Nevertheless, the precise involvement of the dorsal subiculum

in spatial memory processing remains unclear, and nothing is known regarding its network activity across multiple days of learning.

Electrophysiology as a tool to study the brain

Experiments 1-2 in *Chapter 2* attempted to establish a spatial learning paradigm that was sensitive to disruption of the subiculum. *Experiment 3* showed that muscimol infusions into the subiculum during post learning rest had no effect on consolidation of spatial memories of a familiar task, where the animal can reach asymptotic performance within 1-2 days. However, each of these experiments supported the idea that the subiculum plays a role when spatial locations are gradually learnt over the course of several days. It was therefore critical to establish a recording method that enables the tracking of the same subicular units across multiple days. In turn, this will enable the characterization of neuronal activity during maze running and sleep, as the animal gradually learns across days.

In order to understand the information processing that the brain undergoes through electrical signals a variety of different experimental techniques have been developed over the years. These go from measures of intracellular recordings such as voltage clamp, current clamp, and patch-clamp to more brain-wide techniques such as electroencephalography (EEG; see ***Figure 1A-B***). In the field of spatial memory studies in rodents, one of the most popular techniques involves the use of micro-drive arrays of electrodes. First implemented in the hippocampus by O'Keefe and Dostrovsky (1971) to record place cells, these arrays allow detection and discrimination of multiple neurons at the same time by the use of several movable microelectrodes. Electrodes ranged from the 5 initial single-wired ones implanted by O'Keefe and Dostrovsky, to the later implementation of the *tetrode* technique, where 4 electrodes are twisted, which improves both spike separation (into single units) and cell yields (see O'Keefe & Recce; 1993; ***Figure 1C***). Currently, laboratories can implant up to 256-channels drives in the rat (64 tetrodes; Sheng et al., 2021). This allows the experimenter to target with precision multiple structures in the same animal, even when performing complex freely moving behaviour, at a reasonably low cost (Voigts et al., 2020).

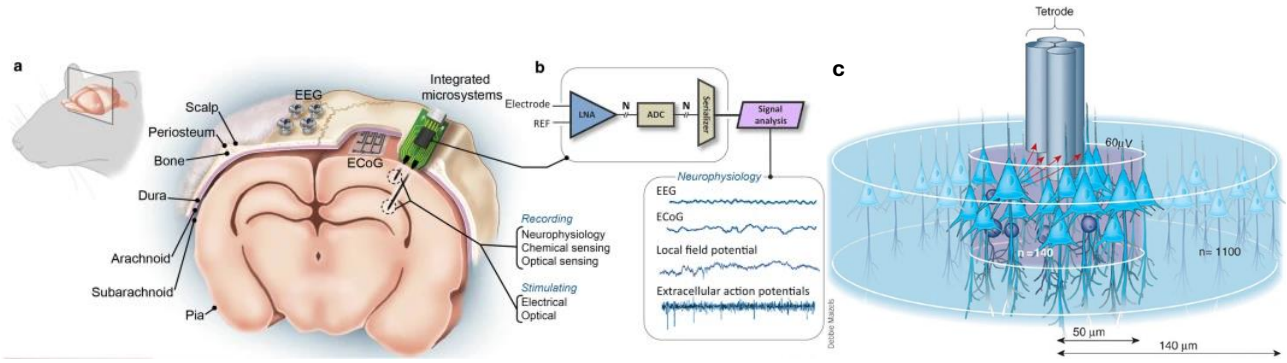

Figure 1. **A variety of electrophysiological techniques can be used to explore the properties of neurons in the brain.** *(A-B) Illustration of a rodent brain and the techniques that can be implemented to study its activity, namely EEG and intracortical microelectrodes. Figure taken from Seymour and colleagues, 2017). (C) Schematics of a tetrode lowered into a layer of pyramidal cells (blue triangles). The red arrows indicate the distance of the four electrodes form a single neuron. The grey cylinder represents the radius (50 μm) inside which spike amplitudes of different neurons are large enough to be separated by clustering. The blue cylinder (14 μm) encapsulates the distance at which neurons can still be detected, albeit with a decreased spike amplitude. Figure taken from Buzsáki (2004).*

One key disadvantage of these micro-drives lies in their difficulty to guarantee stable recordings of individual neurons across days, due to the necessity to move the tetrodes daily to avoid neural degradation or glial migration (Voigts et al., 2020; Zhang et al., 2023). While certain analysis methods claim to produce recording of individual neurons in the span of several weeks (Dickey et al., 2009), silicon probes have recently emerged as an alternative tool for chronic recordings of the same set of neurons.

Probe recordings

Silicon probes can be single or multi-shanked and contain hundreds of electrodes positioned along their length (up to 384 for the Neuropixels probes; see Jun et al., 2017). The possibility to record from a higher number of channels can confer these probes with a larger unit yield than tetrode recordings. They also offer the possibility of higher throughput experiments, by saving on the time and expertise needed for building and implanting the system. Indeed, movable tetrodes can require days or weeks to reach the desired target, while static probes only require one surgery (Voigts et al., 2020). Additionally, implantation of silicon probes offers the possibility of reduced tissue damage, with shank thicknesses as narrow as 15 µm which cause tissue displacement comparable to a single wire electrode (Bragin et al., 2000).

While various companies have developed moveable silicon probes to study the hippocampus (e.g. Buzsáki et al., 1992; Chrobak & Buzsáki, 1996; Ylinen et al., 1995), other companies have focused on developing probes that could be fixedly implanted in an animal's brain, such as the Neuropixels probes. This technique has the potential to precisely target a specific area of the brain without the need to move the electrode in place after surgery. Previous reports also suggest this brings increased recording stability after recovery from surgery, as discussed in the next paragraph.

Neuropixels 1.0 probes

The first generation of Neuropixels (NPX 1.0) probes was tested and published in 2017 (Jun et al., 2017). As mentioned by the authors, these probes were developed with several aims. First, to achieve a wide amount of recording sites for the isolation of multiple neurons, while also minimising the tissue damage that can be caused by the probe insertion in the brain. Moreover, to minimise the noise, maximise the resistance to artefacts and other interference, and build up the efficiency of data transmission. Lastly, to enable the possibility to achieve stable recordings in the long term, while reducing the costs of fabrication.

This led to the development of single shank, 10-mm long probes that contain 960 recording electrodes. The electrodes are placed 13 µm apart from each other in a checkerboard fashion, for a total of 1 cm shank length and 70 x 20 µm thickness (***Figure 2A-B***), and a total weight of around 250 mg. Of the 960 available sites, 384 can be recorded from simultaneously. The data collected is integrated and multiplexed by the probe, which then enables the data to be conducted via a single thin cable (***Figure 2C***), only containing a single signal channel and ground. The resulting data, including both action potential and local field potential amplified and digitised bands (AP: 30 kHz; LFP: 2.5kHz), can then be visualised and recorded with open-source platforms such as SpikeGLX (http://billkarsh.github.io/SpikeGLX/) or OpenEphys (Siegle et al., 2017). Spike-sorting can then be achieved through the KiloSort framework, which is a quick and accurate method of generating data from recordings in a high number of channels (Pachitariu, Steinmetx, et al., 2016).

NPX 1.0 probes have so far been utilised prevalently to record in head-fixed rodents, mostly in mice (see Jun et al., 2017; but also Evans et al., 2018). The technique of insertion requires the animals to be anesthetised during the procedure, and then to perform a behavioural task with the head fixed in place on a stereotaxic frame while the brain is exposed. Thus, it does not require much thought in designing a holder to protect the probe during the experiment. These recordings have been shown to yield from 20 to up to 200 neurons per brain region, with variability due to the specific morphology of the brain regions selected (for example, an area wider or denser in neurons would logically allow for recording of bigger numbers of cells). In these studies, NPX 1.0 probes have

been shown to be re-useable for more than 10 acute insertions, with minimal loss in signal quality levels (computed as the amplitude of spikes relative to a detection threshold in a 30 seconds section of recording).

Few studies have been performed on freely-moving rodents using NPX 1.0 probes, targeting various structures of the cortex and several subcortical regions (e.g. basal ganglia, amygdala, hippocampal formation; see Ghestem et al., 2023; Luo et al., 2020; Van Daal et al., 2021). The number of reported neurons recorded in these studies can vary in the order of 10-200 cells, depending on the brain region, similarly to what has been recorded in head-fixed experiments. Luo and colleagues (2020) reported that variability in the number of recorded neurons could be due to two main factors. First, the anatomical position, with a higher degree of unit loss in more superficial and posterior brain areas. Second, the shank orientation, i.e. the angle of the plane of the probe relative to the brain surface. Here, the probe's thickness makes it more flexible in the axis that is perpendicular to its plane, and thus the angle of insertion can influence the ability of the shank to move with the brain tissue and reduce tissue damage. In addition to identifying large numbers of neurons in a single region, these probes can also help in visualising structural boundaries across regions through measures of neural activity.

Three main studies performed across several days were mentioned by Jun and colleagues (2017), two of which performed on rats. These experiments claimed a good performance of the probes for up to 8 weeks, as assessed by number of spikes recorded (above noise level) and total firing rate. It is important to note that these recordings were usually brief (5-10 minutes a day reported for one of the experiments) and the clustering was computed on each day separately, thus ignoring whether the activity recorded during different sessions belonged to the same neurons. Similarly, other studies have performed recordings for longer sessions (from 30 minutes in some, to up to 12 consecutive hours in Ghestem et al., 2023), and produced good quality results. Some of them did not report stability measures across sessions (Gardner et al., 2019; Krupic et al., 2018), but others reported stability in unit count and signal-to-noise ratio (Ghestem et al., 2023), firing rate (Böhm & Lee, 2020), and spike amplitude (Van Daal et al., 2021; see ***Figure 2F***). Nonetheless, in all of these studies, little effort was made to match units across days, thus a minimal assessment of the ability to record the same cells across different days was provided.

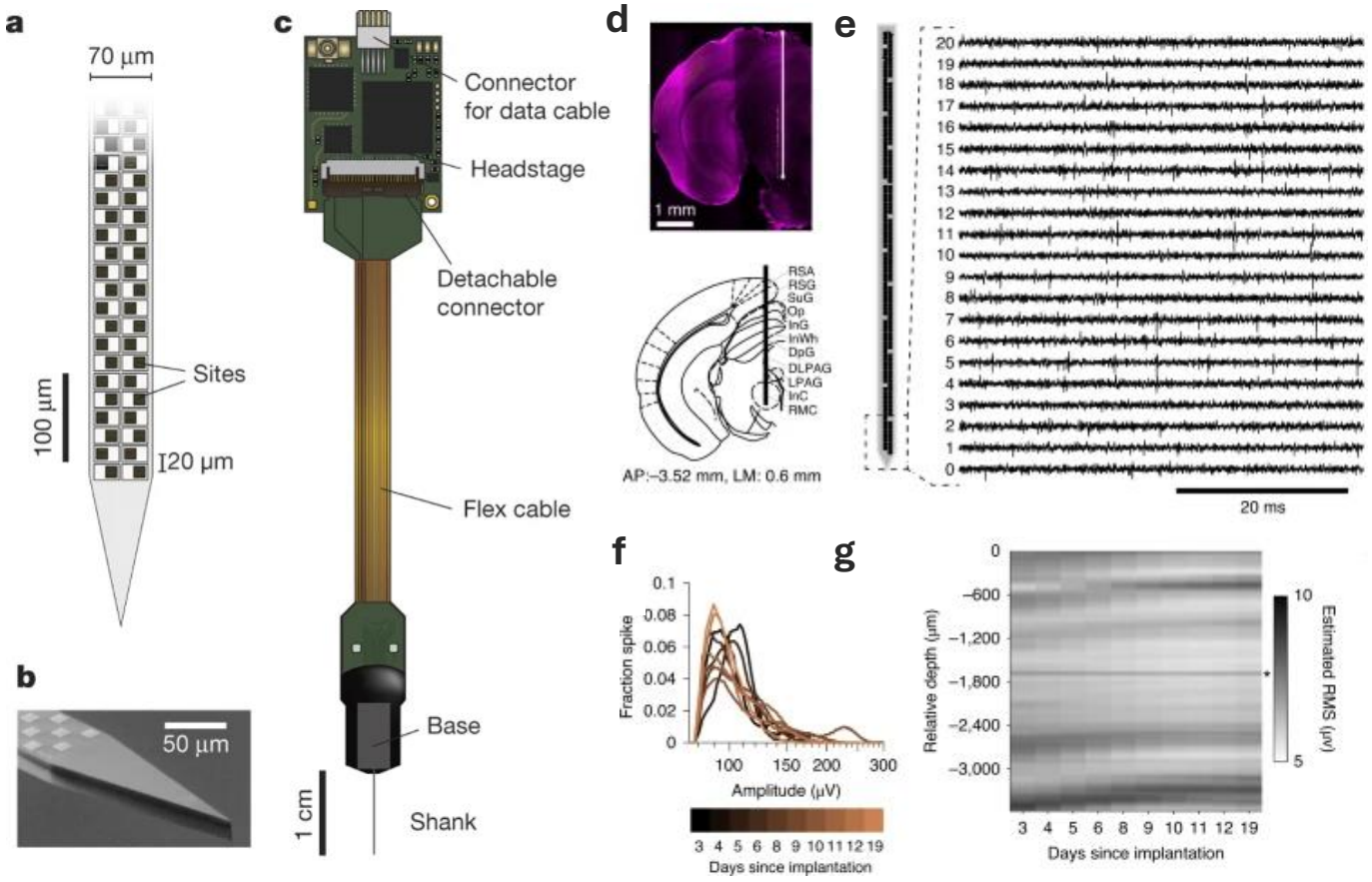

***Figure 2**. **Neuropixels probes are a useful tool to assess neuronal activity in an area**. (A-B) Illustration and microscope image of NPX 1.0 probe tip. (C) Schematics of the NPX 1.0 parts. (D) Histological reconstruction and schematic representation of a probe implanted in a mouse brain. (E) Example of channels voltage traces. (F) Distributions of amplitudes detected over the course of 19 days as a measure of stability of the recording. (G) Estimated neuronal activity relative to the depth of the probe. (A-B-C) taken from Jun and colleagues (2017). (D-E-F-G) taken from Van Daal and colleagues (2021).*

Recordings in the rat's subicular complex across days, to our current knowledge, have only been implemented by two groups (Ghestem et al., 2023; Luo et al., 2020), of which only the second targeted the subiculum proper, while the other aimed at the postsubiculum. Both groups claimed to have developed a sufficiently stable system for chronic recordings. However, Luo and colleagues recorded for only short periods of 10 minutes, while Ghestem and colleagues claimed to have recordings of up to 12-hour blocks. As for the other chronic recording studies mentioned above, the objective of these studies was to assess the ability of NPX probes to record without loss of spike detection, and so no indication was made as to whether it would be possible to identify recordings from the same cells across days.

Neuropixels 2.0 probes

A new version of NPX probes (NPX 2.0*;* Steinmetz et al., 2021) was made available to purchase in 2023. This new version offers the possibility to record from four parallel shanks, instead of just one. This modification allows a better design to record structures that develop perpendicular to the brain surface, such as the hippocampus and its neighbouring regions. The four shanks contain 1280 sites each, organised in a denser (about one-third the size, with centre-to-centre spacing of 15 µm compared to the 25 µm of NPX 1.0), linearised geometry (NPX 1.0 had the sites staggered) that allows post hoc motion correction (performed with the KiloSort 2.5 framework). Of the 5120 total channels, 384 can be recorded from at the same time (similarly to NPX 1.0). The output of the probe is a single wideband of 14-bit data stream, which has been confirmed to be of similar quality to the NPX 1.0's (Steinmetz et al., 2021).

Due to the reduced size and weight (190 mg), NPX 2.0 have been proposed to result in good quality chronic recordings for at least 8 weeks, as measured by the stability of total recorded firing rates across channels, and of clustered neuron count (computed in 20 separate chronic recordings of either mice or rats, see Steinmetz et al., 2021). As an additional consideration to the stability assessments made for NPX 1.0, Steinmetz and colleagues outlined how clustered neurons can be matched between different recordings that are concatenated after acquisition. First, a crucial step relies on the motion correction

algorithm mentioned above, which works under the assumption that spike amplitude decreases across days due to movements of the shanks inside the brain. This assumption was tested in head-fixed mice in which the probe was systematically moved along the dorso-ventral axis. This motion correction algorithm is then implemented automatically when processing the concatenated data with KiloSort, which produces clusters across days independently of their spikes' functional properties. The authors then performed clustering on the separate days and confirmed that the clusters were identified as the same neurons across days by "fingerprinting" the recorded neurons (recorded in the primary visual cortex), which was done by using their unique visual responses to a battery of images (see Steinmetz et al., 2021 for details).

While useful on well-known structures such as the primary visual cortex, this "functional" approach to test the stability of recordings across days could not be implemented in brain regions where the characteristics of the neurons are not so easily identifiable, such as the subiculum. Indeed, it is unclear how features that explain firing pattern of subiculum neurons, such as spatial selectivity or firing rate, develop across time. Moreover, to our knowledge, no recordings of subicular neurons have been performed using NPX 2.0, with the focus being on other regions of the cortex, hippocampus and thalamus.

In order to characterise how network activity in the subiculum changes with learning, this chapter aimed at recording the subiculum using NPX probes during freely moving behaviour performed across the span of multiple days. Both NPX 1.0 and 2.0 were implemented using a modified version of the probe holder designed by Luo and colleagues (2020). First, a method to implant and maintain the probes into the dorsal subiculum of rats for multiple days was established. This method required testing to verify its ability to track the same cells across days. Next, the stability of place coding across repeated exposures to the same environment on different days was quantified. This drift in coding was then examined to show the degree to which it occurred as a result of recording instability, or a physiological change that neurons undergo when coding across time (similar in principle to the visual responses of neurons in the primary visual cortex quantified by Steinmetz et al., 2021). This chapter will give us a first insight into firing properties of neurons in the dorsal subiculum of rats when assessed over multiple days.

Materials and methods

Animals

A total of 5 male rats (*Lister Hooded*, mean age at surgery = 2.86 ± 0.13 m.o.; mean weight = 372.03 ± 32.03 gr) were singly housed in plastic cages, with temperature maintained at approximately 20 °C and humidity at around 40%. Animals were kept on a 12 h light-dark cycle with food and water available *ad libitum*. Prior to the beginning of the experiments, rats were placed on a restricted food diet to maintain 85-90% of their *ad libitum* weight. Access to water was given *ad libitum*. The experiments were performed in accordance with the UK Animals (Scientific Procedures) Act, 1986.

Probe preparation

All parts of the probe implant were adapted from Luo and colleagues (2020) and 3D printed with Vero pure white glossy material (3D Print Bureau). Before surgery, the probe was glued to the internal holder using quick set epoxy adhesive (RS), and a low resistance electrical wire soldered onto the REF/GND input pads (on the probe head for the NPX 1.0, and on the flex cable for the NPX 2.0). A layer of 50% wax+Vaseline was applied on top of the probe base to protect it from anything possibly touching and bending or breaking it. An external chassis was screwed in place to encase all the other components and allow future retrieval. The probe shank was then left to soak in Tergazyme (Alconox) for at least 2 hours, and then in isopropyl alcohol overnight, to ensure the probe shank(s) was completely clean before use. On the morning of the implant, the probe was lifted out of the isopropyl alcohol soak, air-dried, and then lowered into saline solution until before insertion. A schematic of the probe assembly can be found in ***Figure 3A***.

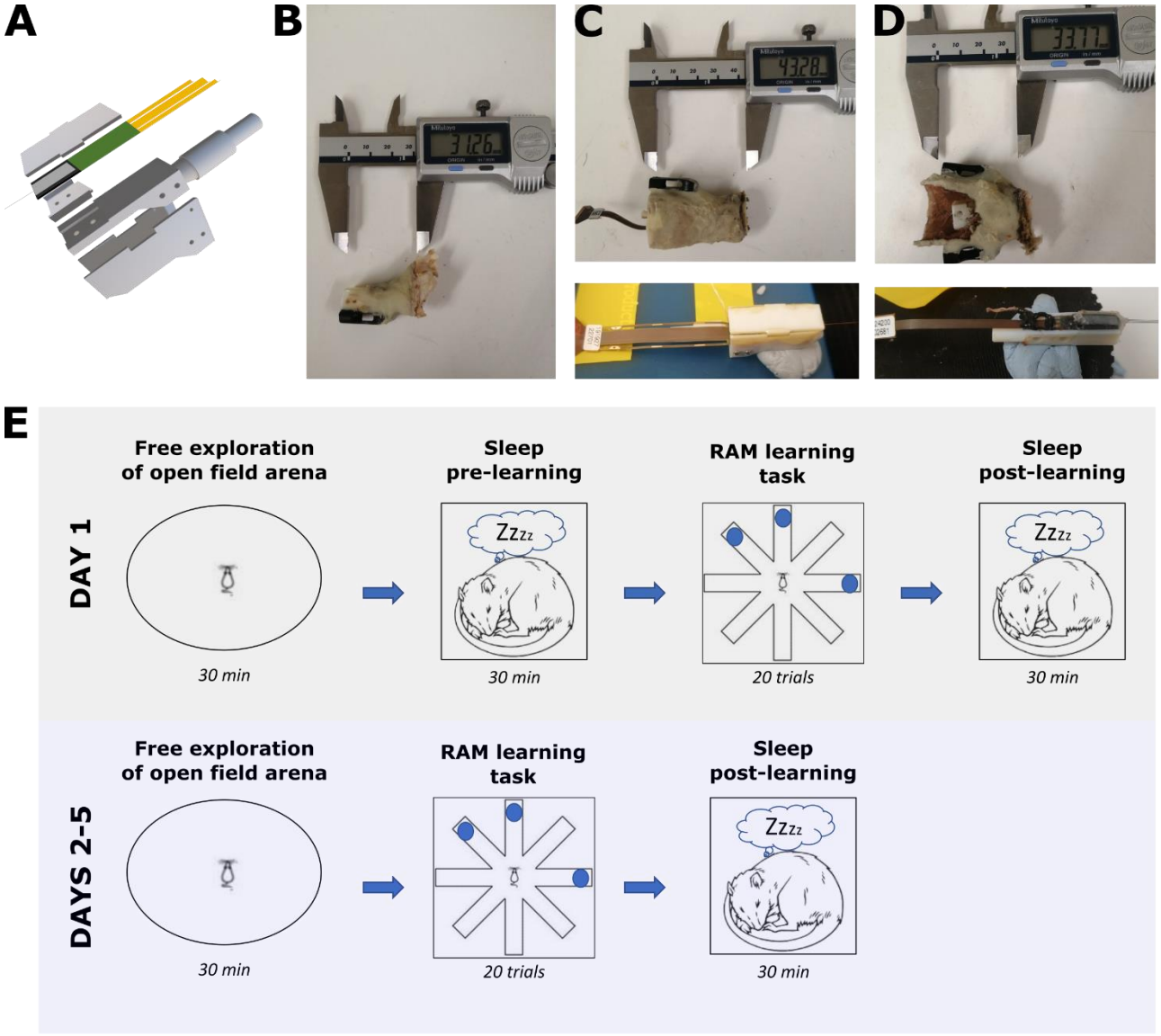

Figure 3. Development of a probe holder design for NPX 1.0 and 2.0 chronic implants in rats. *(A) Shows a schematic of the probe holder design, 3D-printed with Vero pure white glossy material. (B-D) Pictures showing the stages of development of the technique, including the resulting lengths. First, the probe holders were covered in cement, and a layer of copper mesh was applied, to which a clip was attached that would be used to secure the headstage and the LED*

lights. This design, while relatively light and small, did not allow for stable recordings, due to the lack of proper protection from mechanical hits given by the thin layer of cement. The second design, implemented to record from NPX 1.0 probes in this chapter, involves a copper mesh + cement wall separated from the probe holder (seen the insert below the image). This design makes for a bulkier, slightly heavy but more resistant structure. Lastly, an adaptation of this design was made to record with NPX 2.0, which are smaller in nature than the 1.0 counterparts. This adapted design allows for a slightly smaller frame (almost comparable to the first NPX 1.0 design). The two modifications made to this design can be seen in the insert above the picture. First, the modification in shape for the screw holes, which allows for better grip of the screws to the plastic material. Second, the addition of a protective plastic-based layer to cover the points where the ground wires are soldered into the probe flex cable, which allows to reduce possible external noise generated by movements of the electric parts. (E) Shows an example of histology with the visible track of a NPX 1.0 probe (left, red arrow), going across the subiculum, and two coronal slices of the NPX 2.0 animal (right, red arrows show tracks of the 4 shanks). More histology figures and evaluation of probe placement is provided in the next chapter. (F) Schematics of the different stages of the experiment, which was carried out for 5 consecutive days. It involved, on day one, a first period of exploration of an open field, followed by a session of sleep, then the RAM task described in the previous chapter, and lastly a period of at least 30 min of sleep in a sleep box. On days 2-5, the same paradigm was carried out with the exclusion of the first sleep between the open field and the RAM task.

Probe surgery

Rats were anaesthetised with ISO gas at 4% concentration. They were then given Meloxicam (0.06 ml of 5 mg/ml solution; Boehringer Ingelheim) and Baytril (0.2 ml of 20 mg/kg solution) subcutaneously, and Buprenorphine (1 ml/kg in 0.4 mg/ml concentration) intraperitoneally. They were then moved to a stereotaxic frame (David Kopf Instruments) with ISO kept at around 2%. Lidocaine (0.1 ml of 20 mg/ml solution; B. Braun) was administered topically to the scalp during the procedure as an additional analgesic. Of the 5 surgeries, 2 were performed using one single-shank NPX 1.0 probe, 2 were performed with two NPX 1.0 probes inserted bilaterally, and a last one was performed using a four-shanked NPX 2.0 probe (see ***Table 1***).

For the unilateral surgeries, 6 screws were implanted into the skull, two anterior to bregma, two on the contralateral hemisphere to the probe implant site, and two above the cerebellum, acting as reference electrodes. Screws were stabilised with dental cement before a craniotomy was performed above the target region, and the dura cut to expose the cortex. NPX 1.0 probes were lowered at either AP -6.0 and ML -3.0 coordinates, maintaining an angle of insertion of 0 degrees, or at AP -5.76 and ML -2.0, in a 15 degrees angle. The NPX 2.0 four-shanked probe was inserted at AP -5.9, ML -2.7 (shank 1) and AP -6.3, ML -3.3 (shank 4), in a 0 degrees angle on the DV plane. The coordinates for the NPX 2.0 probe would allow to insert the four shanks at a 45 degrees angle in the ML plane, thus allowing each shank to target the dorsal subiculum (as the area has a peculiar shape that extends both in the ML and in the AP planes). See ***Figure 2*** *Chapter 4* for detailed histology.

Animal	*Type of implant*	*Coordinates*	*Angle*	*Success of recording*
#1	*NPX 1.0 unilateral*	*AP -5.76, ML -2.0*	*-15 degrees*	*successful*
#2	*NPX 1.0 unilateral*	*Ap -6.0, ML -3.0*	*0 degrees*	*Successful*
#3	*NPX 1.0 bilateral*	*(L) AP -6.0, ML -3.2*	*0 degrees*	*Successful*
		(R) AP -6.0, ML -3.0	*0 degrees*	*Successful*
#4	*NPX 1.0 bilateral*	*(L) AP -6.0, ML 3.2*	*5 degrees*	*Successful*
		(R) AP -6.0, ML -3.2	*0 degrees*	*Unsuccessful (probe broke during surgery)*
#5	*NPX 2.0 unilateral*	*(Shank 2) AP -6.05, ML -2.9*	*0 degrees*	*Successful*
		(Shank 3) AP -6.15, ML -3.1	*0 degrees*	*Successful*

Table 1. Implant details. *Of the 5 animals, 4 were implanted with NPX 1.0, two of which in a dual implant (one probe per hemisphere). The fifth animal was implanted with a four-shanked NPX 2.0, of which only two shanks were analysed.*

In the bilateral surgeries, 4 screws were implanted into the skull, two anterior to bregma and two above the cerebellum acting as reference electrodes. The coordinates of implantation were AP -6.0, ML either ± 3.2 or + 3.0, and probes were lowered at a 0 degrees angle (with one exception, see details in ***Table 1***).

The position of the probes on the DV axis was monitored by using both the stereotaxic frame, and the live signal displayed on the OpenEphys software. Once the desired target and depth were reached, a layer of 50% wax was applied to completely cover the probe shank(s) and prevent mechanical damage, followed by a thick layer of cement to fix the implant in place. In the latest version of the probes design, a wall of copper mesh was then applied around the implant, with the care of it being separated from any of the probe-and-holder assembly. This would prevent any of the mechanical hits that could be received by the animal moving its head to transfer to the probe. The reference electrodes and the probe reference wires were soldered together onto the copper mesh wall, and the wall covered in enough cement to make it sturdy and resistant to impact.

At the end of the procedure, glucose saline solution was administered subcutaneously, and the rats were left in a heating chamber until awake. They were then transferred to their home cage, in which they underwent a recovery period of minimum 7 days.

Behavioural paradigm

The behavioural design implemented for the freely moving recordings consisted of multiple days of alternating between an open field environment, a radial-arm maze (RAM task described in *Chapter 2*), and sleep sessions (see ***Figure 3E***).

During the surgery recovery period, animals were habituated to the open field environment (a circular, 120 cm in diameter, matte black painted wooden apparatus) with pellet chasing sessions (small pieces of honey cereals used as food reward), and to the sleep environment (a cardboard box filled with bedding and covered with a towel), for 10-15 minutes each. Then, a habituation stage of at least 3 days was carried out, in which the animals were introduced to the RAM. The maze consisted of a central octagonal chamber

of 30 cm in diameter, with eight equidistant spaced arms, each 70 cm long. Wells were positioned at the end of each arm, so that the bait would be unseen from the central chamber. To minimise the possibility of the rat picking up odour cues, dust obtained from the food rewards was sprinkled on the apparatus. During habituation, the 8 arms were each baited with multiple food rewards, and rats were left free to explore the environment for 10-15 minutes each day. All the phases of the experiment were carried out in the same room containing a series of distal room cues to aid the rat in navigating the environment, with the open field and RAM positioned in the same place every day (see ***Figure 4A***).

After habituation, rats performed the behavioural paradigm for 5 consecutive days. On each day, the rat was brought to the room and the probe connected to the acquisition computer. The rat was then placed inside the open field arena, where he would chase food rewards for at least half an hour while the brain activity was being recorded. After being given a water break, the animal would be positioned inside the central chamber of the RAM. The RAM task was carried out in a similar fashion to what was done in the previous behavioural experiments (see *Chapter 2*). However, this was performed with some additional constraints. First, intra-trial periods in the central chamber that lasted precisely 30 seconds were given before the doors were lifted. Second, every 3-6 trials, the animal would be positioned inside a temporary apparatus (see ***Figure 4A***), so that the arms (which could be disconnected from the maze) could be swapped between each other and then re-baited without the need to disconnect the probe. Finally, at the end of each trial, the rat was guided back to the centre of the maze, before the doors were closed and a new trial would begin.

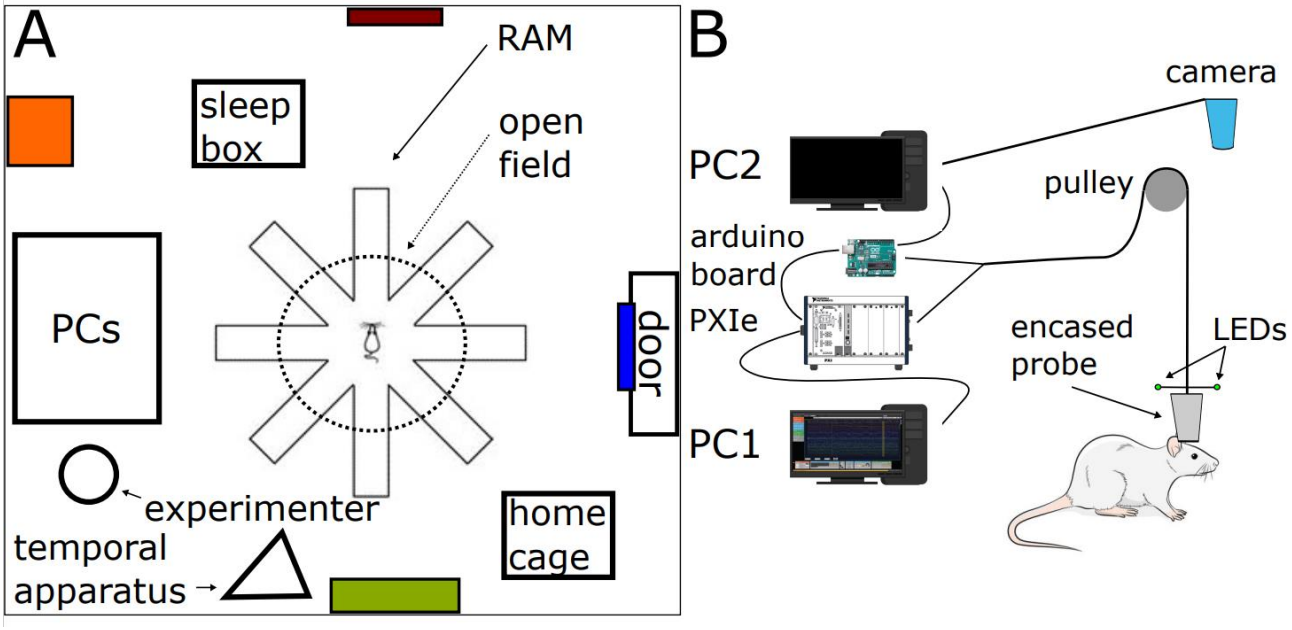

Figure 4. Lay out of the recording procedure. *(A) Shows a layout of the experimental room, in which the open field, RAM, and sleep sessions were all carried out. Coloured rectangles represent different extra-maze cues positioned along the walls, which remained constant throughout the whole experiment. (B) Shows the hardware set up for the recordings.*

The rat would perform a maximum of 20 trials on the RAM, before being moved inside the sleeping box, where he was left to rest for at least 30 minutes. Only on day 1 of the recording an additional sleeping session was introduced after the open field exploration, to allow recording of brain activity before any learning task was carried out. Brain activity was monitored and recorded throughout all sessions, and a camera positioned directly above the environments was used to record tracking of the animal through LED lights attached to the probe's cement cage (***Figure 4B***). A pulley system with a counterweight affixed to the ceiling was used to counterbalance the weight of the cable that connected the probe to the computer, and that powered the LED lights (powered by the Arduino board; see ***Figure 4B***).

Recording equipment

The recording equipment consisted of various components. First, the probe was connected to a PXIe chassis containing a PXIe card (Imec; https://www.neuropixels.org/system1-0) to acquire the data and transmit it to a desktop computer (PC1 in ***Figure 4B***), in which OpenEphys had been previously installed. Connected to the PXIe card was also an Arduino board (Arduino MEGA 2560; see https://www.arduino.cc/en/hardware) that enabled transmission of a TTL signal. The same board was also connected to a digital camera affixed on the ceiling above the maze(s). The camera was driven by the TTL signal and data was collected and stored by a second computer (PC2 in ***Figure 4B***).

Histology

Rats were perfused under a biological hood at the end of each experiment. They were first given a lethal dose of sodium pentobarbital (2 ml/kg, Dolethal; Vetoquinol UK Ltd) through intraperitoneal injection. They were transcardially perfused with 0.1 M PBS, followed by 4% PFA in 0.1 M PBS. Brains were collected in 4% PFA and left on a stirring plate for at

least 4 hours, before being transferred in 25% sucrose solution overnight at room temperature on a stirring plate.

The tissues were cut using a freezing microtome (8000 sledge microtome; Bright Instruments). Brains were sectioned coronally in 80 µm-thick slices. Slices were then cresyl stained, mounted on gelatine subbed glass slides and coverslipped using DPX (Thermo Fisher Scientific). Images were acquired using the Leica Microscope and the Leica Software. Two examples of NPX 1.0 and 2.0 probes histology can be seen in ***Figure 3F.*** More pictures of the other probes can be found in *Chapter 4*.

Data analysis

Data acquisition. Probe data was collected through the OpenEphys software (Siegle et al., 2017), with LPF and AP gain indices parameters set at 250x (for NPX 1.0) and using an external reference channel. All recordings belonging to an individual animal (both LFP and AP data, which were collected into separate binary files for NPX 1.0 but not for NPX 2.0) were merged. Bad channels (i.e. channels that presented a visible amount of noise when observed through the software) were removed from the data and analysed. Channels outside of the target area (identified by the live signal on the OpenEphys software and knowledge of the position of the probe) were also removed to reduce the size of the data. A TTL pulse was used to synchronise the videos and the electrophysiological recordings. The pulse was generated by an Arduino board which then triggered the camera to capture a frame, while being simultaneously recorded as an input sync channel on the OpenEphys software (via the PIXe card, see section above). Spike detection from the resulting data was computed with the open-source software KiloSort 2.5 (Pachitariu, Steinmetz, et al., 2016; see next section). Channels were selected based on the activity registered with the probe during implantation, and anatomical knowledge of the brain areas at the coordinates used. This allowed us to estimate the probe trajectory during implantation, and the number of channels present in each brain area, which was then confirmed through visualisation of brain slices.

Pre-processing and clustering. After collection, the electrophysiological data was pre-processed using Kilosort 2.5, using the default filter settings and parameters (Pachitariu, Steinmetx, et al., 2016; see https://github.com/MouseLand/Kilosort). This framework enables sorting of overlapping spikes for hundreds of channels simultaneously and using a template matching framework, with a motion correction algorithm that identifies drifting of spike amplitudes across time and corrects for them in order to match spikes to the correct cluster (see this chapter's *Introduction*). Clustering was then computed through Phy (Rossant et al., 2016). All clusters generated where visually inspected for manual curation considering three exclusion criteria. First, the presence of spikes in the refractory period of the autocorrelation. Then, the presence of non-physiological waveform shapes. Lastly, the presence of any extreme drifts in cluster points during the recording, which was evaluated using the software. Any clusters flagged by these three criteria were deleted. This process follows what has been done previously by other authors when using NPX probes (Böhm & Lee, 2020; Ghestem et al., 2023; Krupic et al., 2018; Van Daal et al., 2021). Spike times were then subsequently down sampled to 20 kHz, with the LFP data up-sampled to 5 kHz, to align with the lab standard data format.

Tracking data. Tracking data was collected by a camera set up above the two environments. The camera frames were triggered by a ~50 Hz TTL signal which synchronised each frame with the electrophysiological data, and the files were stored in a separate computer to that running the OpenEphys software (see ***Figure 4B***). After the end of each experiment, the data was analysed through DeepLabCut (DLC; Mathis et al., 2018) by marking the position of the two LED lights. Separate DLC projects were created for the two environments (open field and RAM), and for each rat, using sample videos from day 1 of recording. The procedure used for tracking matches what has been described in the *Methods* section of *Chapter 2*. Forty frames were extracted from each video and labelled manually through the DLC GUI. The resulting DLC output was then ran through a custom-made R code to remove any misidentified points that would fit any of 3 different criteria. First, a distance between consecutive tracked points > 11 cm. Then, a distance between the two LED points > 10 cm. Lastly, a distance between the centre of the environment and the point greater than the diameter of the environment. Finally, the position of the rat was taken as the mean distance between the two LED points for each

frame. The resulting data was then aligned to the electrophysiology data by extracting time stamps of the TTL pulse onset from the raw binary data. In this way, each rat location extracted from the DLC analysis was allocated a time stamp that aligned with the electrophysiological data. The resultant tracking was then resampled at a rate of 1 frame per 0.0256 seconds, to align with the lab standard data format.

Waveform reconstruction. Once clusters and their associated spike times were identified, the data was first band pass filtered (800-5000 Hz) and then spike waveforms for each cluster were extracted in 1.3 ms time windows for a total of 40 samples. The first 15 samples were averaged for each spike waveform and used as baseline. A smoothed spline was fit into the datapoints of the spike waveforms and then up-sampled 3 times the amount of data points (i.e. for a total of 120 samples). The reconstructed waveform was then centred around its minimum peak (identified through the smoothed spline as the lowest point in the waveform), and cut to fit into a time window of 1 ms. This process allowed all spike waveforms of one cluster to present their minimum peak in the same time bin. With this, spike waveforms belonging to the same cluster could be averaged together to generate a mean waveform, which would be then used in later analyses.

Waveform shape measures and firing properties. Three measures related to waveform shape were calculated in this chapter. First, spike amplitude, which was computed as the baseline-to-through difference in each cell's mean waveform. In addition, spike width was calculated as the time elapsed between the maximum positive peak before the trough, and the positive peak after. Finally, a waveform asymmetry score was employed, using the following formula: $(b-a)/(a+b)$, where b is the amplitude of the maximum peak before the trough, and a is the amplitude of the one after (all three measures followed the work done by Sirota et al., 2008; see ***Figure 5A***). These measures were either used as a first stability assessment *(waveform stability* paragraph below), or as features to classify cells into distinct groups (*cell type classification analysis* paragraph below). Two main firing properties were also computed for the cell classification: mean firing rate, calculated during awake periods of open field exploration (animal speed > 5 cm/s), and burstiness score,

calculated as the time (in ms) of the peak bin (i.e. the mode) in the autocorrelation histogram (Barthó et al., 2004; Csicsvari et al., 1999; Sirota et al., 2008).

Cell type classification analysis. In order to classify the clusters into distinct groups, four spike properties were considered: spike width, waveform asymmetry score, mean firing rate, and burstiness score (***Figure 5C***). The specifics of why these features were used in the analysis will be outlined in this chapter's *Discussion*. All properties were computed using custom R and C code and were normalised to their min-max scores. A hierarchical clustering algorithm was used to split the data into distinct clusters using the *NbClust* function (R NbClust package). Five parameters are necessary to perform a hierarchical clustering analysis. First, the Euclidean distance between the two vectors of data, which generates a dissimilarity matrix. Second, the aggregation method that will determine the within-cluster variance (ward.D2; for details, see Murtagh & Legendre, 2014). Third, the minimum and maximum number of clusters (in our analysis, 2 and 5). A minimum of 2 distinct groups were expected, namely inhibitory and excitatory neurons, while a maximum of 5 was specified, to include possible distinctions in excitatory cells such as burstiness and theta modulation (see *General Introduction*). The *gap index* was finally used to determine the final number of clusters (see Tibshirani et al., 2001). In this way, the clustering algorithm identified the optimal number of clusters to fit the data (rather than the experimenter).

Once the hierarchical clustering was computed, the resultant classification was validated using a nonparametric naïve Bayesian classifier (*naivebayes* R package) to perform a cross validation of the data. This algorithm creates a model in which the cluster features are estimated using kernel density and are assumed to be independent. Bayes theorem was used: $P(A|B) = P(B|A)*P(A)/P(B)$. The model was then trained on all the data, i.e. the cluster ID, the waveform and firing properties for each cell, while dropping the data for a single neuron. This model was then used to calculate the probability that the dropped neuron belonged to either cluster. This operation was performed iteratively for each cell. The probability that a given dropped neuron belonged to either cluster was subtracted from each other, to provide a confidence measure. Values closer to -1 or 1 indicated that the

neuron was confidently classified as belonging to one of the two clusters, whereas a value of 0 indicated that it was equally likely that the neuron was a member of either cluster.

Waveform stability. To verify that the clustered units maintained stable waveforms, a range of measures was calculated that capture how spike shapes change in time. First, distributions of amplitude and spike width were computed across each day for each cell and visualised through a kernel density estimator (*density* function of the *stats* R package). Then, amplitude and spike width values (for each cell on each day) were transformed into Z scores using the distribution of values on day 5. The resulting distributions were compared using multiple paired Wilcoxon rank sum tests (with Holm-Sidak corrections). Moreover, the waveform score was assessed (Jackson & Fetz, 2007), computed as Pearson's r correlation between two average waveforms. This measure gives an indication of how similar waveform shapes are, independently of their absolute amplitude differences.

Lastly, to assess waveform stability, a PCA was performed (Principal Component Analysis; Pearson, 1901) using the *prcomp* function in the *stats* R package. A PCA is a reduction method that allows to assess the data based on the variance of its features, thus minimising possible biases that could appear when only considering one feature. The PCA was computed on the points of the waveform. To reduce the computational weight of the analysis, the waveform data was reduced to half a millisecond size (centred around the minimum peak) and down-sampled by taking every other point of the waveform. The scores of the first three principal components were used to calculate the total variance explained by each principal component. A mean value was computed for each cell cluster by averaging the first principal component of all the spikes belonging to that cluster. Then, Z scores were computed by taking the mean and SD of the values of day 5 (i.e. the reference distribution). The absolute values of the Z scores were then computed to create a waveform stability score for each cell.

Place field generation. Place fields were calculated following the method of Harris and colleagues (2001). Briefly, the environment was first subdivided into a grid of 2x2 cm bins. A same-size square was overlaid to the grid, for each spike of each cell, and centred around the position of the animal when the spike was recorded. Each bin was then incremented by the amount of overlap between the square and the grid. This procedure was performed on both spike data (creating a spike matrix) and tracking data (creating an occupancy map). Both spike matrix and occupancy map were smoothed with the use of a Gaussian kernel (1 SD = 12 cm), and then divided by each other to produce place field maps. This chapter only focuses on the data collected during exploration of the open field, as some of the features analysed in this chapter might vary with learning (as explored in the next chapter).

Spatial information. The subiculum has a mixture of spatial and non-spatial neurons (see *General Introduction*). The spatial selectivity of these two types of neurons can be calculated by first computing the spatial information (Markus et al., 1994; Skaggs et al., 1992; Skaggs & McNaughton, 1996) for each cell. First, the unsmoothed place fields were constructed for each cell, as described above, but now without a convolution with the Gaussian kernel. Next, the spatial information (SI) was computed as bits per second. SI is given by the following formula: $\sum P_i(R_i/R)log_2(R_i/R)$, *where* P_i is the probability for occupancy of bin *i*, and *R* is the mean firing rate. SI measures can be influenced by two features: (1) number of bins, (2) firing rate (with few spike tending to show higher SI; see Markus et al., 1994). The same bin size (6) and number of bins was maintained throughout the analysis to control the first issue. To compensate for biases that may occur as a result of firing rate, and to classify whether a given cell could be considered spatial, a shuffling procedure was implemented. The resultant data was used to test whether the SI was higher than expected by chance, similarly to Markus and colleagues. On each round of each shuffling, the same SI was calculated, but now with the tracked position of the animal randomly shifted in time relative to the spike data (minimum shift: 5 seconds). This shuffling procedure allowed to maintain the same structure of spike trains for each cell, as well as the behaviour of the animal, while disrupting the relationship between the two. Given that exploration is marked by periods of both foraging and immobility, shifts in the tracking data were restricted to periods of active exploration (i.e. when the animal was

running at > 5 cm/sec), to ensure that the same behavioural data was used to generate both the original and the random SI. This procedure was then repeated 500 times for each cell, providing a distribution of random SI scores. Cells were considered spatial if their SI exceeded the 95% of this distribution ($p < 0.05$). The SI for each cell was normalised by transforming it into a standardised Z score, using the mean and standard deviation of the shuffled distribution (see ***Figure 8D***). This score represents the spatial information of cells, unbiased by firing rate or the behaviour of the animal.

Spatial remapping. Spatial remapping was computed as a correlation coefficient (Pearson's r) between place fields across two days, pixel by pixel. Only cells with a mean firing rate across the whole recording > 0.25 Hz and that were spatial (i.e. $p < 0.05$ using the spatial information analysis described above) on all days of recording were included in the spatial remapping analysis.

Change in rate scores. In order to evaluate how cells change across days, a change in rate score (see equation below) was calculated. This produces a score between -1 and 1, where positive numbers represent an increase in rate on day 5 and a negative drop. This score allows comparisons of rate change amongst a population of neurons, which have widely distributed firing rates (Leutgeb et al., 2004). As instability of firing rate may manifest through both increases and decreases in rate (and so potentially produce a population net change of 0), a sign-less absolute value was used (so that the score ranged between 0 and 1) in order to capture the magnitude of change. This gave the following formula:

$$change\ in\ rate = \left|\frac{(rate\ on\ day\ 5) - (rate\ on\ day\ x)}{(rate\ on\ day\ 5) + (rate\ on\ day\ x)}\right|$$

Where x is day 1-4. Change in rate scores were taken in their absolute values (i.e. Z becomes SD), to compare absolute changes between days, independently of directionality of the change. Spearman correlation coefficients were calculated between the PCA results, change in rate scores, and spatial remapping. Only cells that had a mean firing rate > 0.25 Hz during the whole recording were included in the rate changes analysis.

Results

1. Developing a framework to obtain high quality electrophysiological data across days using NPX probes

Electrophysiological recording of neurons in a specific brain region of the rodent brain can be acquired with a variety of techniques (see *Introduction* section). NPX probes have recently started to be implemented in a variety of rodent studies, as they allow recordings from a high number of channels (384), with minimal tissue damage during insertion, and reported recordings with high single unit activity across multiple days. The aim of this chapter was to implement a protocol that would allow to record the same cells in the span of different days in the dorsal subiculum in freely moving animals performing a series of spatial tasks.

To achieve that, a series of different designs was validated, while keeping in mind three objectives. First, to create a holder design that would allow the probes to be recycled for more than one use. Second, to reduce any possible noise coming from external sources to the brain. Lastly, to reduce any possibility of movement of the probe during the recording that could impact its quality.

Progression of the designs can be seen in ***Figure 3B-D***. In Version 1 (***Figure 3B***), a wall of copper mesh was wrapped directly onto the probe holder and soldered to the ground wires connecting the probe and the animal skull. The probe holder was then covered in cement to prevent movements due to mechanical impacts (e.g. the animal hitting the side of the home cage while moving). This version, while allowing protection from external noise with the addition of the grounded copper mesh wall, presented some issues that

impacted the quality of the recordings. Most relevant was its susceptibility to movements of the probe inside the holder, as early implants made with this design resulted in damage to the probe. In Version 2 of the design (***Figure 3C***), the copper mesh wall was physically separated from the probe holder, while still being connected to the ground and probe wires. This allowed better recording outputs, with only one instance of the probe breaking (during the surgery). The data that will be presented in the next paragraphs for the NPX 1.0 recordings was acquired using this version of the design.

A possible source of movement of the probe across days, while minimal, could still be attributed to the design of the screws used to fix the probe holder in place. In the latest version of our design, implemented in our NPX 2.0 recording, smaller screws were used, and a hexagonal nut was added to further reduce the possibility of movement. A considerable difference between the NPX 1.0 and 2.0 probes design consists in where the ground wires can be soldered: in the early version, wires can be soldered directly onto the head of the probe, while in the newest version this can only happen on the flex cables. This second design raises the concern of noise being generated by the flex cable rubbing against the probe holder or the external copper mesh wall. For this reason, another modification implemented in Version 3 of our design consisted of a layer of plasti-dip being added to the points of contact between the flex cable and the ground wires, as seen in ***Figure 3D (inserts on the bottom)***.

In summary, in order to guarantee high quality recordings in the dorsal subiculum during freely moving behaviour in rats in the span of multiple days, several steps were made. The resulting designs, one for NPX 1.0 and a similar, adapted version for NPX 2.0, are shown in ***Figure 3C-D***.

2. Clustering cells based on spike properties revealed two distinct populations of cells

Five rats were implanted with NPX probes aimed at the dorsal subiculum for a total of 7 implanted probes, 4 being NPX 1.0 probes, and one NPX 2.0. Of the 7 implants, 6 were successful (including 1 bilateral implant), while one was partially successful (two probes were implanted bilaterally, but one of them broke during surgery). Animals were recorded

performing two different tasks (a non-learning and a learning one, see *Methods* for details), followed by a period of rest (see ***Figure 3F, bottom row***), for 5 consecutive days. On day 1, an additional resting period was introduced between the two behavioural tasks, in order to record a session of pre-learning sleep (data presented and analysed in the next chapter). When analysing NPX 2.0 data, only 2 shanks were taken into consideration, due to the position of the other two on the medio-lateral axis (see next chapter). The clustering analysis revealed a total of 321 cells (see ***Table 3*** for a breakdown of each rat)***.***

Animal	***Total n of cells***	***Excitatory cells***	***Inhibitory cells***
#1	35	*24 (68.57%)*	*11 (31.42%)*
#2	41	*35 (85.36%)*	*6 (14.63%)*
#3	51	*49 (96.07%)*	*2 (3.92%)*
#4	17	*17 (100%)*	*0*
#5	177	*158 (89.26%)*	*18 (10.16%)*
All rats	321	*283*	*38*

Table 3. Number of cells recorded for each rat. *The table shows the total number of clustered cells (computed following the procedure described in the Methods section of this chapter) and the number and relative percentage of cells classified as either excitatory or inhibitory based on a hierarchical clustering approach (see Methods).*

In order to classify the recorded cells into inhibitory and excitatory neurons, a hierarchical algorithm was implemented using 4 features of neuronal spiking: spike width, spike asymmetry and burstiness (calculated across the whole recording), and mean firing rate (calculated only during periods of free exploration in the open field). Each feature was first transformed into a score with min-max normalization (range of values being 0-1; see clouds of points distributions of **Figure 5B**). The results revealed 2 groups. The first group presented with low width (mean = 0.331; SD = 0.231), high burstiness scores (mean = 0.549; SD = 0.261), high asymmetry (mean = 0.476; SD = 0.202) and high firing rate

(mean = 0.207; SD = 0.263). This group will be referred to as *inhibitory* neurons (see explanation of why in the *Discussion* of this chapter). The other group presented with opposing characteristics (width: m = 0.45, SD = 0.164; burstiness: m = 0.087, SD = 0.044; asymmetry: m = 0.249, SD = 0.109; rate: m = 0.037, SD = 0.053), and will thus be referred to as *excitatory* neurons (see distribution of features of **Figure 5C**). Of the 321 cells, the hierarchical algorithm identified n = 38 (11.84%) as belonging to the inhibitory group, while n = 283 (88.16%) were identified as excitatory neurons.

To validate the hierarchical clustering results, a non-parametric naïve Bayes algorithm was implemented, using a cross-validation classifier approach (see *Methods*). From this, the percentage of cells predicted as belonging to either of the two groups was calculated. The probability that a cell belonged to the "inhibitory" or "excitatory" clusters was computed for each cell and subtracted (excitatory probability – inhibitory probability). In this way, neurons classified as belonging to the excitatory cluster would have positive probabilities, while cells belonging to the inhibitory cluster will have negative probabilities. A cell was considered to be "misclassified" if it had been clustered as excitatory, but had a probability < 0.5, or if it had been clustered as inhibitory, but had a probability > - 0.5 (see ***Figure 5D***).

Using this method, 304 out of 321 neurons (94.7%) were correctly classified -i.e. the cross validation identified the neuron as belonging to the same group as identified through the hierarchical clustering. Classification was particularly accurate for neurons in the "excitatory" cluster. Here, 274 out of 283 excitatory cells (as classified through the clustering) were correctly classified with the Bayesian cross validation. However, this classification accuracy of > 95% was not maintained when considering the interneuron population. Only 78.9% of cells in the "inhibitory" cluster (30 out of 38 cells) were identified as belonging to that group. This drop in accuracy may reflect the diversity in interneurons characteristics, as explored in the *Discussion* of this chapter.

After cross validation of our two clusters, these clusters were tested to check if they showed different spatial information characteristics, as highlighted in previous literature. That is, that excitatory neurons would be more spatially selective that inhibitory cells (i.e. carry a higher degree of spatial information; O'Mara, 2005; Sharp & Green, 1994). This method of assessment follows a similar logic to that of Steinmetz and colleagues (2021) on the visual responses of neurons in the primary visual cortex.

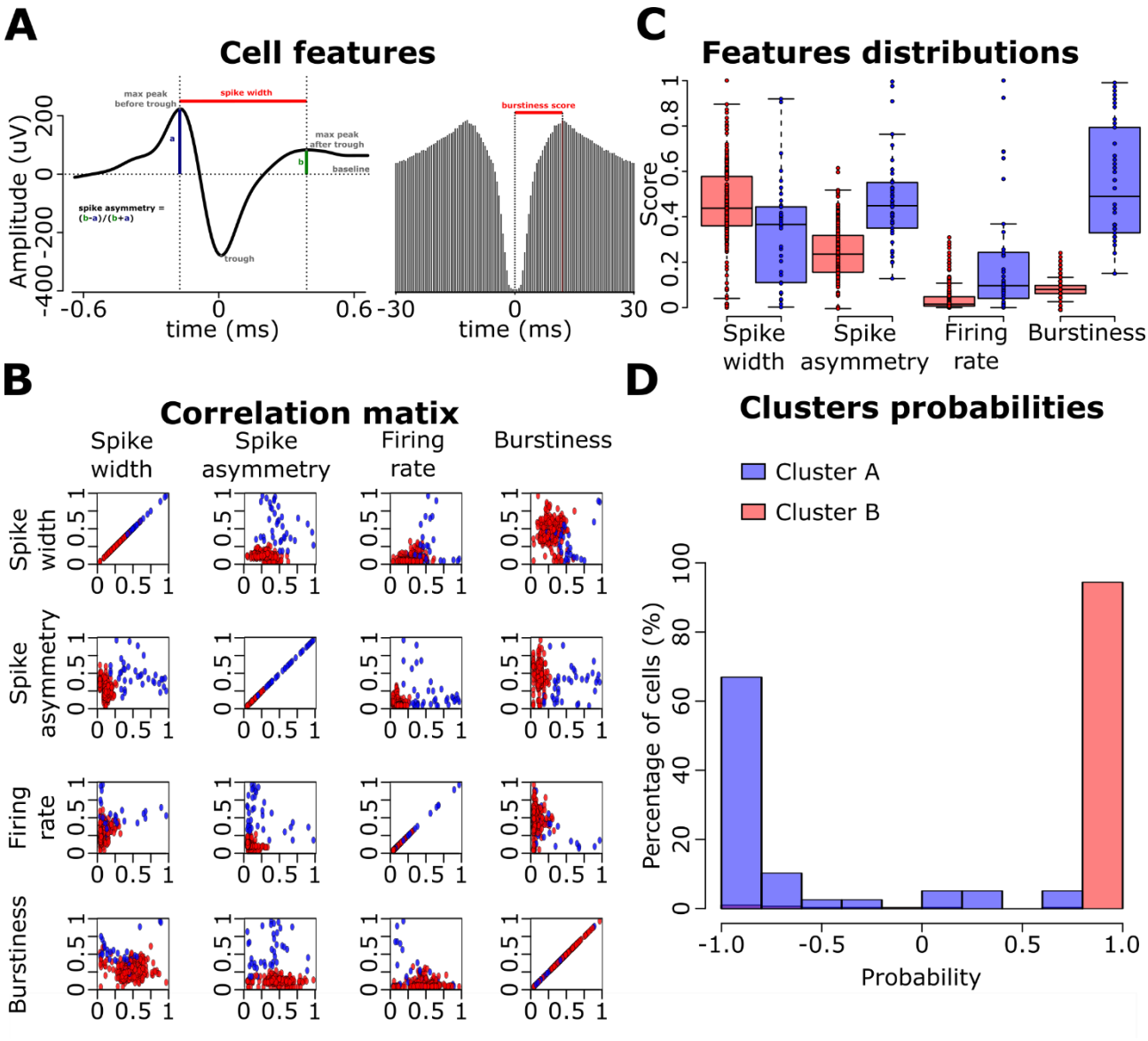

Figure 5. Classification of cells recorded into two distinct groups. *Cells were classified based on four main features, measured across the whole recording: spike width, spike asymmetry, mean firing rate and burstiness. Each feature was min-max normalised, and the resulting scores implemented to generate a hierarchical clustering model. The accuracy of the classifier was then validated using a non-parametric naive Bayes algorithm (see Methods). (A) Visualization of how spike width, asymmetry and burstiness were calculated. Example on the left shows a waveform shape typical of an inhibitory cell, while example on the right shows the autocorrelogram of a cell that, in the subiculum, could be either an excitatory or an inhibitory cell. (B) Correlation matrix between each feature. Highlighted in red and blue are the cells classified into the two clusters by the classifier. (C) Distribution of scores of each feature, split by the two classified clusters. (D) Distribution of probabilities of the cells to belong to the excitatory cluster. The y axis indicates the percentage of cells within each of the two groups. Boxplots error bars represent 95% confidence level, and each dot represents a single cell.*

The mean spatial information was computed across the whole recording (see *Methods*), for both inhibitory and excitatory cells. A positive spatial information score indicates that the SI of the cell is higher than the mean of the shuffle distribution. A total of 217 (n = 183 excitatory, and n = 34 inhibitory) cells were selected for the analysis based on the exclusion criteria mentioned in the *Methods* section, of which 72.35% (n = 138 excitatory, and n = 19 inhibitory neurons) showed significant spatial information (SI > 95th percentile of the shuffled distribution, $p < 0.05$) on at least one of the recorded days. Since spatial information may vary across days, the SI was calculated for each cell on each day (***Table 4*** shows cells that pass the significance criterion, i.e. SI > 95th percentile). As expected, there was a significant difference between inhibitory and excitatory neurons in their spatial information (Kruskal-Wallis rank sum test; $\chi^2 = 32.784$, df = 1, $p < 0.001$), consistent with previous reports in the CA1 (Christian & Deadwyler, 1986; Kubie et al., 1990; McNaughton et al., 1983; also see **Figure 6A** for place fields examples). SI did not vary across days, for either group. Separate pairwise Wilcoxon rank sum tests for the inhibitory and excitatory cells showed no differences across days for either group (all $p > 0.05$ for each day compared to the other days for each group; ***Figure 6B***).

Animal	***Spatially selective cells***	***Day 1***	***Day 2***	***Day 3***	***Day 4***	***Day 5***
#1	*12/7*	*8/2*	*9/6*	*8/2*	*6/0*	*8/0*
#2	*11/4*	*5/1*	*7/2*	*5/2*	*7/3*	*3/3*
#3	*24/0*	*17/0*	*18/0*	*20/0*	*18/0*	*18/0*
#4	*8/0*	*6/0*	*7/0*	*7/0*	*7/0*	*7/0*
#5	*83/8*	*65/2*	*69/2*	*68/4*	*70/3*	*71/4*
All rats	138/19	*101/5*	*110/10*	*108/8*	*108/6*	*107/7*

Table 4. Number of spatially selective cells. *The table shows the total number of spatially selective cells (excitatory/inhibitory) for each animal (SI > 95th percentile) across the whole recording, and for each separate day. Two criteria were used to consider cells to be spatially*

selective across the whole recording: (1) the cell would show significant spatial information on at least one of the 5 recorded days; (2) firing rate of the cell was > 0.25 Hz across the recording. For days 1-5, only cells that met the second criterion were considered.

In summary, the cell classification approach implemented here identified two groups of cells with spiking properties similar to that recognised in literature as inhibitory and excitatory hippocampal neurons. This was validated using a Bayesian classifier, which showed that a small percentage (< 6%) of cells might have been “misclassified”. Additionally, the spatial information analysis showed that the method of classifying inhibitory and excitatory cells reproduces differences in the amount of spatial information carried between the two groups. When looking inside the two groups, no differences were found across days, indicating that spatial information does not seem to change with time during exploration of a familiar environment.

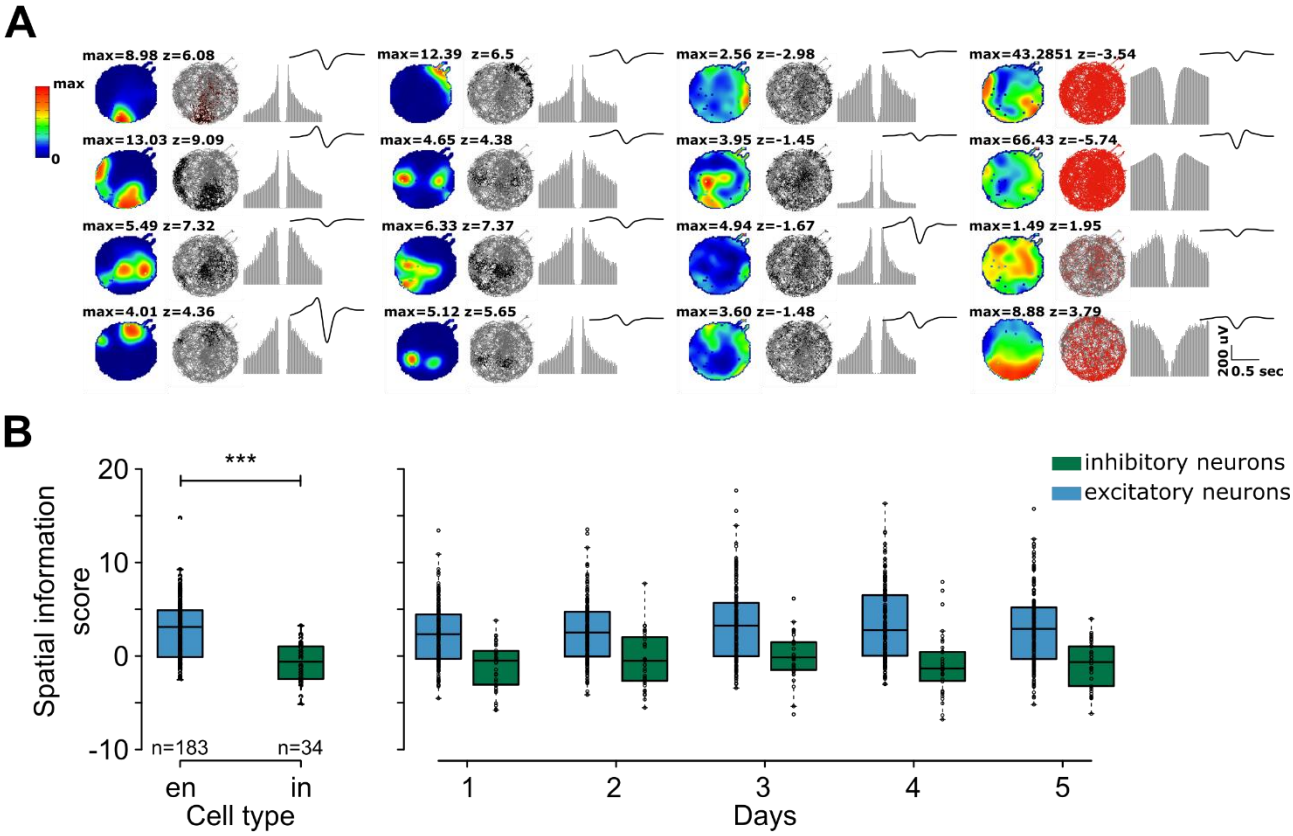

Figure 6. Spatial information differs between excitatory and inhibitory neurons. *(A) Examples of place fields, tracking data, autocorrelation and spike waveform of some of the neurons recorded. The first and second column of examples shows spatially selective excitatory cells; the third column shows non-spatial excitatory cells, while the last column shows inhibitory neurons (first two rows are non-spatial, while the last two are spatial). (B) Boxplots showing the distribution of spatial information scores for excitatory (blue) and inhibitory (green) neurons, both across the whole recording (left), and for each day of exploration of the open field (right). Error bars of the boxplots represent 95% confidence interval. Single points represent individual cells. Significance level: *** p < 0.001.*

3. Analysis of waveform characteristics revealed the stability of our recording across days

The initial analysis of our data showed the possibility to classify the recorded data into two distinct groups with similar characteristics to those found in hippocampal literature for inhibitory and excitatory neurons. The next step in this chapter was to check if our recording method allowed us to track the same neurons across days. To do so, waveforms characteristics were tracked across days, to check whether neuronal activity remained stable throughout the recording.

First, the distribution of two main waveform characteristics, mean amplitude and mean width, were compared across days. Both features showed similar distributions across the 5 days of recordings, as can be seen in ***Figure* 7A**. To quantify how spike amplitude and width changed on each day with respect to day 5 for each individual neuron, these measures were transformed to Z scores using the mean and SD of day 5, for a given cell (as described in the *Methods* section of this chapter). Paired Wilcoxon rank sum tests for both neuronal width and amplitude showed that the Z scores did not change between days 1-4 for the two measures (all $p > 0.05$; see ***Figure 7A insert for spike amplitude***). That is, width and amplitude tended to be as different to day 5 on day 1 as on each of the other days.

To further test waveform stability, the Pearson's correlation was calculated between two average waveforms (***Figure 7C***). Waveform scores, generated by correlating waveforms recorded on day 5 with those recorded on a different day by the same neurons, were compared with the distribution of waveform correlations between each cell with every other cell. A correlation of 1 between waveforms indicates identically shaped spikes, independently of the absolute waveform amplitude. ***Figure 7C*** showed how waveforms of the same cell on day 5 compared to each of the other days tended to be highly similar (> 60% of cells with a waveform score of 1), while waveforms of different cells on different days less so (< 30% of cells with a waveform score of 1).

As a last stability check, a PCA was computed on all the spikes of a cell during each day, from which the first principal component could be compared between days 1-4 and day 5, for each cell. The percentage of total variance explained by the first three principal components was calculated. On average, the percentage of variance explained by the first

component was never < 35% for any of the animals, and the sum of the first three principal components was > 70%, indicating that the first three principal components were accurately representing the data (see ***Table 5***). To quantify stability, a waveform stability score was computed (see *Methods*) for each cell, where the first PCA for each neuron on days 1-4 was transformed into a Z score using the mean and SD from day 5. Overall, the percentage of cells deviating more than ± 2 SDs from the population on day 5 was never > 2% (mean percentage calculated from the percentages of deviating cells on each recorded shank: day 1: m = 1.25, SD = 2.23; day 2: m = 0.833, SD = 1.51; day 3: m = 0.577, SD = 1.53; day 4: m = 0.389, SD = 0.76). Moreover, only around 6% of cells showed waveforms on one or more days that deviated by more than +/- 2 SDs from the mean PCA on day 5 (***Figure 7B***).

Animal	***First component***	***Second component***	***Third component***	***First three components***
#1	*37.22%*	*26.57%*	*11.45%*	*75.24%*
#2	*36.92%*	*21.10%*	*16.56%*	*74.68%*
#3	*51.52%*	*16.01%*	*8.81%*	*76.34%*
#4	*39.79%*	*32.41%*	*7.26%*	*79.46%*
#5	*45.41%*	*22.68%*	*11.90%*	*79.99%*

Table 5. Percentages of variance explained by principal components. *The percentage was calculated for each rat for the first three principal components (first 3 columns), and for the three components put together (last column).*

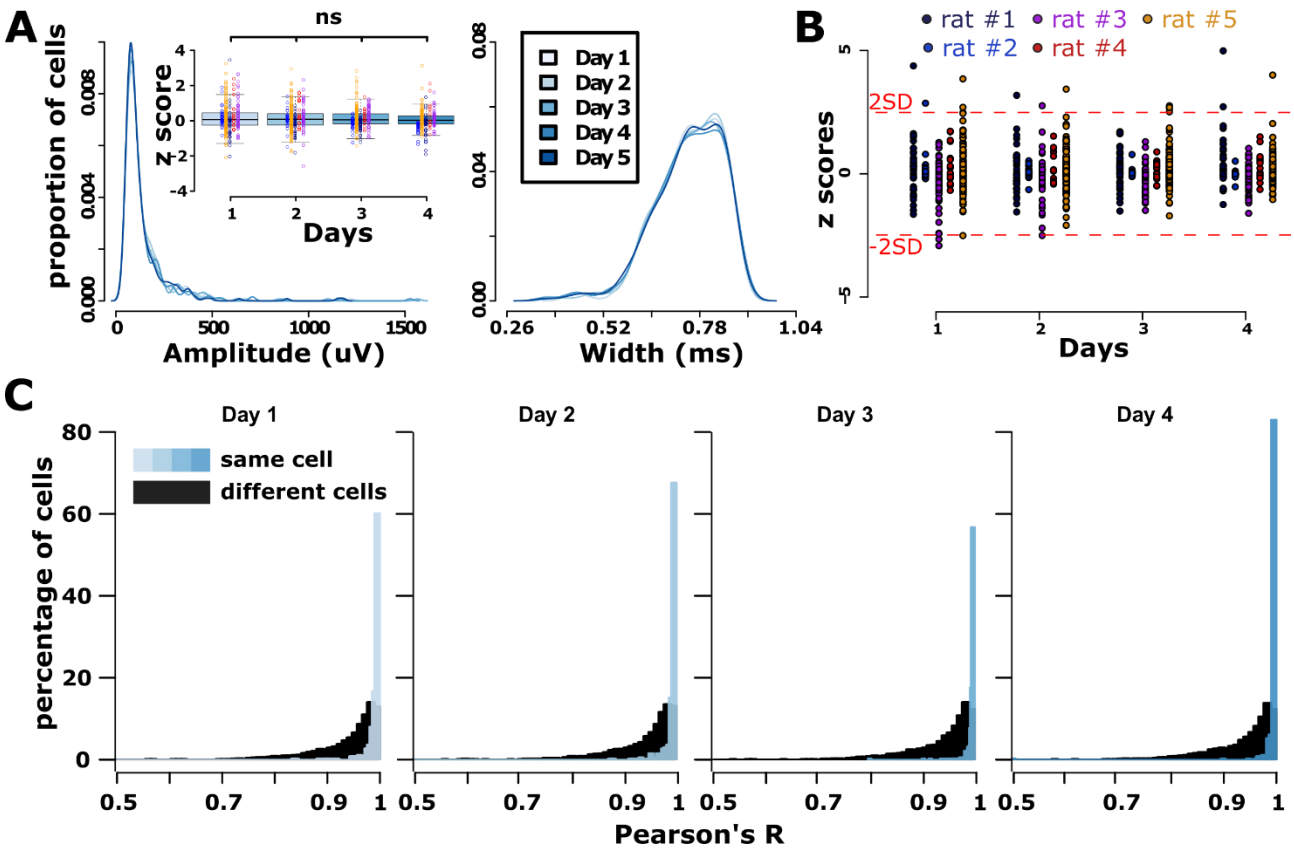

Figure 7. Measures of stability of the recordings confirm stability of the recording. *(A) Distribution of spike waveform and widths across days for each cell. The insert shows the distributions of Z scores for each animal (coloured dots) on each day. (B) Distributions of the Z scores calculated from the first component of the PCA analysis for each animal. Red dotted lines highlight cells which PCA Z score was above |2| SD. (C) Distributions of waveform scores for the same cell across days (blue gradients), and different cells on the same day (black). Error bars of the boxplots represent 95% confidence interval. Single points represent individual cells.*

4. Neurons in the dorsal subiculum of rats show remapping of place fields across days but no changes in firing rate.

The analysis above indicates that spike sorting of neurons across five days produced single units with waveforms that remained stable across the 5 days. However, this stability was not absolute, and it remained possible that some recording “drift” might drive changes in the electrophysiological features of recorded neurons. Changes in rate might reflect physiological or even cognitive processes (Leutgeb et al., 2004). Indeed, previous work in the CA1 indicates that neuronal codes evolve across days, diverging in both spatial coding and firing rates (Ziv et al., 2013). Alternatively, firing rates and spatial coding may vary due to the movement of electrodes in the brain. In this case, movement of the probe itself (so called “drift”) can lead to apparent changes in waveform shape and potentially spike sorting errors (Voigts et al., 2020). Thus, changes in firing rates and spatial selectivity in the open field were examined and analysed to check if such changes could be explained by waveform stability. Firing rates during sleep or the RAM task were not considered, as sleep states or learning processes may also drive changes in neuronal firing patterns (which will be explored in the next chapter).

Firing rate was established across all days for cells that had a mean firing rate > 0.25 Hz during open field exploration, concatenated across days (excitatory cells: n = 183, inhibitory cells: n =34). This data was used to calculate a “change in rate score” as the difference in rate between two days, divided by the sum of these rates. The absolute value of this score was used, which reflected the magnitude of change in rate without considering if the rate had increased or decreased. Scores were constructed to evaluate the change in rate between day 5 (the reference day) and days 1-4, and a nonparametric Friedman Rank Sum Test was computed to compare the 4 distributions. The test was performed on both the excitatory and the inhibitory group and showed no differences across days, for either (excitatory group: $\chi^2 = 1.151$, df = 3, p = 0.7646; inhibitory group: $\chi^2 = 0.933$, df = 3, p = 0.8173; ***Figure 8B***). However, within each day, some cells showed greater changes in rate with day 5 than others. To check whether such changes may be explained by changes in waveform (as an indicator of drift), the changes in rate scores were correlated with the waveform similarity scores (z transformed PCA, as described above). Here, the absolute value of the waveform stability measure was used. This value provides a distance from the mean of the first PCA on day 5, in standard deviations.

Overall, change in rate with day 5 and waveform stability (i.e. change in first principal component of the PCA with day 5) were not correlated when days 3 and 4 were considered, with only a weak, yet significant correlation on days 1 and 2 for the excitatory neurons ($p < 0.05$ for day 1, and $p < 0.01$ for day 2; ***Figure 8C***). These results suggest that any changes in firing rate across days during open field exploration were minimally due to changes in stability of the recordings.

Next, spatial remapping across daily exposure to the open field was examined, by testing whether spatially selective excitatory cells show changes in their place fields across days (i.e. spatial remapping). Only those continually spatially selective cells (i.e. that had a significant SI score on each exposure to the open field, see *Methods*) that had a firing rate in the open field in the open field > 0.25 Hz were included in this analysis (n = 63, 22.26% of all excitatory cells). First, spatial remapping scores were computed as the pixel-by-pixel correlation between place fields across two days (day 5 used as reference day, see *Methods*). Here, a strong positive correlation indicates place fields are similar across days, while a negative correlation indicates that place fields fire in different locations. A Friedman Rank Sum test found there to be a significant difference between the median remapping on days 1 to 4 ($\chi 2 = 31.902$, $df = 3$, $p < 0.001$). Post-hoc pairwise Wilcoxon rank sum tests revealed significant differences between day 1 and day 4 ($W = 1266.5$, $p < 0.05$), and day 2 and day 4 ($W = 1252.5$, $p < 0.01$). However, no difference between day 3 and 4 was found ($W = 1589.5$, $p = 0.426$). These results suggest that spatially selective neurons in the subiculum gradually remap across days (***Figure 8D***), even in a familiar open field with consistent external cues.

Could these results be explained by waveform instability? To address this question, a Spearman correlation between the waveform scores and spatial remapping was performed, to test whether the former could be predicted by the latter. No significant correlation was found on any of the four days (day 1: $r = -0.139$, $p = 0.249$; day 2: $r = 0.054$, $p = 0.646$; day 3: $r = -0.113$, $p = 0.347$; day 4: $r = -0.07$, $p = 0.56$), indicating that any changes in spatial remapping across days were not due to changes in waveform shape (***Figure 8E***).

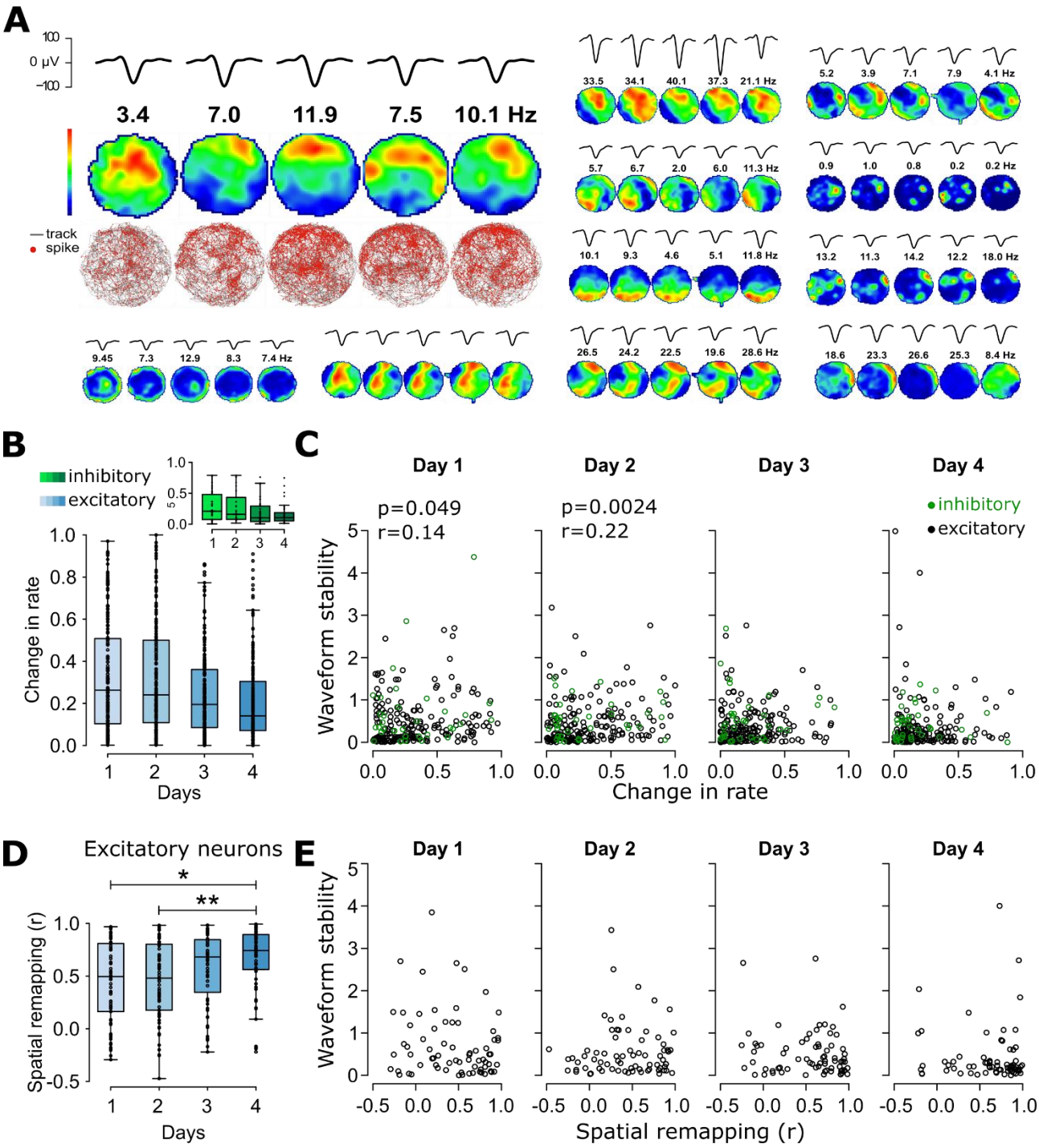

Figure 8. Changes in rate and spatial remapping computed across days during the open field exploration task. *(A) Examples of mean waveform (each top row) and place fields (middle row) for some of the recorded cells. Big example also shows tracking (bottom row), with red dots representing spiking of the cell. (B) Distributions of change in score rates for excitatory (blue) and inhibitory (green) cells across the first four days, compared to day 5. The Friedman Rank Sum test computed for each of the two neuronal types showed no significant differences across days. (C) Scatterplots highlighting any possible correlation between change in rate scores and the waveform stability. Only days 1 and 2 showed a significant correlation, computed with Spearman's r.*

*Correlations were computed for both inhibitory and excitatory cells, yielding similar results (with the exception of days 1 and 2, where the correlation for inhibitory cells was not significant). (D) Distributions of spatial remapping scores for excitatory cells across the first four days, compared to day 5. The Friedman Rank Sum test showed a significant difference among days, which revealed a difference between days 1 and 4 and days 2 and 4 with a post-hoc pairwise Wilcoxon rank sum test. (E) Scatterplots of possible correlations between spatial remapping scores and waveform stability. No significant correlation was found. Error bars of the boxplots represent 95% confidence interval. Single points represent individual cells. Significance level: * $p < 0.05$, ** $p < 0.01$.*

In summary, this chapter outlines the development of a design which allows chronic recordings in the subiculum of freely moving rats using NPX 1.0 and 2.0 probes. Analysis has been presented that tests the stability of these recordings and assessed firing rate and spatial information of the recorded cells during exploration of an open field. Lastly, the data shows that place fields of spatially selective excitatory cells remap across days, and that this spatial remapping is unlikely to be related to changes in stability of our recordings.

Discussion

An effective methodology to implant and recover NPX probe in rats

The aim of this chapter was to test the feasibility of recording with NPX 1.0 and 2.0 probes in the dorsal subiculum of rats for multiple consecutive days and to characterise the firing properties of subicular cells during the recordings.

As a first step, a design was developed that would allow the insertion (and later removal without damaging the pricey equipment) of probes in the targeted area. The design of the probe holder was adapted from Luo and colleagues (2020), who were among the first to propose a design for chronic recordings in rats with re-usable probes. For NPX 1.0 recordings, the main difference in this design consisted in the introduction of a copper mesh wall that would act with one main goal. This modification protected the probe from any mechanical hits generated by the rat moving close to the walls of either the home cage or the experimental environments. Subsequent to the start of this work, a similar approach for protection from mechanical hits has been proposed by Ghestem and colleagues (2023) who 3D-printed an enclosure not mechanically connected to the probe.

In the NPX 2.0 recording, the design was adapted for the smaller probe structure, resulting in a reduction in weight and volume which could, potentially, aid to the implant of multiple probes in the same animal with better results than those yielded with NPX 1.0. Two additional modifications aided in reaching our previously mentioned goal. First, a modification of the screws used to fix the probe inside the probe holder, which in the previous design might allow the probe to move, which in turn would generate instability of

the recording. Second, the addition of isolating the ground wires connected to the probe with a plastic-based protective layer that would reduce any noise generated by the wires moving inside the probe holder.

The ultimate design proposed in this chapter is relatively small and light, which allows the animals to adapt to it quickly in the 7 days of recovery from the surgery. Of the 5 surgeries performed, with insertion of 7 probes (2 unilateral NPX 1.0, 2 bilateral NPX 1.0, and one unilateral NPX 2.0), only one implant was unsuccessful, due to the probe breaking while being lowered into the brain. This result is an improvement compared to previously proposed designs, which resulted in many broken implants, particularly when recording in rats (Juavinett et al., 2019; Luo et al., 2020; Van Daal et al., 2021).

Analysis of electrophysiological recordings in the dorsal subiculum of rats using NPX probes produces two clusters of cells with distinct properties

Using the proposed design, 5 animals were recorded performing the behavioural paradigm, consisting of both a learning and a non-learning task, followed by a sleep session, for 5 consecutive days. The first step in the analysis of these recordings consisted in identifying which different groups of cells are present in the dorsal subiculum of rats.

Our approach revealed two distinct groups, each with different characteristics. The features of these groups reflected the general characteristics of inhibitory and excitatory neurons in the hippocampus. One group had, in general, low spike width, high spike asymmetry, high burstiness and high firing rate, which is in line with inhibitory neurons in the hippocampus (Csicsvari et al., 1999; Sirota et al., 2008). The other group had opposing features, in line with previous literature on hippocampal excitatory neurons (e.g. Csicsvari et al., 1999; Sirota et al., 2008). In addition, the percentage of cells belonging to each of the two groups also reflected previous reports (~11% inhibitory cells against the 8% found by Anderson & O'Mara, 2003; or the 25% found by Böhm et al., 2015b).

Some considerations should be taken into account when looking at these results. First, while other authors have previously implemented clustering methods to classify inhibitory

and excitatory cells in the hippocampus (e.g. Sirota et al., 2008), the increase in variability of features (in particular, firing rate and burstiness) that is intrinsic of subicular cells has made it more difficult in this thesis to produce reliable results. Classification of subicular neurons into excitatory/inhibitory groups has previously been done on single characteristics (e.g. spike width, Kitanishi et al., 2021; or bursting versus regular-firing, Kim et al., 2012b), but a clustering based on features of both spike shape and timing has not yet been attempted for this area. However, there are multiple alternative approaches to quantifying these spike shapes and firing mode features. For example, there are other measures of “burstiness” that could have been considered, including the inter-spike interval (ISI, used by Harris et al., 2001), or the burst index, computed as the ratio between the number of spikes in the 3-5 ms bins and the average number of spikes in the 200-300 ms bins (Royer et al., 2012). Moreover, to distinguish inhibitory and excitatory cells, some studies have used half width (Avermann et al., 2012), or the time from the inflection point on the waveform that marks the initial negativity to the time when the waveform returns to baseline (Rao et al., 1999), or again the width of the waveform at half height (Kyriazi et al., 1996). Some of these alternatives did not seem appropriate to our dataset. For example, Rao’s width measure assumes a return to baseline that, considering the small window selected in the current dataset for waveform extraction, might prove inaccurate. This small window was chosen to avoid multiunit activity and thus reduce the risk of clustering multiple cells together.

There is also the consideration of previous works having recognised different sub-populations of inhibitory and excitatory cells in the subiculum (O’Mara, 2005; Sharp & Green, 1994). Here, authors have identified 5 potential types of subicular neurons: excitatory bursting (with low firing rates and theta modulated), regular spiking (low firing, but no theta modulation), “depolarised bursters” (with relatively high firing rates), fast-spiking interneurons (with low firing, short widths, and theta modulation), and finally theta-modulated neurons. While this thesis clustering approach investigated up to 5 possible clusters for this very reason, only 2 were eventually recognised. The cells in the recordings that were recognised as “misclassified” by the Bayesian model could perhaps belong to one of these different sub-populations, which have been shown to present atypical firing rates and burstiness scores. Additionally, different neuronal types in the hippocampus show distinct morphology features, which could influence spike shape (Buzsáki, 2004; Henze et al., 2000). An extended dataset with a bigger number of recorded neurons might

improve the precision of our classifier and be able to identify these sub-groups as distinct clusters.

To further validate the classifier, spatial selectivity was compared between clusters (i.e. spatial information carried by the cell). In previous studies, it has been shown that excitatory neurons in the subiculum, similarly to CA1 pyramidal cells, can be spatially selective in an environment (Sharp, & Green, 1994; O'Mara, 2005), while inhibitory neurons tend not to be. A similar tendency was evident in these results, with a significant difference in spatial selectivity between the two clustered groups. Looking at the two distributions of data in ***Figure 6B***, one could question the classifier by pointing out that there are some units identified as interneurons that appear to have some degree of spatial selectivity. Two examples are shown in ***Figure 6A*** of such neurons (last column, last two rows). These two examples show how these neurons present with low width, relatively high asymmetry, and low burstiness in their autocorrelograms, correctly marking them as inhibitory neurons, while also presenting a distinct place field. So how do these two notions fit together? While it has been less explored, some studies have pointed out how some inhibitory neurons in the hippocampal formation (Maurer et al., 2006), and particularly in the subiculum (Wilent & Nitz, 2007), can, in fact, exhibit place fields.

Cells recorded in the dorsal subiculum of rats show stability across 5 consecutive days

A key problematic with chronic recording is that the data could be tainted by instability of the recording across multiple days. As a result, spikes identified as belonging to a specific cell on one day might not, for example, be correctly identified as belonging to the same cell on a different day (due to, for example, movements of the cell compared to the electrode; Emondi et al., 2004; Steinmetz et al., 2021). In order to test this possibility in the current dataset, a range of measures of recording stability was implemented, similarly to previous studies (Luo et al., 2020; Steinmetz et al., 2021), albeit only when testing in shorter recordings (~10 minutes for Luo et al., 2020). Moreover, these studies focused on assessing the stability of the recording *in general*, while failing to establish whether they recorded *the same cells* across multiple days.

The distribution of amplitudes and spike widths across the 5 days were evaluated, similar to Van Daal and colleagues (2021). The distributions in this dataset seemed to vary minimally across the different days. Nevertheless, this assessment does not confirm that the same neurons are recorded across days. Instead, these results show that the recording does not degrade (e.g. through the widespread loos of high amplitude spikes over time) and that they contain a similar range of spikes.

The shape of the waveforms was then compared across 5 days and found that the correlation between waveforms of the same cell on different days are generally closer to 1 than those of different cells on the same days (> 60% for same cells vs ~30% for different cells). These results demonstrate that waveforms that belong to the same cell are generally more similar in shape (independently of possible differences in amplitude) than waveforms belonging to separate cells. However, the waveforms were strongly correlated between different neurons -indicating that this measure, to some degree, lacks sensitivity. This suggests that spike shape on its own cannot be a conclusive proof of cell stability across different days, as suggested previously by Jackson and Fetz (2007).

Lastly, a PCA was performed to avoid any potential biases inherent to the measures mentioned above. Only a small percentage of cells (~6%) had PCA scores on days 1-4 that were more than 2 SDs apart from the mean on day 5, indicating that the large majority of cells maintained stable waveform shapes across days. The number of cells with stability scored > |2| SD was, on average, higher on days further away in time from day 5 (mean day 1 = 1.25 vs mean day 4 = 0.389), consistent with some degree of drift over time. However, the majority of drift could have occurred prior to recording: previous studies show that neuronal cell loss is prevalent during the first week following surgery (Luo et al., 2020), after which the stability of the recordings improves. Due to the design of this chapter's experiment, which allowed 7 days of recovery plus 3-6 days of habituation between the day of the surgery and the first experimental day, there was no chance to verify the claims made by Luo and colleagues.

To validate the stability of the recordings, an approach was used that parallels one previously implemented by Steinmetz and colleagues (2021) to assess the stability of their NPX 2.0 recordings in the primary visual cortex. They utilised a functional property of visual neurons, their distinctive visual responses, to "track" the position of the recorded

neurons and confirm that it matched their clustering output. Similarly, two functional properties of subicular neurons, their firing rate and place field similarity were considered here. Changes in firing rate were weak (median change in rate < 0.25) and not strongly correlated to waveform stability. However, stability did predict rate changes for excitatory cells on days 1 and 2, although only weakly ($r < 0.3$). The inclusion criteria for this dataset only considered cells that, *across all open field recordings,* had a firing rate > 0.25 Hz. As a result, there could be instances of sessions with cells that fire very few spikes, followed by sessions with high firing rates. In other words, the stability score may be impacted by under sampling of waveforms on some days.

On the other hand, the spatial remapping analysis (i.e. the correlation between place fields across days), showed that subiculum neurons exhibited a degree of spatial remapping across time, and that this is not predicted by the waveform stability. What might drive such changes in spatial firing patterns across days? Previous work in the CA1 indicates that place field representations of a given environment evolve over time, with few neurons maintaining the same firing location and rates across days (Ziv et al., 2013). Despite this turnover of spatial representation, sufficient spatial information is maintained by the network to decode the position from maps established days before (which is also the case in the current data; see ***Figure 6B***). This arrangement allows for the long-term maintenance of cognitive maps, while providing the possibility that evolving cell assemblies can encode other aspects of memory, associated with a given environment. It has been suggested that such a turnover of neuronal firing patterns may itself encode time within the network. Consistent with this idea, previous work indicates that CA1 spatial representations of a given environment differ, depending on whether the exploration is performed in the morning or afternoon (Mankin et al., 2012). Moreover, so called “time cells” in the CA1 show a turnover across days similar to CA1 place cells. This allows time to be decoded from activity on short (in the order of seconds, during a delay between trials) and long (across days) timescales. Subiculum neurons may in part inherit this turnover of spatial selectivity from CA1 inputs. Additional NPX 2.0 recordings, which bring high numbers of single unit activity, could allow the use a decoding approach (as implemented by Ziv et al., 2013) to stablish if spatial information is maintained in the network, despite the drift in representation. Moreover, joint recordings with the CA1 or CA1 inhibition would enable an assessment of how CA1 input may be driving changes in subicular spatial selectivity over days.

One argument that could be made about these results is the claim of a “stable” environment for the rats to explore during each day. One could argue that changes in environmental cues could cause remapping of place cells, as has been shown to happen in CA1 (Bostock et al., 1991; Muller & Kubie, 1987; O’Keefe & Conway, 1978). However, great care was taken to avoid this possibility in this experiment. The experimental design included a series of environmental cues which remained constant for the whole duration of each experiment (see ***Figure 4A***). Additionally, care was taken to make sure not only that the environment was positioned at the same distance from the walls as it was on previous days, but also that it maintained the same orientation relative to those cues, to avoid a conflict between internal and external cues (Fenton et al., 1998).

While electrophysiological recordings have been sparingly used to track neuronal activity across days, calcium imaging techniques have been widely used to track multiple neurons in time (reviewed by Grienberger et al., 2022; Grienberger & Konnerth, 2012). This includes dissecting the role of the subiculum projections to the CA1 (Sun et al., 2019). However, such methods have several disadvantages over electrode approaches. First, temporal resolution is 30 kHz in the current recordings, which allows the experimenter to establish spike timing information on sub-millisecond time scales. In contrast, calcium imaging methods have temporal resolution of around 30 Hz (Grienberger et al., 2022). Second, while calcium imaging can be used in freely moving animals, two-photon imaging in particular is mostly used in head-fix preparation. Lastly, electrodes provide LFP recordings, alongside single unit activity. As a result, NPX probes provide a cost-effective method for recording network activity across days.

Taken together, these results indicate how the experimental paradigm implemented in this chapter allows for stable recordings across at least 5 consecutive days. They also reassure that the observed changes in firing and spatial properties of the recorded neurons do not seem to be related to the stability of the recordings. Finally, the results show that excitatory subicular neurons during exploration of a familiar environment across multiple days undergo spatial remapping across days.

Conclusions and future steps

This chapter aimed at assessing the quality of recording in the dorsal subiculum across days using NPX 1.0 and 2.0 probes and provided evidence of stable single unit recordings over five days. This will enable a characterization of the role of the subiculum network in in spatial long-term memory, across days, computed in the next chapter.

Chapter 4 – Tracking subicular neurons and their spatial properties across multiple days

Introduction

The introduction to this thesis has highlighted some key characteristics of the subiculum that suggest the need to investigate the role for this area in long-term spatial memory, including its connectivity to other brain regions, or the generation of oscillatory events often linked to consolidation of mnemonic information (Sharp Wave/Ripple events or SWRs; *see General Introduction*). The first experimental chapter showed how inhibiting the dorsal subiculum during either acquisition of information, or its consequent consolidation during rest, results in an impairment in animals performing a spatial memory task. Moreover, the results delineated in *Chapter 3* demonstrate a methodology that allows tracking the electrophysiological activity of subicular neurons across multiple days. This allows the examination of how neuronal firing patterns in the subiculum evolve while the animal learns, across several days performing a behavioural task.

As highlighted in the *General Introduction*, the spike timing of neuronal populations is coordinated with network oscillations, which likely play a role in encoding mnemonic information. Examples include the phenomenon of “theta phase procession” (Huxter et al., 2003; O’Keefe & Recce, 1993) and reactivation of learning-related assembly patterns during SWRs (Buzsáki, 2015). In all regions of the hippocampus (including the subiculum), cells have a tendency to fire during specific phases of the 7-12 Hz theta oscillation (Buzsáki, 2002; Patel et al., 2012).Theta phase preference segregates the spike timing of different neurons, facilitating the formation of cell assemblies coding for discrete features of the environment or events. The timing of inputs to neurons in the subiculum are also organised in time by theta oscillations. For example, CA1 neurons fire at the trough of theta, while layer III cells of the MEC (which projects directly to the CA1 and distal subiculum, see *General Introduction*) fire on the descending phase (Mizuseki et al., 2009). Thus, the phase preference of neurons in the subiculum influences how they are coordinated in time with each other and their presynaptic inputs. Previous work indicates that subicular cells exhibit a gradual shift of this theta preference along both the proximo-

distal and the radial axes (Kitanishi et al., 2021). In concert, the distribution of projections from the subiculum to cortical and subcortical regions varies as a function of the same axes (Aggleton & Christiansen, 2015; Cembrowski et al., 2018; Kitanishi et al., 2021; O'Mara, 2005). In this way, theta modulation orchestrates the flow of information through the subiculum and the computations performed by different grouping of cells.

This begs the question of whether these differences in firing related to the theta cycle could highlight any differences in the way the cells contribute to the processing of mnemonic information. There is a wide variability of neurons in the subiculum (O'Mara, 2005), which have specific firing characteristics and differently contribute to the encoding of spatial information (e.g. bursting and non-bursting excitatory cells, spatial and non-spatial; see *General Introduction*). Could neurons with different phase preferences present with different spatial and firing characteristics? Would that imply a different role for these groups of neurons in contributing to the mnemonic processing of information?

While the spatial coding (and likely the initial phases of spatial memory formation) is accompanied by theta oscillations (O'Neill et al., 2006), sleep-related memory consolidation has been associated with SWR events (Buzsáki, 1989, 2015). SWRs have been shown to not only be present, but also generated in the subiculum (Imbrosci et al., 2021; Kitanishi et al., 2021). However, how subicular spatial information is represented during these events has yet to be fully explored. One report has suggested that neurons in this area could either increase or suppress their firing during SWRs (Kitanishi et al., 2021; see *General Introduction*), but whether these differences reflect in the ability of these neurons to carry spatial/mnemonic information is yet to be determined. Could there be differences among neuronal populations in the subiculum in the way they fire during sleep? And could these differences reflect variations in reactivation?

The aim of this next chapter is to answer the above questions regarding both theta preference and reactivation. To do so, the possible differences in the characteristics of subicular neurons were explored when recorded for multiple consecutive days. The data collected in *Chapter* 3 was utilised, where animals performed a non-mnemonic (open field) and a spatial memory (RAM) tasks, intermingled with sleep sessions, for five consecutive days. Given that neuronal activity varies as a function of anatomical location on the transverse and dorso-ventral axes, a detailed description of network activity during

learning might involve sampling from the subiculum across multiple compartments of the structure. However, such an endeavour would require sufficient sampling across millimetres of the brain. This approach would come with significant costs (e.g. in time, expense of multi-shanked probes, etc.). Alternatively, one could focus on a restricted region. In the experiments of this thesis, electrodes were aimed at the dorsal compartment of the subiculum which, as suggested by *Chapter 2*, plays a role in memory processing during waking and sleep, at least during the initial phases of task learning. In addition, electrode penetrations were targeted to the central portion of the subiculum on the transverse axis. This region contains a homogeneous mix of neuronal firing patterns (Böhm et al., 2015; Kim & Spruston, 2012) and molecular markers (Cembrowski et al., 2018). In this way, these experiments aimed to densely sample from a heterogeneous mix of neuronal types and characterise their spatial firing properties.

To do so, the phase preference of neurons was examined during exploration of the open field environment. The data was clustered based on such “phase preference” and interrogated in regard to how the different subgroups of subicular cells played a role in the reactivation of waking firing patterns during sleep.

Methods

Data acquisition

The data analysed in this chapter is taken from data acquired and pre-processed according to the *Methods* described in *Chapter 3*. This includes the number of animals (n = 5), probe preparation and surgery, behavioural paradigm, histology, data acquisition, pre-processing and clustering, and tracking data. Additional analysis performed on the data is described below.

Data analysis

Behavioural results. Performance of the animals was measured in number of visits, WME and RME (see *Methods Chapter 2*), which were first manually scored by the experimenter. The resulting performance measures (mean number of visits, WME and RME) were then used to confirm the performance generated through the tracking of the animals. To assess learning across days, a one-way repeated measures ANOVA was performed (within variable: days) for each of the three measures. Post-hoc pairwise comparisons t-tests were performed to establish any differences across the 5 recorded days, using Holm-Sidak corrections.

Tracking. The steps for extracting and cleaning the tracking data are described in the *Methods* section of *Chapter 3*. Once the position of the animal was obtained, custom-made R code was used to extract the beginning and end of each trial, as well as visits to each arm. Rat behaviour of the RAM includes both runs to the end of the arms (where a reward might be located) and exploration of the arms without reaching goal location. To extract timestamps of these mixed behavioural epochs DLC was used to first identify the position of the end of each arm, as well as the centre of the maze. From this, three zones of interest were defined as concentric circles, radiating from the centre of the maze. The first zone delimited the central chamber of the RAM. Next, the “choice” area, which extended from the outside of the central zone to 10 cm into the eight arms of the maze. Any traversal into this portion of the arms was counted as a visit, even if the animal did not ultimately reach the end. In addition, the remaining portion of the arms (60 cm) was defined as the “reward” area, in which food rewards may be located (in three of the eight arms).

Next, the specific arm occupied for each visit was identified. To do so, the angle between each arm end and the centre of the maze was calculated. The Euclidean distance and the angle from the centre point were established for each tracked position, providing the exact position of the animal in relation to the centre for each timeframe. Each arm visit was then defined as when the animal entered the “arm” area, at an angle that was ± 0.3 radians from either of the 8 defined arm angles. Based on these two measures, each tracked point

was assigned to one of the three zones, as well as the specific arm being traversed (if the animal was in the choice or reward zone).

These data was then reprocessed to remove any errors in the tracking. First, tracked locations were identified as “outside” of the environment if the distance from the centre point was > 105 cm (length of the arms + 35 cm to accommodate for the animal leaning over the edge of the arms). These “outside” points were removed and replaced with interpolated data (± 1 tracked location). Rapid jumps back and forth between zones (across a single tracked point) were reassigned to smooth the transition between zones.

Next, a matrix was created which contained the “zone” for each time point, as well as the associated arm number (1-8, or 0 for the centre). For all exploration, for segments in which the animal reached the reward zone, the arm number associated with it was checked to ensure the tracking was not “jumping” between arms. If the data showed instances where two or more arms were traversed without entering the central chamber, the most frequent arm value was taken. To validate the resultant arm/central zone visit, the data was compared to the behavioural results acquired manually by the experimenter.

Cell position identification. The output of KiloSort provides spike times and the putative single unit to which each spike belongs, as well as the electrode on which the largest spike was detected for a given neuron. The location of this largest spike likely correlates to the position of the soma in the tissue (Henze et al., 2000). To identify the location of each electrode in both the proximo-distal and radial axes, and hence the position of each cell, three factors were taken into consideration. First, the surgery stereotaxic coordinates (Paxinos & Watson, 2007; see ***Table 1*** in *Chapter 3*). Then, the selected channels based on activity during implantation (see *Methods, Chapter 3*). Lastly, the position of the probe track in the brain, as identified through histology (***Figure 3A, right panels***). These three sets of data were integrated to produce a single set of coordinates for each probe shank. These data provided the location of the most superficial and deep electrodes on a given shank, and the position of the intervening recording heads could then be interpolated, accounting for the angle of the probe. These coordinates were then collapsed to a scale ranging from 0-1, both on the transverse (ML) and radial (DV) axes. To do so, the rat brain

atlas (Paxinos & Watson, 2007) was used to define the boundaries of the subiculum in the ML and DV axes, and electrode locations normalised to these values. Here, 0 represented the most superficial-proximal positions, and 1 the deepest (i.e. top of the layer)-distal subiculum (see ***Figure 3A, left panels***). Two notions should be kept in mind regarding these coordinates. First, following anatomical conventions for the hippocampus, superficial refers to the bottom of the layer, with respect to the brain surface, while deep refers to the top of the layer, closer to the brain surface (e.g. Amaral et al., 1991; Cembrowski et al., 2018; Kitanishi et al., 2021; see *General Introduction*). Second, the anterior posterior location of the probe was maintained within a small window (AP -5.76 to -6.0), meaning that stereotaxic coordinates were generated from consecutive AP locations in the atlas (see ***Figure 3A, upper left corner***).

Post-processing of LFP data. In order to analyse network oscillations in the LFP, the format of the wide band data had to be standardised across the NPX 1.0 and 2.0 recordings. For the NPX 1.0, separate 30 kHz sampling rate (high pass filtered at 300 Hz, used for detecting action potentials) and wideband 2.5 kHz files were recorded. NPX 2.0 recordings produced a single wideband data file, again sampled at 30 kHz. Both wide band formats were down sampled to 1.25k (for theta detection) and 5k (for detection of fast oscillations, e.g. SWRs). The sampling rates of these file formats were therefore significantly greater than the Nyquist threshold (Nyquist, 2002), while being significantly smaller than the source data files.

Theta detection. Theta detection was performed in two steps, by first identifying periods of high theta power during locomotion, and then detecting individual theta oscillations within them (Csicsvari et al., 1999; O'Neill et al., 2006). First, periods of high theta power were detected by calculating the ratio of theta (6-12 Hz) and delta power (2-4 Hz) in overlapping 1600 ms segments of 800 ms steps, using Thomson's multi-taper method (Mitra & Pesaran, 1999; Thomson, 1982). The average running speed of the animal was then calculated in the same windows. Windows with running speed > 2 cm and theta/delta ration of > 2 were designated as theta epochs. A custom-made graphical interface was

then used to manually adjust the exact beginning and end of theta epochs when needed. This software also allows the experimented to mark non-theta periods during rest/sleep in the sleep box. Here, periods of high theta power while the animal settles down or during REM-sleep could be excluded from further analysis. These non-REM epochs were thus used for sleep analysis (see below).

Second, individual theta oscillations were detected inside these identified theta epochs. To do so, the LFP was band-pass filtered at 5-28 Hz. This band was chosen in previous work to minimise errors in peak detection (see Csicsvari et al., 1999). Next, the negative peaks (or “troughs”) were detected in the filtered data to identify individual oscillations on each channel, selecting only those with wavelengths that fell in the range of 83.3-166.6 ms (i.e. 6-12 Hz). The phase of each spike was then calculated using theta oscillations detected on the same channel in which a given neuron was clustered (i.e. the channel with the largest spike). The trough-to-trough time interval could then be used to calculate the phase of spikes that fell within. The troughs, or negative peaks, were designated as 0/360 degrees, and the phase of spikes that fell between the negative peaks of theta were established through linear interpolation. This enabled the calculation of mean phase (or “phase preference”) for each cell. Rayleigh statistic was then used to test whether cells exhibited significant modulation (Zar, 2010). Phase preference of neurons was calculated in the open field, for those cells with ≥ 0.25 Hz firing rate across all experimental days.

“Theta group” analysis. Previous reports have suggested that neurons in the subiculum exhibit a range of theta phase preferences (Kitanishi et al., 2021; Lever et al., 2009). As a result, the distribution of phase preferences may show multiple peaks, reflecting different groups of cells with specific phase preferences. However, the number of observable peaks in a distribution is influenced by the bin size and/or smoothing applied to the histogram. To establish a significance to the observed number of modes, the Silverman method was implemented (Senior et al., 2008; Silverman, 1981). Significance in this test is calculated by first generating a smoothed kernel density estimate of the distribution of excitatory cell phase preferences and calculating the minimal smoothing bandwidth, which results in the number of modes being tested. Bootstrapped samples, each with the same number of data points as the original data, are then drawn from the smoothed distribution. Applying

the kernel density estimate to this bootstrapped data to achieve the same number of modes should require a smaller kernel bandwidth. By repeating this procedure multiple times, a p value can be calculated from the proportion of iterations where the minimal bandwidth required to produce the same number of modes was ≥ to the original data (< 5% = $p < 0.05$). The Silverman Mode Estimation Method was implemented in R (*silverman.test* function of the *silvermatest* package) using 10000 bootstrap replications. To avoid edge effects due to the circular nature of the distribution, the data was first shifted by 90 degrees. To validate this procedure, multiple tests were iteratively performed, testing for the presence of 2 to 10 modes. Once the number of modes had been confirmed with this method, the boundaries of each subgroup were identified, that is the minimum and maximum phase for a given mode, or "phase group". To do so, circular clustering of the data was computed with the circular algorithm implemented in the *CircClust* function of the *OptCircClust* R package, by inputting the number of clusters as determined with the Silverman test and using the fast and optimal ("FOCC") clustering method (see Debnath & Song, 2021). Once the boundaries of each "phase group" had been defined by the circular clustering, all excitatory neurons were assigned to one of the identified groups, independent of their mean firing rate.

SWR detection during sleep/rest epochs. SWRs are marked by a negative deflection of the LFP in the superficial portion of the cell layer and a concomitant 150-250 Hz oscillation, both in the CA1 (Buzsáki et al., 1983; Csicsvari et al., 1999) and subiculum (Böhm et al., 2015). SWRs were identified in this dataset by detecting bursts of ripple oscillations during periods marked as sleep/rest, using previously reported methods (Csicsvari et al., 1999; O'Neill et al., 2006). First, electrodes with high ripple power during sleep/rest were identified through manual inspection of the raw wideband signal. Next, the LFP data was band-pass filtered (150-200 Hz), and the "ripple" power (root mean square) calculated in the resultant signal for the selected electrodes and summed across them. In order to reduce false positive rates (for example due to muscle artifacts, caused by chewing), ripple power recorded on an electrode without ripples was subtracted from the signal. Like the SWRs observed in the CA1 area, subicular SWRs were accompanied by large increases in ripple power, lasting between ~60-120 ms. As a result, the envelop of ripple epochs could be defined, with the peak of ripple power marking the centre of the event, and the

onset/offset times determined by a return to baseline. Only events in which the peak ripple power passed 7 SDs above baseline power were included for further analysis.

SWR response. To quantify the firing responses of the four theta groups during SWRs, unit activity was cross correlated to the peak of ripple power from each SWR identified in sleep, across all days of recording. For each neuron, spike counts were calculated in 1 ms bins, ± 250 ms from the peak of the ripple power, and smoothed with a Gaussian kernel (1 SD = 4 ms). Neurons with spike trains resulting in sparse histograms (< 50 spikes in the cross-correlation) were excluded from further analysis. The first and last 50 ms of bins of the cross-correlation histogram served as a baseline, providing mean and standard deviation. The resultant histogram was then Z-scored using these values. Further analysis was conducted on ± 200 ms bins. In this way, histograms constructed from spike trains of neurons with diverse baseline firing rates could be averaged and compared. In addition to average responses, the time/Z of the peak (i.e. the bin with the maximal increase in rate) and trough (the bin with minimal response) was calculated for each neuron, across all theta groups.

Burstiness scores. To assess differences in firing properties of the identified theta groups, different measures were computed. The burstiness score was calculated as the first moment of the autocorrelation of spike trains (i.e. the mean value, see Csicsvari et al., 1999). As excitatory neurons in the subiculum exhibit a range of bursty and non-bursty properties, this measure was preferred over the one used in *Chapter 3,* as it would allow a more graded assessment of differences within the group of excitatory cells. This burstiness score was computed on the whole recording for each separate theta group (groups 1-4: n = 86, 22, 35, 140 respectively).

Firing rate and spatial information (SI). These two measures were calculated as described in *Chapter 3*. Firing rate was computed separately for the open field and the RAM data, for

each of the theta groups. Only neurons that had an average firing rate > 0.25 Hz across the whole recording were included in this analysis (groups 1-4 open field: n = 55, 17, 25, 86; RAM: n = 62, 18, 28, 102). Firing rates in the hippocampus are log-normally distributed (Battaglia et al., 2005; Mizuseki & Buzsáki, 2013) , thus firing rates were log transformed for comparisons across theta groups. SI was also computed separately for the two environments, on each day of the recording, for each theta group. Here, neurons that showed > 0.25 Hz firing rate on at least one day were included in the analysis (groups 1-4: n = 74, 19, 30, 133 for both environments). SI was only calculated for neurons that exceeded the firing rate threshold on a given day. Average SI across all days was calculated for each neuron, while again only including data from days where firing rates exceeded > 0.25 Hz.

Rate remapping. Rate remapping was expressed as the change between the firing rates during the open field exploration and the RAM task, divided by the sum (see equation below). Neurons were included if their firing rate was > 0.25 Hz in either of the two environments. The absolute value of this score was taken for each theta group on each day, and as an average across all days (groups 1-4: n = 76, 20, 29, 119). Only cells with firing rates > 0.25 Hz on at least one of the 5 days, in either of the two environments, were included. The chance change in rate score was established for each theta group on each day. This was performed by shuffling the rate established in the open field among neurons and recalculating the change in rate score. This procedure was repeated 1000 times, from which the median of the distribution was used as chance level.

$$rate\ remapping = \left| \frac{mean\ rate\ open\ field + mean\ rate\ RAM}{mean\ rate\ open\ field - mean\ rate\ RAM} \right|$$

Assembly similarity score. In order to compare how groups of neurons show changes in firing patterns across environments with different geometric shapes, an “assembly similarity score” was generated (O’Neill et al., 2008). This measure captures the tendency

of cell pairs to fire together (or “cofire”) in two behavioural epochs, which are then in turn correlated, to provide a measure of similarity in joint firing patterns across the two conditions. First, “cofiring” (Dupret et al., 2010; Kudrimoti et al., 1999; O’Neill et al., 2006, 2008, 2017) waw calculated for each possible cell pair of excitatory cells for members of a “theta group”. During exploration, theta epochs were divided into equal 100 ms windows and the instantaneous firing rate (IFR) calculated in each window, for each cell. The resultant series of IFRs was correlated between each pair of neurons, using a Pearson’s correlation. This correlation matrix could then be correlated (again with Pearson’s) with those generated in a second behavioural epoch, to produce a measure of similarity. While network encoding involves joint activity beyond pairwise interactions, such correlations likely capture higher order population representations (Schneidman et al., 2006). To account for the wide range of cell numbers recorded in different animals, pairwise correlations were concatenated across animals to produce a single assembly similarity measure, per group. The displayed confidence intervals represent Fisher CI (Zar, 2010). Correlations were compared with a “Z-test”, using the formula below. This calculation provides a Z score, from which a probability can be obtained (Zar, 2010).

$$Z = \frac{\zeta_1 - \zeta_2}{\sigma(\zeta_1 - \zeta_2)}$$

Where ζ is the Fisher transform of the correlation coefficient and σ ($\zeta_1 - \zeta_2$) is:

$$\sqrt{\frac{1}{n_1 - 3} + \frac{1}{n_2 - 3}}$$

With n being the sample size used to generate each correlation. Where multiple comparisons were performed, p values were corrected using Holm-Sidak correction.

This assembly similarity score was then generated to compare the first and second halves of the open field exploration, or firing patterns during the open field vs firing during the RAM task, for each day of the recording, for groups 1 and 4. The same measure was also used to evaluate the change in joint firing patterns at goal locations at the start and end of learning on each day, and during sleep, although this time during “high synchrony periods” (see below). Only cells with firing rates > 0.25 Hz across the whole recording in either the open field or RAM were included for pairwise analysis, for each of the assembly scores.

Reactivation and high synchrony periods. Reactivation during sleep has been shown to be strongest during SWRs in the CA1 (Kudrimoti et al., 1999; O’Neill et al., 2008). However, times of network synchrony in the CA1 are not restricted to SWRs (McHugh et al., 2024). This situation is further complicated by the lack of published data regarding the sleep architecture of the subiculum. An issue is that previous work shows how the subiculum has the capacity to generate SWRs, without input from the CA1 (Imbrosci et al., 2021). Thus, sleep reactivation was analysed during “high synchrony periods” using a method developed by Wilson and colleagues (Davidson et al., 2009; Ji & Wilson, 2007; O’Neill et al., 2017). These periods are correlated with SWR epochs, but also capture high synchrony epochs outside of them, denoting “frames” of activity that relate to cortical up-states (Ji & Wilson, 2007; Saleem et al., 2010), which were detected using the approach described by O’Neill and colleagues (2017). High synchrony periods were detected using the multiunit activity of all neurons designated as excitatory (see *Chapter 3*). The combined activity of excitatory cells was binned into 1 ms bins and smoothed with a Gaussian kernel (1 SD = 15 ms) to produce a curve representing fluctuations in multiunit activity. High synchrony epochs were detected if this curve passed 3 SD from the mean of the multiunit activity. The envelop of the event was extended until the curve again reached the mean rate, either side of the crossing. The peak synchrony represented the peak of the curve within this envelop.

Power spectra centred on the peak of high synchrony. ***Figure 9C*** shows an example of a high synchrony triggered spectrogram, for a channel with high ripple power (chosen by visual inspection of the wideband LFP data), from the third shank of rat #5. This was computed using the multi-taper method, with 100 ms overlapping temporal bins (step = 6 ms). A Z-score was computed for each frequency band using the mean and standard deviation of the power calculated across the entire sleep session. For each bin, a normalised measure of power was obtained for each frequency band, in units of standard deviation from the mean.

Reactivation. Reactivation in sleep was detected using the same cofiring "assembly similarity" analysis described above, from pairs of neurons with > 0.25 Hz firing rate in the RAM across the whole recording. Here, cofiring patterns were correlated between waking exploratory activity in the goal arms and sleep before (pre) and after (post) exploration of the RAM. As above, cofiring values were concatenated across animals to produce a single score per measure. On day 1, both sleep sessions occurred within the same day (sleep after the open field and sleep after the RAM). On subsequent days, the sleep session following maze learning on the previous day served as pre-sleep. Pairwise correlations may in part arise due to the pre-wired anatomical connectivity of the network. In order to account for pre-existing or hardwired joint firing patterns during sleep, as well as establish if reactivation reflects newly formed assembly activity, a partial correlation approach was employed, similar to Kudrimoti and colleagues (1999). Here, the relationship between waking patterns during learning were correlated with post-sleep, while holding constant the variability during explained by cofiring in pre-sleep. Reversing this order (waking vs pre-sleep accounting for post-sleep) provides a control for learning. Pre-sleep on the first day cannot reflect learning related assemblies, as no learning has yet taken place, and there is simply familiarisation with the maze. However, from day 2 onwards, pre-sleep may reflect learning from the previous day.

Statistics. All statistics were generated with R and |stats (Gary Pearlman, https://garyperlman.com/stat/). Throughout the chapter, p values are corrected for multiple

comparisons with the Holm-Sidak correction (Zar, 2010). Boxplots depicted in the figures, unless otherwise specified, show median of the distribution (thick line inside the box) and 95% confidence intervals ("whiskers"). All Z-scores are reported as positive, regardless of direction.

Results

1. Animals recorded while performing the RAM task showed improved performance across days

The main objective of this chapter was to assess possible differences in electrophysiological properties of subicular neurons during a learning and a non-learning task. To do so, the data from the animals described in *Chapter 3* was further analysed. The animals were recorded exploring an open field apparatus (non-learning context) and performing the RAM task described in *Chapter 2*. ***Figure 1A*** shows an example of the tracking of an animal performing both tasks for each of the 5 recorded days. To verify that the animals were learning across days in the RAM, number of visits, RME and WME were assessed, similarly to the analysis performed in *Chapter 2*. When assessing the number of visits, a one-way repeated measures ANOVA revealed a significant difference in performance across days ($F(4,16) = 25.229$, $p < 0.05$, $\eta^2g = 0.74$; ***Figure 1B***). The post-hoc pairwise comparisons t-tests highlighted a difference between day 1 and day 4 ($df = 4$, $t = 5.59$, $p < 0.05$), as well as between day 5 and days 1, 2 and 3 ($df = 4$, $t = 7.30, 5.73, 6.88$ respectively, all $p < 0.05$). No other differences were found (all $p > 0.05$). This suggested a difference in number of visits between at least the first and the last day of recording, pointing towards the animals learning the location of the food rewards, consistent with the behaviour shown in *Chapter 2*.

The same pattern was uncovered for the RME analysis (ANOVA: $F(4,16) = 31.3232$, $p < 0.05$, $\eta^2g = 0.799$; ***Figure 1C, top***). The post-hoc t-tests revealed, again, a significant difference between day 4 and days 1, 2 and 3 ($df = 4$, $t = 8.67, 4.95, 10.9$ respectively, $p < 0.01, 0.05, 0.01$ respectively), along with significant differences between day 1 and days 3 and 4 ($df = 4$, $t = 7.38, 5.85$, $p < 0.05$). The repeated measures ANOVA for WME also

showed to be significant ($F(4,16) = 7.49$, $p < 0.05$, $\eta^2g = 0.503$; ***Figure 1C, bottom***), but the post-hoc multiple comparisons did not withstand the Holm-Sidak corrections (all $p > 0.05$).

These results confirm a general pattern of learning for the recorded animals during the 5 days of the RAM task. ***Figure 1B-C*** overlays the performance of the animals to the performance of the cohorts of control animals that performed the same task in *Chapter 2* (*Experiments 1 and 2*), which showed similar results to those highlighted in this chapter. Thus, the behaviour during the task matched that observed in *Chapter 2*, despite the presence of the implant and the attached cable.

With this behavioural paradigm, neurons can be characterised in the open field, examined in their changes between the open field and the learning in the RAM, and finally evaluated on how neuronal activity changes with learning. Given that excitatory neurons in the subiculum present a heterogeneous mix in terms of firing properties and connectivity, it is possible that different “types” of subicular neurons play different role in cognitive processes (Cembrowski et al., 2018; Kitanishi et al., 2021; O’Mara et al., 2009).

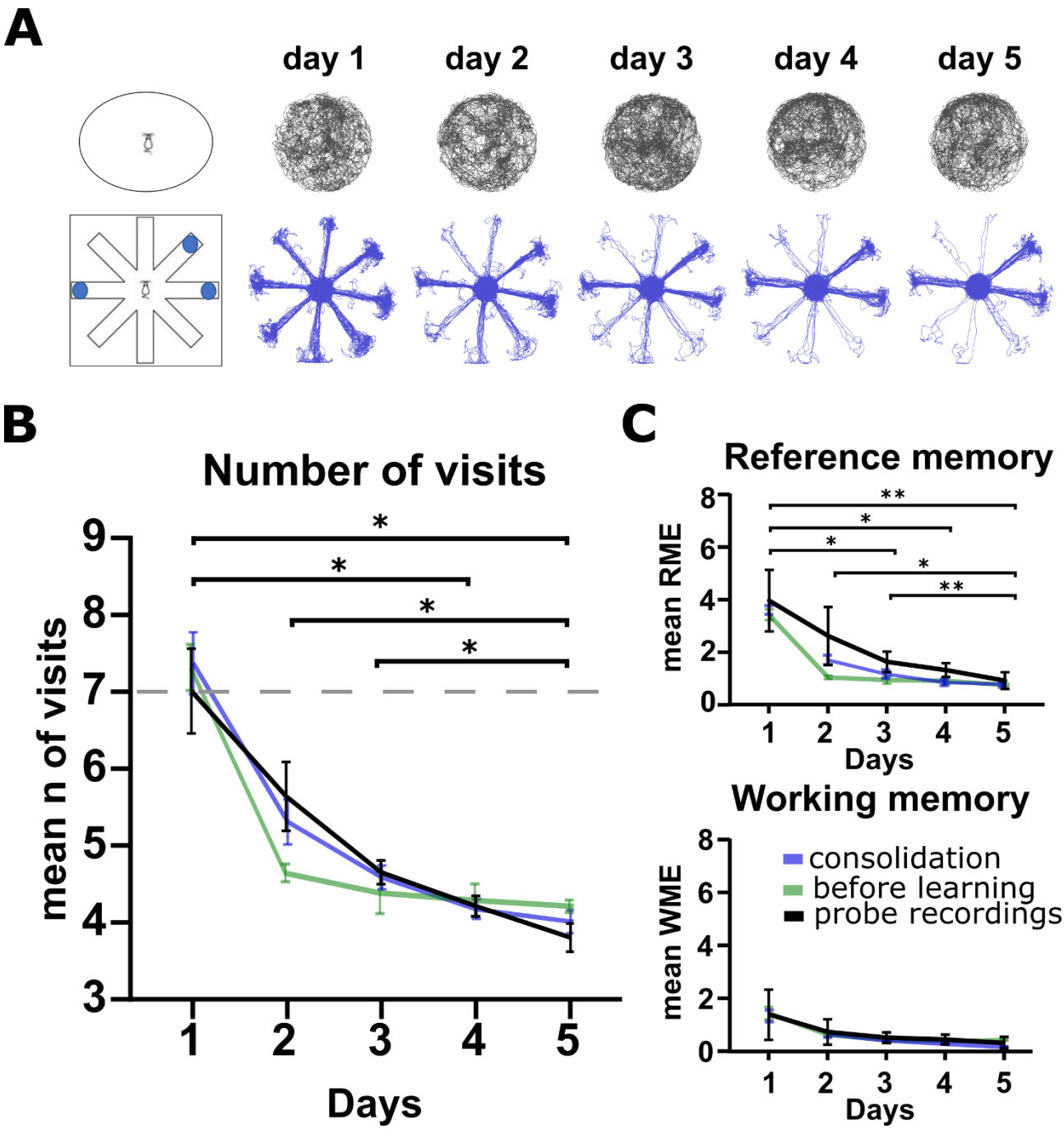

Figure 1. Animals performing the RAM task show learning across days. *(A) Example tracking of one animal on the RAM (top) and open field (bottom) sessions. (B) Mean number of visits across days for the 5 recorded animals (black), overlayed with the performance recorded in Chapter 2 during Experiments 1 and 2. Dotted grey line represents chance level of performance with zero WME. (C) Mean RME (top) and WME (bottom) across the 5 days for the 5 recorded animals (black), overlayed with the performance of animals in Experiments 1 and 2 of Chapter 2. Errors bars represent SEM. Significance values: * p < 0.05, ** p < 0.01.*

2. Pyramidal cells in the subiculum can be classified into four groups based on their theta preference

Electrophysiological recordings in the hippocampus of freely moving animals have identified in the past how neurons in this region are “locked” to specific phases of the theta oscillation (Buzsáki et al., 1983; Fox & Ranck, 1981; Ranck, 1973). In the subiculum, the distribution of these “theta preferences” varies across neurons, and some have reported the presence of different groups based on their location in the area (Kitanishi et al., 2021).

The first aim of this chapter was to explore the presence of these “theta groups” in the recorded dataset. Neurons in the subiculum were tracked across 5 consecutive days while animals explored a circular arena for ~30 minutes a day. Neurons were selected with firing rates > 0.25 Hz during open field exploration over 5 days (183 out of 283 excitatory cells; data pooled across the 5 days). First, the mean theta phase of spiking by each excitatory neuron was computed. Of the sample of 183 selected excitatory neurons, 182 showed significant modulation (Rayleigh test, $p < 0.05$). In addition, all 34 interneurons were significantly theta modulated, which also showed a greater depth of modulation than the excitatory cells (median vector length, interneurons: $r = 0.22$; excitatory cells: $r = 0.18$; Mann-Whitney U test, $z = 0.1704$, $p < 0.05$). Examination of the distribution of excitatory phase preferences revealed a multi-peaked distribution (see ***Figure 2A***), with 4 visible modes. To test if the distribution significantly presented four modes, the Silverman test was computed (see *Methods*), which confirmed the presence of 4 peaks ($p < 0.01$; ***Figure 2***). Indeed, further testing with this method only revealed a significance for 4 modes, when iteratively asking if 2 through to 10 peaks were present in the data. These four peaks represent discrete sets of cells with similar phase preference, which will be referred to as groups 1-4. Next, the boundaries of each group were identified. To do so, a circular data clustering algorithm was used (see *Methods*). Here, the algorithm was instructed to separate the data into 4 clusters, which then provided the minimum and maximum phase for each group. These four bands were then used to calculate the mean preferred phase in each group. Group 1 ($n = 86$) tended to fire just after the trough of theta oscillation (trough of theta = 0 degrees, group 1 mean angle = 42.1 degrees), while group 2 ($n = 22$) on the ascending phase (mean angle = 125.05). Groups 3 ($n = 35$) and 4 ($n = 140$) prevalently fired on the descending phase, the first at an earlier phase (mean angle = 227.15 degrees)

than the second (mean angle = 342.2 degrees). **Table 1** shows a breakdown of the number of neurons belonging to each group for each rat.

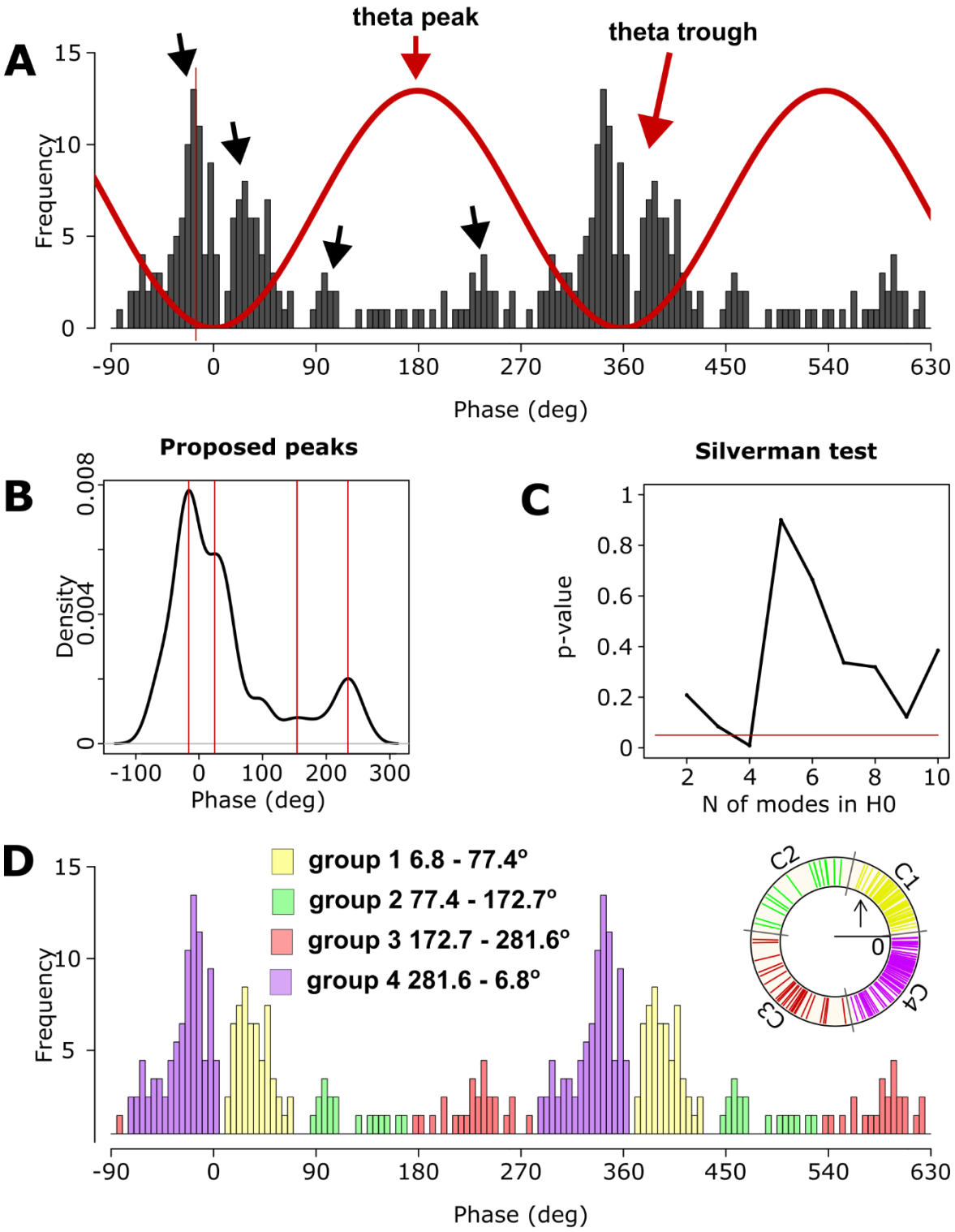

Figure 2. Subicular excitatory cells can be divided into 4 categories based on their theta phase preference. *(A) Distribution of theta phase preferences of excitatory neurons during exploration of the open field. Red arrows mark the trough (0/360 degrees) and peak of theta (180 degrees). Black arrows mark 4 possible peaks in the distribution. (B) Proposed peaks of the shifted distributions, as identified using the Silverman's mode estimation method (see Methods), highlighted by the red vertical lines. (C) P-values of the Silverman test run on 2-10 possible modes*

of the data. Red horizontal line represents the significance level at p = 0.05. (D) Circular clustering identified the theta phase boundaries of the 4 groups (see insert). This analysis provided 4 subsets of neurons, grouped by theta phase preference. Theta band is marked for each group in the figure key.

Figure 2D highlights the distributions of the four groups relative to their phase preference. No significant differences were observed between the groups in the depth of theta modulation, as measured through the median vector length (median r = 0.2, 0.15, 0.17, 0.18, groups 1-4 respectively. Kruskal-Wallis test: df = 3, χ^2 = 6.77, p = 0.08). However, the near significance of the analysis and under sampling of groups 2 and 3 indicates that further data may be required to clarify this result.

Animal	***Total number of excitatory cells***	***Group 1***	***Group 2***	***Group 3***	***Group 4***
#1	*24 (8.48%)*	*0*	*3 (13.64%)*	*3 (8.57%)*	*18 (12.86%)*
#2	*35 (12.37%)*	*2 (2.32%)*	*0*	*3 (8.57%)*	*30 (21.43%)*
#3	*49 (17.31%)*	*12 (13.95%)*	*10 (45.45%)*	*9 (25.71%)*	*18 (12.86%)*
#4	*17 (6.01%)*	*7 (8.14%)*	*0*	*3 (8.57%)*	*7 (5%)*
#5	*158 (55.83%)*	*65 (75.58%)*	*9 (40.91%)*	*17 (48.57%)*	*67 (47.86%)*
All	*283*	*86*	*22*	*35*	*140*

Table 1. Number of cells belonging to each theta group for each recorded animal. *Last row shows the numbers for all animals together. Interneurons were excluded from this analysis. Percentages refer to the total number of cells for each individual group.*

3. Location of the "theta groups" in the transverse and radial axes.

Previous reports in the subiculum suggest that there is a gradient of theta preferences based on the location in the layer, with deep neurons in the distal portion of the subiculum firing at earlier phases of theta than superficial cells (Kitanishi et al., 2021). The recordings of this thesis aimed at collecting data from the mid-area of the subiculum (on the proximo-distal axis, see *Chapter 3* for surgery coordinates), to minimise possible differences to the radial axis only. As the analysis identified 4 groups of neurons based on their theta preference, the distribution of these groups was explored along the radial axis, and the restricted range of locations in the transverse axis. First, the position of the probes was normalised on both the proximo-distal and the radial axes (see *Methods* and ***Figure 3A***). The distributions of cells by group along the proximo-distal axis revealed similar clustering of the cells along the mid-portion of the subiculum, as expected from the surgery coordinates (Krustal-Wallis test performed on the 4 distributions revealed no significant difference: $\chi^2 = 7.4$, df = 3, $p = 0.0538$; ***Figure 3B***). However, the near significance of this result indicates that more data is required. Next, the position of neurons in each of the four groups was identified along the radial axis. A Kruskal-Wallis test performed on the four distributions revealed a significant difference ($\chi^2 = 15.19$, df = 3, $p < 0.01$). Post-hoc Mann-Whitney U tests confirmed significant differences between group 1 and groups 3 and 4 (1 vs 3: $z = 2.46$, $p < 0.05$; 1 vs 4: $z = 3.53$, $p < 0.005$), while no difference was found in the median position of cells for groups 1 and 2 ($z = 0.29$, $p = 0.39$; see ***Figure 3C***).

The results of this section highlight the presence of four distinct groups of neurons that fire at separate theta phases during free exploration of a familiar environment. These groups seem to be differently distributed along the radial axis, with group 1 being more superficial than groups 3 and 4.

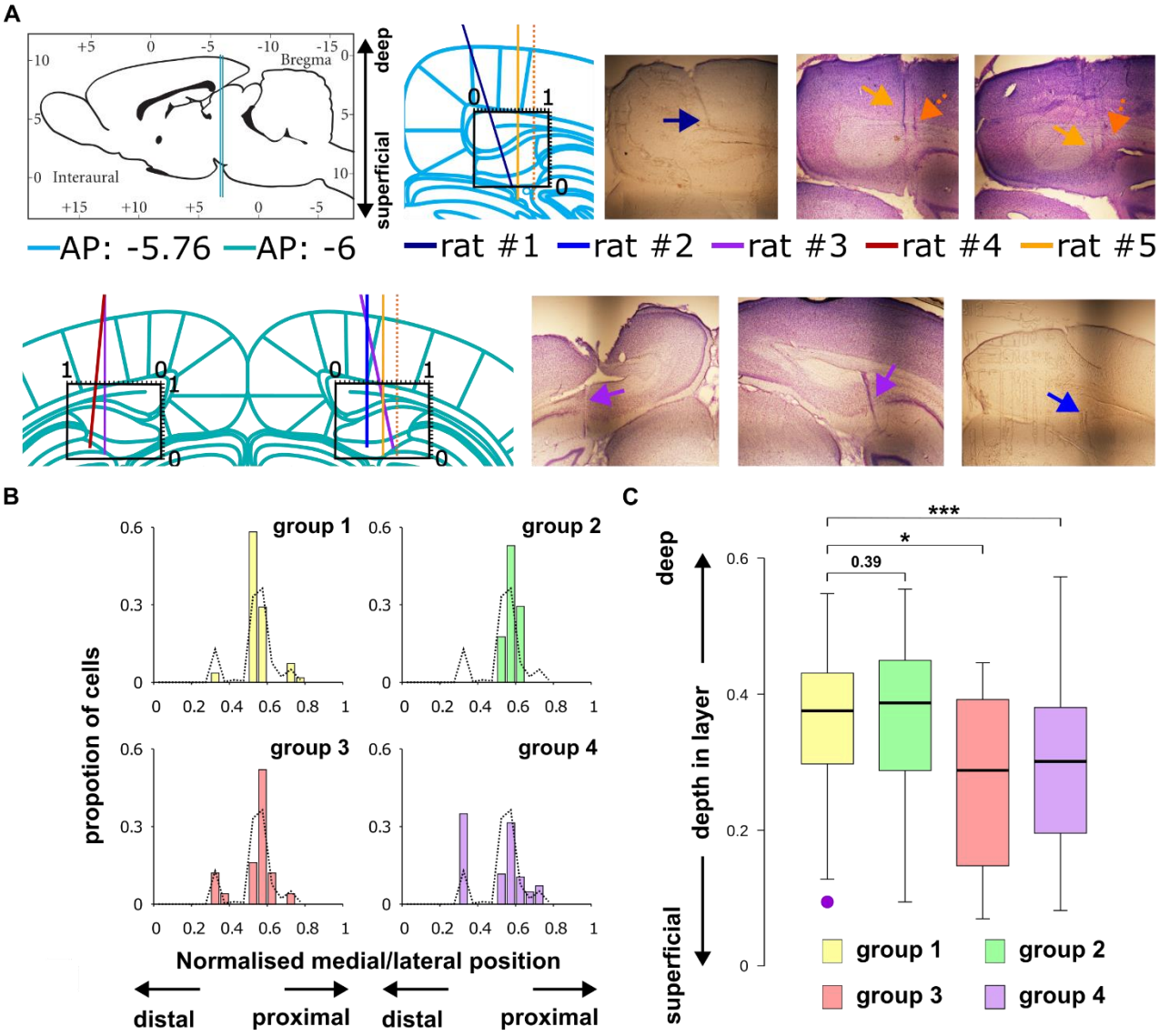

Figure 3. Location of cells in theta groups 1-4 by proximal-distal location and depth. *(A) Schematic representation of probe tracks (left) and histological pictures (right). Probes for each animal are represented by a different coloured line/arrow. Dotted lines/arrows represent un-analysed probe shanks. Histology for rat #4 was not collected therefore only the proposed probe track is shown. Schematic on the upper left corner shows the two coordinates of implant on the anterior-posterior axis, represented by two coloured lines, while schematic of the brain slices shows the normalised coordinates system for each plane, which were adjusted to fit the area of the subiculum. (B) Distributions of normalised proximal position for each neuron on each NPX shank. The proportions of cells are shown at each recoded location, separately for groups 1 to 4 (coloured histograms). Dotted line represents the distribution of all cells. (C) Boxplot showing the distributions of each theta group's cells along the radial (deep-superficial) axis. Significance levels: * $p < 0.05$, *** $p < 0.005$.*

4. Firing characteristics of subicular neurons differ based on their theta preference

Some firing and spatial properties of neurons in the subiculum have been shown to have a high degree of variability (see *General Introduction*). As different groups of neurons have been identified based on their theta preference, the next step involved testing whether these groups would show different firing and spatial characteristics.

Differences in burstiness were first examined as a measure of firing characteristics amongst the four theta groups. Excitatory bursty and non-bursty cells (Stewart & Wong, 1993; Taube, 1993) have been previously identified in the subiculum, distributed along a gradient on the proximo-distal and radial axis (Böhm et al., 2015; Cembrowski et al., 2018; Kim et al., 2012; Kim & Spruston, 2012; Kitanishi et al., 2021; Sharp & Green, 1994). While the data collected in this thesis was recorded in similar positions along the proximo-distal axis, it showed a different distribution of cells in group 1 compared to groups 3 and 4 along the radial axis, with groups 1 cells showing to be generally deeper in the layer than the other groups. *In vitro*, bursty cells seem to be more concentrated in deep layers of the subiculum, while regular-firing neurons prevalently being in the most superficial part (Greene & Totterdell, 1997; Menendez De La Prida et al., 2003).

In *Chapter 3*, burstiness was assessed as the mode of the autocorrelation. While this measure can help in highlighting differences between the burstiness of excitatory versus inhibitory cells, when looking at a population of excitatory neurons only, a more sensitive method is required to tease apart any differences. For this reason, the first moment of the autocorrelation (see *Methods*) was calculated for each of the four theta groups, across the whole recording. A Kruskal-Wallis test was performed to compare the four groups, which showed to be significant ($\chi^2 = 13.12$, df = 3, $p < 0.01$; ***Figure 4A***). The post-hoc Mann-Whitney U test revealed significant differences between groups 1 and 2 ($z = 1.97$, $p < 0.05$) and groups 1 and 4 ($z = 3.6$, $p < 0.001$), but no difference between group 1 and 3 ($z = 1.21$, $p = 0.11$). These results suggest that group 1 cells are in general more bursty than cells in groups 3 and 4, in line with the data from previous *in vitro* experiments.

Another distinctive feature of neurons in the hippocampus is their firing rate. In the subiculum, previous reports have shown a gradient of the distribution of firing rates along the proximo-distal axis, with more distal cells having a higher mean firing rate than

proximal ones (Kim et al., 2012). Additionally, bursty cells in the subiculum have been shown to have higher mean firing rates compared to non-bursty ones (Kim et al., 2012; Lever et al., 2009). While the analysis of this chapter did not include clustering of cells into these two categories, examining the general burstiness of the four theta groups has revealed that group 1 tends to have cells that are more bursty than the others (see results above). With this in mind, one would expect group 1 cells to show a higher mean firing rate compared to the other groups. Thus, a comparison between the firing rates of the four theta groups was made, during both the open field exploration and the RAM task (calculated across all days of recording; ***Figure 4B***). Here, as above, neurons were selected if their firing rate was > 0.25 Hz across the whole recording (for the two environments separately). A Kruskal-Wallis test was performed for the two environments separately, which both showed significant results (open field: $\chi^2 = 26.52$, df =3, $p < 0.001$; RAM: $\chi^2 = 15.06$, df = 3, $p < 0.01$). When post-hoc Mann-Whitney U tests were run for each group, both the open field and the RAM analyses showed a significant difference between group 1 and groups 2 (open field: $z= 3.18$, $p < 0.005$; RAM: $z = 3.05$, $p < 0.005$), 3 (open field: $z = 1.67$, $p < 0.05$; RAM: $z = 2.68$, $p < 0.01$), and 4 (open field: $z = 4.73$, $p < 0.005$; RAM: $z = 3.22$, $p < 0.005$; see ***Figure 4D***). Additionally, a difference was found between groups 1 and 3 in the RAM ($z = 2.68$, $p < 0.01$). These results suggest a different pattern that what is reported in literature, with group 1 cells (identified in our previous analysis are “more bursty”) showing lower firing rates compared to the other, “less bursty” groups.

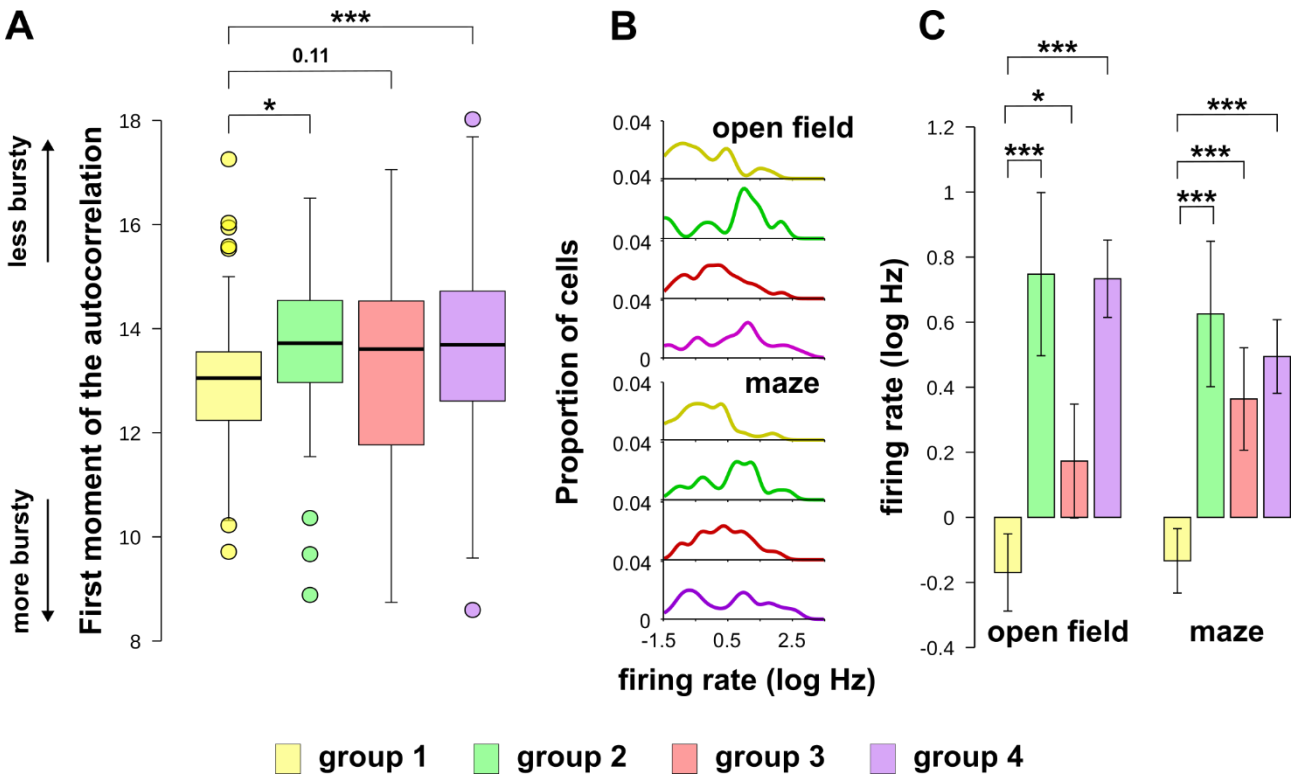

Figure 4. Group 1 neurons are bursty and show sparse firing. *(A) Group 1 neurons are more bursty than groups 2 and 4, based on their first moment of the spike train autocorrelation calculated from the whole recording. (B) Log-transformed firing rate distributions of excitatory neurons, shown separately for each cell group and for each environment. (C) Group 1 shows sparser mean firing rate than the other 3 groups, in both the open field and the RAM. Significance levels: * p < 0.05, *** p < 0.005. Error bars show SEM.*

5. Firing characteristics of subicular neurons during SWRs differ based on their theta preference.

In the hippocampus, during quiet restfulness or sleep, high-frequency field oscillations are generated locally in ~60-100 ms bursts (SWRs; see *General Introduction*). During such events, neurons throughout the hippocampal circuit show robust increases in firing rate (Buzsáki, 2015; Buzsáki et al., 1983; O'Keefe et al., 1978). However, previous work suggests that neurons in the subiculum show heterogeneous responses to SWRs, with a minority of neurons showing suppressed firing rates during SWRs, while other exhibiting increases.

To verify that this was happening in this thesis' dataset, SWR events were detected in the sleep data (see *Methods*). Time periods with SWRs were then selected to analyse the distributions of firing rates for each of the four theta groups (***Figure 5B***). The firing response (see *Methods*) of all groups presented a distinct profile, with a "peak" around the middle of the SWR events (time zero, the black arrow in ***Figure 5B***), and a consequent "trough" shortly after (the blue arrow). The next analysis focused on these two distinct phases in the firing rate response to SWRs for each group.

The firing rate at the peak of the SWR firing response varied between the 4 groups (Kruskal-Wallis, $\chi^2 = 57.27$, df = 3, $p < 0.00001$; groups 1-4 firing rate median z = 35.3, 3.9, 6.6, 27.6 respectively), with group 1 showing a stronger SWR response than groups 2-4 (Mann-Whitney U test, z = 6, 6.4, 3.12, all $p < 0.001$; ***Figure 5C, left***). Similarly, the drop in firing rate during the trough also varied between groups (Kruskal-Wallis test, $\chi^2 = 42.2$, df = 3, $p < 0.00001$, groups 1-4 firing rate median z = 2.59, 7.59, 5.53, 3.72 respectively). Group 1's minimum response showed to be significantly different than groups 2-4 (Mann-Whitney U test, z = 5.54, 4.46, 3.64, all $p < 0.00001$, $p < 0.0001$, $p < 0.001$). As group 2 showed the lowest median firing rate Z-score (7.59), it was quantified whether this would be significantly different than any of the other groups (groups 3 and 4). This was analysed with a Mann-Whitney U test, which showed significant in both cases (group 2 vs 3: z = 1.68, $p < 0.05$; group 2 vs 4: z = 3.59, $p < 0.001$). These results suggest that group 2 showed the largest drop in firing rate (***Figure 5C, right***).

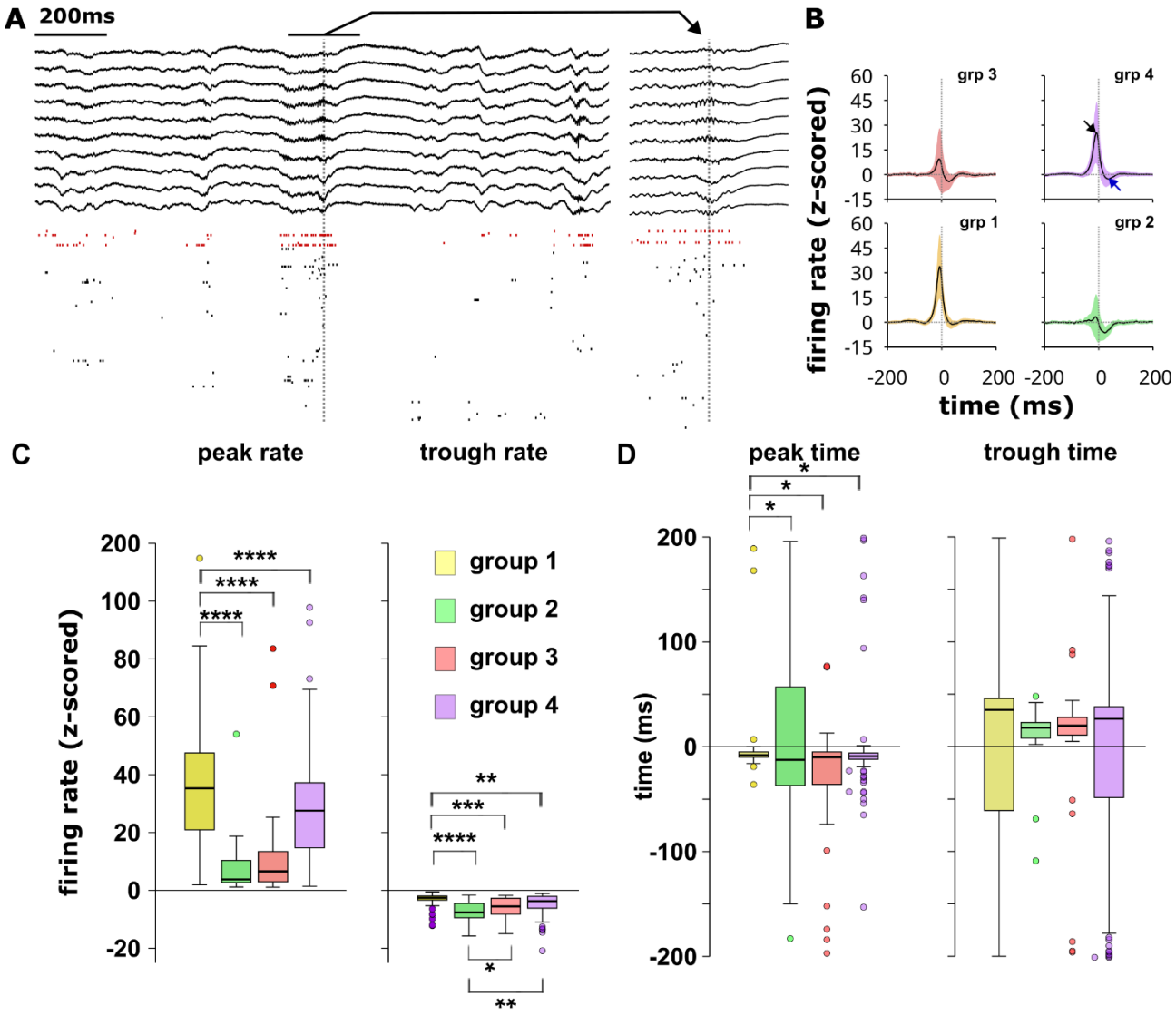

Figure 5. Sharp wave response differs across the four theta groups. *(A) Example of SWR event detected on shank 3 of the NPX 2.0 probe. Dotted line represents the peak of the ripple power. Right: expansion of the section marked by the solid bar in the left panel (± 200 ms from the peak of the detected ripple power). Raster plot shows the spike times of recorded neurons in the shank. Each row represents the spike times of a single cell. Red tics are interneurons, while black are excitatory cells. (B) Firing response of groups 1-4 neurons to SWRs. The average of the Z transformed cross-correlation (see Methods) is shown for each theta group. Shaded regions represent ± 1SD from the Z distribution. Black arrow points to the "peak" of the SWR response, while blue to the "trough", or minimum response. (C) Subiculum neurons have a biphasic response to SWRs. Left: boxplots showing the distributions of Z-transformed firing rates for each theta group. Right: firing rates during the below baseline drop after the peak. (D) Timeline of firing of each theta group. Left: group 1 neurons fire significantly before the peak of the ripple power (marked as time 0). Right: all neuronal groups fire around the same time after the peak of ripple power. Significance levels: * p < 0.05, ** p < 0.001, *** p < 0.0001, **** p < 0.00001.*

The timing of the maximal response (***Figure 5D, left***; Krustal-Wallis test, $\chi^2 = 11.8$, df = 3, $p < 0.01$), but not of the trough (***Figure 5D, right***; Krustal-Wallis test, $\chi^2 = 4.7$, df = 3, p = 0.19) differed amongst the groups. All groups showed a maximal firing response before peak of ripple power (groups 1-4, median time = -8, -12.5, -10, -9 ms from the peak of ripple power), with group 1 firing significantly later than the other groups (group 1 vs 3-4, Mann-Whitney U test, z = 2.3, 2.6, 2.2, all $p < 0.05$).

These results suggest that cells that fire during specific theta phases during exploration also show a different time course of firing during SWRs, with group 1 showing the most robust response to SWR, while firing closer to the peak.

6. Spatial characteristics of subicular neurons differ based on their theta preference.

While differences in spiking dynamics have been suggested in the subiculum, less data has been gathered in the past on differences in spatial information profiles of neuronal populations in this area. Previous reports have suggested that subicular neurons carry a similar degree of spatial information compared to pyramidal cells in the CA1 region (Kitanishi et al., 2021). In both the proximal CA1 and distal subiculum, cells have a higher degree of spatial selectivity, while distal CA1 and proximal subicular neurons are thought to carry less spatial information (Henriksen et al., 2010). Moreover, superficial CA1 cells are more likely to form spatial maps than cells in the deeper layer (Mizuseki et al., 2011). With this in mind, the next analysis compared the spatial information profiles of the four theta groups across the 5 recording days (see *Methods*). First, the amount of spatial information carried out during exploration of the open field environment was quantified (***Figure 6A***). A mixed repeated-measures ANOVA was computed (between: groups, within: days), which revealed a significant main effect for both factors (group: F = 47.764, df = 3, $p < 0.001$; day: F = 2.656, df = 4, $p < 0.05$) but no interaction effect (F = 0.496, df = 12, p = 0.918). To further explore the effect of time on the spatial information carried across time, a one-way ANOVA was run for each group separately, which revealed a significant effect for both groups 1 and 2 (group 1: F(3.3, 135) = 3.21, $p < 0.05$; group 2: F(4, 48) = 3, $p < 0.05$) but not for groups 3 and 4 (group 3: F(4, 84) = 1.29, p = 0.282; group 4: F(4, 252) = 1.9, p = 0.111). However, these significant differences disappear with Holm-Sidak correction (p =

0.84 for both groups 1 and 2). Such a trend may require further data to fully test. However, the mixed ANOVA highlighted a difference between groups regardless of the time of recording, which showed robust differences in spatial information. To test this, a one-way ANOVA was performed between the average spatial information scores of the four groups (n = 74, 19, 30, 113; ***Figure 6A, right***). This, as expected from the previous analysis, revealed a significant effect of the group variable ($df = 3$, $F = 7.272$, $p < 0.001$). This effect reflected on a difference between group 1 and any of the other groups (post-hoc pairwise t-tests, group 1vs2, 1vs3, 1vs4: $t = 2.65$, $p < 0.05$; $t = 2.789$, $p < 0.05$; $t = 4.317$, $p < 0.001$, respectively). Overall, these results suggest a different way of processing spatial information in a familiar environment by group 1 (and in part group 2, although the small number of cells of this group makes drawing conclusions problematic; see *Discussion*).

Could these groups process spatial information differently when performing a learning task? To test this, the same set of analyses was performed on the spatial information scores of the four groups when the animals undertook the RAM task. The mixed repeated-measures ANOVA only revealed an effect of the group variable ($F = 59.059$, $df = 3$, $p < 0.001$; ***Figure 6B, left***), while no effect was registered for either the day variable or the interaction between group and day (day: $F = 0.177$, $df = 4$, $p = 0.95$; interaction: $F = 0.638$, $df = 12$, $p = 0.811$). As no time effect emerged from the analysis, focus was next given to the spatial information regardless of day, by averaging the spatial information scores for each theta group (***Figure 6B, right***). This resulted in a similar pattern than the one revealed in the open field analysis. The one-way ANOVA performed between the four groups (n = 74, 19, 29, 144) highlighted a significant effect of the group variable ($df = 3$, $F = 7.998$, $p < 0.001$), and the post-hoc t-tests confirmed significant differences between group 1 and any of the other groups (group 1vs2, 1vs3, 1vs4: $t = 3.433$, $p < 0.001$; $t = 2.702$, $p < 0.05$; $t = 4.464$, $p < 0.001$, respectively). These results highlighted how cells in group 1 tend, on average, to be more spatial than cells in the other three groups, both during a non-learning (open field) and a learning (RAM) task. However, spatial selectivity did not appear to change with experience in the open field, or learning in the RAM.

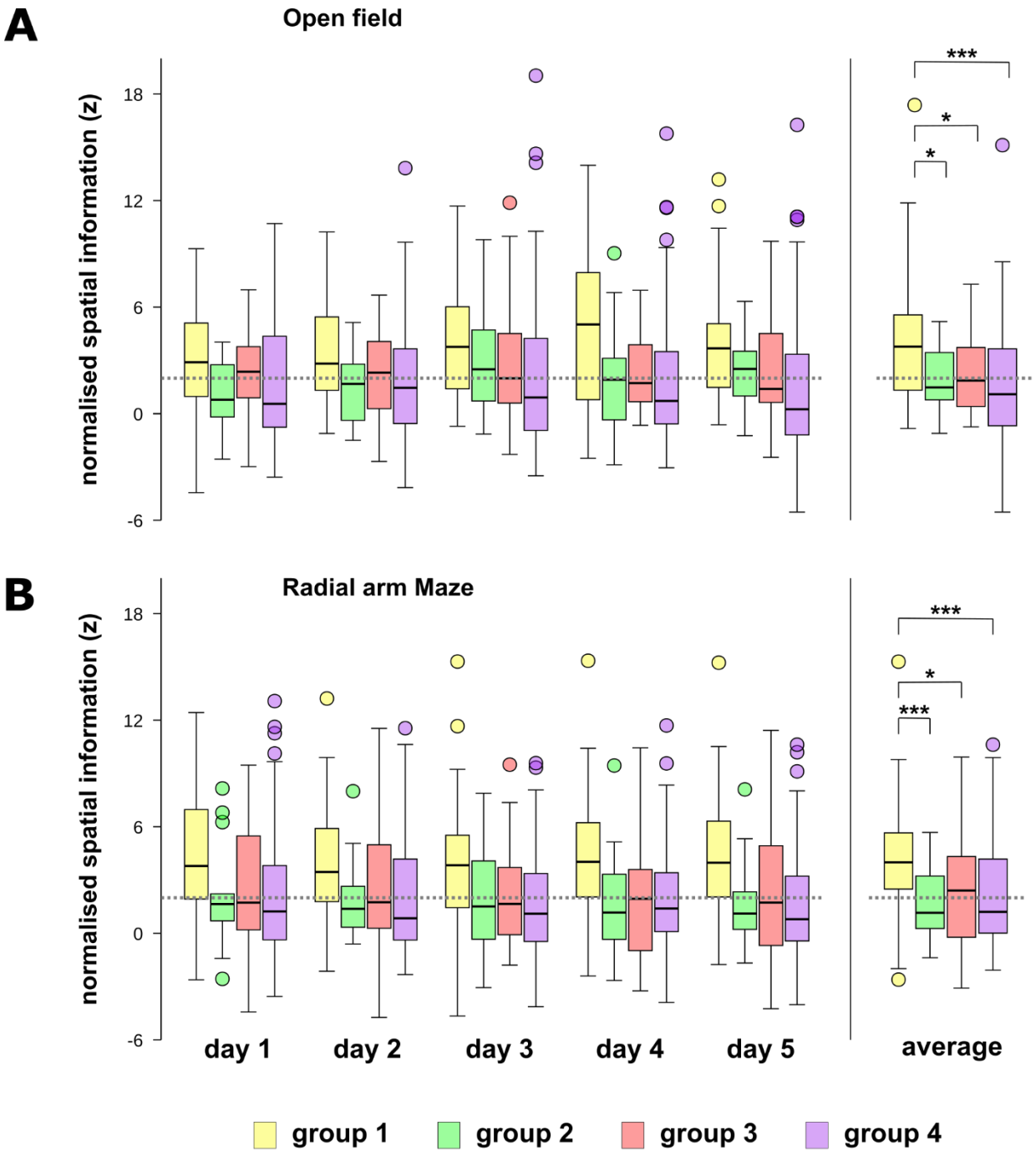

Figure 6. Group 1 neurons are more spatial than groups 2-3-4 during exploration of the open field and during learning on the RAM. *(A-B) Left: spatial information (see Methods) was calculated for each excitatory neurons, on each day in both the open field (A) and the RAM (B). Right: spatial information averaged across each day, for each cell. Dotted line represents + 2 SD from the Z distribution. Significance levels: * p < 0.05, *** p < 0.001.*

7. Theta groups show differences in rate coding during a learning and a non-learning task based on their theta preference.

Having established that group 1 neurons are more bursty, have lower firing rates, fire more robustly during SWRs, and are more spatial than groups 2-4, this thesis then looked at the plasticity of these cells. That is, do neurons in each of the groups show generalised neural coding across environments/tasks, or do these representations diverge? In the CA1, firing rates have been shown to change in the hippocampus over time in familiar environments (Mankin et al., 2012; Mau et al., 2018; Ziv et al., 2013), as well as between different environments (Leutgeb et al., 2005) . Leutgeb and colleagues showed that neurons in the CA1 and CA3 regions have decorrelated rates in different arenas, which can occur independently of place field remapping. This prompted them to hypothesise that firing rates could encode aspects of episodic memory, potentially beyond space, in concert with the spatial information provided by place field selectivity. A limited number of reports have addressed the degree to which neurons in the subiculum reorganise their firing rate across environments. Kim and colleagues (2012) report that firing rates remain similar (correlation between rates: $r > 0.8$) across two geometrically similar environments. This occurs in spite of spatial map reorganisation, at least in some neurons (Kim et al., 2012; Sharp & Green, 1994). Thus, both spatial (i.e. changes in the location of place maps relative to external cues) and rate remapping has been shown to be weaker amongst principal cells in the subiculum than the CA1 area. With these notions in mind, the next analysis sought to explore the rate remapping of subicular recorded cells both in a learning and a non-learning context. Here, the change in rate score used by Leutgeb and colleagues (2005) was used to compare rate remapping between the two environments (open field and RAM) in the four theta groups (see *Methods*). Given that some neurons may increase their rate in the RAM relative to the open field, while other show decreases, the score was calculated as the absolute difference in rate between the two environments, divided by the sum of the rates (see ***Figure 7***). This score provides a measure of the magnitude in change of rate, normalised for the firing rate of the cell, which results in a sign-less value between 0 (no change) and 1 (for neurons with a firing rate of zero in one of the two environments). To assess any differences in rate remapping between groups across the 5 recorded days, a mixed repeated-measures ANOVA was performed (between: groups, within: days). This revealed a significant effect of the group variable ($df = 3$, $F = 72.580$, $p < 0.001$), but no effect of either days or the interaction between group and days (days: df =

4, F = 0.024, p = 0.866; interaction: df = 12, F = 0.582, p = 0.858). Due to these results, the following analysis focused on exploring possible differences among the four theta groups, independent of time. A series of Mann-Whitney U tests was performed to compare the change in rate between groups 1 and 4 for each day (***Figure 7, left***). Results showed no difference between the two groups on day 1 (z = 1.62, p = 0.105), but a significant difference on every other day (day 2: z = 3.24, p < 0.01; day 3: z = 3.12, p < 0.01; day 4: z = 2.09, p < 0.05; day 5: z = 2.07, p < 0.05). This difference was reflected in the analysis of the average change in rate score over the whole recording, in which only group 1 showed a significant difference compared to groups 3 and 4 (unpaired Wilcoxon Rank Sum tests with Holm-Sidak correction; day 3: W = 860, p < 0.01; day 4: W = 2474, p < 0.05), while no other differences were found comparing the other groups (groups 1vs2: W = 471, p = 0.082; 2vs3: W = 158, p = 1; 2vs4: W = 508, p = 1; 3vs4: W = 788, p = 1).

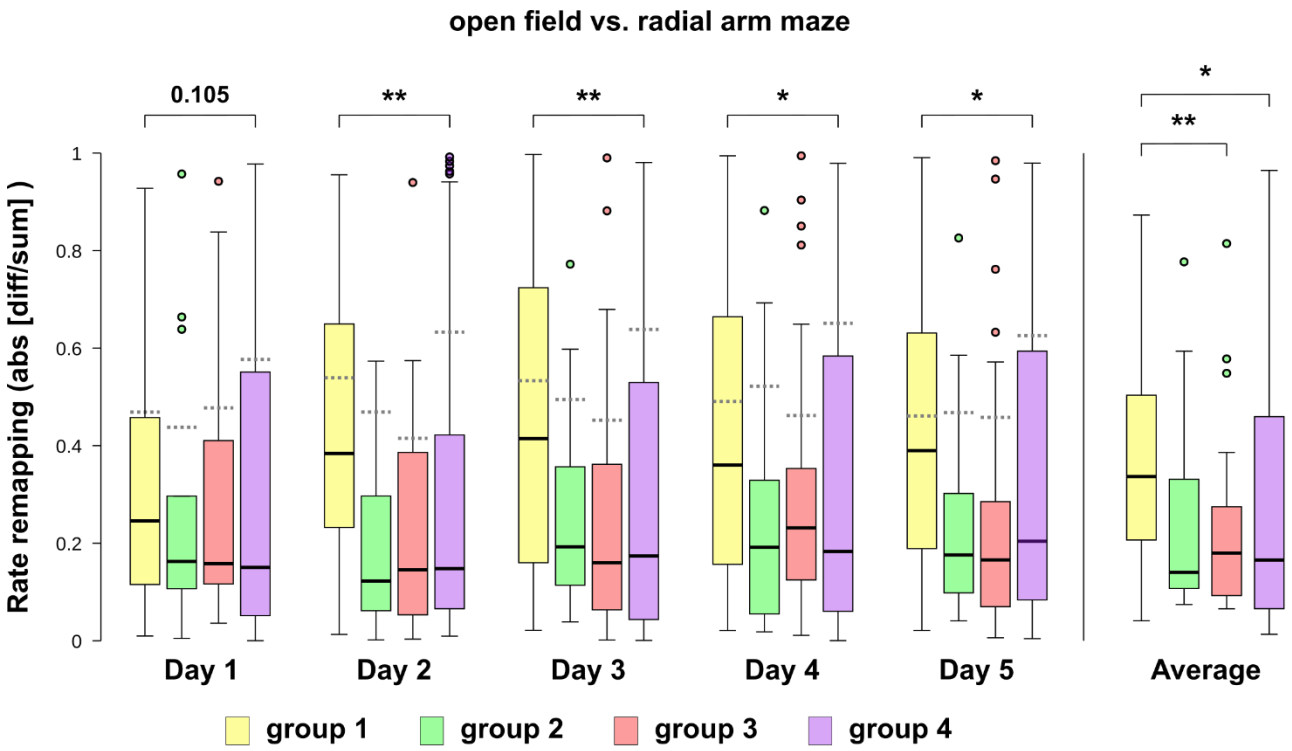

Figure 7. Rate remapping between the open field and the RAM is stronger in group 1 than group 4. *Mean firing rate was calculated during theta epochs in the open field and RAM for each theta group, which were then used to calculate a change in rate score (see Methods). Dashed grey lines mark the chance level of change in rate score (see Methods). Left: change in rate score for each theta group by day. Right: change in rate score was averaged for each neuron across all 5 days. Significance levels: * p < 0.05, ** p < 0.01.*

8. Theta group 1 shows greater plasticity in assembly coding during a learning and a non-learning task that group 4.

Neuronal remapping in the hippocampus reflects changes in both rate and spatial selectivity. However, comparing how spatial representations differ between the open field and the RAM, or indeed across days in the RAM, presents two problems. First, the two environments are geometrically dissimilar. Second, the spatial selectivity of recorded neurons varies between theta groups and, at least at the level of individual neurons, across days (although the average SI remains stable).

Previous work has bypassed the first problem by considering the place field similarity between multiple pairs of neurons and comparing these "similarity" correlations across environments (O'Neill et al., 2008). If neurons remap independently, then two neurons with overlapping place field in environment A may code for different locations in environment B, and vice versa. In this scheme, a near zero correlation between place field similarity across environments would indicate that the *organisation* of the "cognitive map" had changed, i.e. had remapped. However, this measure is influenced by spatial selectivity of the cells, since place field correlations between non-spatial neurons would provide spurious results.

Indeed, as shown in *Chapter 3*, > 70% of neurons were significantly spatially modulated (SI, $p < 0.05$) on at least one day of open field exploration. However, fewer than 25% of neurons were spatially selective on all days. Moreover, spatial selectivity varies between theta groups, with group 1 neurons showing higher spatial selectivity than group 4.

To circumvent this issue, a related measure was implemented that instead captures the degree to which neurons fire together ("cofiring", see *Methods*, and O'Neill et al., 2008, 2017). Here, the instantaneous firing rates are correlated between all possible pairs of neurons, providing a measure of cofiring in a specific behavioural epoch, for each pair. Analogous to the remapping measure described above, correlating cofiring between different environments or time points provides an indication of how the organisation of joint firing patterns changes, or stays the same. While network encoding involves joint activity beyond pairwise interactions, such pairwise "cofiring" correlations likely capture higher order population representation (Schneidman et al., 2006). In this way, this measure

provides an indication of how populations of neurons show similar or dissimilar “assembly” coding in different behavioural epochs.

Given the low numbers of group 2 and 3 neurons in the data set, this next analysis was restricted to group 1 and 4 neurons, and as a comparison, all excitatory neurons, regardless of theta group. Only neurons with > 0.25 Hz firing in the open field or RAM on each day were included for the cofiring analysis (number of cell pairs days 1-5: group 1: n = 938, 654, 789, 897, 927; group 4: n = 867, 1065, 1029, 1011, 1081; all cells: n = 4308, 4288, 4440, 4689, 4761). To establish a baseline of assembly similarity within the same environment, cofiring was correlated between the first and second half of exploration for each group. As expected, assembly patterns were highly correlated within each day, for all groups of neurons ($r > 0.6$, $p < 0.00001$, for all groups across days; see ***Figure 8A***). This indicates that, in the absence of learning, subicular assembly firing patterns remain stable during exploration. Next, the change in assembly firing patterns between the open field and the RAM was assessed. That is, are the joint firing patterns in the open field similar to those in the maze? Cofiring patterns were significantly correlated between the open field and the RAM (all $p < 0.00001$; ***Figure 8B***), when all neurons were included in the analysis. However, these correlations were significantly weaker than the assembly similarity between the first and second half of the open field exploration (all excitatory cells, day 1-5, $z = 31.2, 29.8, 37.5, 36.6, 35.4$; all $p < 0.00001$, Z-test, see *Methods*). This indicates that neurons in the region of the subiculum show a degree of assembly reorganisation between the two arenas. These firing patterns marginally diverged between the arenas across days, as assembly similarity was greater on day 1 than days 3-5 (day 1 vs 2: $z = 0.9$, $p = 0.37$; day 1 vs 3-5: $z = 4.0, 3.4, 3.5$, all $p < 0.005$). Next, the degree to which groups 1 and 4 might show independent representations between the two environments was tested (***Figure 8C***). Group 1 showed weak assembly similarity across all days (all $r > 0.18$), with a complete reorganisation (i.e. a non-significant correlation) of joint firing patterns between the open field and the RAM on day 3 ($r = 0.024$, $p = 0.5$). In contrast, group 4 neurons showed more robust correlations on each day (all $r = 0.24$-0.33, all $p < 0.00001$), indicating that assembly patterns are more generalised between these two environments. Indeed, assembly similarity was significantly stronger in group 4 than amongst group 1, across all days (day 1-5: $z = 3.56, 2.6, 4.9, 3.0, 4.6$; all $p < 0.005$). Taken together, the data indicates that group 1 neurons show more divergent assembly representations between the open field and the RAM than group 4. However, there was little change across days, with no

difference between days 1 and 5 in assembly similarity, for either group 1 or 4 (group 1: $z = 1.99$, $p = 0.07$; group 5: $z = 1.16$, $p = 0.12$).

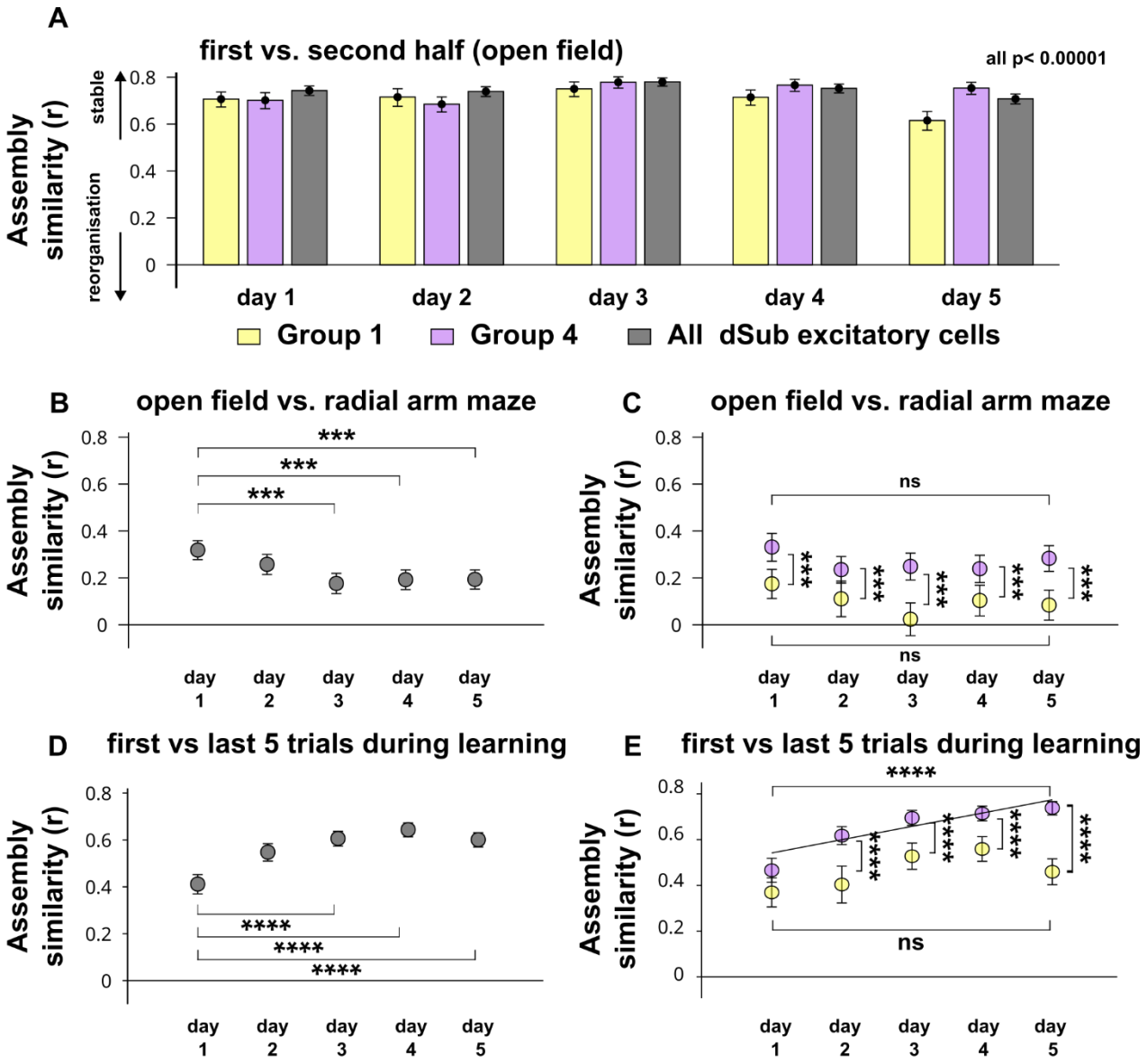

Figure 8. Assembly reorganization between open field and RAM is more pronounced in group 1 than group 4. *(A) Cofiring patterns (computed as assembly similarity, see Methods) calculated for all cells (grey), and separately for each pair of groups 1 (yellow) and 4 (purple). (B) Assembly similarity scores in the open field correlated to the RAM, for all subicular excitatory cells. (C) Cofiring between open field and RAM for both group 1 (yellow) and group 4 (purple) on each day. Results show that group 4 neuronal assemblies are more similar across the two environments than group 1. (D) Cell pair cofiring between the first 5 trials in the RAM, and the last 5 trials, for each day for all excitatory cells. (E) Assembly similarity patterns of groups 1 and 4 between the first and last 5 trials of each task day on the RAM. While group 4 assembly similarity increases with time, group 1 stays stable and always lower than the other group after day 1. Significance levels: * p < 0.05; *** p < 0.005; **** p < 0.00001. Error bars represent Rayleigh's CI.*

9. Theta group 1 shows greater plasticity in assembly coding during a learning task than group 4.

Given that neurons in the subiculum show a greater reorganisation of assembly firing patterns between two different environments than during exploration in the open field, the next question is whether assembly coding reorganises with learning. Previous work in the CA1 suggests that place coding gradually remaps, as the animal learns to find hidden food locations in the RAM within a single day (Xu et al., 2019). Thus, one synapse upstream from the subiculum, assembly coding reorganises as the animal learns. In this thesis, the animal gradually learns across 100 trials, divided into 5 days. In order to quantify how cofiring patterns evolve during learning, cofiring during the first and last five trials was compared on each day. Since improvements in performance across days would necessarily be accompanied by fewer visits to non-baited arms, this analysis was restricted to joint firing patterns on the three rewarded arms. If neurons in the subiculum encode mnemonic features of the task, one might expect the greatest changes in joint firing patterns (i.e. a weaker assembly similarity score) while the animal shows improvement in performance across the first few days of learning. On the other hand, such patterns should become more stable as the animal reaches asymptotic performance, from day 3 or 4 onwards. Consistent with this idea, assembly similarity increases between the first and last five trials, when considering all excitatory neurons (see ***Figure 8D***). Indeed, assembly similarity was greater on days 2-5 than on day 1 ($z = 5.7, 6.0, 8.3, 6.5$; all $p < 0.00001$). However, this pattern was not reflected when considering groups 1 and 4 neurons separately.

Group 4 showed a consistent increase in assembly similarity across days (***Figure 8E***). Days 2-5 all showed a greater similarity than day 1 in joint firing patterns between the first and last 5 trials of the day (day 1 vs 2-5: $z = 4.58, 7.47, 8.14, 9.29$; all $p < 0.00001$). Group 1, on the other hand, showed weaker changes across days. Days 3, 4 and 5 showed increases in assembly similarity within a day (day 1 vs 3-5: $z = 3.6, 4.45, 2.1$; all $p < 0.05$), while day 5 was not significantly different than day 1 (day 1 vs 5: $z = 0.7$, $p = 0.12$). In addition, group 1 showed a much greater assembly reorganisation during learning than group 4 after the first day of the RAM task (days 2-5: $z = 4.93, 5.18, 5.03, 9.12$; all $p < 0.00001$).

Taken together, these results show an emerging pattern for two of the four theta groups identified in our analysis. Indeed, group 1 shows more rate remapping and lower assembly similarity scores across the two environments and learning than group 4, suggesting a tendency for cells belonging to this group to modify their firing to reflect either changes in environment or newly learnt information.

10. Reactivation during sleep.

There is mounting evidence for the role of sleep in memory processing and its likely role in systems consolidation (Brodt et al., 2023). Central to this is the idea that the hippocampus rapidly encodes spatial information during learning and reactivates this data to the cortex during sleep. A prerequisite for this process is that cell assemblies reorganise during learning to encode the newly acquired information, such as the location of food rewards (Dupret et al., 2010). The analysis outlined above supports the notion that joint firing patterns in the subiculum do reorganise across different environments, or indeed during learning. This begs the question, do neurons in the subiculum participate in reactivation during sleep? Given that group 1 neurons show a greater degree of reorganisation during learning than group 4, how might these two groups then participate in reactivation? To address these questions, subicular joint firing patterns were next analysed in sleep.

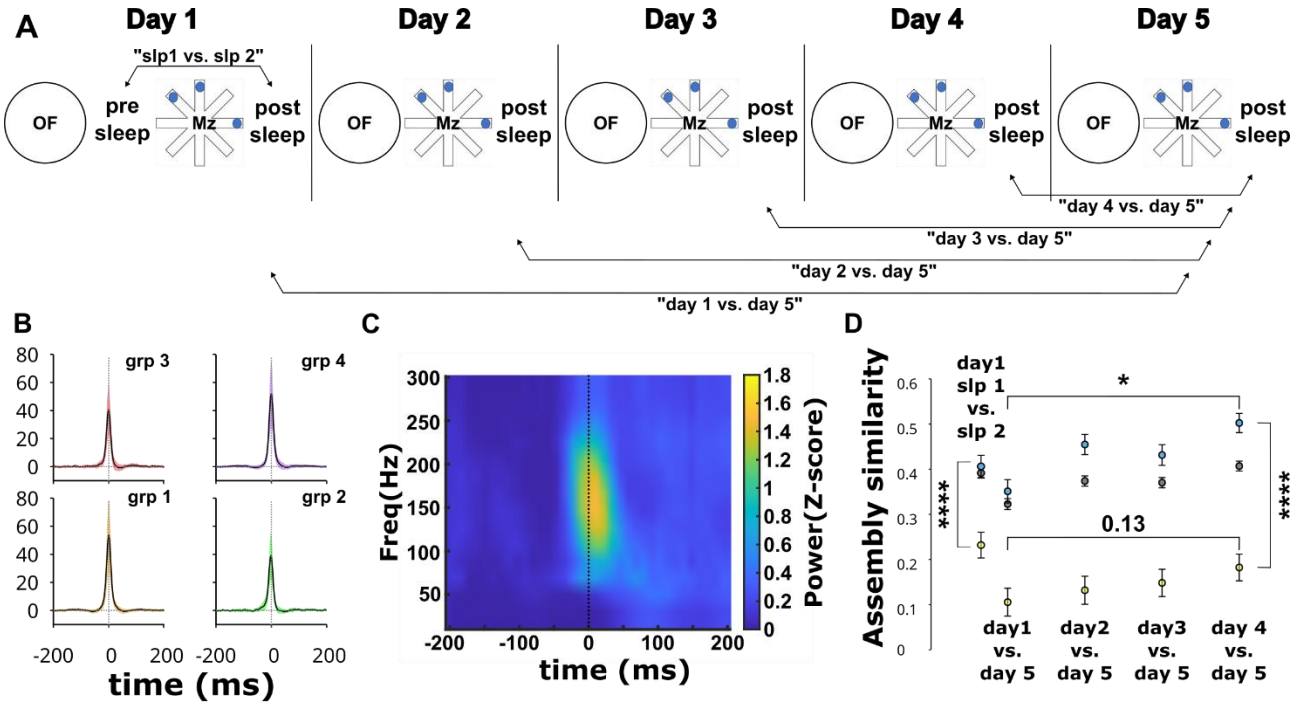

Figure 9. Group 4 firing patterns evolve with learning across days, while group 1 neurons show significant reorganization on each day. *(A) Schematic depicting the analysis of the assembly similarity shown in (D). (B) Firing rate response of groups 1-4 during detected high synchrony events (see Methods). (C) Heat map of normalised frequency over time around the time of highest density of firing (dotted line) for one session of sleep. This shows that high synchrony events are accompanied by an increase in ripple power. (D) Assembly similarity correlations between pairs of cells on two separate sleep sessions (as depicted by the schematic in (A)). Significance levels: * p < 0.05; **** p < 0.00001. Error bars represent Rayleigh's CI.*

Non-REM sleep firing patterns in the cortex are modulated by slow oscillations (0.5-4 Hz), which are accompanied by synchronous depolarisation of cortical neurons, or “up-state”, along with synchronous firing by populations of cells. This is followed by a “down-state” in which neurons are hyperpolarised and silent (Steriade et al., 1993). Hippocampal networks are also modulated by varying degrees by slow oscillations. While CA1 region neurons do not show this modulation of membrane potential in concert with slow oscillations (Isomura et al., 2006), SWR emissions tend to occur around specific phases of cortical slow waves (Battaglia et al., 2005). In contrast, neurons in the subiculum show “up and down” bimodality in membrane potential (Isomura et al., 2006), and consequently tend to show bursts of activity followed by periods of silence. These events contain SWR events, as well as periods of high firing outside of SWR epochs. Given this, the approach taken here to analysing assembly activity in sleep was to first establish periods of high synchrony, reflecting these “frames” of up-states (see *Methods*, and Ji & Wilson, 2007; O’Neill et al., 2017). In our dataset, these events contained moments of robust firing by excitatory neurons, from each theta group (***Figure 9B***), and were often marked by high frequency oscillations (***Figure 9C***).

To compare how assembly patterns evolve over time (i.e. show plasticity over time), all neurons that fired > 0.25 Hz across concatenated maze exploration sessions were taken, from each day. This yielded 4876 pairs when considering all excitatory neurons, 939 in group 1 and 1070 in group 4, which were used in the analysis for each recording day. Again, the low number of neurons identified as belonging to groups 2 and 3 prevented their inclusion in this analysis. First, the assembly similarity, as described above and in the *Methods* was computed, for each pair of cells firing on day 1 in the sleep session preceding the RAM task (pre-sleep) or in the session following the task (post-sleep; see explanatory schematics in ***Figure 9A***). Group 1 showed a significantly lower assembly similarity score compared to group 4 ($z = 4.39$, $p < 0.00001$; ***Figure 9D***). Next, the evolution of sleep joint firing patterns was analysed by comparing assembly patterns in sleep after maze learning on each day with the last sleep session. Across days 1-4, group 1 assembly patterns during sleep were only weakly similar to firing patterns in the sleep on day 5 ($r = 0.1$-0.18, all $p < 0.005$). At the same time, assembly similarity with day 5 did not significantly increase between days 1-4 ($z = 0.58, 0.94, 1.69$; $p = 0.34, 0.35, 0.13$). Overall, group 1 assembly patterns resulted dissimilar between sleep sessions, implying that such cells tend to reorganise on each day following maze learning. In contrast, group 4 neurons

showed a more robust similarity in firing patterns between sleep on days 1-4 and day 5 ($r = 0.34$-0.51, all $p < 0.00001$).

Indeed, sleep firing patterns after RAM were more correlated with day 5 on each day for group 4 than group 1 ($z = 5.57, 7.9, 7.4, 8.5$; all $p < 0.00001$). At the same time, group 4 showed a gradual increase in similarity with day 5 across learning ($z = 2.88, 2.6, 4.5$; all $p < 0.05$). In this way, group 1 neurons appear to show a reorganisation of assembly patterns during sleep each day, regardless of whether the animal was at asymptotic performance in the previous RAM session (on day 4), or was learning the goal locations for the first time (on day 1). In contrast, group 4 neurons showed more limited changes in assembly patterns across sleep sessions (i.e. sleep session cofiring was more correlated between days), but became more similar to day 5 across days. To what degree are sleep assembly patterns driven by waking activity? And do groups 1 and 4 contribute differently to reactivation? And finally, how does reactivation evolve over the 5 days of learning?

To address these questions, cofiring patterns on the baited arms of the maze were correlated with firing in sleep before and after each RAM session (see schematic in ***Figure 10A***), using an approach previously implemented by other authors (Kudrimoti et al., 1999; see *Methods*). Cofiring patterns during learning amongst all excitatory neurons reactivated robustly in subsequent sleep ($r = 0.19$-0.32, all $p < 0.00001$). This was most evident in the first two days of behaviour, after which reactivation declined (***Figure 10B***). Here, the assembly similarity between learning and the subsequent sleep was significantly greater than on day 5 for days 1 and 2 ($z = 6.8, 4.15$, both $p < 0.0005$), but was similar on days 3 and 4 ($z = 0.03, 0.72$; $p = 0.48, 0.23$). Hence, reactivation was stronger in subsequent sleep after those RAM sessions in which performance was still improving. If new assemblies are formed/established as a result of learning, one should expect a weaker similarity between RAM cofiring patterns and the sleep before (pre-sleep). Consistent with this, assembly similarity was significantly weaker with pre- than post-sleep on each day (days 1-4: $z = 13.4, 6.8, 3.2, 3.6$, all $p < 0.005$; day 5: $z = 1.71$, $p < 0.05$). While the animal had been familiarised with the maze, no learning had taken place prior to the first sleep on day 1 (pre-sleep for day 1). However, for all other days, the sleep prior to the RAM exploration (pre-sleep) itself had occurred after learning. Consistent with the idea that learning influences joint firing patterns in sleep, “reactivation” during pre-sleep on day 1 as significantly weaker than on day 5 ($z = 5.2$, $p < 0.00001$).

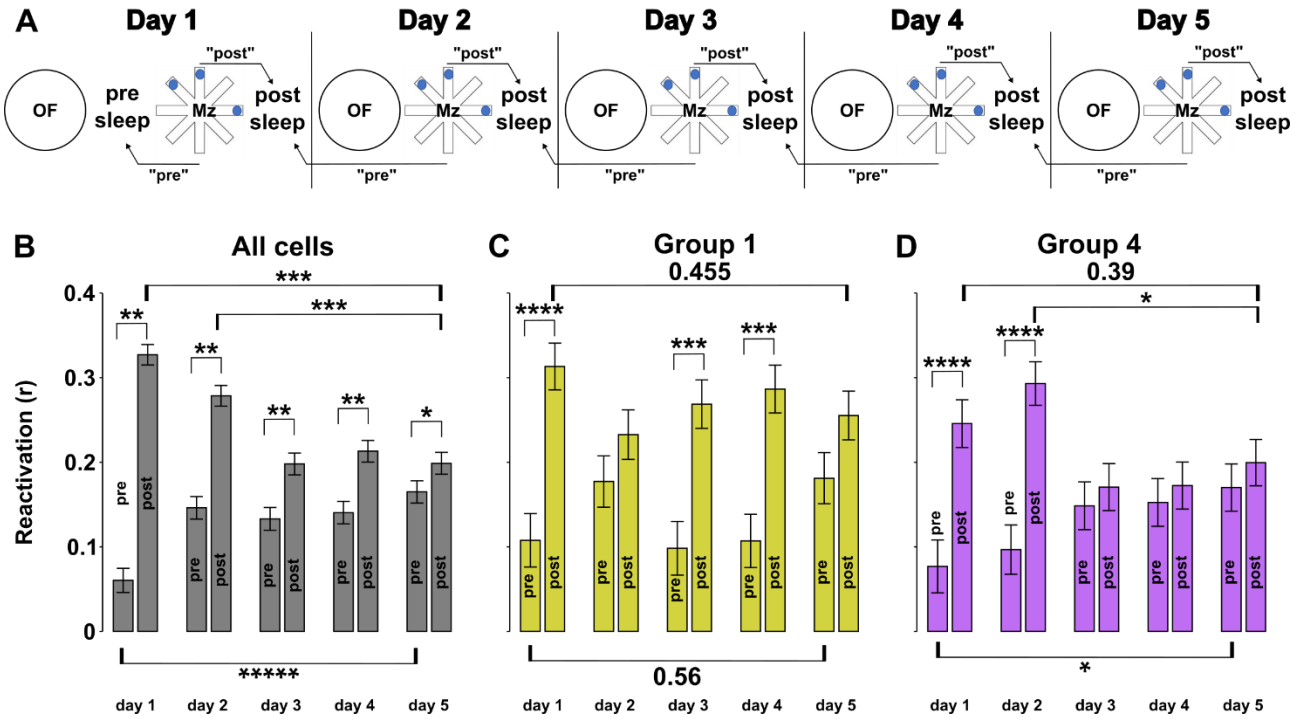

Figure 10. Group 1 cells show high degrees of reactivation in the post-task sleep sessions across the 5 days of recording. *(A) Schematic depicting the analysis of B-C-D. (B-C-D) Bar plots of reactivation coefficients (see Methods) in sleep sessions before and after the RAM task for each day of recording. (B) Reactivation of all recorded excitatory cells. (C) Reactivation of cells belonging to theta group 1. (D) Reactivation of cells belonging to theta group 4. Significance levels: * p < 0.05; ** p < 0.005; *** p < 0.0005; **** p < 0.0001; ***** p < 0.00001. Error bars represent Rayleigh's CI.*

How do groups 1 and 4 participate in reactivation? Group 1 (***Figure 10C***) also showed significant reactivation with post-sleep ($r = 0.23$-0.32, all $p < 0.00001$). In contrast to the analysis using all cells, group 1 showed a similar reactivation of RAM assemblies in post-sleep across all days ($z = 1.3, 0.5, 0.3, 0.7$; all $p > 0.4$). With the exception of day 2 ($z = 1.23$, $p = 0.11$) and day 5 ($z = 1.65$, $p = 0.09$), reactivation was stronger in post-sleep than in pre-sleep (day 1: $z = 4.57$, $p < 0.0001$; day 3: $z = 3.74$, $p < 0.0005$; day 4: $z = 3.96$, $p < 0.0005$). However, pre-sleep sessions on day 1 and day 5 were not significantly different from one another ($z = 1.58$, $p = 0.56$). Reactivation of the RAM during sleep by group 4 neurons was more similar to that observed when considering all excitatory cells (***Figure 10D***). The relationship between cofiring in the RAM and pre-sleep on day 1 was significantly smaller than that observed on day 5 ($z = 2.19$, $p < 0.05$). At the same time, the correlation between cofiring on the RAM and that in post-sleep reduced across days, at least when comparing day 2 with day 5 ($z = 2.31$, $p < 0.05$), although not when considering day 1 and day 5 ($z = 1.12$, $p = 0.39$). Importantly, reactivation in post-sleep was only significantly greater than pre-sleep on days 1 and 2 (day 1-2: $z = 3.8, 4.73$, all $p < 0.0001$; days 3-5: $z = 0.52, 0.47, 0.7$, $p = 0.3, 0.32, 0.24$).

Discussion

Neurons in the subiculum can be subdivided into four groups based on their theta preference

The aim of this chapter was to characterise firing and spatial properties of neurons in the subiculum during a non-learning and a learning task. To do so, the behavioural and electrophysiological data collected in *Chapter 3* was analysed.

Integration of spatial information for mnemonic processing in the hippocampus is facilitated by theta modulation (Dragoi & Buzsáki, 2006; Lisman & Idiart, 1995; Raghavachari et al., 2001), which is the tendency of neurons to fire at specific phases of the theta oscillation (e.g. Buzsáki et al., 1983; Fox & Ranck, 1981; Ranck, 1973). As a first step in the characterization of subicular neurons, theta phase preference was explored amongst the identified excitatory neurons. This analysis revealed four groups in the dataset: one firing

just after the trough (group 1), a second firing on the ascending phase of theta (group 2), and two on the descending phase (groups 3 and 4; see ***Figure 2***).

Only one study prior to this thesis has tried to identify different groups of subicular neurons based on their theta preference (Kitanishi et al., 2021). This study identified three main preferred angles, two firing on the descending phase of theta (on two consecutive timepoints: 285 and 321 degrees), and a third firing immediately after the trough (~ 9 degrees). The theta preferences highlighted by this study related to the position of cells on the proximo-distal and radial axes, with the first group (firing earlier on the descending phase) comprising of cells in the distal-deep part of the subiculum (closest to the surface of the brain), followed by cells on the distal but more on the superficial (more ventral) part of the structure (at ~321 degrees on the theta cycle), and finally proximal cells (spanning across the whole radial axis, firing at ~ 9 degrees). As the electrophysiological features of subicular neurons have been shown to considerably vary on the proximo-distal axis (Cembrowski et al., 2018; Kim et al., 2012), the current experiment aimed at sampling cells situated in the mid-part of the subiculum. While two groups were indeed identified with theta preference on the descending phase (groups 3 and 4), the other two groups identified by the circular clustering method fired later in the theta cycle than Kitanishi's third one (42.1 degrees for group 1 and 125.05 for group 2). As their dataset comprised of a wider sampled area on the transverse axis, it might have been difficult for the authors to have sampled sufficient neurons to identify the clusters of neurons presenting the theta phase preferences highlighted in this thesis.

The distribution on the radial axis that Kitanishi and colleagues identified does not completely match with this thesis findings either. The "distal-deep" group had a mean theta preference of 285 degrees. In this thesis' dataset, this would possibly coincide with group 4, which instead comprised of neurons in the superficial layer of the subiculum (see ***Figure 2C***). On the other hand, the theta preference of the "distal-superficial" group of Kitanishi and colleagues (~321 degrees) could also be associated with group 4. In this case, the results of this experiment would reflect the findings of Kitanishi and colleagues. Lastly, Kitanishi's study identified a group of proximal cells, that spanned across the whole radial axis, which had a theta preference that covered the phase preferences of groups 1 and 4, which, together, are indeed located both at the top and bottom part of the layer (***Figure 2C***). Group 2, located in the deep subiculum, does not seem to have an equivalent in

Kitanishi's dataset, while group 3 (located in the current dataset in the most superficial part of the layer) could comprise cells of the "distal-superficial" group in Kitanishi's results. In summary, there are differences with the two datasets, likely due to location of the recordings in the proximo-distal axis of the subiculum. Future experiments, sampling across the whole area of dorsal subiculum, could allow a more detailed comparison of the results found in this chapter with the previous literature.

Kitanishi and colleagues found a gradient of distributions of theta preferences not only based on position of the cell, but also based on the type of projections associated with those neurons. They found that neurons that projected to the antero-ventral nucleus of the thalamus (AV) fired at the earliest phases of theta (i.e. what this thesis consider the descending phase; mean phase = 250 degrees), followed by neurons projecting to the restrosplenial cortex (RSC;~292 degrees), the medial mammillary body (MMB; ~ 297 degrees), and lastly the nucleus accumbens (NAC; ~ 29 degrees). Based on the preferred theta phase alone, AV-, RSC-, and MMB-projecting neurons, in this thesis' dataset, would all represent neurons belonging to group 4, while NAC-projecting cells would be part of group 1. While the authors did not quantify positional differences on the radial axis for these projecting neurons, their tracing images, combined with a previous study conducted by Ishizuka (2001), allow to create an approximate picture of the position of these projecting cells in the layer. Cells in the deep subiculum prevalently project to the anterior thalamus, while cells in the middle of the layer project to mammillary bodies, and cells in the superficial subiculum project to the nucleus accumbens. This does not reflect the results presented here (as group 4 comprises of neurons in the deep part of the layer, while group 1 neurons are in the superficial part). An explanation for this discrepancy can come from two main arguments. First, subicular projection neurons have shown to vary along the proximo-distal axis based on genetic markers (Cembrowski et al., 2018). More specifically, NAC-projecting neurons are mostly found in the proximal subiculum, while RSC-projecting one are found in the distal part. The middle portion of the subiculum could comprise both NAC- and RSC-projecting neurons (along with neurons projecting to other areas). Second, while initial reports state that projection neurons typically target a single downstream region (Naber & Witter, 1998), recent work has recognised that many subicular neurons project to more than one area (Cembrowski et al., 2018; Kinnavane et al., 2018; Kitanishi et al., 2021; Winnubst et al., 2019). If that is indeed the case, making a

clear link between preferred theta phases, location on the radial axis, and projection targets would become particularly complicated.

A potential limitation of this work lies in the discrepancy in sample sizes for the four groups. Indeed, groups 1 and 4 make up most of the population of cells (86 and 140 respectively, which together make up almost 80% of all excitatory cells recorded), while groups 2 and 3 are comparatively small. A bigger sample size might be required to confirm these results. The recordings in this thesis utilised a NPX 2.0 four-shanked probe, but the data analysed only considers two of those four shanks. Analysing the other two shanks would give a first indication of the presence (or not) of these four groups in more proximo-distal areas. Additional recordings with these probes, orientate to record along the proximo-distal axis, would allow a better comparison of these results with the available literature.

Neurons that fire at different phases of theta show distinct firing characteristics in behaviour and sleep, and differently contribute to learning of a spatial task

Excitatory neurons in the subiculum have been principally identified based on their burstiness profiles: bursting, and regular-firing (O'Mara, 2005; Sharp & Green, 1994). These classes of neurons have been shown to be distributed along a gradient on the proximo-distal axis (Cembrowski et al., 2018), although others claim them to not be segregated by their anatomical position (Simonnet & Brecht, 2019). The central transitional portion of the transverse axis, might represent a mixture of both populations (Böhm et al., 2015b; Cembrowski et al., 2018). *In vitro* studies have reported that bursty excitatory neurons tend to be prevalently in the top layers of the subiculum, while regular-firing cells are concentrated in the most bottom part (Greene & Totterdell, 1997; Menendez De La Prida et al., 2003). This aligns with our results, with group 1 neurons (which are significantly more present in the deep layer than neurons of the other groups) shown to be more bursty than neurons in group 4 (which are prevalently located in the superficial part of the layer). Based on the current knowledge of the field, this is the first *in vivo* report of a laminar organization along the radial axis of subicular cells based on their burstiness profiles.

The results of this chapter highlighted that group 1 cells, along with presenting more bursts of spikes, generally tend to have sparser firing than cells in the other three groups, both in a non-learning and in a learning context. High firing rates has been associated with burstiness (Lever et al., 2009). While this contrasts with this chapter's results, Lever and colleagues analysed a small number of cells compared to the recordings of this thesis (11 bursty and 25 non-bursty), which were widely distributed along the proximo-distal axis. These cells were also all boundary-vector cells, a specific subpopulation of subicular neurons. BVCs are also only one of the so-far identified subpopulations of subicular neurons (others include vector-trace cells, head-direction cells, and axis-tuning cells; see Kitanishi et al., 2021; Muller et al., 1991; Olson et al., 2017; Poulter et al., 2021; and *General Introduction*), and could thus present with specific firing characteristics and anatomical distribution that are not necessarily shared by other subicular groups.

Overall, group 1 cells were found to generally carry more spatial information. This was true both during exploration of the open field, and during performance on the RAM task (see ***Figure 5***). A recent report suggests that there is a positive correlation between firing rate and spatial information in the subiculum, with neurons that have high per-second information content also presenting with generally high firing rates (Kitanishi et al., 2021). This is not evident in this dataset, where sparser firing neurons in group 1 also exhibit more spatial information content. Recent work by Simonnet and Brecht (2019) suggests that subsets of bursting neurons with lower firing rates show greater selectivity, however these neurons appeared to be less "bursty", or at least fire fewer bursts. Taken together with the above, the population of neurons recorded in this area set appears, to some degree, contain neurons with distinct characteristics to those previously described in the more proximal and distal regions of the subiculum.

The four groups identified in this chapter also present different firing responses during SWR events. In the hippocampus, neuronal populations generally increase their firing during SWRs (Buzsáki, 1989), which is supposed to reflect a mechanism of consolidation of mnemonic information. Increases in firing rates during SWRs have also been recorded in the subiculum, but some neuronal populations in the deep layers have also shown suppression of their firing rates (Kitanishi et al., 2021). In the current dataset, while mean firing rate was variable among the different theta groups, all four showed an increase in firing at the peak of the ripple power. Interestingly, group 1 neurons showed a higher firing

rate during peak SWRs activity compared to the other three groups. This peak response was also significantly sooner in group 1 neurons compared to the other groups. The increase in rate was subsequently followed by a below baseline drop, in which group 1 neurons still fired at a higher rate than any of the other groups. This biphasic response, more visible in some of the groups, could in part reflect the results found by the authors mentioned above.

Another novel result in this dataset comes from the rate reorganization/remapping analysis (***Figures 7 & 8***). Here, group 1 cells showed to remap within days (and on average) more than group 4 cells, along with exhibiting a greater degree of reorganization of their firing assemblies. These results suggest that group 1 cells might represent a more “plastic” group of cells in the subiculum, and might process information to aid in learning across days. Previous work has indicated that firing rates are correlated between environments (Kim et al., 2012), and different neurons exhibit varying degrees of remapping between different contexts (Sharp & Green, 1994). However, the data in this work indicates that specific subsets of neurons show reorganisation of both rate and firing associations. The cofiring measure is likely driven, in part, by the degree to which place fields overlap or not. However, spiking is not restricted to within the place field, and spike dynamics within the place field are highly variable (Fenton & Muller, 1998), meaning that cofiring is likely explained by more than spatial selectivity. Thus, one unexplored topic in this dataset involved remapping during learning of the task.

This chapter showed that remapping is different across days between group 1 and group 4 cells. In the CA1, excitatory cells remap their firing on learning of the location of food rewards (Danielson et al., 2016; Dupret et al., 2010). This phenomenon seems to be more present in neurons in the deep layers of the area, where cells have been recognised to have a more dynamic representation of space. In this dataset, group 1 cells are predominantly in the deep layer of the subiculum. Looking at the remapping to goal locations in the RAM of the different theta groups might reveal a similar pattern than what is shown in CA1 cells. Moreover, CA1 and subicular cells have shown both rate and place remapping (see Kim et al., 2012), but our analysis only considers rate remapping, and changes in cofiring. Indeed, within a day, neurons in group 1 show a low similarity between the beginning and the end of learning on each day, consistent with spatial remapping during learning. At the same time, group 4 neurons show less changes in remapping within

each day, but show a gradual increase in similarity across days, as the animals performance improves.

Neurons in the superficial layer of the subiculum undergo more firing reorganization during sleep

The last group of analyses carried out in this chapter concerns the data acquired during sleep sessions before and after the RAM task. The results presented here provide the first demonstration of reactivation of waking patterns by subicular neurons. When considering all excitatory neurons, there is a greater degree of reactivation in sleep sessions following the RAM task than compared to the sleep that precedes it (***Figure 10***). However, the strength of reactivation declines after day 2, as performance in the task improves. One might speculate that reactivation in the subiculum is most pronounced following learning of new information and declines when performance on the task is driven by recall rather than the formation of memory. However, when considering group 1 and group 4 neurons separately, reactivation amongst group 4 declines, similar to that seen with all excitatory neurons, while group 1 maintained robust reactivation across days. This indicates that these two groups may serve different purposes in reactivation. Decoding the information within the reactivation activity might shed light to this issue. Additional NPX 2.0 recordings, with higher cell yields within a single animal, would allow for decoding approaches to identify locations reactivated by neurons of groups 1 and 4 (for example goal locations).

Indeed, along with the general reactivation of memory traces, hippocampal neurons that fire consecutively during exploration have been shown to preserve that firing order during sleep (indicating a “replay” mechanism; Lee & Wilson, 2002; Skaggs & McNaughton, 1996). This process is believed to aid in consolidation of specific events. The analysis of this thesis only focused on reactivation of memory traces, without considering the preservation of the order of firing. Investigating this mechanism in the subicular network could further solidify the notion of the contribution of this area in long-term mnemonic processing. Additionally, newly learnt goal locations have been shown to be preferentially activated during subsequent sleep in the CA1 (Dupret et al., 2010). This leads to an increase in firing frequency of cells that encode for these locations during sleep. A next

step in the analysis could include quantifying whether any specific group of subicular cells in our dataset preferentially fires at the goal locations of the RAM, and whether these cells belong to theta group 1. However, given the variability in spatial selectivity on each day, such analysis would require a larger dataset.

Conclusions and future steps

This chapter focused on characterising firing and spatial properties of subicular neurons in both a learning and a non-learning context across consecutive days. In the analysed neuronal population, four groups have been identified based on their preferential firing during theta oscillations. These groups have shown differences in location on the radial axis, burstiness, mean firing rate, spatial information content and reorganization and remapping of their firing between environments and across days. This has allowed to identify a group (group 1) that generally shows plasticity between environments and within a day. At the same time, group 4 neurons showed to be less plastic within a day, while showing indications of plasticity across days. Together, these neurons may provide differential contributions to processing mnemonic information, both on the short and on the long-term.

GENERAL DISCUSSION

This thesis explored the role of the subiculum in spatial long-term memory, which has been a disputed topic in previous literature. While its role in spatial working memory had been delineated in previous behavioural studies (e.g. Morris et al., 1990; Potvin et al., 2007), its contribution to spatial reference (long-term) memory has been object of debate (see *General Introduction*). The first aim of this thesis was to test the involvement of the subiculum in working and reference memory by inhibiting the area during a spatial memory task.

The results of *Chapter 2* suggest an involvement of the subiculum in different types of mnemonic processes. Information in the brain can be stored over hours, days, or even years. The methods established in this thesis allowed the recording of the same cells across consecutive days, along with network activity in the LFP. With these data, neurons can be characterised, as well as the change in features of these cells during learning of a task across days.

The data in this thesis supports two roles for the subiculum in learning. First, that the subiculum is involved in on-line processing of spatial information, which can be seen by both inhibiting the area during acquisition of spatial information, and by the analysis of its neuronal coding during performance of a spatial task. Second, that the subiculum also has a role in off-line processing of spatial information. This can be observed in changes in neuronal coding both across days in performing a spatial task, and in analysing firing assemblies during sleep following the task.

1. The subiculum is involved in on-line/short-term processing of spatial information

The hippocampal formation has been implicated in on-line processing of spatial information since O'Keefe and Dostrovsky's (1971) discovery of place cells. Lesioning the hippocampus in behavioural studies impacts performance of animals on different spatial

memory tasks, where keeping in mind a goal location (i.e. through working memory) was needed (Jarrard, 1993; Morris et al., 1982, 1990; Olton, 1977; Potvin et al., 2007). The RAM task chosen for this thesis allows for testing of the working memory function: whenever the animal makes a visit to one of the arms, re-visiting that same arm during the same trial is considered a “working memory error” (WME; Olton et al., 1979). The impairment of subicular function has been demonstrated to impact the number of WME animals make when exploring the maze. This has been previously assessed in a version of the task where all 8 arms are baited, thus the aim of the task is for the animal to get all food rewards by visiting the lowest number of arms (Potvin et al., 2007). In the version of the task used in this thesis, only 3 out of the 8 arms contain a food reward. While others have used similar partially baited mazes to evaluate performance following damage of the hippocampus (e.g. Jarrard, 1995), or of other brain regions involved in spatial processing (for example assessing the function of the anterior thalamic nuclei; Harvey et al., 2017), to the current knowledge of the field this is the first experiment that conducts a similar paradigm while impacting subicular function.

The results of the behavioural study conducted in *Chapter 2* highlight a contribution of the subiculum in the working memory function. This was evaluated by assessing WME, which showed significantly higher for the treatment group on days in which inhibition of the subiculum was carried out (*Experiment 1*), consistent with previous reports (Cembrowski et al., 2018; Galani et al., 1998). This remained true even when the animal was highly familiar with both the environment and the task (through training, see ***Figure 6,*** *Chapter* 2).

From a behavioural standpoint, the results of *Experiment 1* of *Chapter 2* confirm a role of the subiculum in processing spatial information. This conclusion is supported by the electrophysiological data recorded from animals performing the same task (*Chapter 3 and 4*). Here, > 70% of subicular neurons showed to be significantly spatially selective on at least one of the recorded days. Spatial selectivity was computed as the amount of spatial information, that is, how much the firing of the cell says about the current location of the animal (Skaggs et al., 1992). In the CA1, estimates of the percentage of spatially selective cells can vary, with some reporting ~37% (Markus et al., 1994) and others finding > 90% (Henriksen et al., 2010). The proportion of spatially selective cells can depend on the position along the proximo-distal (Henriksen et al., 2010) and radial axes (Mizuseki et al., 2011), which seems to be a characteristic of subicular neurons as well (Kim et al., 2012;

Kitanishi et al., 2021). Indeed, in the current dataset, spatial selectivity was also a feature of depth in the layer, with groups 1 cells (located deeper in the layer) carrying more spatial information than cells belonging to groups 3 and 4 (more superficial). While varying based on position in the layer, spatial information does not seem to change across days. Indeed, when looking at both the general population of subicular cells (***Figure 6*** *Chapter 3*) or subpopulations based on theta preference (***Figure 6****, Chapter 4*), subicular neurons did not become more or less "spatial" with experience (in the open field) or learning (in the RAM).

Online processing of information in the hippocampus is believed to be coordinated by theta oscillations (Dragoi & Buzsáki, 2006; Lisman & Idiart, 1995; Raghavachari et al., 2001). The analysis of theta modulation amongst excitatory neurons uncovered four distinct neuronal groups based on their preferred firing on different phases of the theta rhythm. These groups presented with different spiking dynamics (i.e. burstiness, mean firing rate, spatial selectivity) which might imply different profiles of information processing by subpopulation of neurons in the subiculum. Indeed, burstiness is a feature of hippocampal cells that has been implicated in synchrony detection (Harris et al., 2001) and could thus implicate different contributions to the temporal coding of information for the different groups. Moreover, different phases of the theta rhythm could separate or "parse" the dynamics of information encoding and retrieval in the CA1, with the encoding phase being enhanced at the trough of local theta, and retrieval at the peak (Hasselmo et al., 2002). Group 1 cells fire just after the trough of theta, immediately after CA1 neurons, and were shown to greatly reorganise their firing patterns within a day. One could speculate that this subpopulation of subicular neurons might be the main contributor to the acquisition of information throughout the task. Indeed, due to their propensity to carry more spatial information than neurons of the other theta groups, these cells could be constantly updating the "cognitive map" that represents the RAM environment and the location of food rewards. Indeed, these neurons also show a greater reorganisation of firing patterns between the two environments than group 4. Thus, these neurons may provide distinct spatial representations of different environments.

Previous work conducted in the CA1 shows that neurons change their place fields when the animals are exposed to new environments or are learning new goal locations ("place remapping", which shows a certain degree of correlation with cofiring; reviewed by Fenton,

2024). A difference in firing assemblies in this dataset was evident between the open field and the RAM, which showed a decrease across days (i.e. firing patterns in the maze became less similar to the firing patterns in the open field). However, the recordings conducted in this thesis did not include changes in task conditions, such as recording in a new RAM environment and changing the position of the baited arms that was done in the *Experiment 3* of *Chapter 2*. Extending the recording paradigm to include such changes could then uncover whether there is a neuronal correlate to the increased performance on day 1 of the "test" phase compared to day 1 of "training" that was seen in this thesis' behavioural experiment. One could hypothesise that, if joint firing patterns in the maze reflect the familiarity of the task, these would be more strongly correlated on day 1 in a second environment compared to the first day of training.

2. The subiculum has a role in off-line/long-term processing of spatial information

2.1. Subicular processing during learning.

The behavioural task utilised in this thesis consisted in placing food rewards at the end of 3 out of the 8 arms of a RAM. This allows the simultaneous assessment of both working memory and reference (or long-term) memory. A "reference memory error" is defined as the animal entering one of the non-baited arms (RME; Olton et al., 1979). When inhibition of the subiculum was carried out before acquisition (*Experiment 1* of *Chapter 2*), a significant difference between groups in RME was registered on the days of treatment, *and* on the first treatment-free day. This suggests that the role of the subiculum is not simply linked to working memory, but might involve processing of information across several days. A suggestion similar to this was previously made by Bolhius and colleagues (1994) and Morris and colleagues (1990). This is supported by the electrophysiological data collected on animals performing the RAM task without any treatment. Indeed, the results obtained when analysing the joint firing patterns of cells during performance on the maze (*Chapter 4)* follow a pattern that resembles that of the measure of overall performance (i.e. number of visits) in animals free of subicular inhibition. First, excitatory neurons in the subiculum showed a (slightly) higher level of reorganisation of joint firing patterns compared to the cofiring in the free exploration of the open field on day 5 than they did on

day 1 (***Figure 8B,*** *Chapter 4*). This suggests that the way information was processed by the subicular network in the maze had a more similar organization of the first day of recording (when the animals were first performing the task) compared to the last day. While changes in encoding of spatial features between two different environments have been shown in the past in both the CA1 (Bostock et al., 1991; Muller & Kubie, 1987) and the subiculum (Kim et al., 2012), reorganisation of joint firing patterns (or "cofiring") has only been analysed in the CA1. In addition to that, one could initially assume that place remapping and cofiring across different environments are dependent measures. However, cofiring patterns likely reflect more than just place field overlap between pairs of neurons, with recent work suggesting that cofiring among cells predicts around 20% of the variance in their place fields (Fenton et al., 1998; Kelemen & Fenton, 2016; Levy et al., 2023). Other features such as theta phase, head direction, and speed (Kitanishi et al., 2021) may also be driving correlations in joint firing patterns. Beyond this, cell assembly patterns are likely driven by internal dynamics beyond these factors, including the degree of recurrent connectivity amongst neurons and faster network oscillations (e.g. gamma; Harris et al., 2003).

The results of this thesis regarding cofiring in the subiculum point to a new feature of the subicular network in processing information during learning. While changes in cofiring could reflect a simple feature of changes in the environments (same as the remapping of place fields found in CA1 and subiculum), great care was applied during the recordings to make sure that there were no differences in the two environments within days. The results showing a change in firing assemblies diverging between the two environments across days suggest that these changes might be a feature of the different learning contexts. To support this notion, assembly similarity between the first and second half of the open field sessions showed a low degree of reorganisation on any day, while the first and last 5 trials of the RAM across days revealed a different pattern. Here, joint firing patterns of all excitatory cells at the goal locations were less similar on day 1 than they were on day 5. This suggests that the representation of the reward locations change across days: when the animal is first exploring the maze, the representation that its neuronal network might create at the first encounter of a goal location is quite different than the representation formulated towards the end of the day. On the other hand, the representation at the start of day 5, when the animal has had several days to learn the location of the food rewards, is now much more similar at the start and end of trials. This convergence of assembly

patterns progresses in accordance with the performance of animals on the task, where the number of visits necessary to correctly identify all three goal locations is higher at the start compared to the end of learning. Of note, different subicular populations seem to process information related to learning of the task in different ways. Indeed, while neurons of the theta group 4 have a similar pattern of assembly similarity in the maze as the general population of excitatory neurons (i.e. their joint firing patterns are more less similar on day 1 compared to day 5), group 1 neurons seem to reorganise their population firing patterns independently of day (***Figure 8E**, Chapter 4*). Overall, these results show a connection between subicular assembly processing and learning of the spatial RAM task. An additional level of analysis of these results could come by comparing the reorganisation of firing assemblies between two non-learning tasks (which is shown in areas such as the CA1, see above) to the reorganization between a learning and a non-learning task. This could help tease apart any differences in both the response of the general population of subicular cells, while also allow a comparison of the reorganisation of firing patterns of the theta groups identified in this thesis (particularly, groups 1 and 4).

2.2. The role of the subiculum in memory consolidation

As mentioned above, while some behavioural studies did not recognise a role of the subiculum in long-term memory processing (Cembrowski et al., 2018; Galani et al., 1998), both Bolhius and colleagues (1994) and Morris and colleagues (1990) reached the same conclusions that have been delineated by this thesis. In both studies, reference memory was assessed in the MWM as the time spent exploring a specific quadrant of the environment during probe trials. In these two cases, performance was assessed based on lesions produced *after* acquisition of information about the task, to focus on the effects of subicular impairment on the *retention* of information, unbiased by acquisition. This procedure parallels *Experiment 2* of this thesis, where the contribution of the subiculum to memory processing during the *off-line* was tested. It also circumvented the issue of subicular inhibition having an impact on working memory that could itself cause a disruption of the reference memory measurement (Sanderson et al., 2010; Schmitt et al., 2003). This was born out of the results in which inhibition of the subiculum during rest left WME unaffected, while RME increased. However, this deficit was only observed on days 5

and 6 of the task. What could be the reason for this delay between the day of subicular inhibition and the presence of performance deficits?

An explanation may lie in the type of learning required to perform the task. Non-spatial procedural components of the task, such as the task “rules” (e.g. there are three baited arms, once all three are visited the trial stops and re-starts) are acquired over time. The first few times the animal is exposed to the task, performance might mainly increase as a product of the animal learning the rules. Over the course of the next 2-5 days, performance improvements occur as a result of correctly learning the additional spatial information required to reach the goal arms with a minimum number of visits. In this way, deficits in spatial memory might only be revealed after improvements driven by assimilating the rules of the task.

This first scenario is supported by the electrophysiological data acquired during resting periods following the task. Indeed, when looking at the reactivation of firing patterns during the sleep preceding or following the task (pre- and post-sleep; ***Figure 10,*** *Chapter 4*) analysis of all cells revealed that the reactivation during periods of high synchrony in sleep is always stronger in the post-sleep. The difference between reactivation in the post-sleep on days 1 and 2 versus day 5 is also striking. One could hypothesise that, while on the first days of the task the animals are consolidating information necessary to solve the task, the more they are exposed to the task the less that information requires consolidating. Theta group 4 excitatory neurons showed differences in reactivation between pre- and post-sleep on days 1 and 2, but showed no differences on any of the following days. Thus, reactivation was distinct during the first stages of learning, which may correlate to when the procedural components of the task are being learnt. Consistent with this, neurons in this group show, in general, to be less spatially selective than neurons of group 1. It could then be that group 4 neurons play a bigger role in consolidating information regarding the rules of the task, while group 1 cells (which pre- and post-sleep reactivation scores are significantly different on days 3 and 4 of the task) predominantly contribute to the consolidation of spatial information. However, further work is required to confirm this speculation.

Thus, another possible explanation of a delay in performance impairment following the consolidation block is as follows. Instead of the subicular function being necessary for a

correct consolidation of spatial information, the subiculum contribution to consolidation could solely involve non-spatial information about the task. Galani and colleagues (1998) explored the contributions of the subiculum in non-spatial tasks (novel object recognition) and found that lesioning the area leads to a general deficit in performance. This role in non-spatial memory has been also recognised for the hippocampus (Cohen et al., 2013). Additionally, the CA1 has been showed to have a role in consolidation of non-spatial information, where animals are impaired in a novel-object recognition task when muscimol is infused into the dorsal hippocampus during a resting period that follows encoding (Sawangjit et al., 2018). In this scheme, animals would still manage to show *some* improvement in the task (by relying on their intact spatial working memory), but would show a delay in reaching a performance level comparable to their control counterparts, due to a delay in learning the task's procedural components. Indeed, spatial and non-spatial components of memory have been shown to relate to different processes (Bannerman et al., 1995). While more than 70% of recorded excitatory neurons in the subiculum showed significant spatial selectivity, around 30% did not reach the significance level to be considered "spatial" cells. These cells might have a role in processing the nonspatial information needed to complete the task when animals are first exposed to it. Nonetheless, this theory is inconsistent with the strength of reactivation in the post sleep of almost every day seen in group 1 neurons, which are the "most spatial" group identified in the recordings (***Figure 6,*** *Chapter 4*). The use of more silicon probes allowing dense sampling of cells in this area could allow to test the contribution of different subpopulations of neurons in leaning of the RAM task.

One last possible explanation of the results highlighted in *Experiment 2* of *Chapter 2* is that the subicular function could be implicated in remote, but not recent, recall. The consolidation process in the brain takes place over days, weeks, and even years. These multiple timeframes might implicate the presence of different mechanisms in the brain. Indeed, the previously mentioned studies that did not report a deficit in reference memory performance when manipulating subicular activity involved testing of performance immediately after training in the task (Galani et al., 1998), or with a one-day delay (Cembrowski et al., 2018). If the assessment of performance of the RAM task as computed in this thesis was only considered on the day following subicular inhibition, no deficit would have been detected either. Bolhius and colleagues (1994) encountered a deficit in reference memory with subicular impairment when testing was delayed by two

weeks. In the current electrophysiological data, reactivation during post-task sleep was still significant on day 5 of recording, which implies a repeated use of the subicular neuronal network to consolidate information even on the last days of the task. On the other hand, reactivation profiles of the two theta groups found in this analysis might suggest that there are distinct neuronal populations that differently contribute to recent or remote recall. One might speculate that group 4 could be involved in facilitating “recent” recall, by processing behavioural information on the first days the animal is introduced to the task. In contrast, group 1 cells may play a bigger role in more “remote” recall, by the repeated reactivation firing patterns later in the task, even after the animal has reached asymptotic performance.

In trying to differentiate the possible contributions of learning the “rules” of the task, and thus allowing to make an inference about the first two scenarios mentioned above, the last behavioural experiment of this thesis involved “training” the animals to the task for 7 drug-free days. The animals were then “tested” in a second environment, where the location of external cues and food rewards were randomly changed. Results of *Experiment 3* in *Chapter 2* showed that, when animals are trained on the task, inhibiting subicular consolidation on the first day of the “test” phase did not lead to any impairments in performance. This was true even when the “test” was carried out for 6 consecutive days (***Figure 8****, Chapter 2*). What possible conclusions can be drawn from these results?

One possibility is that the subiculum might be preferentially involved in consolidation of spatial information only when it involves learning a novel task. In the CA1, the novelty of a presented stimulus elicits changes in neuronal encoding (Bostock et al., 1991; Muller & Kubie, 1987), but repeated exposure to the same environment also elicit changes in the place fields of the cells (Mehta et al., 1997). On the other hand, there is evidence suggesting that there are two distinct molecular mechanisms for novelty detection (Kafkas & Montaldi, 2018). In this scheme, there could be a preferential mechanism that involves subicular neurons more during performance on a novel memory task than a familiar one.

Another possibility is that training animals on the task allows the information to “skip” the subiculum and to be processed directly by other output regions of the hippocampus. While the subiculum is the main output region from the CA1, there are some connections between the CA1 and downstream regions that run parallel to subicular projections (Aggleton & Christiansen, 2015; see ***Figure 2,*** *General Introduction*). Running the same

behavioural paradigm while inhibiting the CA1 region might help in exploring this alternative hypothesis.

The work conducted throughout this thesis suggests that there is a contribution of the subiculum in reference memory, and in consolidation of information acquired during performance on the RAM task. To the current knowledge of the field, this is the first report of reactivation of cell assemblies in the subiculum during sleep.

3. A proposed role for the subiculum in the hippocampal network

The experiments in which inhibiting the subiculum during memory consolidation was carried out showed that there might be differences in how this area processes information based on different factors. These include the familiarity with the task itself, but also the differential contributions of distinct sub-population of subicular neurons. Identifying groups of excitatory neurons in the subiculum is still a work in progress. Past attempts have focused on the characteristics of their spike trains (i.e. burstiness; see Stewart & Wong, 1993; Taube, 1995), genetic markers (Cembrowski et al., 2018), or theta preference (Kitanishi et al., 2021). In this thesis, four groups were identified based on theta phase preference of the neurons. Each showed different characteristics in terms of spatial properties and spike train dynamics, which may imply a differential processing of information.

Previous literature has shown a mixture of spatial coding schemes for subicular neurons, with some showing similar activity to that of CA1 place cells, while others show a range of spatial motifs (e.g. grid, border, … etc; see *General Introduction*). Some of these examples were encountered in this thesis (see examples in ***Figure 6 and 8,*** *Chapter* 3). Nonetheless, a precise quantification of these cells has not been conducted in this thesis. On the other hand, spatial information, which reflects how much of the firing of a cell can predict the position of the animal, was shown to differ among the various sub-populations of subicular cells. Whether these sub-populations have a tendency to have multipeaked place fields or not could be explored in the future. Additionally, both EC and CA1 neurons have been shown to have specific firing preferences during theta oscillations, with EC

neurons preferentially firing at the peak, and CA1 neurons firing at the trough of theta (Mitchell & Ranck, 1980). In the subiculum, distinct groups of neurons were found that fired at different phases of the theta oscillation. As theta oscillations drive the timing of spike sequences (Dragoi & Buzsáki, 2006; Lisman & Idiart, 1995; Raghavachari et al., 2001), exploring the link between these sub-populations of subicular cells and the inputs they receive from upstream regions might delineate differential contributions in processing spatial information. This could be acquired through retrograde tracing techniques similar to the ones used by Cembrowski and colleagues (2018) or optogenetics, as used by Kitanishi and colleagues (2021).

Along with its two main input regions, the subiculum has a variety of other regions it projects to. Distinct sub-populations based on projections targets have been characterised before (Cembrowski et al., 2018; Kim & Spruston, 2012; Kitanishi et al., 2021). While these authors recognise that some cells project to only one output region, they also show that a distinct number of subicular excitatory neurons have multiple projection targets. Optogenetics techniques could help to “tag” those subpopulations in the subiculum. This would add to the results found in this thesis about characteristics of the four distinct theta groups.

Moreover, both the two input regions (EC and CA1) and some of the output regions (e.g. Sweeney-Reed et al., 2021; Vann et al., 2009; Vann & Aggleton, 2004) of the subiculum have been implicated in long-term spatial memory processing, and memory consolidation. How is consolidation then processed across these different regions? One main theory of memory consolidation states that the hippocampus is fundamental in processing of recently acquired memories. Strengthening of the connections between neurons in this area allow formation of long-term memories. With time, the communication between the hippocampus and the neocortex allows the “transfer” of memories between the two areas (Buzsáki, 1989; Marr et al., 1991; McClelland et al., 1995). The neocortex is then believed to store those memories, which can then be recalled at a later time, allowing “remote” recall. In this proposed model, consolidation processes would have two stages, that involve different brain regions. A “recent” consolidation stage that would be carried out by the hippocampus, and a “remote” consolidation, carried out by the neocortex. One of the possible explanations for the delayed effects of consolidation inhibition seen in the behavioural experiments of this thesis suggests that the subiculum could be preferentially

involved in remote recall, rather than recent. Here, the subiculum could act as the “link” between the consolidation of information in the hippocampus and its subsequent strengthening in neocortical areas. Strengthening of synapses between subicular neurons might aid in developing of long-term memories for relatively long periods of time. This is supported by the reactivation of joint firing patterns seen in post-task sleep particularly for group 1 neurons, which is evident on any of the 5 post-task sleep sessions. To test whether this is true, performing the “consolidation block” experiment while inhibiting both hippocampal and neocortical areas involved in the different stages of memory consolidation (e.g. the prefrontal cortex; Frankland & Bontempi, 2005), along with tracking possible changes in neuronal activity for the various subicular groups, would help in pinpointing the temporal contribution of the subiculum.

On the other hand, the involvement of the subiculum in “remote” recall might suggest that this area is less involved in earlier stages of memory consolidation. These stages might be predominantly computed by the CA1 and information communicated to downstream regions without the need to involve the subiculum first. Indeed, while the subiculum uniquely projects to some targets, a lot of downstream areas receive projections from both the subiculum and the CA1 (e.g. Trouche et al., 2019; but also see Aggleton & Christiansen, 2015). In this scheme, these targets might preferentially receive “recent” memory information from the CA1, while the subiculum would become more dominant during “remote” recall. Joint recordings in CA1, subiculum, and downstream regions might help in understanding this phenomenon better, as well as behavioural experiments aimed at addressing remote recall.

In conclusion, while a precise contribution of the subiculum to consolidation of spatial information is yet to be provided, the work carried out in this thesis suggests that the subiculum is much more than just a “relay” station between the hippocampus and the neocortex, and that it most certainly plays a role in processing/consolidating information regarding learning of a task during off-line periods of rest.

4. The challenges of exploring the subicular contribution to the mnemonic component of spatial information processing

Some considerations should be addressed when interpreting the results of this thesis. First, the cohort of animals used for the behavioural experiments was relatively small (n = 8, 8, 6 and 12 for, respectively, *Experiment 1, 2, and 3, first and second part*). Repeating the experiments with a bigger cohort of animals might help in drawing stronger conclusions on the effect of subicular inhibition on spatial memory processing. In addition to this, the timeline of inhibition of the consolidation processes should be considered carefully. In *Experiment 2* and the second part of *Experiment 3*, muscimol infusions were delivered immediately after the end of all trials, after which the animals were left to rest in their home cages. Monitoring of sleep activity was not conducted. For this reason, the effect of the muscimol would have impacted both awake and sleep periods. While consolidation is not only limited to periods of sleep, but it is considered a mechanism that is carried out during general “rest” (e.g. see Wamsley, 2022), the lack of precise monitoring of activity of the animals may signify that other, non-consolidation processes may have been impacted by the treatment (Sawangjit et al., 2022). Implementation of electromyography and monitoring LFP/EEC might provide a more accurate timing of muscimol infusions (Sawangjit et al., 2018, 2022). Additionally, an important consideration comes from the type of treatment chosen to inhibit the subiculum. Muscimol has been widely used in studies that inhibited the hippocampal function (e.g. Holt & Maren, 1999; McEown & Treit, 2010; Melo et al., 2020), but precisely targeting the subicular area, due to its peculiar shape, is challenging. Other techniques have been developed over the years that can result in targeted inhibition of specific areas. For example, DREADDs (Designer Receptors Exclusively Activated by Designer Drugs; Roth, 2016) can be a useful tool to induce specific changes in neural activity in an area, and present the added bonus of being easily paired with electrophysiological recordings (review by Whissell et al., 2016).

One substantial feat of this thesis is in regard to the electrophysiological tracking of the activity of several neurons across multiple consecutive days. Other techniques have been implemented in the past to quantify features of neuronal coding across time (e.g. calcium imaging, see for example Sun et al., 2019). However, these do not allow the temporal precision that probe recordings allow, and do not provide LFP recordings of network events, such as theta oscillations. With the NPX probes implemented in this thesis, a

stable signal was recorded across days, which allowed tracking of the activity of a great number of cells (n = 321) in the span of 5 consecutive days. Nonetheless, the recording approach used in this thesis comes with some limitations. A first consideration should be made in regard to the clustering method that is implemented in probe recordings to identify neurons. In classical tetrode analysis, each laboratory would have a validation of their own clustering and data processing (e.g. Csicsvari et al., 1999; Hazan et al., 2006), which was easily accessible and possible to implement in further studies. Silicon probes, which allow sampling of data from a wide variety of recording points (e.g. 384 in NPX probes), come with their own clustering and processing software (in the case of NPX probe, KiloSort), which has been designed specifically to deal with such a large quantity of data. However, there is a risk that such software becomes a “black box” which is difficult to validate. Implementation of spike sorting in this thesis relied on the publications describing the KiloSort software (Pachitariu, Steinmetz, et al., 2016) and the github manual for later versions (e.g. this thesis used KiloSort 2.5). The danger of using common software has been reported by authors in the past (e.g. Eklund et al., 2016). While a series of validations were made in this, caution should then be taken when implementing such packages.

In addition to the general validity of the recording technique, some other limitations are worth mentioning in regard to the results of this thesis. While a considerable number of neurons was registered in the 5 recorded animals, the majority of cells were recorded from a single animal (n = 177, more than 50%), in which a four-shanked NPX 2.0 probe was implanted. This might have skewed the results of the analysis towards mechanisms that are not generalised across animals, but might instead be due to individual differences. Additionally, while the clustering analysis identified four distinct groups of cells based on their theta preference during exploratory behaviour, the low of number of cells belonging to some of the groups (particularly, groups 2 and 3) made it impossible to include those groups in certain analyses. Performing additional probe recordings of animals during this experimental paradigm might reveal a better picture of some of the results highlighted in this thesis. With the use of NPX 2.0 probes, which come with four shanks and can thus record across different sites in the proximo-distal axis of the subiculum, comparisons related to theta preference, burstiness, firing rate and spatial selectivity could be made with previous work (e.g. Cembrowski et al., 2018; Kim et al., 2012; Kim & Spruston, 2012; Kitanishi et al., 2021).

Despite some of its limitations, this thesis is the first body of work that quantifies a contribution of the subiculum in spatial reference memory, and that finds neuronal correlates to the consolidation of spatial information in the area during rest periods.

5. Conclusions

The work undertaken in this thesis has shown a contribution of the subiculum in processing spatial information both on-line and off-line, during memory consolidation. This has a series of implications on how memories are stored and processed in the hippocampal system, and what is transmitted to other brain regions. The subiculum is one area that is greatly affected by brain diseases such as dementia and Alzheimer's (e.g. Carlesimo et al., 2015; Mak et al., 2019). This work provides an additional step in creating a better understanding of the complications that arise from the disruption of the subicular network in these instances. More work is needed to create a complete picture of the function of this area, but with the recording method validated in this thesis, and with the aid of additional techniques that allow neuronal manipulation, this should now be a feasible goal. These techniques might include silencing of projections to and from the subiculum and assessment of the same spatial memory task, or concomitant recording of subicular activity during these manipulations to assess the type of information that is communicated between the subiculum and its up- and down-stream regions. Nonetheless, this thesis provides evidence that the subiculum is indeed involved in the processing of spatial reference memory.

References

Aggleton, J. P. (2012). Multiple anatomical systems embedded within the primate medial temporal lobe: Implications for hippocampal function. *Neuroscience & Biobehavioral Reviews*, *36*(7), 1579–1596. https://doi.org/10.1016/j.neubiorev.2011.09.005

Aggleton, J. P., & Brown, M. W. (1999). Episodic memory, amnesia, and the hippocampal–anterior thalamic axis. *Behavioral and Brain Sciences*, *22*(3), Article 3. https://doi.org/10.1017/S0140525X99002034

Aggleton, J. P., & Christiansen, K. (2015). The subiculum. In *Progress in Brain Research* (Vol. 219, pp. 65–82). Elsevier. https://doi.org/10.1016/bs.pbr.2015.03.003

Aguirre, G. K., Detre, J. A., Alsop, D. C., & D'Esposito, M. (1996). The Parahippocampus Subserves Topographical Learning in Man. *Cerebral Cortex*, *6*(6), 823–829. https://doi.org/10.1093/cercor/6.6.823

Aimone, J. B., Deng, W., & Gage, F. H. (2011). Resolving New Memories: A Critical Look at the Dentate Gyrus, Adult Neurogenesis, and Pattern Separation. *Neuron*, *70*(4), 589–596. https://doi.org/10.1016/j.neuron.2011.05.010

Amaral, D. G. (1993). Emerging principles of intrinsic hippocampal organization. *Current Opinion in Neurobiology*, *3*(2), 225–229. https://doi.org/10.1016/0959-4388(93)90214-J

Amaral, D. G., Dolorfo, C., & Alvarez-Royo, P. (1991). Organization of CA1 projections to the subiculum: A PHA-L analysis in the rat. *Hippocampus*, *1*(4), 415–435. https://doi.org/10.1002/hipo.450010410

Amaral, D. G., Ishizuka, N., & Claiborne, B. (1990). Chapter 1 Chapter Neurons, numbers and the hippocampal network. In *Progress in Brain Research* (Vol. 83, pp. 1–11). Elsevier. https://doi.org/10.1016/S0079-6123(08)61237-6

Amaral, D. G., & Witter, M. P. (1989). The three-dimensional organization of the hippocampal formation: A review of anatomical data. *Neuroscience*, *31*(3), 571–591. https://doi.org/10.1016/0306-4522(89)90424-7

Anderson, M. I., & O'Mara, S. M. (2003). Analysis of Recordings of Single-Unit Firing and Population Activity in the Dorsal Subiculum of Unrestrained, Freely Moving Rats. *Journal of Neurophysiology*, *90*(2), 655–665. https://doi.org/10.1152/jn.00723.2002

Atkinson, R. C., & Shiffrin, R. M. (1968). Human Memory: A Proposed System and its Control Processes. In *Psychology of Learning and Motivation* (Vol. 2, pp. 89–195). Elsevier. https://doi.org/10.1016/S0079-7421(08)60422-3

Avermann, M., Tomm, C., Mateo, C., Gerstner, W., & Petersen, C. C. H. (2012). Microcircuits of excitatory and inhibitory neurons in layer 2/3 of mouse barrel cortex. *Journal of Neurophysiology*, *107*(11), 3116–3134. https://doi.org/10.1152/jn.00917.2011

Bannerman, D. M., Deacon, R. M. J., Offen, S., Friswell, J., Grubb, M., & Rawlins, J. N. P. (2002). Double dissociation of function within the hippocampus: Spatial memory and hyponeophagia. *Behavioral Neuroscience*, *116*(5), 884–901. https://doi.org/10.1037/0735-7044.116.5.884

Bannerman, D. M., Good, M. A., Butcher, S. P., Ramsay, M., & Morris, R. G. M. (1995). Distinct components of spatial learning revealed by prior training and NMDA receptor blockade. *Nature*, *378*(6553), 182–186. https://doi.org/10.1038/378182a0

Barnes, C. A., McNaughton, B. L., Mizumori, S. J. Y., Leonard, B. W., & Lin, L.-H. (1990). Chapter 21 Chapter Comparison of spatial and temporal characteristics of neuronal activity in sequential stages of hippocampal processing. In *Progress in Brain Research* (Vol. 83, pp. 287–300). Elsevier. https://doi.org/10.1016/S0079-6123(08)61257-1

Barry, C., & Burgess, N. (2007). Learning in a geometric model of place cell firing. *Hippocampus*, *17*(9), 786–800. https://doi.org/10.1002/hipo.20324

Barthó, P., Hirase, H., Monconduit, L., Zugaro, M., Harris, K. D., & Buzsáki, G. (2004). Characterization of Neocortical Principal Cells and Interneurons by Network Interactions and Extracellular Features. *Journal of Neurophysiology*, *92*(1), 600–608. https://doi.org/10.1152/jn.01170.2003

Battaglia, F. P., Sutherland, G. R., Cowen, S. L., Mc Naughton, B. L., & Harris, K. D. (2005). Firing rate modulation: A simple statistical view of memory trace reactivation. *Neural Networks*, *18*(9), 1280–1291. https://doi.org/10.1016/j.neunet.2005.08.011

Berger, T. W., Swanson, G. W., Milner, T. A., Lynch, G. S., & Thompson, R. F. (1980). Reciprocal anatomical connections between hippocampus and subiculum in the rabbit: Evidence for subicular innervation of regio superior. *Brain Research*, *183*(2), 265–276. https://doi.org/10.1016/0006-8993(80)90463-1

Bezaire, M. J., & Soltesz, I. (2013). Quantitative assessment of CA1 local circuits: Knowledge base for interneuron-pyramidal cell connectivity: Quantitative Assessment Of Ca1 Local Circuits. *Hippocampus*, *23*(9), 751–785. https://doi.org/10.1002/hipo.22141

Bliss, T. V. P., & Collingridge, G. L. (1993). A synaptic model of memory: Long-term potentiation in the hippocampus. *Nature*, *361*(6407), 31–39. https://doi.org/10.1038/361031a0

Boccara, C. N., Nardin, M., Stella, F., O'Neill, J., & Csicsvari, J. (2019). The entorhinal cognitive map is attracted to goals. *Science*, *363*(6434), 1443–1447. https://doi.org/10.1126/science.aav4837

Böhm, C., & Lee, A. K. (2020). Canonical goal-selective representations are absent from prefrontal cortex in a spatial working memory task requiring behavioral flexibility. *eLife*, *9*, e63035. https://doi.org/10.7554/eLife.63035

Böhm, C., Peng, Y., Maier, N., Winterer, J., Poulet, J. F. A., Geiger, J. R. P., & Schmitz, D. (2015). Functional Diversity of Subicular Principal Cells during Hippocampal Ripples. *The Journal of Neuroscience*, *35*(40), 13608–13618. https://doi.org/10.1523/JNEUROSCI.5034-14.2015

Bolhius, J. J., Stewart, C. A., & Forrest, E. M. (1994). Tetrograde amnesia and memory reactivation in rats with ibotenate lesions to the Hippocampus or Subiculum. *The Quarterly Journal of Experimental Psychology. B. Comparative and Physiological Psychology*, *47(2b)*, 129–150. https://doi.org/10.1080/14640749408401353

Bostock, E., Muller, R. U., & Kubie, J. L. (1991). Experience-dependent modifications of hippocampal place cell firing. *Hippocampus*, *1*(2), 193–205. https://doi.org/10.1002/hipo.450010207

Bragin, A., Engel, J., Wilson, C. L., Fried, I., & Buzs□ki, G. (1999). High-frequency oscillations in human brain. *Hippocampus*, *9*(2), 137–142. https://doi.org/10.1002/(SICI)1098-1063(1999)9:2<137::AID-HIPO5>3.0.CO;2-0

Bragin, A., Hetke, J., Wilson, C. L., Anderson, D. J., Engel, J., & Buzsáki, G. (2000). Multiple site silicon-based probes for chronic recordings in freely moving rats: Implantation, recording and histological verification. *Journal of Neuroscience Methods*, *98*(1), 77–82. https://doi.org/10.1016/S0165-0270(00)00193-X

Brodt, S., Inostroza, M., Niethard, N., & Born, J. (2023). Sleep—A brain-state serving systems memory consolidation. *Neuron*, *111*(7), 1050–1075. https://doi.org/10.1016/j.neuron.2023.03.005

Brotons-Mas, J. R., Schaffelhofer, S., Guger, C., O'Mara, S. M., & Sanchez-Vives, M. V. (2017). Heterogeneous spatial representation by different subpopulations of neurons in the subiculum. *Neuroscience*, *343*, 174–189. https://doi.org/10.1016/j.neuroscience.2016.11.042

Brown, E. N., Frank, L. M., Tang, D., Quirk, M. C., & Wilson, M. A. (1998). A Statistical Paradigm for Neural Spike Train Decoding Applied to Position Prediction from Ensemble Firing Patterns of Rat Hippocampal Place Cells. *The Journal of Neuroscience*, *18*(18), 7411–7425. https://doi.org/10.1523/JNEUROSCI.18-18-07411.1998

Burke, S. N., Maurer, A. P., Nematollahi, S., Uprety, A. R., Wallace, J. L., & Barnes, C. A. (2011). The influence of objects on place field expression and size in distal hippocampal CA1. *Hippocampus*, *21*(7), 783–801. https://doi.org/10.1002/hipo.20929

Buzsáki, G. (1989). Two-stage model of memory trace formation: A role for "noisy" brain states. *Neuroscience*, *31*(3), 551–570. https://doi.org/10.1016/0306-4522(89)90423-5

Buzsáki, G. (2002). Theta Oscillations in the Hippocampus. *Neuron*, *33*(3), 325–340. https://doi.org/10.1016/S0896-6273(02)00586-X

Buzsáki, G. (2004). Large-scale recording of neuronal ensembles. *Nature Neuroscience*, *7*(5), 446–451. https://doi.org/10.1038/nn1233

Buzsáki, G. (2015). Hippocampal sharp wave-ripple: A cognitive biomarker for episodic memory and planning. *Hippocampus*, *25*(10), 1073–1188. https://doi.org/10.1002/hipo.22488

Buzsáki, G., & Chrobak, J. J. (1995). Temporal structure in spatially organized neuronal ensembles: A role for interneuronal networks. *Current Opinion in Neurobiology*, *5*(4), 504–510. https://doi.org/10.1016/0959-4388(95)80012-3

Buzsáki, G., Horváth, Z., Urioste, R., Hetke, J., & Wise, K. (1992). High-frequency network oscillation in the hippocampus. *Science*, *256*(5059), 1025–1027. https://doi.org/10.1126/science.1589772

Buzsáki, G., Lai-Wo S., L., & Vanderwolf, C. H. (1983). Cellular bases of hippocampal EEG in the behaving rat. *Brain Research Reviews*, *6*(2), 139–171. https://doi.org/10.1016/0165-0173(83)90037-1

Carlesimo, G. A., Piras, F., Orfei, M. D., Iorio, M., Caltagirone, C., & Spalletta, G. (2015). Atrophy of presubiculum and subiculum is the earliest hippocampal anatomical marker of Alzheimer's disease. *Alzheimer's & Dementia: Diagnosis, Assessment & Disease Monitoring*, *1*(1), 24–32. https://doi.org/10.1016/j.dadm.2014.12.001

Cassel, J.-C., Pereira De Vasconcelos, A., Loureiro, M., Cholvin, T., Dalrymple-Alford, J. C., & Vertes, R. P. (2013). The reuniens and rhomboid nuclei: Neuroanatomy, electrophysiological characteristics and behavioral implications. *Progress in Neurobiology*, *111*, 34–52. https://doi.org/10.1016/j.pneurobio.2013.08.006

Cembrowski, M. S., Phillips, M. G., DiLisio, S. F., Shields, B. C., Winnubst, J., Chandrashekar, J., Bas, E., & Spruston, N. (2018). Dissociable Structural and Functional

Hippocampal Outputs via Distinct Subiculum Cell Classes. *Cell*, *173*(5), 1280-1292.e18. https://doi.org/10.1016/j.cell.2018.03.031

Cenquizca, L. A., & Swanson, L. W. (2007). Spatial organization of direct hippocampal field CA1 axonal projections to the rest of the cerebral cortex. *Brain Research Reviews*, *56*(1), 1–26. https://doi.org/10.1016/j.brainresrev.2007.05.002

Chevaleyre, V., & Siegelbaum, S. A. (2010). Strong CA2 Pyramidal Neuron Synapses Define a Powerful Disynaptic Cortico-Hippocampal Loop. *Neuron*, *66*(4), 560–572. https://doi.org/10.1016/j.neuron.2010.04.013

Christian, E. P., & Deadwyler, S. A. (1986). Behavioral functions and hippocampal cell types: Evidence for two nonoverlapping populations in the rat. *Journal of Neurophysiology*, *55*(2), 331–348. https://doi.org/10.1152/jn.1986.55.2.331

Chrobak, J., & Buzsaki, G. (1994). Selective activation of deep layer (V-VI) retrohippocampal cortical neurons during hippocampal sharp waves in the behaving rat. *The Journal of Neuroscience*, *14*(10), 6160–6170. https://doi.org/10.1523/JNEUROSCI.14-10-06160.1994

Chrobak, J. J., & Buzsáki, G. (1996). High-Frequency Oscillations in the Output Networks of the Hippocampal–Entorhinal Axis of the Freely Behaving Rat. *The Journal of Neuroscience*, *16*(9), 3056–3066. https://doi.org/10.1523/JNEUROSCI.16-09-03056.1996

Cohen, S. J., Munchow, A. H., Rios, L. M., Zhang, G., Ásgeirsdóttir, H. N., & Stackman, R. W. (2013). The Rodent Hippocampus Is Essential for Nonspatial Object Memory. *Current Biology*, *23*(17), 1685–1690. https://doi.org/10.1016/j.cub.2013.07.002

Collingridge, G. L., Kehl, S. J., & McLennan, H. (1983). Excitatory amino acids in synaptic transmission in the Schaffer collateral-commissural pathway of the rat hippocampus. *The Journal of Physiology*, *334*(1), 33–46. https://doi.org/10.1113/jphysiol.1983.sp014478

Csicsvari, J., Hirase, H., Czurkó, A., Mamiya, A., & Buzsáki, G. (1999). Oscillatory Coupling of Hippocampal Pyramidal Cells and Interneurons in the Behaving Rat. *The*

Journal of Neuroscience, *19*(1), 274–287. https://doi.org/10.1523/JNEUROSCI.19-01-00274.1999

Csicsvari, J., Hirase, H., Mamiya, A., & Buzsáki, G. (2000). Ensemble Patterns of Hippocampal CA3-CA1 Neurons during Sharp Wave–Associated Population Events. *Neuron*, *28*(2), 585–594. https://doi.org/10.1016/S0896-6273(00)00135-5

Danielson, N. B., Zaremba, J. D., Kaifosh, P., Bowler, J., Ladow, M., & Losonczy, A. (2016). Sublayer-Specific Coding Dynamics during Spatial Navigation and Learning in Hippocampal Area CA1. *Neuron*, *91*(3), 652–665. https://doi.org/10.1016/j.neuron.2016.06.020

Davidson, T. J., Kloosterman, F., & Wilson, M. A. (2009). Hippocampal Replay of Extended Experience. *Neuron*, *63*(4), 497–507. https://doi.org/10.1016/j.neuron.2009.07.027

Davis, H. P., Tribuna, J., Pulsinelli, W. A., & Volpe, B. T. (1986). Reference and working memory of rats following hippocampal damage induced by transient forebrain ischemia. *Physiology & Behavior*, *37*(3), 387–392. https://doi.org/10.1016/0031-9384(86)90195-2

Debnath, T., & Song, M. (2021). Fast Optimal Circular Clustering and Applications on Round Genomes. *IEEE/ACM Transactions on Computational Biology and Bioinformatics*, *18*(6), 2061–2071. https://doi.org/10.1109/TCBB.2021.3077573

Deshmukh, S. S., & Knierim, J. J. (2011). Representation of Non-Spatial and Spatial Information in the Lateral Entorhinal Cortex. *Frontiers in Behavioral Neuroscience*, *5*. https://doi.org/10.3389/fnbeh.2011.00069

Dickey, A. S., Suminski, A., Amit, Y., & Hatsopoulos, N. G. (2009). Single-Unit Stability Using Chronically Implanted Multielectrode Arrays. *Journal of Neurophysiology*, *102*(2), 1331–1339. https://doi.org/10.1152/jn.90920.2008

Diekelmann, S., & Born, J. (2010). The memory function of sleep. *Nature Reviews Neuroscience*, *11*(2), 114–126. https://doi.org/10.1038/nrn2762

Dragoi, G., & Buzsáki, G. (2006). Temporal Encoding of Place Sequences by Hippocampal Cell Assemblies. *Neuron*, *50*(1), 145–157. https://doi.org/10.1016/j.neuron.2006.02.023

Drieu, C., & Zugaro, M. (2019). Hippocampal Sequences During Exploration: Mechanisms and Functions. *Frontiers in Cellular Neuroscience*, *13*, 232. https://doi.org/10.3389/fncel.2019.00232

Dudai, Y. (2004). The Neurobiology of Consolidations, Or, How Stable is the Engram? *Annual Review of Psychology*, *55*(1), 51–86. https://doi.org/10.1146/annurev.psych.55.090902.142050

Dupret, D., O'Neill, J., Pleydell-Bouverie, B., & Csicsvari, J. (2010). The reorganization and reactivation of hippocampal maps predict spatial memory performance. *Nature Neuroscience*, *13*(8), 995–1002. https://doi.org/10.1038/nn.2599

Ego-Stengel, V., & Wilson, M. A. (2010). Disruption of ripple-associated hippocampal activity during rest impairs spatial learning in the rat. *Hippocampus*, *20*(1), 1–10. https://doi.org/10.1002/hipo.20707

Eklund, A., Nichols, T. E., & Knutsson, H. (2016). Cluster failure: Why fMRI inferences for spatial extent have inflated false-positive rates. *Proceedings of the National Academy of Sciences*, *113*(28), 7900–7905. https://doi.org/10.1073/pnas.1602413113

Ekstrom, A. D., Kahana, M. J., Caplan, J. B., Fields, T. A., Isham, E. A., Newman, E. L., & Fried, I. (2003). Cellular networks underlying human spatial navigation. *Nature*, *425*(6954), 184–188. https://doi.org/10.1038/nature01964

Emondi, A. A., Rebrik, S. P., Kurgansky, A. V., & Miller, K. D. (2004). Tracking neurons recorded from tetrodes across time. *Journal of Neuroscience Methods*, *135*(1–2), 95–105. https://doi.org/10.1016/j.jneumeth.2003.12.022

Epstein, R. A., Patai, E. Z., Julian, J. B., & Spiers, H. J. (2017). The cognitive map in humans: Spatial navigation and beyond. *Nature Neuroscience*, *20*(11), 1504–1513. https://doi.org/10.1038/nn.4656

Evans, D. A., Stempel, A. V., Vale, R., Ruehle, S., Lefler, Y., & Branco, T. (2018). A synaptic threshold mechanism for computing escape decisions. *Nature*, *558*(7711), 590–594. https://doi.org/10.1038/s41586-018-0244-6

Fanselow, M. S., & Dong, H.-W. (2010). Are the Dorsal and Ventral Hippocampus Functionally Distinct Structures? *Neuron*, *65*(1), 7–19. https://doi.org/10.1016/j.neuron.2009.11.031

Fenton, A. A. (2024). Remapping revisited: How the hippocampus represents different spaces. *Nature Reviews Neuroscience*, *25*(6), 428–448. https://doi.org/10.1038/s41583-024-00817-x

Fenton, A. A., & Muller, R. U. (1998). Place cell discharge is extremely variable during individual passes of the rat through the firing field. *Proceedings of the National Academy of Sciences*, *95*(6), 3182–3187. https://doi.org/10.1073/pnas.95.6.3182

Fenton, A. A., Wesierska, M., Kaminsky, Y., & Bures, J. (1998). Both here and there: Simultaneous expression of autonomous spatial memories in rats. *Proceedings of the National Academy of Sciences*, *95*(19), 11493–11498. https://doi.org/10.1073/pnas.95.19.11493

Fox, S. E., & Ranck, J. B. (1981). Electrophysiological characteristics of hippocampal complex-spike cells and theta cells. *Experimental Brain Research*, *41–41*(3–4), 399–410. https://doi.org/10.1007/BF00238898

Frank, L. M., Brown, E. N., & Wilson, M. (2000). Trajectory Encoding in the Hippocampus and Entorhinal Cortex. *Neuron*, *27*(1), 169–178. https://doi.org/10.1016/S0896-6273(00)00018-0

Frankland, P. W., & Bontempi, B. (2005). The organization of recent and remote memories. *Nature Reviews Neuroscience*, *6*(2), 119–130. https://doi.org/10.1038/nrn1607

Galani, R., Weiss, I., Cassel, J.-C., & Kelche, C. (1998). Spatial memory, habituation, and reactions to spatial and nonspatial changes in rats with selective lesions of the

hippocampus, the entorhinal cortex or the subiculum. *Behavioural Brain Research*, *96*(1–2), 1–12. https://doi.org/10.1016/S0166-4328(97)00197-6

Galvao, J., Davis, B., Tilley, M., Normando, E., Duchen, M. R., & Cordeiro, M. F. (2014). Unexpected low-dose toxicity of the universal solvent DMSO. *The FASEB Journal*, *28*(3), 1317–1330. https://doi.org/10.1096/fj.13-235440

Gardner, R. J., Lu, L., Wernle, T., Moser, M.-B., & Moser, E. I. (2019). Correlation structure of grid cells is preserved during sleep. *Nature Neuroscience*, *22*(4), 598–608. https://doi.org/10.1038/s41593-019-0360-0

Ghaem, O., Mellet, E., Crivello, F., Tzourio, N., Mazoyer, B., Berthoz, A., & Denis, M. (1997). Mental navigation along memorized routes activates the hippocampus, precuneus, and insula: *NeuroReport*, *8*(3), 739–744. https://doi.org/10.1097/00001756-199702100-00032

Ghestem, A., Pompili, M. N., Dipper-Wawra, M., Quilichini, P. P., Bernard, C., & Ferraris, M. (2023). Long-term near-continuous recording with Neuropixels probes in healthy and epileptic rats. *Journal of Neural Engineering*, *20*(4), 046003. https://doi.org/10.1088/1741-2552/ace218

Gigg, J. (2006). Constraints on hippocampal processing imposed by the connectivity between CA1, subiculum and subicular targets. *Behavioural Brain Research*, *174*(2), 265–271. https://doi.org/10.1016/j.bbr.2006.06.014

Gilbert, P. E., Kesner, R. P., & Lee, I. (2001). Dissociating hippocampal subregions: A double dissociation between dentate gyrus and CA1. *Hippocampus*, *11*(6), 626–636. https://doi.org/10.1002/hipo.1077

Girardeau, G., Benchenane, K., Wiener, S. I., Buzsáki, G., & Zugaro, M. B. (2009). Selective suppression of hippocampal ripples impairs spatial memory. *Nature Neuroscience*, *12*(10), 1222–1223. https://doi.org/10.1038/nn.2384

Green, J. D., Maxwell, D. S., Schindler, W. J., & Stumpf, C. (1960). RABBIT EEG ‘THETA’ RHYTHM: ITS ANATOMICAL SOURCE AND RELATION TO ACTIVITY IN SINGLE

NEURONS. *Journal of Neurophysiology*, *23*(4), 403–420. https://doi.org/10.1152/jn.1960.23.4.403

Greene, J. R. T., & Totterdell, S. (1997). Morphology and distribution of electrophysiologically defined classes of pyramidal and nonpyramidal neurons in rat ventral subiculum in vitro. *The Journal of Comparative Neurology*, *380*(3), 395–408. https://doi.org/10.1002/(SICI)1096-9861(19970414)380:3<395::AID-CNE8>3.0.CO;2-Y

Gridchyn, I., Schoenenberger, P., O'Neill, J., & Csicsvari, J. (2020). Assembly-Specific Disruption of Hippocampal Replay Leads to Selective Memory Deficit. *Neuron*, *106*(2), 291-300.e6. https://doi.org/10.1016/j.neuron.2020.01.021

Grienberger, C., Giovannucci, A., Zeiger, W., & Portera-Cailliau, C. (2022). Two-photon calcium imaging of neuronal activity. *Nature Reviews Methods Primers*, *2*(1), 67. https://doi.org/10.1038/s43586-022-00147-1

Grienberger, C., & Konnerth, A. (2012). Imaging Calcium in Neurons. *Neuron*, *73*(5), 862–885. https://doi.org/10.1016/j.neuron.2012.02.011

Hafting, T., Fyhn, M., Molden, S., Moser, M.-B., & Moser, E. I. (2005). Microstructure of a spatial map in the entorhinal cortex. *Nature*, *436*(7052), 801–806. https://doi.org/10.1038/nature03721

Harris, K. D., Csicsvari, J., Hirase, H., Dragoi, G., & Buzsáki, G. (2003). Organization of cell assemblies in the hippocampus. *Nature*, *424*(6948), 552–556. https://doi.org/10.1038/nature01834

Harris, K. D., Hirase, H., Leinekugel, X., Henze, D. A., & Buzsáki, G. (2001). Temporal Interaction between Single Spikes and Complex Spike Bursts in Hippocampal Pyramidal Cells. *Neuron*, *32*(1), 141–149. https://doi.org/10.1016/S0896-6273(01)00447-0

Hartley, T., Burgess, N., Lever, C., Cacucci, F., & O'Keefe, J. (2000). Modeling place fields in terms of the cortical inputs to the hippocampus. *Hippocampus*, *10*(4), 369–379. https://doi.org/10.1002/1098-1063(2000)10:4<369::AID-HIPO3>3.0.CO;2-0

Harvey, R. E., Thompson, S. M., Sanchez, L. M., Yoder, R. M., & Clark, B. J. (2017). Post-training Inactivation of the Anterior Thalamic Nuclei Impairs Spatial Performance on the Radial Arm Maze. *Frontiers in Neuroscience*, *11*. https://doi.org/10.3389/fnins.2017.00094

Hasselmo, M. E., Bodelón, C., & Wyble, B. P. (2002). A Proposed Function for Hippocampal Theta Rhythm: Separate Phases of Encoding and Retrieval Enhance Reversal of Prior Learning. *Neural Computation*, *14*(4), 793–817. https://doi.org/10.1162/089976602317318965

Hazan, L., Zugaro, M., & Buzsáki, G. (2006). Klusters, NeuroScope, NDManager: A free software suite for neurophysiological data processing and visualization. *Journal of Neuroscience Methods*, *155*(2), 207–216. https://doi.org/10.1016/j.jneumeth.2006.01.017

Henriksen, E. J., Colgin, L. L., Barnes, C. A., Witter, M. P., Moser, M.-B., & Moser, E. I. (2010). Spatial Representation along the Proximodistal Axis of CA1. *Neuron*, *68*(1), 127–137. https://doi.org/10.1016/j.neuron.2010.08.042

Henze, D. A., Borhegyi, Z., Csicsvari, J., Mamiya, A., Harris, K. D., & Buzsáki, G. (2000). Intracellular Features Predicted by Extracellular Recordings in the Hippocampus In Vivo. *Journal of Neurophysiology*, *84*(1), 390–400. https://doi.org/10.1152/jn.2000.84.1.390

Herman, J., & Mueller, N. (2006). Role of the ventral subiculum in stress integration. *Behavioural Brain Research*, *174*(2), 215–224. https://doi.org/10.1016/j.bbr.2006.05.035

Hitti, F. L., & Siegelbaum, S. A. (2014). The hippocampal CA2 region is essential for social memory. *Nature*, *508*(7494), 88–92. https://doi.org/10.1038/nature13028

Hok, V., Lenck-Santini, P.-P., Roux, S., Save, E., Muller, R. U., & Poucet, B. (2007). Goal-Related Activity in Hippocampal Place Cells. *The Journal of Neuroscience*, *27*(3), 472–482. https://doi.org/10.1523/JNEUROSCI.2864-06.2007

Hollup, S. A., Molden, S., Donnett, J. G., Moser, M.-B., & Moser, E. I. (2001). Accumulation of Hippocampal Place Fields at the Goal Location in an Annular Watermaze Task. *The Journal of Neuroscience*, *21*(5), 1635–1644. https://doi.org/10.1523/JNEUROSCI.21-05-01635.2001

Holt, W., & Maren, S. (1999). Muscimol Inactivation of the Dorsal Hippocampus Impairs Contextual Retrieval of Fear Memory. *The Journal of Neuroscience*, *19*(20), 9054–9062. https://doi.org/10.1523/JNEUROSCI.19-20-09054.1999

Honig, W. K. (1978). Studies of working memory in the pigeon. In *Cognitive processes in animal behaviour* (pp. 211–248). Hillsdale, NJ: Lawrence Erlbaum Associates.

Huxter, J., Burgess, N., & O'Keefe, J. (2003). Independent rate and temporal coding in hippocampal pyramidal cells. *Nature*, *425*(6960), 828–832. https://doi.org/10.1038/nature02058

Igarashi, K. M., Ito, H. T., Moser, E. I., & Moser, M.-B. (2014). Functional diversity along the transverse axis of hippocampal area CA1. *FEBS Letters*, *588*(15), 2470–2476. https://doi.org/10.1016/j.febslet.2014.06.004

Imbrosci, B., Nitzan, N., McKenzie, S., Donoso, J. R., Swaminathan, A., Böhm, C., Maier, N., & Schmitz, D. (2021). Subiculum as a generator of sharp wave-ripples in the rodent hippocampus. *Cell Reports*, *35*(3), 109021. https://doi.org/10.1016/j.celrep.2021.109021

Ishizuka, N. (2001). Laminar organization of the pyramidal cell layer of the subiculum in the rat. *Journal of Comparative Neurology*, *435*(1), 89–110. https://doi.org/10.1002/cne.1195

Ishizuka, N., Weber, J., & Amaral, D. G. (1990). Organization of intrahippocampal projections originating from CA3 pyramidal cells in the rat. *Journal of Comparative Neurology*, *295*(4), 580–623. https://doi.org/10.1002/cne.902950407

Isomura, Y., Sirota, A., Özen, S., Montgomery, S., Mizuseki, K., Henze, D. A., & Buzsáki, G. (2006). Integration and Segregation of Activity in Entorhinal-Hippocampal Subregions by Neocortical Slow Oscillations. *Neuron*, *52*(5), 871–882. https://doi.org/10.1016/j.neuron.2006.10.023

Ito, H. T., Zhang, S.-J., Witter, M. P., Moser, E. I., & Moser, M.-B. (2015). A prefrontal–thalamo–hippocampal circuit for goal-directed spatial navigation. *Nature*, *522*(7554), 50–55. https://doi.org/10.1038/nature14396

Jackson, A., & Fetz, E. E. (2007). Compact Movable Microwire Array for Long-Term Chronic Unit Recording in Cerebral Cortex of Primates. *Journal of Neurophysiology*, *98*(5), 3109–3118. https://doi.org/10.1152/jn.00569.2007

Jacobs, J., Weidemann, C. T., Miller, J. F., Solway, A., Burke, J. F., Wei, X.-X., Suthana, N., Sperling, M. R., Sharan, A. D., Fried, I., & Kahana, M. J. (2013). Direct recordings of grid-like neuronal activity in human spatial navigation. *Nature Neuroscience*, *16*(9), 1188–1190. https://doi.org/10.1038/nn.3466

Jadhav, S. P., Rothschild, G., Roumis, D. K., & Frank, L. M. (2016). Coordinated Excitation and Inhibition of Prefrontal Ensembles during Awake Hippocampal Sharp-Wave Ripple Events. *Neuron*, *90*(1), 113–127. https://doi.org/10.1016/j.neuron.2016.02.010

Jarrard, L. E. (1993). On the role of the hippocampus in learning and memory in the rat. *Behavioral and Neural Biology*, *60*(1), 9–26. https://doi.org/10.1016/0163-1047(93)90664-4

Jarrard, L. E. (1995). What does the hippocampus really do? *Behavioural Brain Research*, *71*(1–2), 1–10. https://doi.org/10.1016/0166-4328(95)00034-8

Jeffreys, H. (1998). *Theory of probability* (3rd ed). Clarendon Press ; Oxford University Press.

Ji, D., & Wilson, M. A. (2007). Coordinated memory replay in the visual cortex and hippocampus during sleep. *Nature Neuroscience*, *10*(1), 100–107. https://doi.org/10.1038/nn1825

Johnston, G. A. R. (2014). Muscimol as an Ionotropic GABA Receptor Agonist. *Neurochemical Research*, *39*(10), 1942–1947. https://doi.org/10.1007/s11064-014-1245-y

Juavinett, A. L., Bekheet, G., & Churchland, A. K. (2019). Chronically implanted Neuropixels probes enable high-yield recordings in freely moving mice. *eLife*, *8*, e47188. https://doi.org/10.7554/eLife.47188

Jun, J. J., Steinmetz, N. A., Siegle, J. H., Denman, D. J., Bauza, M., Barbarits, B., Lee, A. K., Anastassiou, C. A., Andrei, A., Aydın, Ç., Barbic, M., Blanche, T. J., Bonin, V., Couto,

J., Dutta, B., Gratiy, S. L., Gutnisky, D. A., Häusser, M., Karsh, B., … Harris, T. D. (2017). Fully integrated silicon probes for high-density recording of neural activity. *Nature*, *551*(7679), 232–236. https://doi.org/10.1038/nature24636

Jung, M. W., & McNaughton, B. L. (1993). Spatial selectivity of unit activity in the hippocampal granular layer. *Hippocampus*, *3*(2), 165–182. https://doi.org/10.1002/hipo.450030209

Kafkas, A., & Montaldi, D. (2018). How do memory systems detect and respond to novelty? *Neuroscience Letters*, *680*, 60–68. https://doi.org/10.1016/j.neulet.2018.01.053

Kelemen, E., & Fenton, A. A. (2016). Coordinating different representations in the hippocampus. *Neurobiology of Learning and Memory*, *129*, 50–59. https://doi.org/10.1016/j.nlm.2015.12.011

Kerr, K. M., Agster, K. L., Furtak, S. C., & Burwell, R. D. (2007). Functional neuroanatomy of the parahippocampal region: The lateral and medial entorhinal areas. *Hippocampus*, *17*(9), 697–708. https://doi.org/10.1002/hipo.20315

Kesner, R. P., & Hunsaker, M. R. (2010). The temporal attributes of episodic memory. *Behavioural Brain Research*, *215*(2), 299–309. https://doi.org/10.1016/j.bbr.2009.12.029

Khodagholy, D., Gelinas, J. N., & Buzsáki, G. (2017). Learning-enhanced coupling between ripple oscillations in association cortices and hippocampus. *Science*, *358*(6361), 369–372. https://doi.org/10.1126/science.aan6203

Kim, S. M., Ganguli, S., & Frank, L. M. (2012). Spatial Information Outflow from the Hippocampal Circuit: Distributed Spatial Coding and Phase Precession in the Subiculum. *The Journal of Neuroscience*, *32*(34), 11539–11558. https://doi.org/10.1523/JNEUROSCI.5942-11.2012

Kim, Y., & Spruston, N. (2012). Target-specific output patterns are predicted by the distribution of regular-spiking and bursting pyramidal neurons in the subiculum. *Hippocampus*, *22*(4), 693–706. https://doi.org/10.1002/hipo.20931

Kinnavane, L., Vann, S. D., Nelson, A. J. D., O'Mara, S. M., & Aggleton, J. P. (2018). Collateral Projections Innervate the Mammillary Bodies and Retrosplenial Cortex: A New Category of Hippocampal Cells. *Eneuro*, *5*(1), ENEURO.0383-17.2018. https://doi.org/10.1523/ENEURO.0383-17.2018

Kitanishi, T., Umaba, R., & Mizuseki, K. (2021). Robust information routing by dorsal subiculum neurons. *Science Advances*, *7*(11), eabf1913. https://doi.org/10.1126/sciadv.abf1913

Krupic, J., Bauza, M., Burton, S., & O'Keefe, J. (2018). Local transformations of the hippocampal cognitive map. *Science*, *359*(6380), 1143–1146. https://doi.org/10.1126/science.aao4960

Kubie, J., Muller, R., & Bostock, E. (1990). Spatial firing properties of hippocampal theta cells. *The Journal of Neuroscience*, *10*(4), 1110–1123. https://doi.org/10.1523/JNEUROSCI.10-04-01110.1990

Kudrimoti, H. S., Barnes, C. A., & McNaughton, B. L. (1999). Reactivation of Hippocampal Cell Assemblies: Effects of Behavioral State, Experience, and EEG Dynamics. *The Journal of Neuroscience*, *19*(10), 4090–4101. https://doi.org/10.1523/JNEUROSCI.19-10-04090.1999

Kyriazi, H. T., Carvell, G. E., Brumberg, J. C., & Simons, D. J. (1996). Quantitative effects of GABA and bicuculline methiodide on receptive field properties of neurons in real and simulated whisker barrels. *Journal of Neurophysiology*, *75*(2), 547–560. https://doi.org/10.1152/jn.1996.75.2.547

Lee, A. K., & Wilson, M. A. (2002). Memory of Sequential Experience in the Hippocampus during Slow Wave Sleep. *Neuron*, *36*(6), 1183–1194. https://doi.org/10.1016/S0896-6273(02)01096-6

Leutgeb, J. K., Leutgeb, S., Moser, M.-B., & Moser, E. I. (2007). Pattern Separation in the Dentate Gyrus and CA3 of the Hippocampus. *Science*, *315*(5814), 961–966. https://doi.org/10.1126/science.1135801

Leutgeb, S., Leutgeb, J. K., Barnes, C. A., Moser, E. I., McNaughton, B. L., & Moser, M.-B. (2005). Independent Codes for Spatial and Episodic Memory in Hippocampal Neuronal Ensembles. *Science*, *309*(5734), 619–623. https://doi.org/10.1126/science.1114037

Leutgeb, S., Leutgeb, J. K., Treves, A., Moser, M.-B., & Moser, E. I. (2004). Distinct Ensemble Codes in Hippocampal Areas CA3 and CA1. *Science*, *305*(5688), 1295–1298. https://doi.org/10.1126/science.1100265

Lever, C., Burton, S., Jeewajee, A., O'Keefe, J., & Burgess, N. (2009). Boundary Vector Cells in the Subiculum of the Hippocampal Formation. *The Journal of Neuroscience*, *29*(31), 9771–9777. https://doi.org/10.1523/JNEUROSCI.1319-09.2009

Levy, E. R. J., Carrillo-Segura, S., Park, E. H., Redman, W. T., Hurtado, J. R., Chung, S., & Fenton, A. A. (2023). A manifold neural population code for space in hippocampal coactivity dynamics independent of place fields. *Cell Reports*, *42*(10), 113142. https://doi.org/10.1016/j.celrep.2023.113142

Li, X. -G., Somogyi, P., Ylinen, A., & Buzsáki, G. (1994). The hippocampal CA3 network: An in vivo intracellular labeling study. *Journal of Comparative Neurology*, *339*(2), 181–208. https://doi.org/10.1002/cne.903390204

Lisman, J. E., & Idiart, M. A. P. (1995). Storage of 7 ± 2 Short-Term Memories in Oscillatory Subcycles. *Science*, *267*(5203), 1512–1515. https://doi.org/10.1126/science.7878473

Liu, X.-S., Xue, Q., Zeng, Q.-W., Li, Q., Liu, J., Feng, X.-M., & Yu, B.-W. (2010). Sevoflurane impairs memory consolidation in rats, possibly through inhibiting phosphorylation of glycogen synthase kinase-3β in the hippocampus. *Neurobiology of Learning and Memory*, *94*(4), 461–467. https://doi.org/10.1016/j.nlm.2010.08.011

Logothetis, N. K., Eschenko, O., Murayama, Y., Augath, M., Steudel, T., Evrard, H. C., Besserve, M., & Oeltermann, A. (2012). Hippocampal–cortical interaction during periods of subcortical silence. *Nature*, *491*(7425), 547–553. https://doi.org/10.1038/nature11618

Lorente de Nó, R. (1934). Studies on the structure of the cerebral cortex. II. Continuation of the study of the ammonic system. *Journal Für Psychologie Und Neurologie*.

Luo, T. Z., Bondy, A. G., Gupta, D., Elliott, V. A., Kopec, C. D., & Brody, C. D. (2020). An approach for long-term, multi-probe Neuropixels recordings in unrestrained rats. *eLife*, *9*, e59716. https://doi.org/10.7554/eLife.59716

Luscher, C., & Malenka, R. C. (2012). NMDA Receptor-Dependent Long-Term Potentiation and Long-Term Depression (LTP/LTD). *Cold Spring Harbor Perspectives in Biology*, *4*(6), a005710–a005710. https://doi.org/10.1101/cshperspect.a005710

Maguire, E. A., Burgess, N., Donnett, J. G., Frackowiak, R. S. J., Frith, C. D., & O'Keefe, J. (1998). Knowing Where and Getting There: A Human Navigation Network. *Science*, *280*(5365), 921–924. https://doi.org/10.1126/science.280.5365.921

Mahmmoud, R. R., Sase, S., Aher, Y. D., Sase, A., Gröger, M., Mokhtar, M., Höger, H., & Lubec, G. (2015). Spatial and Working Memory Is Linked to Spine Density and Mushroom Spines. *PLOS ONE*, *10*(10), e0139739. https://doi.org/10.1371/journal.pone.0139739

Mak, E., Donaghy, P. C., McKiernan, E., Firbank, M. J., Lloyd, J., Petrides, G. S., Thomas, A. J., & O'Brien, J. T. (2019). Beta amyloid deposition maps onto hippocampal and subiculum atrophy in dementia with Lewy bodies. *Neurobiology of Aging*, *73*, 74–81. https://doi.org/10.1016/j.neurobiolaging.2018.09.004

Mankin, E. A., Sparks, F. T., Slayyeh, B., Sutherland, R. J., Leutgeb, S., & Leutgeb, J. K. (2012). Neuronal code for extended time in the hippocampus. *Proceedings of the National Academy of Sciences*, *109*(47), 19462–19467. https://doi.org/10.1073/pnas.1214107109

Markus, E. J., Barnes, C. A., McNaughton, B. L., Gladden, V. L., & Skaggs, W. E. (1994). Spatial information content and reliability of hippocampal CA1 neurons: Effects of visual input. *Hippocampus*, *4*(4), 410–421. https://doi.org/10.1002/hipo.450040404

Marr, D. (1971). Simple memory: A theory for archicortex. *Philosophical Transactions of the Royal Society of London. B, Biological Sciences*, *262*(841), 23–81. https://doi.org/10.1098/rstb.1971.0078

Marr, D., Willshaw, D., & McNaughton, B. (1991). Simple Memory: A Theory for Archicortex. In L. Vaina (Ed.), *From the Retina to the Neocortex* (pp. 59–128). Birkhäuser Boston. https://doi.org/10.1007/978-1-4684-6775-8_5

Mathis, A., Mamidanna, P., Cury, K. M., Abe, T., Murthy, V. N., Mathis, M. W., & Bethge, M. (2018). DeepLabCut: Markerless pose estimation of user-defined body parts with deep learning. *Nature Neuroscience*, *21*(9), 1281–1289. https://doi.org/10.1038/s41593-018-0209-y

Mau, W., Sullivan, D. W., Kinsky, N. R., Hasselmo, M. E., Howard, M. W., & Eichenbaum, H. (2018). The Same Hippocampal CA1 Population Simultaneously Codes Temporal Information over Multiple Timescales. *Current Biology*, *28*(10), 1499-1508.e4. https://doi.org/10.1016/j.cub.2018.03.051

Maurer, A. P., Cowen, S. L., Burke, S. N., Barnes, C. A., & McNaughton, B. L. (2006). Phase Precession in Hippocampal Interneurons Showing Strong Functional Coupling to Individual Pyramidal Cells. *The Journal of Neuroscience*, *26*(52), 13485–13492. https://doi.org/10.1523/JNEUROSCI.2882-06.2006

McClelland, J. L., McNaughton, B. L., & O'Reilly, R. C. (1995). Why there are complementary learning systems in the hippocampus and neocortex: Insights from the successes and failures of connectionist models of learning and memory. *Psychological Review*, *102*(3), 419–457. https://doi.org/10.1037/0033-295X.102.3.419

McEown, K., & Treit, D. (2010). Inactivation of the dorsal or ventral hippocampus with muscimol differentially affects fear and memory. *Brain Research*, *1353*, 145–151. https://doi.org/10.1016/j.brainres.2010.07.030

McGaugh, J. L. (2000). Memory—A Century of Consolidation. *Science*, *287*(5451), 248–251. https://doi.org/10.1126/science.287.5451.248

McHugh, S. B., Lopes-dos-Santos, V., Castelli, M., Gava, G. P., Thompson, S. E., Tam, S. K. E., Hartwich, K., Perry, B., Toth, R., Denison, T., Sharott, A., & Dupret, D. (2024).

Offline hippocampal reactivation during dentate spikes supports flexible memory. *Neuron*, *112*(22), 3768-3781.e8. https://doi.org/10.1016/j.neuron.2024.08.022

McHugh, T. J., Jones, M. W., Quinn, J. J., Balthasar, N., Coppari, R., Elmquist, J. K., Lowell, B. B., Fanselow, M. S., Wilson, M. A., & Tonegawa, S. (2007). Dentate Gyrus NMDA Receptors Mediate Rapid Pattern Separation in the Hippocampal Network. *Science*, *317*(5834), 94–99. https://doi.org/10.1126/science.1140263

McNaughton, B. L., Barnes, C. A., & O'Keefe, J. (1983). The contributions of position, direction, and velocity to single unit activity in the hippocampus of freely-moving rats. *Experimental Brain Research*, *52*(1). https://doi.org/10.1007/BF00237147

McNaughton, B. L., Battaglia, F. P., Jensen, O., Moser, E. I., & Moser, M.-B. (2006). Path integration and the neural basis of the 'cognitive map'. *Nature Reviews Neuroscience*, *7*(8), 663–678. https://doi.org/10.1038/nrn1932

McNaughton, B. L., & Morris, R. G. M. (1987). Hippocampal synaptic enhancement and information storage within a distributed memory system. *Trends in Neurosciences*, *10*(10), 408–415. https://doi.org/10.1016/0166-2236(87)90011-7

Mehta, M. R., Barnes, C. A., & McNaughton, B. L. (1997). Experience-dependent, asymmetric expansion of hippocampal place fields. *Proceedings of the National Academy of Sciences*, *94*(16), 8918–8921. https://doi.org/10.1073/pnas.94.16.8918

Melo, M. B. D., Favaro, V. M., & Oliveira, M. G. M. (2020). The dorsal subiculum is required for contextual fear conditioning consolidation in rats. *Behavioural Brain Research*, *390*, 112661. https://doi.org/10.1016/j.bbr.2020.112661

Menendez De La Prida, L., Suarez, F., & Pozo, M. A. (2003). Electrophysiological and morphological diversity of neurons from the rat subicular complex in vitro. *Hippocampus*, *13*(6), 728–744. https://doi.org/10.1002/hipo.10123

Mercer, A., & Thomson, A. M. (2017). Cornu Ammonis Regions–Antecedents of Cortical Layers? *Frontiers in Neuroanatomy*, *11*, 83. https://doi.org/10.3389/fnana.2017.00083

Milczarek, M. M., & Vann, S. D. (2020). The retrosplenial cortex and long-term spatial memory: From the cell to the network. *Current Opinion in Behavioral Sciences*, *32*, 50–56. https://doi.org/10.1016/j.cobeha.2020.01.014

Mitchell, S. J., & Ranck, J. B. (1980). Generation of theta rhythm in medial entorhinal cortex of freely moving rats. *Brain Research*, *189*(1), 49–66. https://doi.org/10.1016/0006-8993(80)90006-2

Mitra, P. P., & Pesaran, B. (1999). Analysis of Dynamic Brain Imaging Data. *Biophysical Journal*, *76*(2), 691–708. https://doi.org/10.1016/S0006-3495(99)77236-X

Mizuseki, K., & Buzsáki, G. (2013). Preconfigured, Skewed Distribution of Firing Rates in the Hippocampus and Entorhinal Cortex. *Cell Reports*, *4*(5), 1010–1021. https://doi.org/10.1016/j.celrep.2013.07.039

Mizuseki, K., Diba, K., Pastalkova, E., & Buzsáki, G. (2011). Hippocampal CA1 pyramidal cells form functionally distinct sublayers. *Nature Neuroscience*, *14*(9), 1174–1181. https://doi.org/10.1038/nn.2894

Mizuseki, K., Sirota, A., Pastalkova, E., & Buzsáki, G. (2009). Theta Oscillations Provide Temporal Windows for Local Circuit Computation in the Entorhinal-Hippocampal Loop. *Neuron*, *64*(2), 267–280. https://doi.org/10.1016/j.neuron.2009.08.037

Moroni, F., Forchetti, M. C., Krogsgaard-Larsen, P., & Guidotti, A. (1982). Relative disposition of the GABA agonists THIP and muscimol in the brain of the rat. *Journal of Pharmacy and Pharmacology*, *34*(10), 676–678. https://doi.org/10.1111/j.2042-7158.1982.tb04702.x

Morris, R. G. M., Garrud, P., Rawlins, J. N. P., & O'Keefe, J. (1982). Place navigation impaired in rats with hippocampal lesions. *Nature*, *297*(5868), 681–683. https://doi.org/10.1038/297681a0

Morris, R. G. M., Schenk, F., Tweedie, F., & Jarrard, L. E. (1990). Ibotenate Lesions of Hippocampus and/or Subiculum: Dissociating Components of Allocentric Spatial Learning.

European Journal of Neuroscience, *2*(12), 1016–1028. https://doi.org/10.1111/j.1460-9568.1990.tb00014.x

Moser, E. I., Kropff, E., & Moser, M.-B. (2008). Place Cells, Grid Cells, and the Brain's Spatial Representation System. *Annual Review of Neuroscience*, *31*(1), 69–89. https://doi.org/10.1146/annurev.neuro.31.061307.090723

Muller, R., & Kubie, J. (1987). The effects of changes in the environment on the spatial firing of hippocampal complex-spike cells. *The Journal of Neuroscience*, *7*(7), 1951–1968. https://doi.org/10.1523/JNEUROSCI.07-07-01951.1987

Muller, R. U., Kubie, J. L., Bostock, E. M., Taube, J. S., & Quirk, G. J. (1991). *Spatial firing correlates of neurons in the hippocampal formation of freely moving rats.*

Murtagh, F., & Legendre, P. (2014). Ward's Hierarchical Agglomerative Clustering Method: Which Algorithms Implement Ward's Criterion? *Journal of Classification*, *31*(3), 274–295. https://doi.org/10.1007/s00357-014-9161-z

Naber, P. A., Lopes Da Silva, F. H., & Witter, M. P. (2001). Reciprocal connections between the entorhinal cortex and hippocampal fields CA1 and the subiculum are in register with the projections from CA1 to the subiculum. *Hippocampus*, *11*(2), 99–104. https://doi.org/10.1002/hipo.1028

Naber, P. A., & Witter, M. P. (1998). Subicular efferents are organized mostly as parallel projections: A double-labeling, retrograde-tracing study in the rat. *The Journal of Comparative Neurology*, *393*(3), 284–297. https://doi.org/10.1002/(SICI)1096-9861(19980413)393:3<284::AID-CNE2>3.0.CO;2-Y

Nádasdy, Z., Hirase, H., Czurkó, A., Csicsvari, J., & Buzsáki, G. (1999). Replay and Time Compression of Recurring Spike Sequences in the Hippocampus. *The Journal of Neuroscience*, *19*(21), 9497–9507. https://doi.org/10.1523/JNEUROSCI.19-21-09497.1999

Nakashiba, T., Buhl, D. L., McHugh, T. J., & Tonegawa, S. (2009). Hippocampal CA3 Output Is Crucial for Ripple-Associated Reactivation and Consolidation of Memory. *Neuron*, *62*(6), 781–787. https://doi.org/10.1016/j.neuron.2009.05.013

Nelson, A. J. D., Powell, A. L., Holmes, J. D., Vann, S. D., & Aggleton, J. P. (2015). What does spatial alternation tell us about retrosplenial cortex function? *Frontiers in Behavioral Neuroscience*, *9*. https://doi.org/10.3389/fnbeh.2015.00126

Nitzan, N., McKenzie, S., Beed, P., English, D. F., Oldani, S., Tukker, J. J., Buzsáki, G., & Schmitz, D. (2020). Propagation of hippocampal ripples to the neocortex by way of a subiculum-retrosplenial pathway. *Nature Communications*, *11*(1), 1947. https://doi.org/10.1038/s41467-020-15787-8

Nyberg, L., McIntosh, A. R., Cabeza, R., Habib, R., Houle, S., & Tulving, E. (1996). General and specific brain regions involved in encoding and retrieval of events: What, where, and when. *Proceedings of the National Academy of Sciences*, *93*(20), 11280–11285. https://doi.org/10.1073/pnas.93.20.11280

Nyquist, H. (2002). Certain topics in telegraph transmission theory. *Proceedings of the IEEE*, *90*(2), 280–305. https://doi.org/10.1109/5.989875

O'Keefe, J., & Conway, D. H. (1978). Hippocampal place units in the freely moving rat: Why they fire where they fire. *Experimental Brain Research*, *31*(4). https://doi.org/10.1007/BF00239813

O'Keefe, J., & Dostrovsky, J. (1971). The hippocampus as a spatial map. Preliminary evidence from unit activity in the freely-moving rat. *Brain Research*, *34*(1), 171–175. https://doi.org/10.1016/0006-8993(71)90358-1

O'Keefe, J. M., Nadel, L., & O'Keefe, J. (1978). *The hippocampus as a cognitive map*. Clarendon Press.

O'Keefe, J., & Recce, M. L. (1993). Phase relationship between hippocampal place units and the EEG theta rhythm. *Hippocampus*, *3*(3), 317–330. https://doi.org/10.1002/hipo.450030307

O'Keefe, John. (2014). *Spatial Cells in the Hippocampal Formation.* Nobel Lecture on, *7*.

Ólafsdóttir, H. F., Carpenter, F., & Barry, C. (2016). Coordinated grid and place cell replay during rest. *Nature Neuroscience*, *19*(6), 792–794. https://doi.org/10.1038/nn.4291

Oliva, A., Fernández-Ruiz, A., Buzsáki, G., & Berényi, A. (2016). Role of Hippocampal CA2 Region in Triggering Sharp-Wave Ripples. *Neuron*, *91*(6), 1342–1355. https://doi.org/10.1016/j.neuron.2016.08.008

Olson, J. M., Tongprasearth, K., & Nitz, D. A. (2017). Subiculum neurons map the current axis of travel. *Nature Neuroscience*, *20*(2), 170–172. https://doi.org/10.1038/nn.4464

Olton, D. S. (1977). Spatial Memory. *Scientific American*, *236*(6), 82–99.

Olton, D. S., Becker, J. T., & Handelmann, G. E. (1979). Hippocampus, space, and memory. *Behavioral and Brain Sciences*, *2*(3), 313–322. https://doi.org/10.1017/S0140525X00062713

Olton, D. S., & Samuelson, R. J. (1976). Remembrance of places passed: Spatial memory in rats. *Journal of Experimental Psychology: Animal Behavior Processes*, *2*(2), 97–116. https://doi.org/10.1037/0097-7403.2.2.97

O'Mara, S. (2005). The subiculum: What it does, what it might do, and what neuroanatomy has yet to tell us. *Journal of Anatomy*, *207*(3), 271–282. https://doi.org/10.1111/j.1469-7580.2005.00446.x

O'Mara, S. M., & Aggleton, J. P. (2019). Space and Memory (Far) Beyond the Hippocampus: Many Subcortical Structures Also Support Cognitive Mapping and Mnemonic Processing. *Frontiers in Neural Circuits*, *13*, 52. https://doi.org/10.3389/fncir.2019.00052

O'Mara, S. M., Commins, S., Anderson, M., & Gigg, J. (2001). The subiculum: A review of form, physiology and function. *Progress in Neurobiology*, *64*(2), 129–155. https://doi.org/10.1016/S0301-0082(00)00054-X

O'Mara, S. M., Sanchez-Vives, M. V., Brotons-Mas, J. R., & O'Hare, E. (2009). Roles for the subiculum in spatial information processing, memory, motivation and the temporal

control of behaviour. *Progress in Neuro-Psychopharmacology and Biological Psychiatry*, *33*(5), 782–790. https://doi.org/10.1016/j.pnpbp.2009.03.040

O'Neill, J., Boccara, C. N., Stella, F., Schoenenberger, P., & Csicsvari, J. (2017). Superficial layers of the medial entorhinal cortex replay independently of the hippocampus. *Science*, *355*(6321), 184–188. https://doi.org/10.1126/science.aag2787

O'Neill, J., Senior, T., & Csicsvari, J. (2006). Place-Selective Firing of CA1 Pyramidal Cells during Sharp Wave/Ripple Network Patterns in Exploratory Behavior. *Neuron*, *49*(1), 143–155. https://doi.org/10.1016/j.neuron.2005.10.037

O'Neill, J., Senior, T. J., Allen, K., Huxter, J. R., & Csicsvari, J. (2008). Reactivation of experience-dependent cell assembly patterns in the hippocampus. *Nature Neuroscience*, *11*(2), 209–215. https://doi.org/10.1038/nn2037

Pachitariu, M., Steinmetx, N. A., Kadir, S. N., Carandini, M., & Harris, K. D. (2016). Fast and accurate spike sorting of high-channel count probes with KiloSort. *Advances in Neural Information Processing Systems*, *29*, 4455–4463.

Pachitariu, M., Steinmetz, N., Kadir, S., Carandini, M., & Kenneth D., H. (2016). *Kilosort: Realtime spike-sorting for extracellular electrophysiology with hundreds of channels*. Neuroscience. https://doi.org/10.1101/061481

Packard, M. G., & McGaugh, J. L. (1996). Inactivation of Hippocampus or Caudate Nucleus with Lidocaine Differentially Affects Expression of Place and Response Learning. *Neurobiology of Learning and Memory*, *65*(1), 65–72. https://doi.org/10.1006/nlme.1996.0007

Palombi, T., Mandolesi, L., Alivernini, F., Chirico, A., & Lucidi, F. (2022). Application of Real and Virtual Radial Arm Maze Task in Human. *Brain Sciences*, *12*(4), 468. https://doi.org/10.3390/brainsci12040468

Patel, J., Fujisawa, S., Berényi, A., Royer, S., & Buzsáki, G. (2012). Traveling Theta Waves along the Entire Septotemporal Axis of the Hippocampus. *Neuron*, *75*(3), 410–417. https://doi.org/10.1016/j.neuron.2012.07.015

Pavlides, C., & Winson, J. (1989). Influences of hippocampal place cell firing in the awake state on the activity of these cells during subsequent sleep episodes. *The Journal of Neuroscience*, *9*(8), 2907–2918. https://doi.org/10.1523/JNEUROSCI.09-08-02907.1989

Paxinos, G., & Watson, C. (2007). *The rat brain in stereotaxic coordinates* (6th ed). Elsevier.

Pearson, K. (1901). LIII. *On lines and planes of closest fit to systems of points in space*. *The London, Edinburgh, and Dublin Philosophical Magazine and Journal of Science*, *2*(11), 559–572. https://doi.org/10.1080/14786440109462720

Petsche, H., & Stumpf, Ch. (1960). Topographic and toposcopic study of origin and spread of the regular synchronized arousal pattern in the rabbit. *Electroencephalography and Clinical Neurophysiology*, *12*(3), 589–600. https://doi.org/10.1016/0013-4694(60)90101-2

Potvin, O., Allen, K., Thibaudeau, G., Doré, F. Y., & Goulet, S. (2006). Performance on spatial working memory tasks after dorsal or ventral hippocampal lesions and adjacent damage to the subiculum. *Behavioral Neuroscience*, *120*(2), 413–422. https://doi.org/10.1037/0735-7044.120.2.413

Potvin, O., Doré, F. Y., & Goulet, S. (2007). Contributions of the dorsal hippocampus and the dorsal subiculum to processing of idiothetic information and spatial memory. *Neurobiology of Learning and Memory*, *87*(4), 669–678. https://doi.org/10.1016/j.nlm.2007.01.002

Potvin, O., Doré, F. Y., & Goulet, S. (2009). Lesions of the dorsal subiculum and the dorsal hippocampus impaired pattern separation in a task using distinct and overlapping visual stimuli. *Neurobiology of Learning and Memory*, *91*(3), 287–297. https://doi.org/10.1016/j.nlm.2008.10.003

Poulter, S., Lee, S. A., Dachtler, J., Wills, T. J., & Lever, C. (2021). Vector trace cells in the subiculum of the hippocampal formation. *Nature Neuroscience*, *24*(2), 266–275. https://doi.org/10.1038/s41593-020-00761-w

Quirk, M. C., & Wilson, M. A. (1999). Interaction between spike waveform classification and temporal sequence detection. *Journal of Neuroscience Methods*, *94*(1), 41–52. https://doi.org/10.1016/S0165-0270(99)00124-7

Raghavachari, S., Kahana, M. J., Rizzuto, D. S., Caplan, J. B., Kirschen, M. P., Bourgeois, B., Madsen, J. R., & Lisman, J. E. (2001). Gating of Human Theta Oscillations by a Working Memory Task. *The Journal of Neuroscience*, *21*(9), 3175–3183. https://doi.org/10.1523/JNEUROSCI.21-09-03175.2001

Ranck, J. B. (1973). Studies on single neurons in dorsal hippocampal formation and septum in unrestrained rats. *Experimental Neurology*, *41*(2), 462–531. https://doi.org/10.1016/0014-4886(73)90290-2

Ranganath, C., & Ritchey, M. (2012). Two cortical systems for memory-guided behaviour. *Nature Reviews Neuroscience*, *13*(10), 713–726. https://doi.org/10.1038/nrn3338

Rao, S. G., Williams, G. V., & Goldman-Rakic, P. S. (1999). Isodirectional Tuning of Adjacent Interneurons and Pyramidal Cells During Working Memory: Evidence for Microcolumnar Organization in PFC. *Journal of Neurophysiology*, *81*(4), 1903–1916. https://doi.org/10.1152/jn.1999.81.4.1903

Remondes, M., & Schuman, E. M. (2004). Role for a cortical input to hippocampal area CA1 in the consolidation of a long-term memory. *Nature*, *431*(7009), 699–703. https://doi.org/10.1038/nature02965

Riedel, G., Micheau, J., Lam, A. G. M., Roloff, E. v. L., Martin, S. J., Bridge, H., Hoz, L. D., Poeschel, B., McCulloch, J., & Morris, R. G. M. (1999). Reversible neural inactivation reveals hippocampal participation in several memory processes. *Nature Neuroscience*, *2*(10), 898–905. https://doi.org/10.1038/13202

Rolls, E. T. (2013). The mechanisms for pattern completion and pattern separation in the hippocampus. *Frontiers in Systems Neuroscience*, *7*. https://doi.org/10.3389/fnsys.2013.00074

Rosene, D. L., & Van Hoesen, G. W. (1977). Hippocampal Efferents Reach Widespread Areas of Cerebral Cortex and Amygdala in the Rhesus Monkey. *Science*, *198*(4314), 315–317. https://doi.org/10.1126/science.410102

Rossant, C., Kadir, S. N., Goodman, D. F. M., Schulman, J., Hunter, M. L. D., Saleem, A. B., Grosmark, A., Belluscio, M., Denfield, G. H., Ecker, A. S., Tolias, A. S., Solomon, S., Buzsáki, G., Carandini, M., & Harris, K. D. (2016). Spike sorting for large, dense electrode arrays. *Nature Neuroscience*, *19*(4), 634–641. https://doi.org/10.1038/nn.4268

Roth, B. L. (2016). DREADDs for Neuroscientists. *Neuron*, *89*(4), 683–694. https://doi.org/10.1016/j.neuron.2016.01.040

Rothschild, G., Eban, E., & Frank, L. M. (2017). A cortical–hippocampal–cortical loop of information processing during memory consolidation. *Nature Neuroscience*, *20*(2), 251–259. https://doi.org/10.1038/nn.4457

Rouder, J. N., Morey, R. D., Speckman, P. L., & Province, J. M. (2012). Default Bayes factors for ANOVA designs. *Journal of Mathematical Psychology*, *56*(5), 356–374. https://doi.org/10.1016/j.jmp.2012.08.001

Royer, S., Zemelman, B. V., Losonczy, A., Kim, J., Chance, F., Magee, J. C., & Buzsáki, G. (2012). Control of timing, rate and bursts of hippocampal place cells by dendritic and somatic inhibition. *Nature Neuroscience*, *15*(5), 769–775. https://doi.org/10.1038/nn.3077

Saleem, A. B., Chadderton, P., Apergis-Schoute, J., Harris, K. D., & Schultz, S. R. (2010). Methods for predicting cortical UP and DOWN states from the phase of deep layer local field potentials. *Journal of Computational Neuroscience*, *29*(1–2), 49–62. https://doi.org/10.1007/s10827-010-0228-5

Sanderson, D. J., & Bannerman, D. M. (2012). The role of habituation in hippocampus-dependent spatial working memory tasks: Evidence from GluA1 AMPA receptor subunit knockout mice. *Hippocampus*, *22*(5), 981–994. https://doi.org/10.1002/hipo.20896

Sanderson, D. J., McHugh, S. B., Good, M. A., Sprengel, R., Seeburg, P. H., Rawlins, J. N. P., & Bannerman, D. M. (2010). Spatial working memory deficits in GluA1 AMPA

receptor subunit knockout mice reflect impaired short-term habituation: Evidence for Wagner's dual-process memory model. *Neuropsychologia*, *48*(8), 2303–2315. https://doi.org/10.1016/j.neuropsychologia.2010.03.018

Sargolini, F., Fyhn, M., Hafting, T., McNaughton, B. L., Witter, M. P., Moser, M.-B., & Moser, E. I. (2006). Conjunctive Representation of Position, Direction, and Velocity in Entorhinal Cortex. *Science*, *312*(5774), 758–762. https://doi.org/10.1126/science.1125572

Saunders, R. C., & Aggleton, J. P. (2007). Origin and topography of fibers contributing to the fornix in macaque monkeys. *Hippocampus*, *17*(5), 396–411. https://doi.org/10.1002/hipo.20276

Savelli, F., Yoganarasimha, D., & Knierim, J. J. (2008). Influence of boundary removal on the spatial representations of the medial entorhinal cortex. *Hippocampus*, *18*(12), 1270–1282. https://doi.org/10.1002/hipo.20511

Sawangjit, A., Harkotte, M., Oyanedel, C. N., Niethard, N., Born, J., & Inostroza, M. (2022). Two distinct ways to form long-term object recognition memory during sleep and wakefulness. *Proceedings of the National Academy of Sciences*, *119*(34), e2203165119. https://doi.org/10.1073/pnas.2203165119

Sawangjit, A., Oyanedel, C. N., Niethard, N., Salazar, C., Born, J., & Inostroza, M. (2018). The hippocampus is crucial for forming non-hippocampal long-term memory during sleep. *Nature*, *564*(7734), 109–113. https://doi.org/10.1038/s41586-018-0716-8

Schacter, G. B., Yang, C. R., Innis, N. K., & Mogenson, G. J. (1989). The role of the hippocampal-nucleus accumbens pathway in radial-arm maze performance. *Brain Research*, *494*(2), 339–349. https://doi.org/10.1016/0006-8993(89)90602-1

Scharfman, H. E. (2007). The CA3 "backprojection" to the dentate gyrus. In *Progress in Brain Research* (Vol. 163, pp. 627–637). Elsevier. https://doi.org/10.1016/S0079-6123(07)63034-9

Schmitt, W. B., Deacon, R. M. J., Seeburg, P. H., Rawlins, J. N. P., & Bannerman, D. M. (2003). A Within-Subjects, Within-Task Demonstration of Intact Spatial Reference Memory

and Impaired Spatial Working Memory in Glutamate Receptor-A-Deficient Mice. *The Journal of Neuroscience*, *23*(9), 3953–3959. https://doi.org/10.1523/JNEUROSCI.23-09-03953.2003

Schneidman, E., Berry, M. J., Segev, R., & Bialek, W. (2006). Weak pairwise correlations imply strongly correlated network states in a neural population. *Nature*, *440*(7087), 1007–1012. https://doi.org/10.1038/nature04701

Scoville, W. B., & Milner, B. (1957). LOSS OF RECENT MEMORY AFTER BILATERAL HIPPOCAMPAL LESIONS. *Journal of Neurology, Neurosurgery & Psychiatry*, *20*(1), 11–21. https://doi.org/10.1136/jnnp.20.1.11

Senior, T. J., Huxter, J. R., Allen, K., O'Neill, J., & Csicsvari, J. (2008). Gamma Oscillatory Firing Reveals Distinct Populations of Pyramidal Cells in the CA1 Region of the Hippocampus. *The Journal of Neuroscience*, *28*(9), 2274–2286. https://doi.org/10.1523/JNEUROSCI.4669-07.2008

Seymour, J. P., Wu, F., Wise, K. D., & Yoon, E. (2017). State-of-the-art MEMS and microsystem tools for brain research. *Microsystems & Nanoengineering*, *3*(1), 16066. https://doi.org/10.1038/micronano.2016.66

Sharp, P. (2006). Subicular place cells generate the same "map" for different environments: Comparison with hippocampal cells. *Behavioural Brain Research*, *174*(2), 206–214. https://doi.org/10.1016/j.bbr.2006.05.034

Sharp, P. E. (1997). Subicular cells generate similar spatial firing patterns in two geometrically and visually distinctive environments: Comparison with hippocampal place cells. *Behavioural Brain Research*, *85*(1), 71–92. https://doi.org/10.1016/S0166-4328(96)00165-9

Sharp, P. E. (1999). Complimentary roles for hippocampal versus subicular/entorhinal place cells in coding place, context, and events. *Hippocampus*, *9*(4), 432–443. https://doi.org/10.1002/(SICI)1098-1063(1999)9:4<432::AID-HIPO9>3.0.CO;2-P

Sharp, P., & Green, C. (1994). Spatial correlates of firing patterns of single cells in the subiculum of the freely moving rat. *The Journal of Neuroscience*, *14*(4), 2339–2356. https://doi.org/10.1523/JNEUROSCI.14-04-02339.1994

Sheng, T., Xing, D., Wu, Y., Wang, Q., Li, X., & Lu, W. (2021). A novel 3D-printed multi-driven system for large-scale neurophysiological recordings in multiple brain regions. *Journal of Neuroscience Methods*, *361*, 109286. https://doi.org/10.1016/j.jneumeth.2021.109286

Siegle, J. H., López, A. C., Patel, Y. A., Abramov, K., Ohayon, S., & Voigts, J. (2017). Open Ephys: An open-source, plugin-based platform for multichannel electrophysiology. *Journal of Neural Engineering*, *14*(4), 045003. https://doi.org/10.1088/1741-2552/aa5eea

Silverman, B. W. (1981). Using Kernel Density Estimates to Investigate Multimodality. *Journal of the Royal Statistical Society Series B: Statistical Methodology*, *43*(1), 97–99. https://doi.org/10.1111/j.2517-6161.1981.tb01155.x

Simonnet, J., & Brecht, M. (2019). Burst Firing and Spatial Coding in Subicular Principal Cells. *The Journal of Neuroscience*, *39*(19), 3651–3662. https://doi.org/10.1523/JNEUROSCI.1656-18.2019

Sirota, A., Montgomery, S., Fujisawa, S., Isomura, Y., Zugaro, M., & Buzsáki, G. (2008). Entrainment of Neocortical Neurons and Gamma Oscillations by the Hippocampal Theta Rhythm. *Neuron*, *60*(4), 683–697. https://doi.org/10.1016/j.neuron.2008.09.014

Skaggs, W. E., & McNaughton, B. L. (1996). Replay of Neuronal Firing Sequences in Rat Hippocampus During Sleep Following Spatial Experience. *Science*, *271*(5257), 1870–1873. https://doi.org/10.1126/science.271.5257.1870

Skaggs, W. E., McNaughton, B. L., Permenter, M., Archibeque, M., Vogt, J., Amaral, D. G., & Barnes, C. A. (2007). EEG Sharp Waves and Sparse Ensemble Unit Activity in the Macaque Hippocampus. *Journal of Neurophysiology*, *98*(2), 898–910. https://doi.org/10.1152/jn.00401.2007

Skaggs, W. E., McNaughton, B. L., Wilson, M. A., & Barnes, C. A. (1996). Theta phase precession in hippocampal neuronal populations and the compression of temporal sequences. *Hippocampus*, *6*(2), 149–172. https://doi.org/10.1002/(SICI)1098-1063(1996)6:2<149::AID-HIPO6>3.0.CO;2-K

Skaggs, W., Mcnaughton, B., & Gothard, K. (1992). An information-theoretic approach to deciphering the hippocampal code. *Advances in Neural Information Processing Systems*, *5*.

Šmejda Haug, F.-M. (1974). Light microscopical mapping of the hippocampal region, the pyriform cortex and the corticomedial amygdaloid nuclei of the rat with Timm's sulphide silver method: I. Area dentata, hippocampus and subiculum. *Zeitschrift Für Anatomie Und Entwicklungsgeschichte*, *145*(1), 1–27. https://doi.org/10.1007/BF00519123

Solstad, T., Boccara, C. N., Kropff, E., Moser, M.-B., & Moser, E. I. (2008). Representation of Geometric Borders in the Entorhinal Cortex. *Science*, *322*(5909), 1865–1868. https://doi.org/10.1126/science.1166466

Soltesz, I., & Losonczy, A. (2018). CA1 pyramidal cell diversity enabling parallel information processing in the hippocampus. *Nature Neuroscience*, *21*(4), 484–493. https://doi.org/10.1038/s41593-018-0118-0

Somogyi, P., & Klausberger, T. (2005). Defined types of cortical interneurone structure space and spike timing in the hippocampus. *The Journal of Physiology*, *562*(1), 9–26. https://doi.org/10.1113/jphysiol.2004.078915

Squire, L. R. (2004). Memory systems of the brain: A brief history and current perspective. *Neurobiology of Learning and Memory*, *82*(3), 171–177. https://doi.org/10.1016/j.nlm.2004.06.005

Staba, R. J., Wilson, C. L., Bragin, A., Fried, I., & Engel, J. (2002). Quantitative Analysis of High-Frequency Oscillations (80–500 Hz) Recorded in Human Epileptic Hippocampus and Entorhinal Cortex. *Journal of Neurophysiology*, *88*(4), 1743–1752. https://doi.org/10.1152/jn.2002.88.4.1743

Staff, N. P., Jung, H.-Y., Thiagarajan, T., Yao, M., & Spruston, N. (2000). Resting and Active Properties of Pyramidal Neurons in Subiculum and CA1 of Rat Hippocampus. *Journal of Neurophysiology*, *84*(5), 2398–2408. https://doi.org/10.1152/jn.2000.84.5.2398

Steinmetz, N. A., Aydin, C., Lebedeva, A., Okun, M., Pachitariu, M., Bauza, M., Beau, M., Bhagat, J., Böhm, C., Broux, M., Chen, S., Colonell, J., Gardner, R. J., Karsh, B., Kloosterman, F., Kostadinov, D., Mora-Lopez, C., O'Callaghan, J., Park, J., … Harris, T. D. (2021). Neuropixels 2.0: A miniaturized high-density probe for stable, long-term brain recordings. *Science*, *372*(6539), eabf4588. https://doi.org/10.1126/science.abf4588

Steriade, M., Nunez, A., & Amzica, F. (1993). A novel slow (< 1 Hz) oscillation of neocortical neurons in vivo: Depolarizing and hyperpolarizing components. *The Journal of Neuroscience*, *13*(8), 3252–3265. https://doi.org/10.1523/JNEUROSCI.13-08-03252.1993

Steward, O. (1976). Topographic organization of the projections from the entorhinal area to the hippocampal formation of the rat. *Journal of Comparative Neurology*, *167*(3), 285–314. https://doi.org/10.1002/cne.901670303

Stewart, M., & Wong, R. K. (1993). Intrinsic properties and evoked responses of guinea pig subicular neurons in vitro. *Journal of Neurophysiology*, *70*(1), 232–245. https://doi.org/10.1152/jn.1993.70.1.232

Strange, B. A., Witter, M. P., Lein, E. S., & Moser, E. I. (2014). Functional organization of the hippocampal longitudinal axis. *Nature Reviews Neuroscience*, *15*(10), 655–669. https://doi.org/10.1038/nrn3785

Sun, Y., Jin, S., Lin, X., Chen, L., Qiao, X., Jiang, L., Zhou, P., Johnston, K. G., Golshani, P., Nie, Q., Holmes, T. C., Nitz, D. A., & Xu, X. (2019). CA1-projecting subiculum neurons facilitate object–place learning. *Nature Neuroscience*, *22*(11), 1857–1870. https://doi.org/10.1038/s41593-019-0496-y

Swanson, L. W., & Cowan, W. M. (1977). An autoradiographic study of the organization of the efferet connections of the hippocampal formation in the rat. *Journal of Comparative Neurology*, *172*(1), 49–84. https://doi.org/10.1002/cne.901720104

Swanson, L. W., Wyss, J. M., & Cowan, W. M. (1978). An autoradiographic study of the organization of intrahippocampal association pathways in the rat. *Journal of Comparative Neurology*, *181*(4), 681–715. https://doi.org/10.1002/cne.901810402

Sweeney-Reed, C. M., Buentjen, L., Voges, J., Schmitt, F. C., Zaehle, T., Kam, J. W. Y., Kaufmann, J., Heinze, H.-J., Hinrichs, H., Knight, R. T., & Rugg, M. D. (2021). The role of the anterior nuclei of the thalamus in human memory processing. *Neuroscience & Biobehavioral Reviews*, *126*, 146–158. https://doi.org/10.1016/j.neubiorev.2021.02.046

Tamamaki, N., & Nojyo, Y. (1995). Preservation of topography in the connections between the subiculum, field CA1, and the entorhinal cortex in rats. *Journal of Comparative Neurology*, *353*(3), 379–390. https://doi.org/10.1002/cne.903530306

Taube, J. (1995). Head direction cells recorded in the anterior thalamic nuclei of freely moving rats. *The Journal of Neuroscience*, *15*(1), 70–86. https://doi.org/10.1523/JNEUROSCI.15-01-00070.1995

Taube, J., Muller, R., & Ranck, J. (1990). Head-direction cells recorded from the postsubiculum in freely moving rats. I. Description and quantitative analysis. *The Journal of Neuroscience*, *10*(2), 420–435. https://doi.org/10.1523/JNEUROSCI.10-02-00420.1990

Taube, JeffreyS. (1993). Electrophysiological properties of neurons in the rat subiculum in vitro. *Experimental Brain Research*, *96*(2). https://doi.org/10.1007/BF00227110

Thomson, D. J. (1982). Spectrum estimation and harmonic analysis. *Proceedings of the IEEE*, *70*(9), 1055–1096. https://doi.org/10.1109/PROC.1982.12433

Tibshirani, R., Walther, G., & Hastie, T. (2001). Estimating the Number of Clusters in a Data Set Via the Gap Statistic. *Journal of the Royal Statistical Society Series B: Statistical Methodology*, *63*(2), 411–423. https://doi.org/10.1111/1467-9868.00293

Tolman, E. C. (1948). Cognitive maps in rats and men. *Psychological Review*, *55*(4), 189–208. https://doi.org/10.1037/h0061626

Torromino, G., Autore, L., Khalil, V., Mastrorilli, V., Griguoli, M., Pignataro, A., Centofante, E., Biasini, G. M., De Turris, V., Ammassari-Teule, M., Rinaldi, A., & Mele, A. (2019). Offline ventral subiculum-ventral striatum serial communication is required for spatial memory consolidation. *Nature Communications*, *10*(1), 5721. https://doi.org/10.1038/s41467-019-13703-3

Trouche, S., Koren, V., Doig, N. M., Ellender, T. J., El-Gaby, M., Lopes-dos-Santos, V., Reeve, H. M., Perestenko, P. V., Garas, F. N., Magill, P. J., Sharott, A., & Dupret, D. (2019). A Hippocampus-Accumbens Tripartite Neuronal Motif Guides Appetitive Memory in Space. *Cell*, *176*(6), 1393-1406.e16. https://doi.org/10.1016/j.cell.2018.12.037

Tsao, A., Moser, M.-B., & Moser, E. I. (2013). Traces of Experience in the Lateral Entorhinal Cortex. *Current Biology*, *23*(5), 399–405. https://doi.org/10.1016/j.cub.2013.01.036

Tsao, A., Sugar, J., Lu, L., Wang, C., Knierim, J. J., Moser, M.-B., & Moser, E. I. (2018). Integrating time from experience in the lateral entorhinal cortex. *Nature*, *561*(7721), 57–62. https://doi.org/10.1038/s41586-018-0459-6

Tulving, E. (1972). Episodic and semantic memory. *Organization of Memory/Academic Press*.

Tulving, E. (2002). Episodic Memory: From Mind to Brain. *Annual Review of Psychology*, *53*(1), 1–25. https://doi.org/10.1146/annurev.psych.53.100901.135114

Turrigiano, G. G., & Nelson, S. B. (2004). Homeostatic plasticity in the developing nervous system. *Nature Reviews Neuroscience*, *5*(2), 97–107. https://doi.org/10.1038/nrn1327

Van Daal, R. J. J., Aydin, Ç., Michon, F., Aarts, A. A. A., Kraft, M., Kloosterman, F., & Haesler, S. (2021). Implantation of Neuropixels probes for chronic recording of neuronal activity in freely behaving mice and rats. *Nature Protocols*, *16*(7), 3322–3347. https://doi.org/10.1038/s41596-021-00539-9

Van De Ven, G. M., Trouche, S., McNamara, C. G., Allen, K., & Dupret, D. (2016). Hippocampal Offline Reactivation Consolidates Recently Formed Cell Assembly Patterns

during Sharp Wave-Ripples. *Neuron*, *92*(5), 968–974. https://doi.org/10.1016/j.neuron.2016.10.020

Van Groen, T., & Wyss, J. M. (1990). Extrinsic projections from area CA_1 of the rat hippocampus: Olfactory, cortical, subcortical, and bilateral hippocampal formation projections. *Journal of Comparative Neurology*, *302*(3), 515–528. https://doi.org/10.1002/cne.903020308

Vanderwolf, C. H. (1969). Hippocampal electrical activity and voluntary movement in the rat. *Electroencephalography and Clinical Neurophysiology*, *26*(4), 407–418. https://doi.org/10.1016/0013-4694(69)90092-3

Vann, S. D. (2010). Re-evaluating the role of the mammillary bodies in memory. *Neuropsychologia*, *48*(8), 2316–2327. https://doi.org/10.1016/j.neuropsychologia.2009.10.019

Vann, S. D., & Aggleton, J. P. (2004). The mammillary bodies: Two memory systems in one? *Nature Reviews Neuroscience*, *5*(1), 35–44. https://doi.org/10.1038/nrn1299

Vann, S. D., Aggleton, J. P., & Maguire, E. A. (2009). What does the retrosplenial cortex do? *Nature Reviews Neuroscience*, *10*(11), 792–802. https://doi.org/10.1038/nrn2733

Varga, V., Petersen, P., Zutshi, I., Huszar, R., Zhang, Y., & Buzsáki, G. (2024). Working memory features are embedded in hippocampal place fields. *Cell Reports*, *43*(3), 113807. https://doi.org/10.1016/j.celrep.2024.113807

Vertes, R. P. (1982). Brain stem generation of the hippocampal EEG. *Progress in Neurobiology*, *19*(3), 159–186. https://doi.org/10.1016/0301-0082(82)90005-3

Voigts, J., Newman, J. P., Wilson, M. A., & Harnett, M. T. (2020). An easy-to-assemble, robust, and lightweight drive implant for chronic tetrode recordings in freely moving animals. *Journal of Neural Engineering*, *17*(2), 026044. https://doi.org/10.1088/1741-2552/ab77f9

Wagner, A. R. (1976). Priming in STM: An information processing mechanism for self generated or retrieval-generated depression in performance. In *Habituation: Perspectives from child development, animal behavior, and neurophysiology* (1st ed., pp. 95–128). Hillsdale, NJ: Lawrence Erlbaum Associates.

Wagner, A. R. (1981). SOP: A model of automatic memory processing in animal behavior. In *Information processing in animals: Memory mechanisms* (1st ed., pp. 5–47). Information processing in animals: Memory mechanisms.

Wamsley, E. J. (2022). Offline memory consolidation during waking rest. *Nature Reviews Psychology*, *1*(8), 441–453. https://doi.org/10.1038/s44159-022-00072-w

Warburton, E. C., & Aggleton, J. P. (1998). Differential deficits in the Morris water maze following cytotoxic lesions of the anterior thalamus and fornix transection. *Behavioural Brain Research*, *98*(1), 27–38. https://doi.org/10.1016/S0166-4328(98)00047-3

Whissell, P. D., Tohyama, S., & Martin, L. J. (2016). The Use of DREADDs to Deconstruct Behavior. *Frontiers in Genetics*, *7*. https://doi.org/10.3389/fgene.2016.00070

Wiener, J. M., Lafon, M., & Berthoz, A. (2008). Path planning under spatial uncertainty. *Memory & Cognition*, *36*(3), 495–504. https://doi.org/10.3758/MC.36.3.495

Wilent, W. B., & Nitz, D. A. (2007). Discrete Place Fields of Hippocampal Formation Interneurons. *Journal of Neurophysiology*, *97*(6), 4152–4161. https://doi.org/10.1152/jn.01200.2006

Wilson, M. A., & McNaughton, B. L. (1993). Dynamics of the Hippocampal Ensemble Code for Space. *Science*, *261*(5124), 1055–1058. https://doi.org/10.1126/science.8351520

Wilson, M. A., & McNaughton, B. L. (1994). Reactivation of Hippocampal Ensemble Memories During Sleep. *Science*, *265*(5172), 676–679. https://doi.org/10.1126/science.8036517

Winnubst, J., Bas, E., Ferreira, T. A., Wu, Z., Economo, M. N., Edson, P., Arthur, B. J., Bruns, C., Rokicki, K., Schauder, D., Olbris, D. J., Murphy, S. D., Ackerman, D. G.,

Arshadi, C., Baldwin, P., Blake, R., Elsayed, A., Hasan, M., Ramirez, D., … Chandrashekar, J. (2019). Reconstruction of 1,000 Projection Neurons Reveals New Cell Types and Organization of Long-Range Connectivity in the Mouse Brain. *Cell*, *179*(1), 268-281.e13. https://doi.org/10.1016/j.cell.2019.07.042

Winson, J. (1974). Patterns of hippocampal theta rhythm in the freely moving rat. *Electroencephalography and Clinical Neurophysiology*, *36*, 291–301. https://doi.org/10.1016/0013-4694(74)90171-0

Witter, M. P. (1986). A Survey of the Anatomy of the Hippocampal Formation, with Emphasis on the Septotemporal Organization of Its Intrinsic and Extrinsic Connections. In R. Schwarcz & Y. Ben-Ari (Eds.), *Excitatory Amino Acids and Epilepsy* (Vol. 203, pp. 67–82). Springer US. https://doi.org/10.1007/978-1-4684-7971-3_5

Witter, M. P. (1993). Organization of the entorhinal-hippocampal system: A review of current anatomical data. *Hippocampus*, *3 Spec No*, 33–44.

Witter, M. P., Griffioen, A. W., Jorritsma-Byham, B., & Krijnen, J. L. M. (1988). Entorhinal projections to the hippocampal CA1 region in the rat: An underestimated pathway. *Neuroscience Letters*, *85*(2), 193–198. https://doi.org/10.1016/0304-3940(88)90350-3

Witter, M. P., Groenewegen, H. J., Lopes Da Silva, F. H., & Lohman, A. H. M. (1989). Functional organization of the extrinsic and intrinsic circuitry of the parahippocampal region. *Progress in Neurobiology*, *33*(3), 161–253. https://doi.org/10.1016/0301-0082(89)90009-9

Wood, E. R., Dudchenko, P. A., Robitsek, R. J., & Eichenbaum, H. (2000). Hippocampal Neurons Encode Information about Different Types of Memory Episodes Occurring in the Same Location. *Neuron*, *27*(3), 623–633. https://doi.org/10.1016/S0896-6273(00)00071-4

Xu, H., Baracskay, P., O'Neill, J., & Csicsvari, J. (2019). Assembly Responses of Hippocampal CA1 Place Cells Predict Learned Behavior in Goal-Directed Spatial Tasks on the Radial Eight-Arm Maze. *Neuron*, *101*(1), 119-132.e4. https://doi.org/10.1016/j.neuron.2018.11.015

Xu, X., Sun, Y., Holmes, T. C., & López, A. J. (2016). Noncanonical connections between the subiculum and hippocampal CA1. *Journal of Comparative Neurology*, *524*(17), 3666–3673. https://doi.org/10.1002/cne.24024

Ylinen, A., Bragin, A., Nadasdy, Z., Jando, G., Szabo, I., Sik, A., & Buzsaki, G. (1995). Sharp wave-associated high-frequency oscillation (200 Hz) in the intact hippocampus: Network and intracellular mechanisms. *The Journal of Neuroscience*, *15*(1), 30–46. https://doi.org/10.1523/JNEUROSCI.15-01-00030.1995

Young, B. J., Otto, T., Fox, G. D., & Eichenbaum, H. (1997). Memory Representation within the Parahippocampal Region. *The Journal of Neuroscience*, *17*(13), 5183–5195. https://doi.org/10.1523/JNEUROSCI.17-13-05183.1997

Zar, J. H. (2010). *Biostatistical analysis* (5th ed). Prentice-Hall/Pearson.

Zhang, F., Wang, L.-P., Brauner, M., Liewald, J. F., Kay, K., Watzke, N., Wood, P. G., Bamberg, E., Nagel, G., Gottschalk, A., & Deisseroth, K. (2007). Multimodal fast optical interrogation of neural circuitry. *Nature*, *446*(7136), 633–639. https://doi.org/10.1038/nature05744

Zhang, Z. J., Li, Q., Dong, Z. Y., Wang, W. T., Lai, S. T., Yang, X., Liang, F., Wang, C. L., Luo, C., Lyu, L. J., Li, Z., Xu, J. M., & Wu, X. (2023). Microscopic Characterization of Failure Mechanisms in Long-Term Implanted Microwire Neural Electrodes. *2023 IEEE International Reliability Physics Symposium (IRPS)*, 1–5. https://doi.org/10.1109/IRPS48203.2023.10117971

Ziv, Y., Burns, L. D., Cocker, E. D., Hamel, E. O., Ghosh, K. K., Kitch, L. J., Gamal, A. E., & Schnitzer, M. J. (2013). Long-term dynamics of CA1 hippocampal place codes. *Nature Neuroscience*, *16*(3), 264–266. https://doi.org/10.1038/nn.3329

Zola-Morgan, S., & Squire, L. R. (1990). The Neuropsychology of Memory: Parallel Findings in Humans and Nonhuman Primatesa. *Annals of the New York Academy of Sciences*, *608*(1), 434–456. https://doi.org/10.1111/j.1749-6632.1990.tb48905.x